THE UNIVERSITY
of LIVERPOOL

Centre for Nanoscale Science, Department of Chemistry

A Generic Approach to Biomolecular Functionality of Gold and Silver Nanoparticles

Thesis submitted in accordance with the requirements of The University of Liverpool for the degree of Doctor of Philosophy

by

Tshinyadzo Robert Tshikhudo

July, 2006

I certify that all material in this thesis which is not my own work has clearly been identified and no material is included for which a degree has previously been awarded.

To.....

"Our deepest fear is not that we are inadequate. Our deepest fear is that we are powerful beyond measure. It is our light not our darkness that frightens us. We ask ourselves 'who am I to be brilliant, gorgeous, talented and fabulous?' Actually, who are you not to be? You are a child of God. Your playing small doesn't serve the world. There's nothing enlightened about shrinking so that other people won't feel insecure around you. We were born to make manifest the glory of God that is within us.

It's not just in some of us; it's in everyone. And as we let our own light shine, we unconsciously give other people permission to do the same. As we are liberated from our own fear, our presence automatically liberates others."

Ndi kona nga a nkonisaho. Wo mmpha vhutshilo Wa mpfuna,
Wa ntonda, Wa nndinda nda vha Wau- Ndi a u livhuwa Murena.

Ndi do dzula ndi tshi renda Iwe Mukona zwothe

Phillipians 4: 15

Acknowledgements

I am extremely grateful to my supervisor Professor Mathias Brust for allowing me to conduct this research work under his supervision. I thank him for his tremendous support, guidance and teaching throughout my PhD studies. Through his extensive chemical knowledge and passion for chemistry, he has been a source of inspiration to me. He has given me an opportunity to learn and explore a lot in this multidisplinary field. This will certainly help me to establish a strong research group at Mintek in South Africa.

Special thanks go to Mintek and Project AuTEK, the financial sponsors of this project. I am indebted to their generous financial support. Thank you to Dr. Elma van der Lingen, a visionary and inspiring leader of the 21st centuary and in particular to Dr. Daven Compton, I cannot forget their help, encouragement and support throughout my studies. Thank you to all my colleagues at Mintek (Advanced Material Division) for their support and in particular to the wonderful administrative officers, Bettie Nell and Shireen Patel.

Many thanks go to Professor Zhenxin Wang for his help in particular AFM analysis and useful discussions throughout my studies. Many thanks go to Dr Rick Cosstic for his support and helpful suggestions. Thanks to Dr. Domenico F. Demuru (Dr. Andrea Secchi, Arturo Arduini, Andrea Pochini, from Parma University, Italy) and Dr. Christopher R. Doty (Prof. Dave Fernig) for our collaborative work on calixarene based gold nanoparticles and peptide stabilised silver nanoparticles respectively. Thanks to Dr. Jennifer. L. Brennan for the collaborative click chemistry work and on exploring the use of "BAB" approach I have developed (particularly the work of Claire Rees). Thanks to Dr. D.S.K. Ikah for evaluating neurotoxic effects of PEGylated AuMPCs and ongoing work on exploring the use of PEGylated BSA MPCs for the removal of billirubin.

I cannot forget to thank Dr. Adam Papworth and Mr John Naylor for their help in using transmission electron microscopy (TEM) and the Chemistry NMR group particularly Sandra for NMR and Mr Steve Apter for elemental analysis.

I would like to acknowledge the wonderful atmosphere of bionanomeetings in Chemistry Dept led by Dr. NTK Thanh and her passion for bionanotechnology. I cannot forget to acknowledge the support and friendship of Dr Irshad Husain, Mr Jorg Wagner, Ms Maria Proupin-Perez. Ms Maryam Bayat. Thanks to my colleagues in the Nanoscale labs G35 and 215 (Dr. Zhen Wang, Ms Paola Nativo, Dr Antonios Kanaras *etc*.). Many thanks go to Dr. Raphael Levy for proof reading chapter 1. Many thanks go to Mr Richard Amewu and his family for their wonderful support and encouragements. I will miss all the wonderful social and spiritual meetings. I appreciate all you have done to me and your wife Kate. God bless you richly. Dr. Xolani Nocanda and Poslet Shumbula, I appreciate all your spiritual support and guidance.

I would like to acknowledge the wonderful support and encouragement I always receive from my fiancée Zwidofhela Munyai. To my mum Tshavhungwe, my brothers Alex and Edzisani, my sisters Rosemary, Sandra, Jane and Mercy, you are ever in my heart and I love you all. Mr Milton Mangenge you are truly a blessing to me. Thank you very much for your support and encouragement. To Pastor E. Nengovhela, Mrs Gloria Nengovhela and your entire family, I cannot thank you enough. You are truly a blessing to me. God ever bless you.

Abstract

A generic method for the modification of monolayer protected clusters (MPCs) of gold and silver with any biomolecular functionality of choice has been developed. For this purpose, thioalkylated polyethylene glycol (PEG) ligands carrying specific functional groups such as amines, azides, carboxylates and biotin, have been employed for the size-selected preparation and stabilization of water-soluble MPCs of gold and silver in the 2-60 nm size range. These MPCs exhibited an unprecedented stability under conditions likely to be encountered in physiological environments, *i.e.* high electrolyte concentration and a wide range of pH.

Before exploring possibilities of biomolecular functionalisation, a calix[4]arene moiety was incorporated in the PEG ligand shell of the MPCs, and it was demonstrated that this, on its own totally water-insoluble species, was solubilised and retained its specific recognition function towards pyridinium ions also in an aqueous environment. In addition, calix[6]arene was used as a wheel for the assembly of pseudorotaxanes and rotaxanes, in which gold nanoparticles served as stoppers. Using these supramolecular structures for the deposition of thin films of particles by drop-casting, it was found that the orientation of the calixarene rim influenced to some extent the nanoscopic ordering observed.

The PEGylated MPCs were then used as precursors for the preparation of biomolecularly functionalised nanoparticles. Three different bioconjugation routes, *i.e.* click chemistry, carbodiimide coupling and avidin-biotin interactions, have been adapted for the preparation of a wide range of biomolecular/inorganic hybrid nanoparticles. In particular, the attachment of proteins (lipase, antibodies, BSA), DNA and sugars, retaining their respective functionality has been demonstrated. Importantly, it is demonstrated that based on biotin-avidin binding an extremely versatile bioconjugation approach can be described, which lends itself to the development of modular biomolecular tool kits for the facile preparation of nanoparticles with desired functionality.

Publications

1. Brennan, J, L., Hatzakis, N. S., **Tshikhudo, T. R.**, Dirvianskyte, N., Razumas, V., Patkar, S., Vind, J., Svendsen, A., Nolte, R.J.M., Rowen, E. A and Brust M., Bioconjugation via click chemistry: The creation of functional hybrids of Lipases and Gold Nanoparticles, *Bioconjugate Chemistry, 2006, in press*

[chapter 5]

2. Ikah, D.S.K, Howard, C. V., Mclean, W. G., Brust, M and **Tshikhudo, T.R.**, Neurotoxic Effects of Monodisperse Colloidal Gold Nanoparticles., *Toxicology*, 2006, **238**, 219

3. Doty, R.C., **Tshikhudo, T.R.**, Brust, M and Fernig, D.G, Extremely Stable, Water-Soluble, Ag Nanoparticles. *Chem Mater*, 2005, **17**, 4630

[chapter 3]

4. **Tshikhudo T.R.**, Demuru, D., Wang, Z., Brust, M., Secchi, A., Arduini, A and Pochini, A, Molecular Recognition by Calix[4]arene-Modified Gold Nanoparticles in Aqueous Solution, *Angew. Chem. Int. Ed.,* 2005, **44,** 2913

[chapter 4]

5. **Tshikhudo T.R.**, Wang, Z and Brust M, Biocompatible Gold Nanoparticles, *Materials Science and Technology*, 2004, **20**, 980

[chapter 2]

Table of Contents

Chapter 2. Functionalised thioalkylated polyethylene glycol (PEG) ligands

CHAPTER 1

INTRODUCTION

1 Introduction

1.1 Overview and Objectives

Metal nanoparticles, in particular those of gold and silver, are probably the most widely studied materials in nanotechnology to date due to their stability, ease of preparation and unique optical properties.[1-8] Gold colloids have long been used as biomolecular labels in electron microscopy [9-11] because they are much more electron-dense than organic molecules and hence yield excellent contrast in comparison to cells and tissues. Exploitation of gold nanoparticles as optical markers in the dark field microscopy of biological samples is a more recent development as this area has always been dominated by fluorescence dyes. These, however, have limitations such as photobleaching, and often a relatively high detection threshold, while light scattering by gold nanoparticles even has the potential for single particle detection.[12] This opens the ability to track single molecules within a cell and hence to monitor single molecular binding events in biological systems. [12] Owing to the limitations accompanying the use of fluorescent dyes, gold and silver nanoparticles and in particular semiconductor quantum dots have now gained popularity as alternative bio-labeling probes. [13-17] Apart from their unique optical properties, gold and silver nanoparticles are also known to act as strong Raman enhancers [18,19] and may also amplify fluorescence under certain circumstances.[20] An important requirement for their biological applications, apart from making them stable in aqueous environment, is the ability to attach biomolecules of interest.

The objective of this project is to design and prepare a wide range of robust biocompatible gold and silver nanoparticles in such a way that each of these particles will have properties that can, in principle, be exploited for bio-labeling purposes, either in optical or electron microscopy. It is not intended to make particles with only one specific biological recognition function but instead provide a generic surface chemistry that will easily allow the incorporation of practically variety of desired recognition motif. The desired bio-gold/silver products schematically shown in Figure 1 are designed to address many biological and pharmaceutical applications.

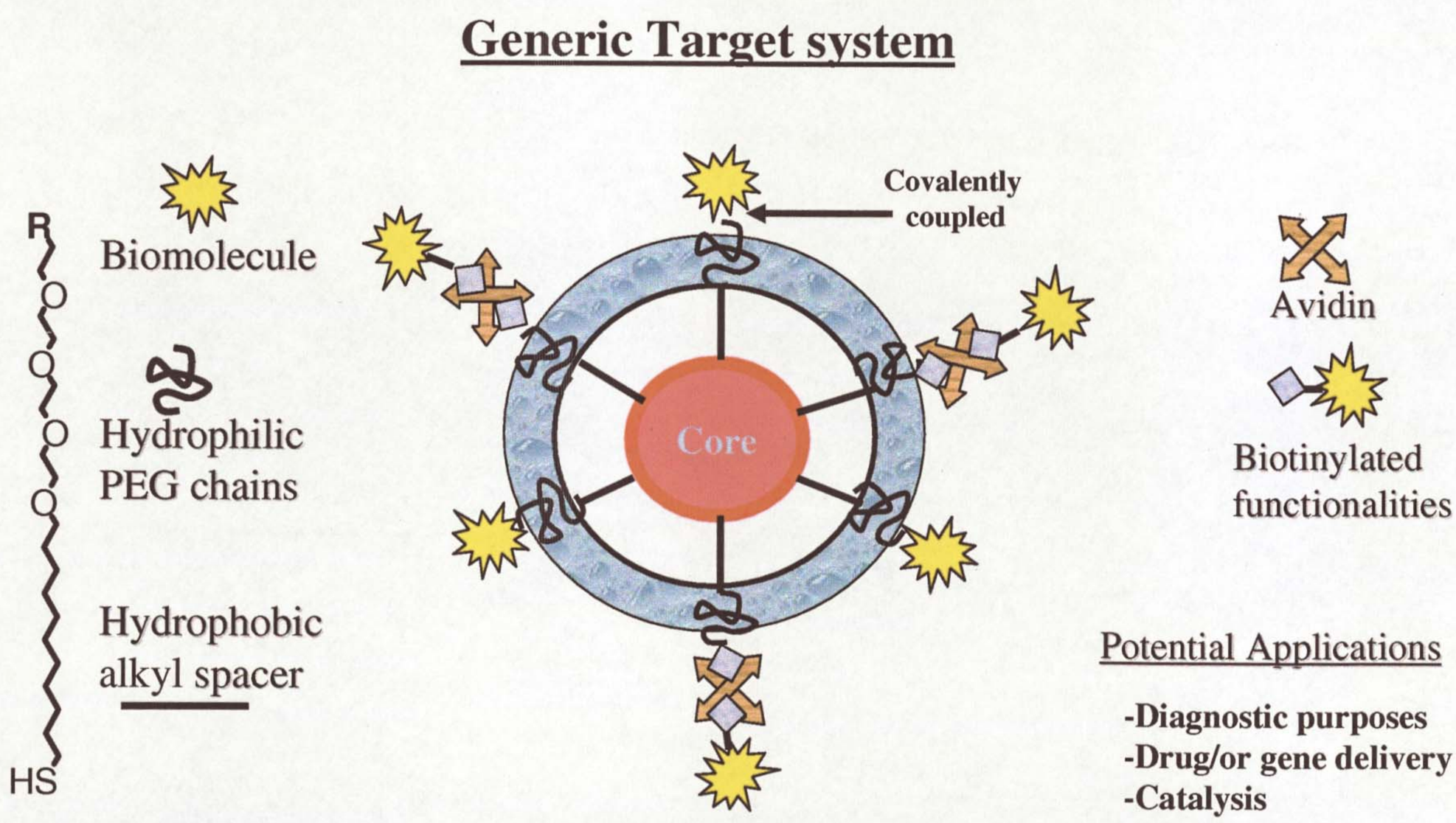

Figure 1. Proposed generic system for the development of biomolecular functionalisation on gold and silver nanoparticles.

Three important milestones were identified for the development of biomolecular functionality on gold and silver nanoparticles.

i) Size-chosen synthesis of water soluble gold/silver nanoparticles

ii) Chemical surface functionalisation without compromising particle stability

iii) A general method for the attachment of variety of biological recognition motif.

The aim is that the final product should accommodate the following criteria:- water soluble and extremely stable in biological environment, functionalized and hence versatile to address a wide range of biological and related applications.

1.2 Synthesis of Gold and Silver nanoparticles

1.2.1 Background and origin of properties

The optical properties of metal nanoparticles in particular those of gold and silver are dependent on size, shape *etc* (as theoretically explained by Mie in 1908).[1] In fact, their unusual optical properties have long been exploited for instance in decorative pigments during the Roman period. They exhibit a strong UV-vis absorption band not present in the spectrum of the bulk. The origin of the light absorption by these noble metal nanoparticles is the collective oscillation of the conduction band electrons induced by the interacting electromagnetic field. The absorption band arises when the incident photon frequency is resonant with the collective oscillation of the conduction electrons and is commonly known as surface plasmon resonance (SPR). An elegant example is the Lycurgus cup (4^{th} century A.D.) [21] shown in Figure 2, exhibited in the British museum. The glass appears green in reflection and red in transmission of light. Chemical analysis revealed that the glass contains gold and silver nanoparticles of approximately 70 nm. [21] The red colour is due to the small fraction of gold nanoparticles contained in it.

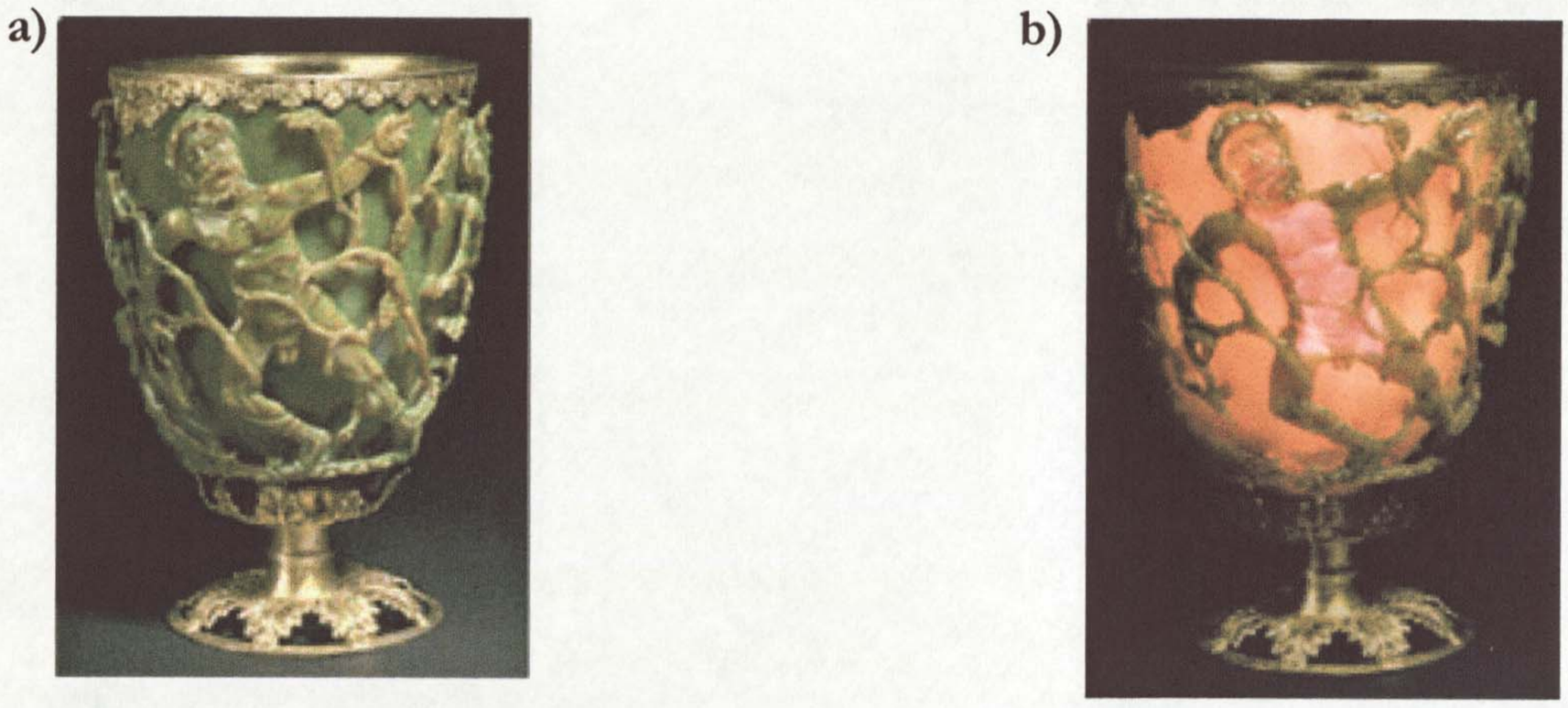

Figure 2. Lycurgus cup in a) reflected light and b) in transmitted light.

1.2.2 General synthetic methods of Nanoparticles

To benefit from the above mentioned properties, many different synthetic methods were developed for the preparation of metal nanoparticles. [22-27] Chemical methods currently used for the preparation of nanoparticles include (i) reduction of metal salts (ii) photochemical reduction (iii) electrochemical synthesis (iv) ligand reduction and (iv) displacement from organometallics.

The reduction of metal salts in solution as shown in Figure 3 is the most widely used method, and the particles discussed in the following chapters are prepared via this approach.

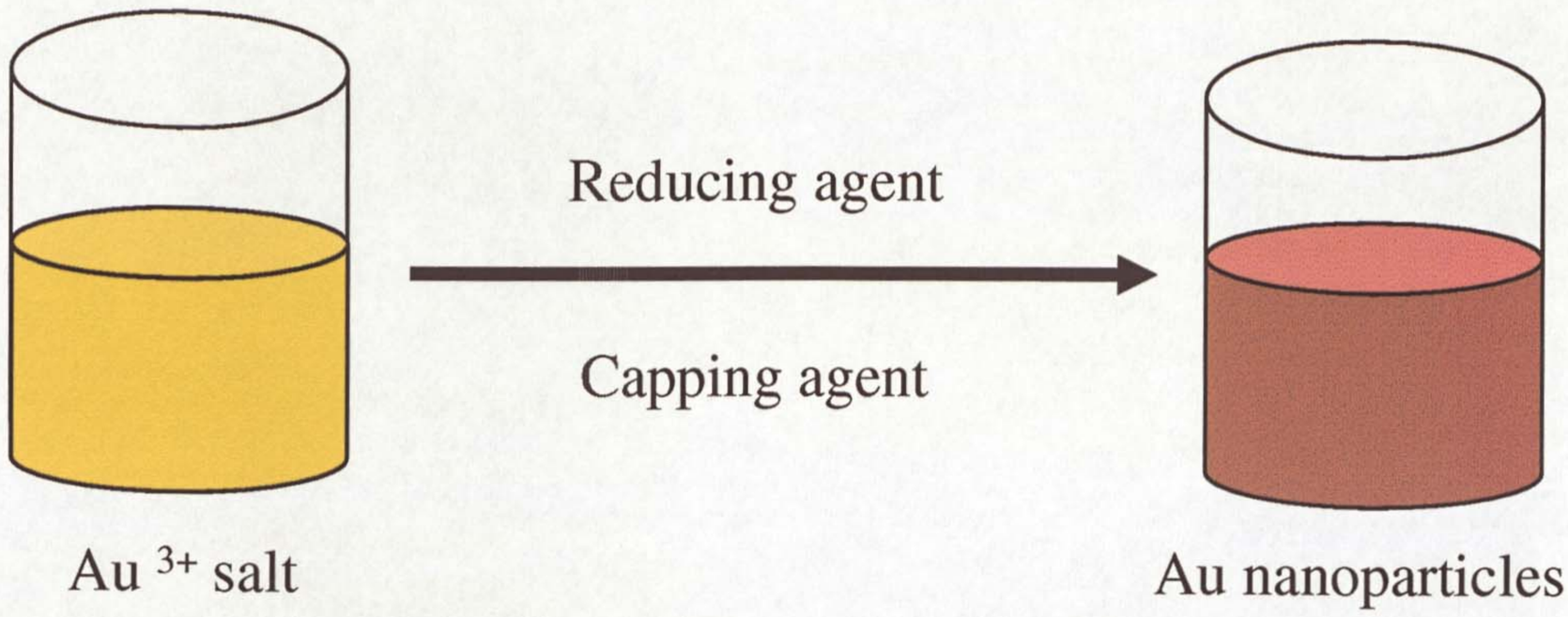

Figure 3. Preparation of gold nanoparticles by chemical reduction route.

Generally, particles are made by reducing a metal salt. The reducing agent can also act as a stabilizing agent or otherwise a suitable capping agent can be added before reduction. [28] While it is beyond the scope of this introduction to mention all reducing or capping agents that have been used to date, a list of some common agents is presented in Table 1.

Metal	**Reducing agent**	**Stabilising agent(s)**	**Refs**
Au, Ag, *etc*	$NaBH_4$ or (KBH_4)	Thiols, polymers, dendrimers, surfactants	29-36
Au	Diborane	Phosphine	37
Au	Sodium citrate	Citrate	38,39
Au	Hydrazine	Cationic or anionic surfactants block copolymers	40,41
Au, Pt,Pd, Rh	Aqueous alcohols	Polymers such as Polyvinyl pyrolidone (PVP), polyvinyl alcohol (PVA),polyvinyl ether (PVE), cyclodextrin	42-44
Au, Pt, Ag, Rh	H_2	PVA	45
Au	CO	Polyvinyl sulfate	46

Table 1. A summary of the most common reducing and stabilising agents employable for the preparation of noble metal nanoparticles.

1.2.2.1 Stabilisation of metal nanoparticles

Nanoparticles are thermodynamically unstable and hence have to be stabilised to prevent aggregation during and after synthesis. [48] This is a basic requirement since van der Waals attraction at short interparticle distance causes particles to aggregate. Therefore, a stabilizing agent is required to induce a repulsive force opposed to van der Waals forces. Generally, stabilisation can be accomplished in two different ways thus; electrostatic and steric stabilization. [48] These two mechanisms are schematically shown in Figure 4. Electrostatic stabilization depicted in Figure 4a, entails the adsorption of negatively charged species (such as carboxylates, or halides) and their counter ions to the surface of the nanoparticles, creating an electrochemical double layer, which is responsible for Coulombic repulsion. Electrostatically stabilised particles are very sensitive to changes in the ionic strength of the medium or thermal motion which disrupt or compress the double layer and hence induce particles aggregation. Steric stabilisation entails the adsorption of ligands, macromolecules or polymers to the surface of the nanoparticles providing a protective layer,[47,49] which causes a steric barrier and hence prevents the nanoparticles from aggregation. As depicted in Figure 4b, a region of high local ligand/polymer concentration builds-up in solution as the particles come closer. The particles are separated by solvent, since the solvent re-establishes the equilibrium by diluting the polymer molecules and hence particles separation. [48]

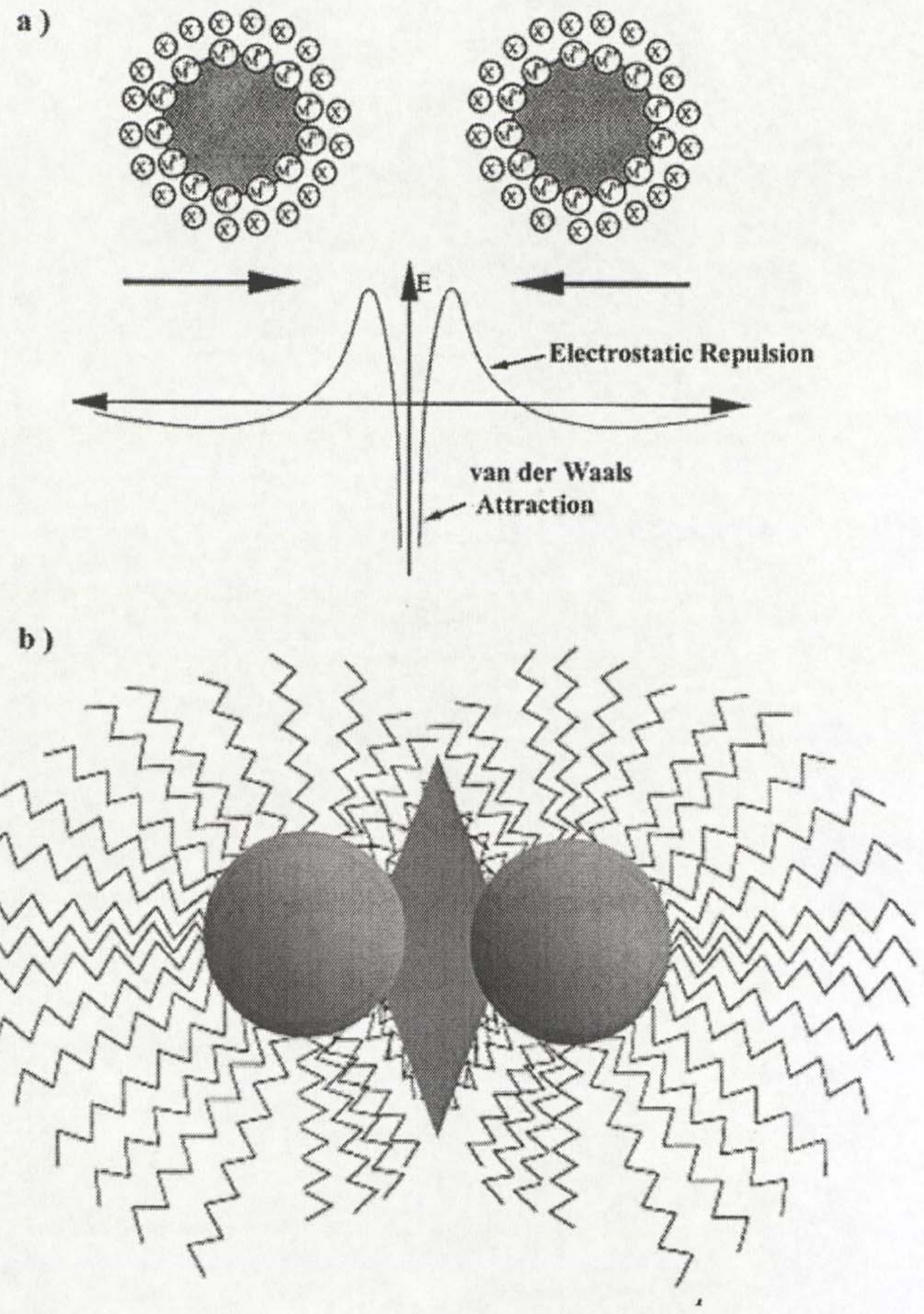

Figure 4. Illustration of a) electrostatic and b) steric stabilisation of metal nanoparticles. [48]

1.2.2.2 Nanoparticles preparation by citrate reduction method

Probably, the first scientific report on the preparation of gold nanoparticles was contributed by Faraday,[50] who had reduced an aqueous solution of $AuCl_4^-$ with white phosphorous in a two-phase (CS_2-water) solvent system and explained that the ruby red colour of the solution was due to the suspension of small metallic gold particles interacting with light. However, it was later in 1951 that Turkevich [39] prepared the classical citrate reduced gold nanoparticles in aqueous solution. Turkevich's method was later modified in 1974 by Frens,[22] who prepared citrate

stabilised gold nanoparticles of different sizes (10-100 nm) by changing the molar ratio between gold and citrate. Today the scientific community follows or modifies his approach for the preparation of uniform charge stabilised gold and silver nanoparticles. The Frens method basically entails the reduction of Au (III) salt by citrate to Au (0) as shown in Figure 3. When the citrate is added to the boiling $AuCl_4^-$, the yellow Au (III) changes colour to the characteristic ruby red of Au nanoparticles. This is evidenced by a typical sharp plasmon absorption band in the UV-vis spectrum $\lambda = 525$ nm. [22]

1.2.2.3 Monolayer Protected Clusters (MPCs)

Ligand stabilised metal nanoparticles were a key to improving the stability and reactivity of metal nanoparticles, and in particular, to allow the facile synthesis of well-defined nanoparticles in an organic phase. The first approach of this kind was the preparation of phosphine stabilised Au clusters ($Au_{55}(PPh_3)_{12}Cl_6$) of about 1.4 ± 0.4 nm size reported by Schmid *et al* in 1981.[51] Despite their delicate synthesis "Schmid clusters" had a great impact on the preparation and application of ligand stabilised metal nanoclusters. Just a decade later, Mulvaney and Giersig in 1993 demonstrated that thiols can be used to stabilize gold colloids, which were electrophoretically deposited onto amorphous carbon film to form hexagonal close packed superlattices.[52] A year later a two-phase liquid-liquid synthesis of alkanethiol stabilised gold clusters was reported by Brust *et al*. [30] This method had a considerable impact in the area of ligand stabilised metal nanoclusters in just a decade simply because of its ease of preparation and the stability of the product. [29]

In addition to the advantage that the method is applicable to various metals, [29] chemical modification of the resulting MPCs can be achieved in different ways. It should be pointed out that the term monolayer protected clusters (MPCs) will be often used in this work and this is by taking assumptions that thioalkylated PEG ligands used also form a monolayer on clusters surface. A schematic illustration of the preparation of MPCs is shown in Figure 6. The term monolayer protected clusters (MPCs) was first introduced by Murray to distinguish them from other clusters or colloids which in

comparison lack stability and tend to be less monodisperse.[29] The diameters of these clusters can tentatively be rationalized by the full-shell or magic number concept to attain a cubic (fcc) close-packed structure. This consists of a central atom surrounded by 12 atoms in the first shell (Figure 5), while the second shell comprises 42 atoms surrounding the first inner shell (*i.e.*55-atoms in total). The third layer consists of 92 atoms (thus 147 total atoms). The total number of atoms *y*, per *n*th shell is given by the equation: $y = 10n^2 + 2$ $(n > 0)$ [47] (Table 2).

The two-phase method follows the synthetic scheme outlined in Figure 6 (route A) in which aqueous $AuCl_4^-$ is transferred to an organic phase (toluene) by the phase transfer agent tetraoctyl ammonium bromide (TOABr) to form an intensely orange coloured Au (III) complex (tetraoctylammonium tetrabromoaurate) in toluene. Thiol ligands are then added to the organic phase followed by reduction with aqueous BH_4^- to form the desired MPCs. [30] The proposed reactions are given in equation 1 and 2.[53]

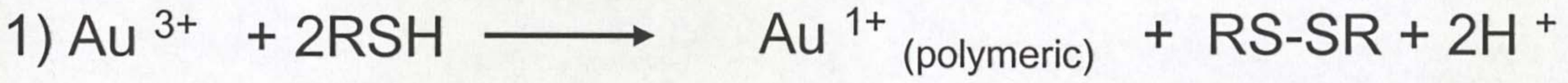

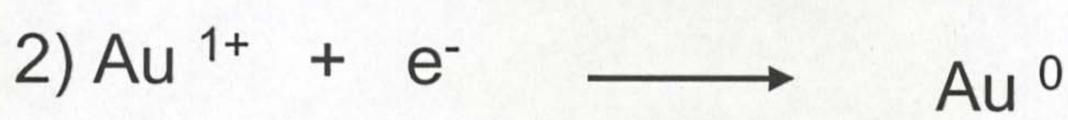

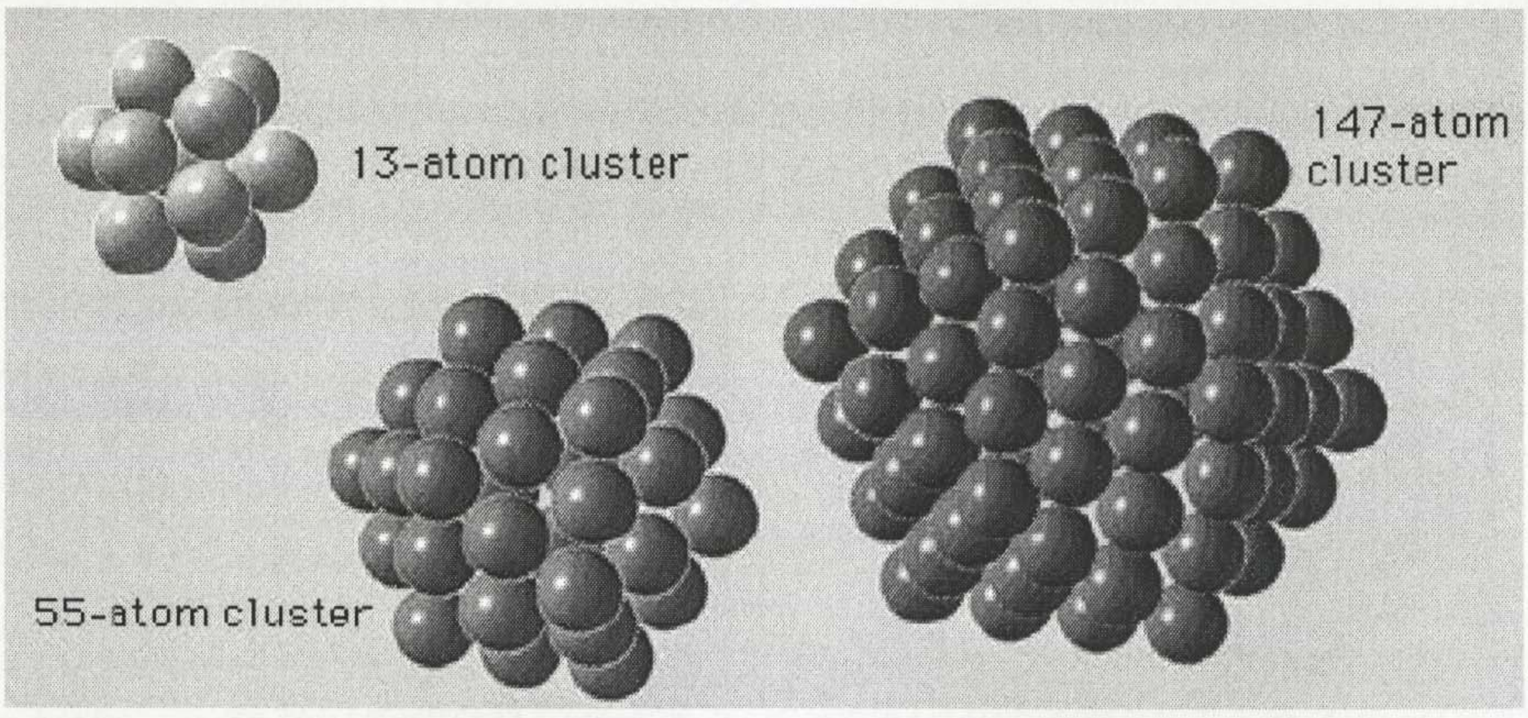

Figure 5. Typical representation of the first three closed-packed full shell (magic numbers) clusters, showing a complete regular outer geometry to have 13, 55 and 147 atoms.[47]

Full Shell Clusters	**Total number of atoms**	**Surface atoms (%)**
1 shell	13	92
2 shell	55	76
3 shell	147	63
4 shell	309	52
5 shell	561	45
6 shell	1415	35

Table 2. The relationship between the total number of atoms in full shell (magic number) clusters and the percentage of surface atoms. [54,55]

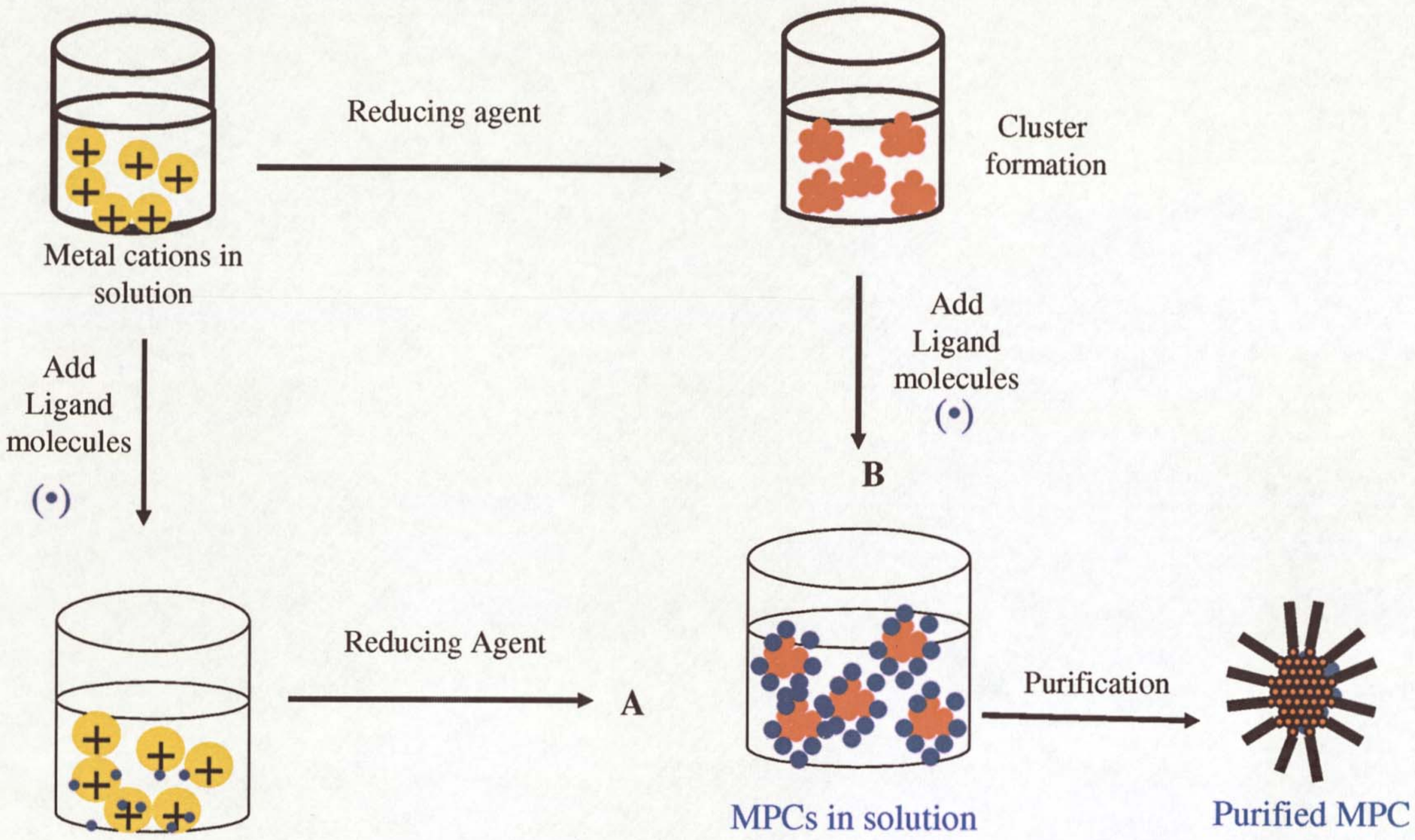

Figure 6. Schematic illustration for the preparation of monolayer protected clusters (MPCs) via two different routes. In route A, metal cations are reduced either in organic or aqueous solution in the presence of ligands to obtain the desired MPCs while in route B, electrostatically stabilised particles are prepared and then ligands (mostly thiols) are added to produce the desired MPCs.

Equation 1 illustrates a route in which thiol is involved in the reduction of Au (III) to a Au (I)-polymeric intermediate. In fact the type of material formed is dependent on the type of thiols used, in that, aromatic thiols such as thiophenol have been shown to form insoluble Au (I) species which cannot be reduced further using sodium borohydride. [56] Moreover, Negishi and Tsukuda showed that some dithiols such as *meso*-2, 3,-dimercaptosuccinic acid are capable of reducing Au (III) to Au (0) completely without the use of sodium borohydride.[57] To complete the reduction, normally, sodium borohydride is added (equation 2) to form the corresponding clusters as illustrated in Figure 6 route A.

Murray carefully investigated this route (A) and showed that by changing parameters such as gold:thiol molar ratio, [58] temperature, [59] and the rate of borohydride addition, size and shape of the resulting MPCs could be manipulated to some extent in the 1-5 nm regime. This is achievable by controlling the nucleation and growth rate during reduction. [60, 61] Following the same route (A), Brust *et al* developed also a single phase method, which allowed the preparation of hydrophilic MPCs by adding aqueous solution of borohydride to an alcoholic solution of $AuCl_4^-$ and *p*-mercaptophenol. [62]

Following synthetic route (B) illustrated in Figure 6, the University of Liverpool group also showed that, if the (tetraoctylammonium tetrabromoaurate) complex in toluene is reduced by aqueous borohydride in the absence of thiols, then, this leads to the formation of electrostatically stabilised particles, in which bromides and ammonium ions stabilize the particles. Addition of thiols to the TOABr stabilised particles converts them to MPCs. [63-67] The Schiffrin group employed Soxhlet extraction to purify dodecane thiol stabilised MPCs since it was found that they contain a significant amount of tetraoctylammoniun bromide as impurity. [64] We have extensively used this route (B) and showed that citrate stabilised or any charge stabilised particles can also be converted to the corresponding MPCs [65] by treating the particles with the thiolated ligands of interest, mostly for the preparation of hydrophilic MPCs. One of the major breakthroughs in the context of MPCs, is the introduction of ligand-exchange reactions pioneered by Murray. [29] In route B, if MPCs are formed instead of charge stabilised particles, then by applying Murray's ligand-exchange, it is possible to introduce any functionality of choice to the MPCs surface. Apart from alkane-thiolated ligands which are normally used, other ligands such as amines, [26, 68-70] thioethers, [71-73] isocyanates [74] and some listed in Table 1 have also been used.

1.3 MPCs ligand structure and reactivity

MPCs of gold and silver can adopt different morphologies such as decahedra, dodecahedra *etc* depending on their size, while truncanted cubeoctahedral is the most common motif.[47] Amongst all chemical functionalities, thiols are crucial for the formation of gold clusters since they form strong Au-S bonds (owing to Au and S both having "soft" character). Both alkyl thiols and dialkyl disulfides have a strong affinity for gold and both are believed to bind as thiolate species to metal surfaces. They are widely used for the formation of self-assembled monolayers (SAMs) on gold and other metal surfaces. [53] The hydrogen is eliminated as molecular hydrogen.[53] Evidence of "intact" thiols on clusters by ^{1}H NMR however showed that the loss of hydrogen can be prevented for some time as long as there is no easy path for hydrogen removal. [73] The general understanding is that the stability of alkane-thiolated molecules on gold clusters is due to the strong Au-S interaction and lateral van der Waals attractions between hydrocarbon chains, which also suggests that the longer the hydrocarbon chains, the greater is the stability.[53]

The MPC ligand shell represents a monolayer in 3D in contrast to the 2D assembly on flat surfaces.[53] Place-exchange reactions allow the incorporation of functionalities on MPCs. The extent of exchange (complete or partial exchange) was carefully studied by Murray, in particular using NMR and FTIR spectroscopy. [75-79] NMR provides information regarding the molecular composition of MPCs. ^{1}H and ^{13}C NMR data of MPCs exhibit peak broadening [58] particularly of the methylene protons closest to the gold core (a phenomenon still subjected to debate). Murray explained this to be based on spin-spin relaxation (T_2), while a distribution of chemical shifts is due to ligand heterogeneity (or differences) in Au-SR binding sites in a mixture of clusters with different shapes and size. [29,80, 81]

Place exchange reactions are understood to proceed according to an associative mechanism *i.e.* the incoming thiols replace thiols on the cluster surface via an S_N2-type mechanism.[76] The hydrogen of the incoming thiol binds to the leaving

thiol during the replacement step. Weakly bound ligands on the gold surface, such as amines or phosphines, can easily be replaced by incoming thiols.[53] Both hydrophobic and/or hydrophilic molecules can be introduced to the MPCs surface allowing simple transfer of particles from organic to aqueous phase or vice versa.[82, 83]

1.4 MPCs characterization

Numerous microscopic and spectroscopic techniques have been used to characterise MPCs (see a review by Finke [47] for details). The main techniques used in this project are listed below.

- Transmission electron microscopy (TEM) which uses a fine beam of electrons to image nanoscale objects is widely used to analyse shape, size, dispersity and structure of the MPCs.

- Atomic force microscopy (AFM) provides 3D topographical information of a sample. A very sharp tip attached to a cantilever is scanned across the surface of the sample, and the change in the vertical position reflects the topography of the surface.

- Ultraviolet and Visible absorption spectroscopy (UV-vis). Gold and silver nanoparticles exhibit a strong UV-vis absorption band. The absorption band results when the incident photon frequency is resonant with the collective oscillation of the conduction electrons (plasmons). The resonance is commonly known as surface plasmon resonance (SPR). Spectra contain information on particle size and shape and the degree of aggregation (inter-particle distance).

- Inductively Coupled Plasma-Atomic Emission Spectroscopy (ICP-AES) was used for elemental analysis. The technique measures the light emitted by an element in a sample introduced to a high temperature argon plasma. Each element emits at specific wavelengths and the intensity of the emission is

proportional to the number of atoms and hence to the concentration of the element in the sample.

- Nuclear magnetic resonance spectroscopy (NMR). Both ^{1}H and ^{13}C NMR data provide information regarding the structure and composition of the ligand shell of MPCs.

- Gel electrophoresis

Gel electrophoresis is a technique used to separate macromolecules (such as proteins and oligonucleotides) based on charge and molecular weight and used often in chapter 5. The word "gel" refers to the matrix or support used during separation. In most cases polyacrylamide and agarose supports, which are the cross-linked polymers of acrylamide and saccharide respectively are used. The composition and porosity of the polyacrylamide and agarose matrix can be varied. When the intended application is to separate proteins and small nucleic acids (DNA and RNA), different mesh sized networks of polyacrylamide support are often used. In separating larger nucleic acids (greater than a few hundreds of bases) agarose (a galactose polymer extracted from seaweed) is a preferred matrix. These matrices can be used to form gels in buffer media. [84]

During preparation, the choice of buffer (its ionic strength and concentration) plays an important role in maintaining the pH constant within the reservoir and the matrix and for uniform macromolecular migration and good resolution. Also, the buffer should not interact with the matrix. Electrophoresis (or the movement of electrically charged molecules under the influence of an electric field) is run, by placing the molecules into the wells of the gel and a voltage is applied to the gel chamber. The molecules then move towards the cathode if they are positively charged or towards anode if they are negatively charged. When separating proteins (having multiple charges and complex shapes) using polyacrylamide gel, the anionic detergent called sodium dodecyl sulfate (SDS) is often used to coat the proteins (making them negatively charged) to maintain constant migration of proteins at pH values that are far

from their isoelectric point (pI). The separated proteins can be visualized on the gel by various staining procedures e.g. ethidium bromide, silver or cooumassi blue dye.

Agarose gel electrophoresis is relatively simple to perform and mostly used for the separation of DNA. DNA is negatively charged due to the phosphate backbone, and the migration is always towards the positive electrode and hence facilitates separation of DNA strands based on molecular weight. Agarose gel electrophoresis was recently applied to the separation of biomolecularly functionalized gold nanoparticles [85, 86] with great success to the extent of isolating particles with only one DNA strand attached.[87-89]

1.5 Biomolecular Functionalisation of Nanoparticles

The ability to integrate nanostructured materials with biomolecules has many advantages over the molecular tags, since nanostructured hybrids provide new and unique optical properties for biotechnological applications. Moreover, molecular tags have many disadvantages and limitations including; photobleaching, and often a relatively high detection threshold.

Gold and silver nanoparticles are more attractive since they are excellent scatterers and absorbers of light. The light scattering from these plasmon resonant particles is known to be in the order of 10^6 more intense than fluorescence emitted from commercially available fluorophores.[18] Noteworthy is that surface plasmon resonance (SPR) is very sensitive to local environmental changes and refractive index. The optical properties of gold and silver nanoparticles make them suited for biological applications. Two methods can be applied for detection by monitoring the change in SPR position; UV-vis extinction (absorption plus scattering) and resonant Raleigh scattering spectroscopy.

If the particles are brought close together in solution (thus, the interparticle spacing is less than the diameter of the nanoparticles), for example, by binding of biomolecules attached to the particles, they are able to interact electromagnetically

through dipolar coupling, resulting in a broadened and red shifted SPR band. [90] This can be monitored by UV-vis spectroscopy. Alternatively, nanoparticles can be immobilized on substrates, making it possible to detect biomolecules of interest.[91] Signal transduction in this case depends on the dielectric environment of the nanoparticles induced by solvent or target molecules.

Typical examples exploring the use of SPR require brief discussion. Probably to begin with, it is important to mention that the use of gold colloids in biological applications dates back to the invention of an immunogold staining procedure developed by Faulk and Taylor in 1971. [93] Since then, gold nanoparticles have been extensively used as labels of targeting molecules particularly proteins. Schultz has recently demonstrated the use of colloidal silver plasmon resonant particles as optical reporters in a typical biological assay. [20] Plasmon resonant particles were surface coated with a ligand, and used as target-specific labels in an *in situ* hybridization and immunocytology assay.

The change in the optical properties of gold nanoparticles resulting from the plasmon-plasmon interaction between locally adjacent gold nanoparticles was demonstrated by Mirkin for the detection of polynucleotides. Mirkin *et al.* developed a gold nanoparticle-bioconjugate based colorimetric assay by attaching thiolated DNA to the nanoparticles. [94] When a complementary strand was introduced to the solution, a polymeric network was formed due to Watson Crick base pairing leading to reversible nanoparticle aggregation, with a concomitant colour change from red to blue. Owing to the sensitivity of SPR, the colorimetric assay used was able to detect 10 fm of a nucleotide, which is 50 times more sensitive than hybridization detection methods used for fluorescence detection. DNA-gold nanotechnology is now a well established area both in applied and fundamental studies. [95, 96]

Halas developed metal nanoshells, a type of nanoparticles consisting of silica-core gold-shell, which act as near IR absorbers. Their plasmon is tunable by controlling the thickness of core-shell materials.[97] Interesting about nanoshell nanoparticles is that they can be exploited to many applications by taking advantage of

their plasmonic properties. They have been used as heat delivery system. [98] The results for nanoshell NIR photothemal tumour therapy for the destruction of carcinoma cells has been demonstrated with success in vitro. In addition, they have been used to trigger drug systems photothemally when conjugated with specific biomolecules. [99]

The SPR of noble metal nanoparticles has the ability to amplify certain behaviour such as fluorescence [100] and Raman scattering.[101] A recent review by Kneipp, [18] highlighted the surface-enhanced Raman scattering in local optical fields of silver and gold nanoaggregates, from single-molecule Raman spectroscopy to ultrasensitive probing in live cells. Gold and silver nanoaggregates formed by individual nanoparticles of between 20 and 60 nm size have been shown to significantly enhance Raman scattering to the order of 10^{14}. [18]

Optical detection techniques are currently available allowing the ability to track and monitor molecular binding events, down to single-molecule experiments. The applications of plasmonic nanostructured materials in biotechnology are rapidly increasing. The ability to engineer stable, biocompatible nanostructured materials with specific biofunctionality will certainly harness these properties.

1.6 Strategies to meet objectives and chapters overview

To meet the objectives presented in section 1.1. Thioalkylated oligo (ethylene glycol) ligands were selected to stabilize the various types of gold and silver nanoparticles

Specific functional groups such as amines, azides and biotin were selected to allow the development of readily functionalized MPCs.

The attachment of biological recognition functionality of choice can then be introduced by three different methods;

i) Biotin-avidin-biotin system (BAB)

ii) Carbodiimide coupling (EDC)

iii) Click chemistry (Click)

As shown in Figure 7, a monohydroxy thioalkylated ligand was chosen to stabilize, solubilise and control the density of functionality to be introduced to the MPCs ligand shell. The plan is that the final product should minimize and overcome the challenges discussed above.

Figure 7 shows how this dissertation will be presented with respect to the work carried out in each chapter. In Chapter 2, ligand design strategies are discussed in detail, including some synthetic efforts that were carried out to prepare readily functionalized thioalkylated ligands.

In chapter 3, thioalkylated PEG ligands are used to stabilize gold and silver nanoparticles in aqueous environment. Size-selective hydrophilic gold and silver MPCs (2-60 nm) were prepared following and modifying common synthetic methods. This discusses key issues of MPCs solubility, stability and functionality. The stability of MPCs is discussed extensively, mainly for Ag-MPCs.

Chapter 4 is mainly devoted to demonstrating the versatility of this PEGylated system by introducing a non-biological recognition element, in this case calix[4]arene, to the MPCs ligand shell and demonstrating that the incorporated calix[4]arene retains its molecular recognition properties in water. The specific molecular recognition properties of calix[4]arene modified MPCs towards pyridinium cations on two substrates will be demonstrated. Rotaxanes and pseudorotaxanes based on Au-MPCs in non-aqueous solvents will also be presented.

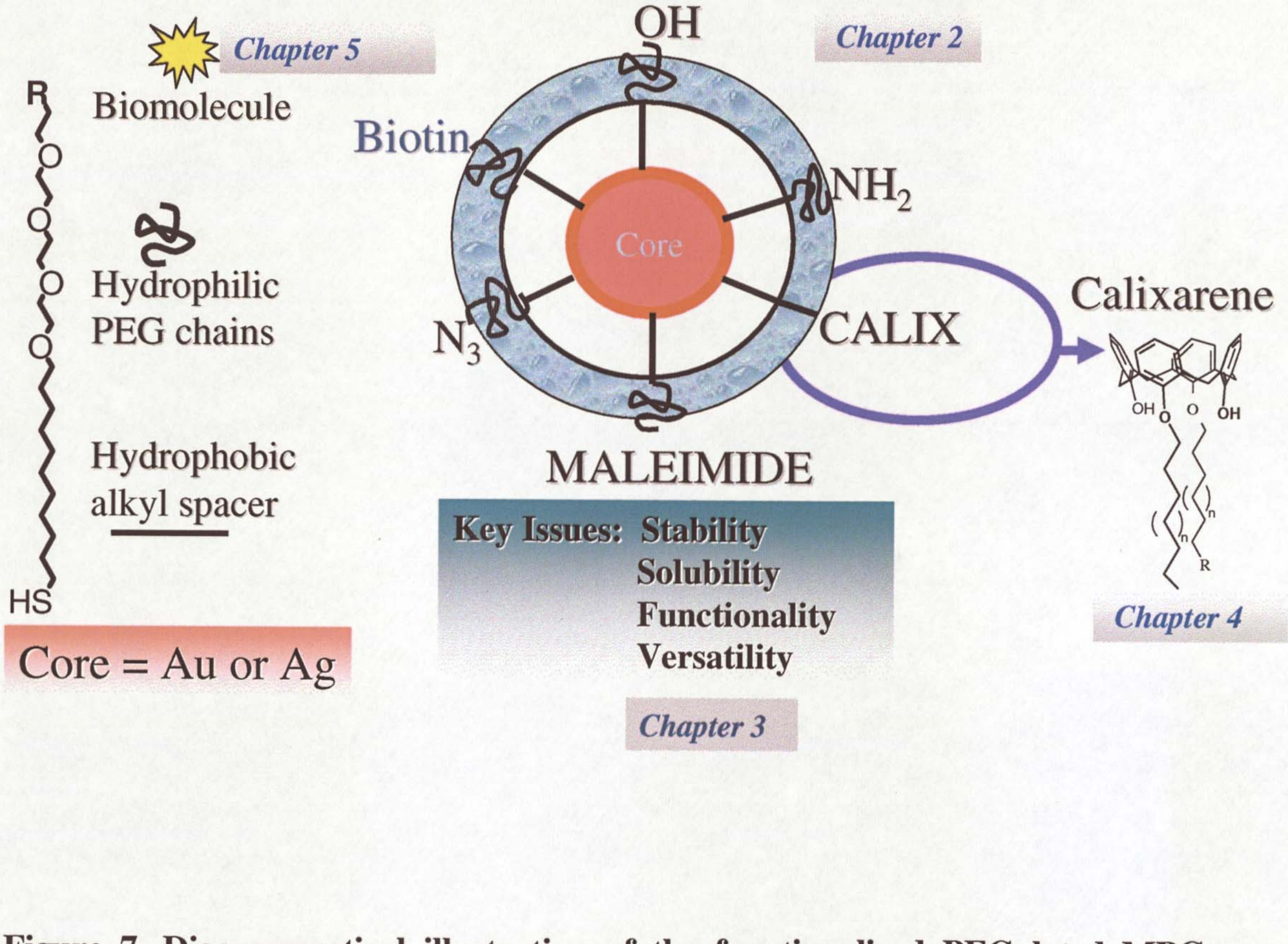

Figure 7. Diagrammatical illustration of the functionalized PEGylated MPCs, representing approaches that were followed to meet our target system illustrated in Figure 1. Milestones were met according to the work described in chapters 2-5.

In chapter 5 biomolecular functionalisation of MPCs is discussed in detail. Two strategies are discussed; the use of biotin-avidin-biotin (non-covalent interaction) and covalent approaches such as carbodiimide coupling and "click" chemistry.

Chapter 6 presents ongoing and future work evaluating applications of PEGylated gold and silver MPCs.

1.7 References

[1] Haes, A. M., Stuart, D. A., Nie, S and Duyne, R. P., *Journal of fluorescence*, 2004, 355

[2] Mulvaney, P., *Langmuir*, 1996, **12**, 788

[3] Pinchuk, A., von Plessen, G and Kreibig, U., *J. Phys. D. Appl. Phys.*, 2004, **37**, 3133

[4] Pinchuk, A., Kreibig, U and Hilger, A., *Surface Science*, 2004, **557**, 269

[5] Pinchuk, A and Kreibig, U., *New Journal of Physics*, 2005, **5**, 151

[6] Liz-Marzan, L. M and Mulvaney, P., *J. Phys. Chem. B.*, 2003, **107**, 7312

[7] Hilger, A., Cuppers, N., Tenfelde, M and Kreibig, U., *Eu. Phys. J. D.*, 2000, **115**, 10

[8] Kreibig, U., Bour, D., Hilger, A and Gartz, M., *Phys. Stat. Sol.*, 1999, **175**, 351

[9] Horisberger, M and Rosset, J., *The journal of Histochemistry & Cytochemistry*, 1997, **25**, 295

[10] Takizawa, T., *The journal of Histochemistry & Cytochemistry*, 1999, **47**, 569

[11] Thoolen, B., *The journal of Histochemistry & Cytochemistry*, 1990, **38**, 267

[12] Raschke, G., Kowarik, S., Franzl., Sonnichsen, C., Klar, T. A and Fieldmann, J., *Nano Lett.,* 2003, **3,** 935

[13] Hayat, M. A, Colloidal Gold: *Principles, Methods and Applications*, Academic Press, New york, 1989

[14] Pellengrino, T., Kudera, S., Liedl, T., Javier, A. M., Manna, L and Parak, W. J., *Small*, 2005, **1**, 48

[15] Rosi, N. L and Mirkin, C. A., *Chem. Rev.*, 2005, **105,** 1547

[16] Alivisatos, P., *Nature biotechnology*, 2004, **22**(1), 47

[17] Tkachenko, A. G., Xie, H., Coleman, D., Glomm, W., Ryan, J., Anderson, M. F., Franzen, S and Fieldheim, D. L., *J. Am. Chem. Soc.*, 2003, **125**, 4700

[18] Kneipp, K., Kneipp, H and Kneipp., *Accounts of Chemical Research*, 2006, ACS ASAP article

[19] Cao, Y. C., Jin, R., Nam, J., Thaxton, S and Mirkin, C. A., *J. Am. Chem. Soc.*, 2003, **125**, 14676

[20] Schultz, S., Smith, D. R., Mock, J. J and Schultz, D. A., *Proc. Natl. Acad. Sci*, 2000, **97**, 996

[21] Sugunan, A and Dutta, J., *Journal of Physics, Science and ideas*, 2004, **4**, 50 (http://www.thebritishmuseum.ac.uk/science/lycurguscup/sr-lycugus-pl.html)

[22] Frens, G., *Nature (London), Phys. Sci.*, 1973, **241**, 20

[23] Morris, R. H and Milligan, W. O., *Morphology of colloidal gold*, 1964, 3461

[24] Duff, D. D and Baiker, A., *Langmuir.*, 1993, **9**, 2301

[25] Brust, M., Bethell, D., Schriffrin, D. J. and Kiely, C. J., *Adv. Mater.*, 1995, **7**(9), 795

[26] Heath, J. R., Knobler, C. M and Leff, D. V., *J. Phys. Chem. B,* 1997, **101**, 189

[27] Korgel, B.A., Fullam, S., Connolly, S and Fitzmaurice, D., *J. Phys. Chem, B*, 1998, **102**, 8379

[28] Marie-Cristine, D and Astruct, D., *Chem. Rev.*, 2004, **104**, 293

[29] Templeton, A. C., Wuelfing, W.P and Murray, R. W., *Acc. Chem. Res.*, 2000, **33,** 27

[30] Brust, M., Walker, M., Bethel, D., Schiffrin, D. J and Whyman, R., *J. Chem. Soc. Chem. Commun.,* 1994, 801

[31] Esumi, K., Kameo, A., Suzuki, A., Torigoe, K., Yoshimura, T., Koide, Y and Shosenji, H, *Collioids and Surfaces A:, Physicochemical and Engineering Aspects*, 2001, **176**, 233

[32] Esumi, K., Kameo, A., Suzuki, A., Torigoe, K., Yoshimura, T., Koide, Y and Shosenji, H, *Collioids and Surfaces A:, Physicochemical and Engineering Aspects*, 2001, **189**, 155

[33] Xu, W., Liu, W., Zhang, D., Tongxin, Y. X and Zhu, D., *Collioids and Surfaces A:, Physicochemical and Engineering Aspects*, 2002, **204**, 201

[34] Johnson, S. R., Evans, S. D., Mahon, S. W and Ulman, A., *Supramolecular Science*, 1997, **4**, 329

[35] Yonezawa, T and Kunitake, T., *Collioids and Surfaces A: Physicochemical and Engineering Aspects*, 1999, **149**, 193

[36] Mayer, A.B.R and Mark, J. E., *Eur. Polym. J.*, 1998, **34**, 103

[37] Schmid, G and Perschel, S., *New J. Chem.*, 1998, **22**, 669

[38] Turkevich, J., *Gold Bull.*, 1985, **18**, 86

[39] Turkevich, J and Enustun, B. V., *J. Am. Chem. Soc.*, 1963, **85**, 3317

[40] Moiseev, I. I., Vargaftik, M.N., Chemysheva, T. V., Stromnova, T. A., Gekhman, A. E., Tsirkov, G. A., Makhlina, A. M., *J. Mol. Catal A*: *Chem*., 1996, **108**, 77

[41] Bonnemann, H., Brijoux, W., Brinkmann, R., Dinjus., Jouben, T and Korall, B., *Angew. Chem. Int. Ed.,* 1991, **30**, 1312

[42] Hirai, H., Nakan, Y and Toshima, M., *J. Macromol. Science. Chem*., 1978, **A12**, 1117

[43] Hirai, H., Nakan, Y and Toshima, M., *J. Macromol. Science. Chem*., 1979, **A13**, 727

[44] Hirai, H., *J. Macromol. Science. Chem*., 1978, **A13**, 633

[45] Tan, C. K., Newberry, V., Webb, T. R and McAuhffe, A. C., *J. Am. Chem, Soc*, *Dalton Trans*., 1987, 1299

[46] Kiwi, J and Cratzel, M., *J. Am. Chem. Soc*., 1979, **101**, 7214

[47] Aiken III, J. D and Finke, R.G., *Journal of Molecular Catalysis A*: *Chemical*, 1999, **145**, 1

[48] Roucoux, A., Schulz, J and Patin, H., *Chem. Rev.,* 2002, **102**, 3757

[49] Schmid, G., *Chem. Rev*., 1992, **92**, 1709

[50] Faraday, M., *Phil. Trans. Roy. Soc*., 1857, **147**, 145

[51] Schmid, G., Pfeil, R., Boese, R., Bandeman, F., Meyer, S., Calis, G. H. M and van der Felden, J. W. A., *Chem. Ber*., 1981, **114**, 3634

[52] Giersig, M and Mulvaney, P., *Langmuir*, 1993, **9**, 3408

[53] Love, J. C., Estroff, L. A., Kriebel, J. K., Nuzzo, R. G and Whitesides, G. M., *Chem., Rev.,* 2005, **105**, 1103

[54] Teo, B. K and Sloane, N. J. A., *Inorganic Chemistry,* 1985, **24**, 4545

[55] Watzky, M. A and Finke, R. G., *J. Am. Chem. Soc.,* 119, **103,** 10382

[56] Brust *et al*. unpublished observation

[57] Negishi, Y and Tsukuda, T., *J. Am. Chem. Soc.*, 2003, **125,** 4046

[58] Hostetler, M. J., Wingate, J. E., Zhong, C. J., Harries, J. E., Vachet, R. W., Clark, M. R., London, J. D., Green, S. J., Stokes, S. J., Wignal, G. D., Glish, G. L., Porter, M. D., Evans, N. D and Murray, R. W., *Langmuir*, 1998, **14**, 17

[59] Jimenez, V. L., Georganopoulou, D. G., White, R. J., Harper, A. S., Mills, A. J., Lee, D and Murray, R.W., *Langmuir,* 2004, **20**, 6864

[60] Schaaff, T. G., Shafigullin, M. N., Khoury, J.T., Vezmar, I., Whetten, R. L., Cullen, W., First, P.N., Gutierrez-Wing, C., Ascensio, J and Jose-Yacaman, M. J., *J. Phys. Chem*. **B**, 1997, **101**, 7885

[61] Alvarez, M. M., Khoury, J. T., Schaaff, T. G., Shafigullin, M. N., Vezmar, I. and Whetten, R. L., *Chem. Phys. Lett*. 1997, **266**, 91

[62] Brust, M., Fink, J., Bethel, D., Schiffrin, D. J and Kiely, C. J., *J. Chem. Soc., Chem. Commun,* 1995, 1655

[63] Bethel, D., Brust, M., Schiffrin, D. J and Kiely, C., *Journal of electroanalytical chemistry,* 1996, **409**, 137

[64] Waters, C. A., Mills, A. J., Johnson, K. A and Schiffrin, D. J., *Chem. Commun*., 2003, 540

[65] Tshikhudo, T. R., Demuru, D. Wang, Z., Brust, M., Secchi, A., Arduini, A and Pochini, A., *Angwew, Chem. Int. Ed.*, 2005, **44,** 2293

[66] Hostetler, M. J., Green, S. J., Stokes, J. J and Murray, R. W., *J. Am. Chem. Soc.*, 1996, **118**, 4212

[67] Ingram, R.S., Hostetler, M. J and Murray, R. W., *J. Am. Chem. Soc.*, 1997, **119**, 9175

[68] Heath, J. R., Brandt, L and Leff, D. V., *Langmuir*, 1996, **12,** 4723

[69] Gamez, S., Philippot, K., Collier, V., Chaudret, B., Senocq, F and Lecante, P., *Chem, Commun.*, 2000, 1945

[70] Bardaji, M., Uznaski, P., Amiens, C., Chaudret, B and Laguna, A., *Chem. Commun.*, 2000, 183

[71] Li, X. M., de Jong, M. R., Inoue, K., Shinkai, S., Huskens, J and Reinhoudt, D. N., *J. Mater. Chem.*, 2001, **11**, 1919

[72] Shelley, E. J., Ryan, D., Johnson, S. R., Couillard, M., Fitzmaurice, D., Nellist, P. D., Chen, Y., Palmer, R. E and Preece, J. A., *Langmuir*, 2002, **18**, 1791

[73] Hasan, M., Bethell, D and Brust, M., *J. Am. Chem. Soc.*, 2002, **124**, 1132

[74] Horswell, S. L., O'Neil, A and Schiffrin, D. J., *J. Phys. Chem. B.*, 2001, **105**, 941

[75] Hostetler, M. J., Templeton, A. C and Murray, R. W., *Langmuir*, 1999, **15**, 3782

[76] Templeton, A. C., Hostetler, M. J and Murray, R. W., *J. Am. Chem. Soc.*, 1998, **120**, 1906

[77] Templeton, A. C., Hostetler, M. J., Warmoth, E. K., Chen, S., Hartshorn, C. M., Krishnamurphy, V. M., Forbes, M. D. E and Murray, R. W., *J. Am. Chem. Soc.*, 1998, **120**, 4845

[78] Buining, P. A., Humbel, B. M., Philipse, A. P and Verkleij, A. J., *Langmuir*, 1997, **13,** 3921

[79] Watson, K. J., Zhu, J., Nguyen, S. T and Mirkin, C. A., *J. Am. Chem. Soc.*, 1999, **121**, 462

[80] Badia, A., Gao, W., Singh, S., Demers, L., Cuccia, L and Reven, L., *Langmuir*, 1996, **12**, 1262

[81] Badia, A., Demers, L., Dickinson, L., Morin, F. G., Lennox, R. B and Reven, L., *J. Am. Chem. Soc.*, 1997, **119**, 11104

[82] Gittins, D. I and Caruso, F., *Chemphyschem*, 2002, **3**, 110

[83] Song, Y., Huang, T and Murray, R. W., *J. Am. Chem. Soc.*, 2003, **125**, 11694

[84] Dunbar, B. S., *Two dimensional electrophoresis and Immunological techniques,* Plenum Press, New York, 1998

[85] Aubin, M. E., Morales, D. G., Hamad-Schifferli, K. *Nano Lett.*, 2005, **5**, 519

[86] Parak, W. J., Pellegrino, T., MIcheel, C. M., Gerion, D., Williams, A. C and Alivisatos, A. P., *Nano Lett.,* 2003, **3**, 33

[87] Zanchet, D., Micheel, C. M., Parak, W. J., Gerion, D and Alivisatos, A. P., *Nano Lett.,* 2001, **1**, 32

[88] Zanchet, D., Micheel, C. M., Parak, W. J., Gerion, D., Williams, S. C and Alivisatos, A. P., *J. Phys. Chem. B.*, 2002, **106**, 11758

[89] Ackerson, C. J., Sykes, M. T and Kornberg, R. G., *Proc. Natl. Acad. Sci.,* 2005, **102,** 13383

[90] Mirkin, C. A., *Inorg. Chem.*, 2000, **39**, 2258

[91] Wang, Z., Lee, J., Cossins, A. R and Brust, M., *Anal. Chem.*, 2005, **77,** 5770

[92] Zheng, J., Petty, J. T and Dickson, R. M., *J. Am. Chem. Soc*., 2003, **125**, 7780

[93] Hayat, M. A, Colloidal Gold: *Principles, Methods and Applications*, Academic Press, New york, 1989

[94] Taton, T. A., Mirkin, C. A and Letsinger, R. L., *Science,* 2000, **289**, 1757

[95] Niemeyer, C. M and Mirkin, C. A., *Nanobiotechnology,* Wiley-VCH, Weinheim, 2004

[96] Niemeyer, C. M., *Angew. Chem. Int. Ed*., *2001*, **113,** 4254

[97] Pham, T., Jackson, J. B., Halas, N. J and Lee, R., *Langmuir,* 2002, **18,** 4915

[98] Hirsh, L. R., Stafford, R. J., Bankson, J. A., Sershen, S. R., Rivera, B., Price, R. E., Hazle, J. D., Halas, N. J and West, J. L., *Proc. Natl. Acad. Sci*., 2003, **100,** 13549

[99] Hirsh, L. R., Stafford, R. J., Bankson, J. A., Sershen, S. R., Rivera, B., Price, R. E., Hazle, J. D., Halas, N. J and West, J. L., *Anal. Chem.,* 2003, **75**, 2377

[100] Zheng, J., Petty, J. T and Dickson, R. M, *J. Am. Chem. Soc*., 2003, **125**, 7780

[101] Jackson, J. B and Halas, N. J., *Proc. Natl. Acad. Sci.*, 2004, **101**, 17930

CHAPTER 2

FUNCTIONALISED THIOALKYLATED POLYETHYLENE GLYCOL (PEG) LIGANDS

2 Functionalised thioalkylated polyethylene glycol (PEG) ligands

This chapter describes the design and synthesis of functionalised thioalkylated polyethylene glycol ligands. They play the important role of imparting high stability, water solubility and functionality to metal nanoparticles. These properties are essential for the development of bio-molecularly functionalized particles discussed in chapter 5. The following sections will present the properties and applications of polyethylene glycol followed by the ligand design and synthesis.

2.1 Background

Polyethylene glycol (PEG) is a linear or branched polyether terminated with two hydroxyl groups and has the following general structure:

$$HO\text{-}(CH_2CH_2O)_n\text{-}CH_2CH_2\text{-}OH$$

This polymer has been widely used both in applied [1]a,b and fundamental research [2] and is commercially available in different molecular weights. It has been approved by the US Food and Drug Administration (FDA) agency to be used in food and cosmetics and it has been employed in pharmaceutical products that are administered by means of parenteral (not through digestive track), topical (applied to skin) and oral (mouth) routes. [1]a,b Particularly attractive in biological, biomedical and biopharmaceutical areas is that PEG has an excellent ability to resist non-specific adsorption of proteins and other macromolecules in its surroundings [4] and this is largely due to the fact that, in addition to its structural inertness, PEG chains are, conformationally flexible [5] and have high water-binding ability. [6] Generally, there are many properties of polyethylene glycol that make it a polymer of choice and ideally suited for many biological and pharmaceutical applications. These properties are summarized below prior to the review on the synthesis of PEG derivatives.

2.1.1 Properties of polyethylene glycol (PEG)

The properties of polyethylene glycol according to Roberts *et al* [7] and Li [8] are summarized below.

i. Forms complex with metal ions, large exclusion volume

ii. Insoluble in diethyl ether and hexane

iii. Soluble in water, methylene chloride and many organic solvents

iv. Forms two phase system with other aqueous solutions of other polymers

v. Solubilise other molecules and move molecules across cell membrane

vi. Reduce rate of clearance through kidney

vii. Weakly immunogenic, alter electro osmotic flow and pharmacokinetics

viii. Non toxic and approved by FAD for in *vivo* use

ix. Can be used to precipitate out proteins and nucleic acid

Due to these remarkable properties the literature is replete with the exploitation of polyethylene glycol in many areas that cannot all be covered here. However, the synthesis of relevant PEG derivatives plays a significant role in achieving successful PEGylation of nanoparticles and will be briefly discussed.

2.1.2 Polyethylene glycol derivatives

2.1.2.1 General concepts

The repeating ethylene oxide units of PEG (or PEG back bone) are inert in biological environments and under most reaction conditions. This makes the terminal hydroxyl groups amenable to chemical modifications without affecting the PEG units. The preparation of polyethylene glycol derivatives is usually carried out by anionic ring-opening polymerization of ethylene oxide induced by initiators [9],[10] such as potassium bis(trimethylsilyl)amide $[(CH_3)_3Si]_2NK$[11] to afford the desired derivatives such as amine functionalized PEG.[9] Generally, there are two approaches employed for the synthesis of PEG derivatives;

i) Converting the end hydroxyl group to introduce the desired functional group.

ii) Reacting bifunctional compounds with PEG under controlled conditions in such a way that one of its reactive groups reacts with PEG and the other remains active.

The resulting functionalised PEG moieties can be homofunctional (*e.g.* PEG with carboxylic acid groups at its terminals), heterobifunctional (*e.g.* PEG with carboxylic acid and amine groups at its terminals) and monofunctional (*e.g.* PEG with amine and methoxy groups at its terminals commonly known as mPEG derivatives). However, in order to fully understand the importance and reactivity of these PEG derivatives, which are often quoted as important derivatives for second-generation PEGylation, it is also important to introduce the so-called first generation chemistry. This will be discussed under the umbrella of PEGylation chemistry to include both the first-and second-generation chemistry of PEG.

2.1.2.2 Chemistry of PEGylation

PEGylation, means the attachment of PEG to a certain component for example a biomolecule, and the technology is widely used today. This is due to the fact that PEG is eminently suitable for use as covalent modifier of biological macromolecules and substrates as well as carrier of low molecular weight drugs. For detailed PEG-polypeptides conjugates and applications, reviews by Zalipsky [4] and Li and Kao [12] are particularly useful. The chemistry involved in peptides and protein PEGylation has been reviewed by Roberts [7] and is described here under first and second generation PEGylation.

2.1.2.2.1 First and second generation PEGylation

PEGylation technology was first realized in the 1970's by Davies who demonstrated that it is an effective means of providing protein protection during drug delivery.[13] This was attributed to the fact that PEG attached to a polypeptide alters many features of the polypeptide while maintaining its biological activities. First generation pegylation was concerned with the use of polyethylene glycol derivatives particularly mPEG derivatives for protein PEGylation through amine conjugation. Examples of first-generation PEG derivatives include;[7] i) PEG dichloroazine, ii) PEG-tresylate, iii) PEG succinimidyl carbonate,[14] iv) PEG succinimidyl succinate *etc.* Basically, many of these acylating PEG derivatives are used for conjugating the polymer to either the alpha or epsilon amino groups of lysine. In this case, peptides containing lysines are conjugated giving rise to different isomers with varied molecular masses and consequently making it difficult to reproduce and obtain reliable drug batches.

Many problems were encountered with the first generation strategies, including the formation of unstable linkages, side reactions and being restricted to mPEG and the use of low molecular weight drugs. In addition, the resulting PEG derivatives had high diol contamination which resulted in the cross-linking of proteins forming inactive aggregates.

These problems led to the establishment of the second generation of PEGylation reactions. The second generation PEGylation is generally regarded as the advancement of PEGylation chemistries employed in the first generation. For example, the problem of diol contamination of the early generation was improved by ion-exchange chromatographic techniques where by carboxylic acid PEG derivatives are purified prior to polypeptide attachment, and in this way about 97 % of diol impurity can be removed. The chemistry for amine conjugation was generally improved and a typical example in this case is the use of mPEG-propionaldehyde which is easier to prepare than mPEG-acetaldehyde analog which is susceptible to dimerisation via aldol condensation.[7]

Another change in the second generation PEGylation was the introduction of mPEG-derivatives for cysteine modification such as PEG-maleimide,[15] PEG-vinylsulfone *etc*, which are good derivatives providing site-specific peptide conjugation. It is generally obvious that PEGylation through the formation of stable bonds improves long-term storage half-life and the conjugates are easy to purify and handle, however, it is also possible that steric crowding of high molecular weight PEGs and the position of PEGylation can reduce the biological activities of certain proteins. To address these challenges, degradable linkages were incorporated between the PEG and the protein and hence allowed the protein to be released at the targeted site.[16] Of particular importance has been the use of heterobifunctional PEG ligands, thus PEG derivatives with dissimilar terminal groups.[17] These are generally special types of PEG derivatives which have also been used in a number of applications such as biosensors and immunoassays. They are very useful for the development of anchors to link macromolecules to surfaces[18] and for targeting of drugs, liposomes or viruses to specific tissues.

Some of the preferred heterobifunctional PEGs contain derivatives mentioned above, including NHS esters, maleimide, vinylsulfone, amines and carboxylic acids moieties. Owing to the remarkable applications of heterobifunctional PEGs, extensive work has been carried out (particularly via anionic polymerization route mentioned above) for the synthesis of simple and complex PEG derivatives containing amines,

esters, aldehydes, acids, vinyl groups *etc.*[19]-[23] As an example, Li and Kao [12] reported the synthesis of a library of 50 polyethylene glycol derivatives.

2.2 Applications of polyethylene glycol

2.2.1 PEGylation of peptides, drugs and surfaces

Polypeptides are important therapeutic agents.[24],[25] However, there are some limitations including poor solubility, short circulation half life, rapid clearance by kidney, a tendency to generate neutralising antibodies and susceptibility to destruction by proteolytic enzymes. PEG has been used to address these problems and examples of drugs attached to PEG are procaine, atropine, aspirin, amphetamine *etc.* [7] Another area where PEG has been extensively used is in modifying surfaces. Biomaterials have to be compatible with blood, plasma and proteins. PEG has received special attention in this area since it was found that it blocks the immunological recognition of proteins and has demonstrated the ability to suppress the binding of blood elements to surfaces to which it is attached. The properties of PEG make it a superior polymer for use as coating for arterial replacement, diagnostic apparatus, blood-contacting devices *etc.* Protein resistance ability of PEG is indeed the major contributing property.[26] Different surfaces, can be modified and made biocompatible with PEG.[27]

2.2.2 PEGylated gold nanoparticles

The use of metal and semiconductor nanoparticles as bio-labels due to their tunable optical properties is an area that is rapidly advancing. [28]-[30] Fundamental studies have been carried out to gain insight into the properties and means of fabrication of these materials. In Chapter 3 these properties will be discussed in detail for gold and silver including the methods which are used to prepare such materials. Considering the development of metal nanoparticles, monolayer protected clusters (MPCs) of gold and to a lesser extent silver are well established.

Basically, MPCs are defined by the stabilization of metallic clusters by a monolayer of ligands, particularly alkanethiols, which form a protective shell around the particles via a strong Au/Ag-S interaction. Due to their extreme stability and ease of preparation MPCs have been extensively studied and used both in applied and fundamental research such as in materials science (nanoelectronics, thin films, decorative coatings *etc*) and biological sciences (microscopy labels *etc*). Generally, Au/Ag MPCs are prepared by a two-phase liquid/liquid synthesis[31]-[33] and they have been found amenable to thiol exchange reactions[31] and hence these properties accelerated the exploitation of MPCs in different areas. Nevertheless, most of these materials are not water soluble. This is, however, a prerequisite for biological applications.

In order to render MPCs water soluble successful attempts have been made recently to stabilize them by thiolated polyethylene glycol. Wuelfing *et al.*[34] used thiolated methoxy PEG (Mw ~ 5000) to produce water soluble gold MPCs. These particles exhibited excellent water solubility and stability but could not undergo thiol exchange reactions. Foos *et al.*[35] synthesised water soluble gold MPCs prepared by a two-phase system[31] using short HS-$(CH_2CH_2O)_n$-CH_3 (n = 2-4) thiolated methoxy PEG that underwent thiol-exchange reaction and the same ligand was used by Zheng *et al.*[36] for the preparation of gold nanoparticles in a methanol/water ratios. In 2002, a new ligand was introduced; monohydroxy thioalkylated tetraethylene glycol, which was used for the stabilisation of 2-4 and 5-8 nm gold nanoparticles in aqueous solution providing MPCs of excellent stability and water solubility.[36]

Otsuka *et al.*[38] made further advances by preparing functionalised gold nanoparticles covered with bifunctionalised PEG (acetal-PEG-SH) based on anionic ring opening polymerisation of ethylene oxide to demonstrate "quantitative and reversible lectin-induced association of gold nanoparticles." They also noted that PEGylation of gold nanoparticles with readily functionalized PEG ligands will expand the traditional use of gold nanoparticles particularly their exploitation in diverse technologies including bioassay and bio-recognition.

In order to explore the usefulness of PEGylation technology taking advantage of stabilizing metal nanoparticles with alkanethiolated ligands we were prompted to design a ligand system that will address not only fundamental questions but provides a unique platform for the exploitation of MPCs in diverse biological and pharmaceutical areas. The design criteria that have been followed are outlined in the following section.

2.3 Ligand design

The ligand design strategy that was followed is outlined in Figure 1. Basically, the primary aim has been to develop a functionalized thioalkylated PEG ligand system for use in the manufacturing of readily functionalized gold nanoparticles.

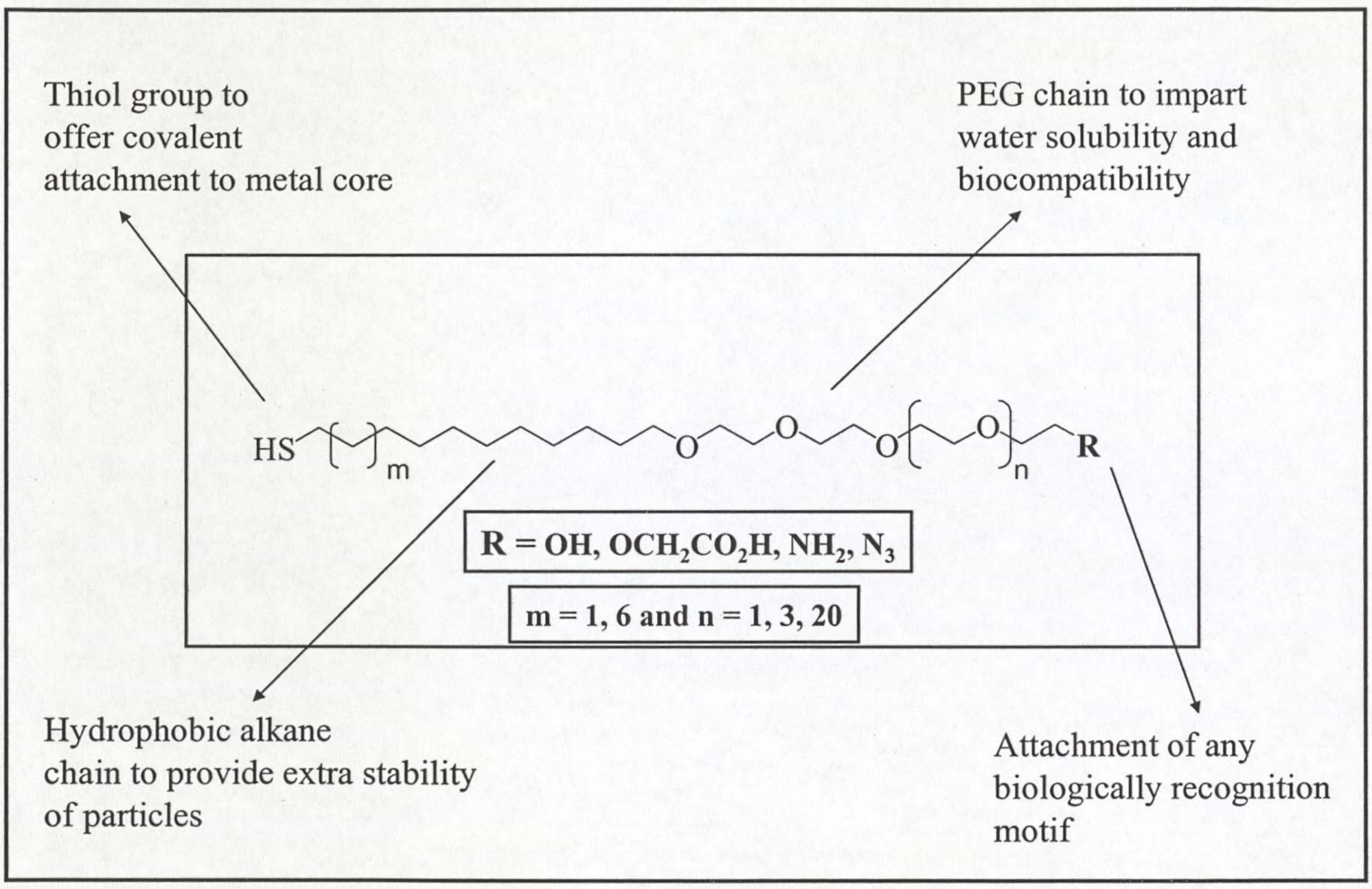

Figure 1. Structural representation of ligand design.

This design permits the stabilization of either Au or Ag nanoparticles by thiolate-ligands which form a protective shell around the particles. The alkyl spacer length is chosen to enhance the stability due to the lateral van der Waals attractions between hydrocarbon chains, which also suggests that the longer the hydrocarbon chain the greater the stability. The oligoethylene glycol segment is selected to make particles water soluble and, of particular importance, to make them compatible with biological conditions. Based on the PEGylation chemistry stated above, the ligand has been designed to contain specific functional groups such as carboxylic acid and amines which are versatile functionalities allowing the development of stable Au/Ag-bioconjugates.

Generally, the design combines the excellent stability offered by the conventional thioalkylated MPCs and solubility imparted by PEG chains (to satisfy physiological conditions) while functionalisation meets the requirements for biological and pharmaceutical applications.

2.4 Ligand Synthesis (Experimental Part)

2.4.1 Materials

Unless specified otherwise, chemicals and solvents were purchased from Sigma-Aldrich, UK and used as received. Flash chromatography was used for purification using standard flash grade silica gel, while thin layer chromatography (TLC) was carried out on silica gel plates (SiO_2, MN ALUGRAM® SIL G/UV_{254}). ^1H and ^{13}C NMR spectra were recorded on a Bruker 400 MRX NMR spectrometer and chemical shifts are quoted relative to the solvent peaks as δ values in ppm.

2.4.2 Synthesis

Thioalkylated PEG ligands illustrated in Figure 1 were either purchased or prepared. The following ligands were obtained from Dr F. S. Kamounah at Copenhagen University (Denmark) thus; monohydroxy thioalkylated PEG ligand (m = 6 and n = 3) (**3b**) and carboxylated thioalkylated PEG ligand (m = 1 and n = 20), (**6c**) while the following ligand was purchased from Prochimia Ltd (Poland) thus; carboxylated thioalkylated PEG ligand (m = 1 and n = 3). (**6b**).

Three target ligands prepared were; monohydroxy (1-mercaptoundec-11yl) tetraethylene glycol (m = 1 and n =1) (later denoted as PEG-OH **3a**), carboxylated thioalkylated PEG ligand (m = 1 and n =1), (PEG-COOH **6a**) and amine functionalized thioalkylated PEG ligand (m = 1 and n =1) (PEG-NH_2.**10**). For a complete structural identification of all these ligands see chapter 3 experimental section, page 104.

Table 1 presents the yields obtained for all the precursors and the target ligands prepared in this study.

	Ligands	Yield [a]/ %	Reference page
Precursor	**1**	75	45
Precursor	**2**	88	47
Target ligand	**3a**	80	47 (scheme pg 46)
Precursor	**4**	90	48
Precursor	**5**	42	49
Target ligand	**6a**	18	50 (Scheme pg 49)
Precursor	**7**	88	51
Precursor	**8**	76	52
Precursor	**9**	70	53
Target ligand	**10**	72	53 (Scheme pg 52)

Table 1. Summary of the yields obtained for all the precursors synthesized leading to the corresponding target ligands 3a, 6a and 10. [[a] Based on pure product obtained from flash chromatography].

2.4.2.1 Synthesis of monohydroxy (1-mercaptoundec-11yl) tetraethylene glycol (PEG-OH 3a) target ligand[39]

2.4.2.1.1 Synthesis of precursor 1

A schematic illustration of the synthesis of monohydroxy (1-mercaptoundec-11yl) tetraethylene glycol (PEG-OH) is shown in Figure 2. An approach for the synthesis of oligo(ethylene glycol)-terminated alkane thiols of this type was first reported by Pale-Grosdemange. *et al.*[39] In our laboratory, alkene terminated monohydroxy PEG **1** was prepared as follows; A solution of 50 % aqueous sodium hydroxide (0.34g, 8.6 mmol) was added while stirring to a solution of tetra ethylene glycol (15 ml, 86.9 mmol) under argon. The reaction mixture was stirred for 30 min in an oil bath at 100 ^{0}C. An equivalent amount of 11-bromoundec-1-ene (1.87 ml, 8.6 mmol) was then added and the reaction mixture was further heated under reflux for 24 h. Then the reaction mixture was cooled to room temperature and extracted seven times with hexane. The hexane extracts were concentrated under reduced pressure by rotary evaporation to give a light yellow oil. Purification of the crude oil by flash chromatography on silica gel (eluent: ethyl acetate) afforded compound **1** in good yield (75 %) as a light yellow oil.

^{1}H NMR ($CDCl_3$; 400 MHz, ppm): 1.28 (br s, 12H), 1.56 (qui, 2H, J = 7 Hz), 1.89 (br s, 1H), 2.03 (q, 2H, J = 6.7 Hz), 3.44 (t, 2H, J = 6.80 Hz), 3.58-3.67 (m, 16H), 4.90-5.01 (m, 2H), 5.80-5.82 (m, 1H).

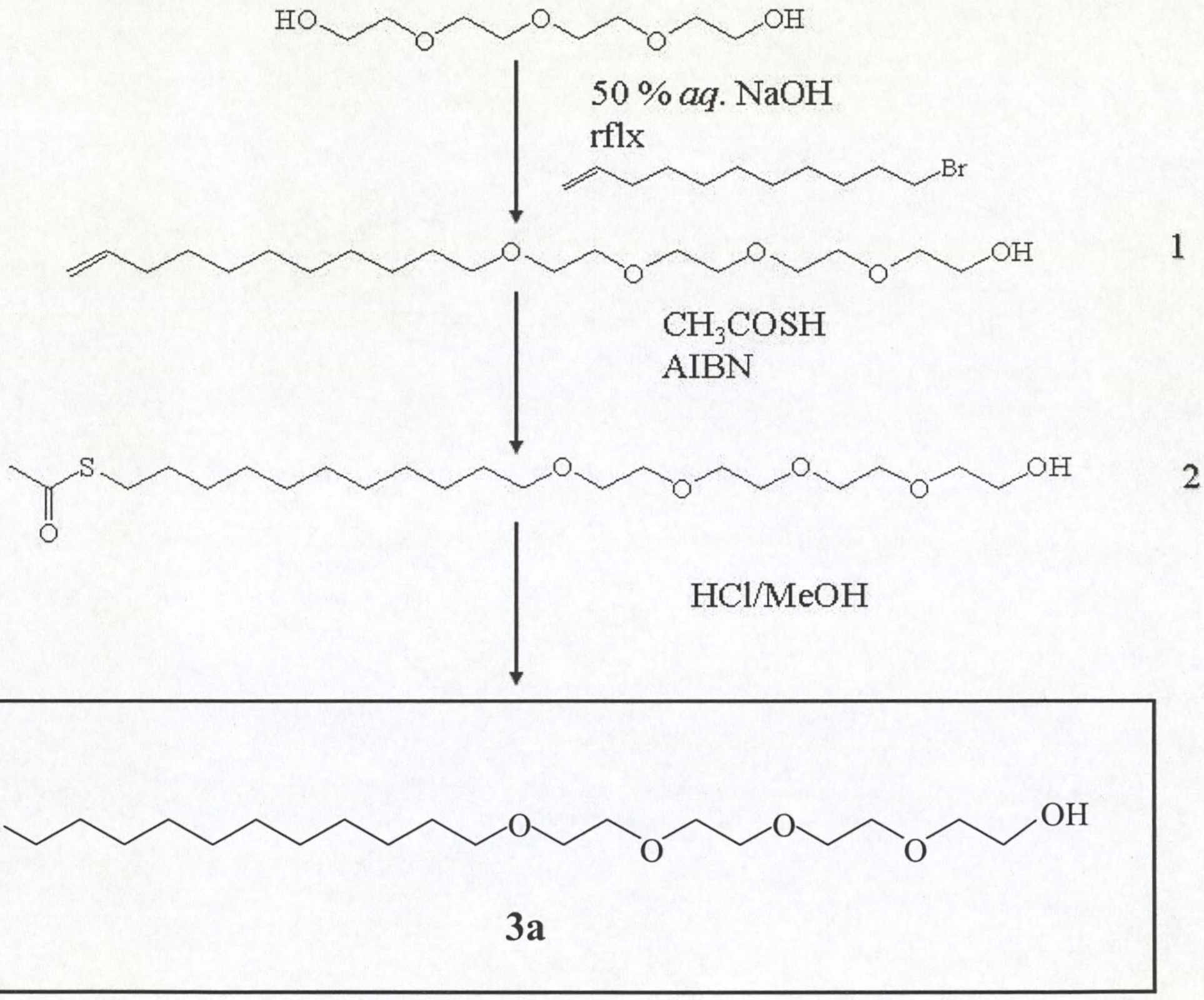

Figure 2. Synthetic scheme for the preparation of monohydroxy (1-mercaptoundec-11yl) tetraethylene glycol (PEG-OH 3a).

2.4.2.1.2 Synthesis of precursor 2

To the stirred solution of compound **1** (1.7 g, 4.9 mmol) in dry methanol (5 ml) was added a catalytic amount of azobis (isobutyronitrile) (AIBN) (51 mg, 0.3 mmol) and the mixture was purged with argon for 30 min at room temperature. Then thiol acetic acid (1.6 g, 21mmol) was added and the reaction mixture was heated under reflux for 6h under nitrogen. After 6h, the mixture was cooled to room temperature and the crude product was concentrated under reduced pressure and worked up by flash chromatography [elution: (hexane: ethyl acetate) (1:1)] to give thioacetate PEG (**2**) in 88 % yield as an oil.

^{1}H NMR ($CDCl_3$; 400 MHz, ppm): 1.25 (br s, 14 H), 1.56 (m, 4H), 2.31 (s, 3H), 2.62 (br s, 1H), 2.86 (t, 2H, J = 7.4 Hz), 3.44 (t, 2H, *J* = 6.78 Hz), 3.56-3.71 (m, 16H).

2.4.2.1.3 Synthesis of target ligand 3

Thioacetate **2** (0.9 g, 2 mmol) was dissolved in 0.1M HCl in MeOH (45 ml) and refluxed for 6 hrs under nitrogen. Then, the mixture was concentrated *in vacuo* and the crude product was purified by flash chromatography [elution: ethyl acetate] to yield 80% of the target ligand **3a**, as a colourless oil.

^{1}H NMR ($CDCl_3$; 400 MHz, ppm): 1.26-1.32 (br s, 15 H), 1.56 (m, 4H), 2.56 (q, br-baseline, 3H, *J* = 7Hz), 3.44(t, 2H, *J* = 6.80), 3.57-3.68 (m, 16H). **^{13}C NMR** ($CDCl_3$, 100 MHz, ppm): 24.65, 26.11, 28.39, 29.08, 29.48, 29.51, 29.57, 29.66, 34.06, 61.84, 70.10, 70.45, 70.64, 70.66, 70.69, 71.57, 72.54.

2.4.2.2 Synthesis of carboxylated thioalkylated PEG ligand (PEG-COOH 6a) target ligand (scheme in Figure 3)

2.4.2.2.1 Synthesis of precursor 4

Sodium hydride (1.38 g, 58 mmol, 60 % dispersion in oil) in dry THF (5 ml) was placed in three-necked flask under argon atmosphere and subsequently compound **1** (2 g, 5.8 mmol) was added and the reaction mixture was stirred at room temperature for 5 hrs. Ethyl bromoacetate (9.6 g, 57mmol) was added dropwise to this mixture (over 1 min) and stirred at room temperature for 60 hrs. The resulting crude product was extracted with hexane and hexane extracts (2 x 15 ml) were combined and concentrated under reduced pressure to give crude yellow oil. Work up by flash chromatography [elution: (ethyl acetate: hexane) (7:3)] afforded compound **4** as a light yellow oil (90 % yield).

^{1}H NMR ($CDCl_3$; 400 MHz, ppm): 1.25-1.28 (m, 15H), 1.37 (m, 2H), 2.04 (q, 2H, J= 6.0Hz), 3.45 (t, 2H, J = 6.70 Hz), 3.58-3.67 (m, 16H), 4.15 (q, 2H, J = 7Hz), 4.16 (s, 2H), 4.90-5.01 (m, 2H), 5.80-5.82 (m, 1H). **^{13}C NMR** ($CDCl_3$, 100 MHz, ppm): 14.46, 26.11, 28.95, 29.14, 29.45, 29.49, 29.55, 29.66, 33.81, 60.76, 61.55, 68.39, 70.10, 70.66, 71.04, 71.57, 114.11, 139.23, 169.95.

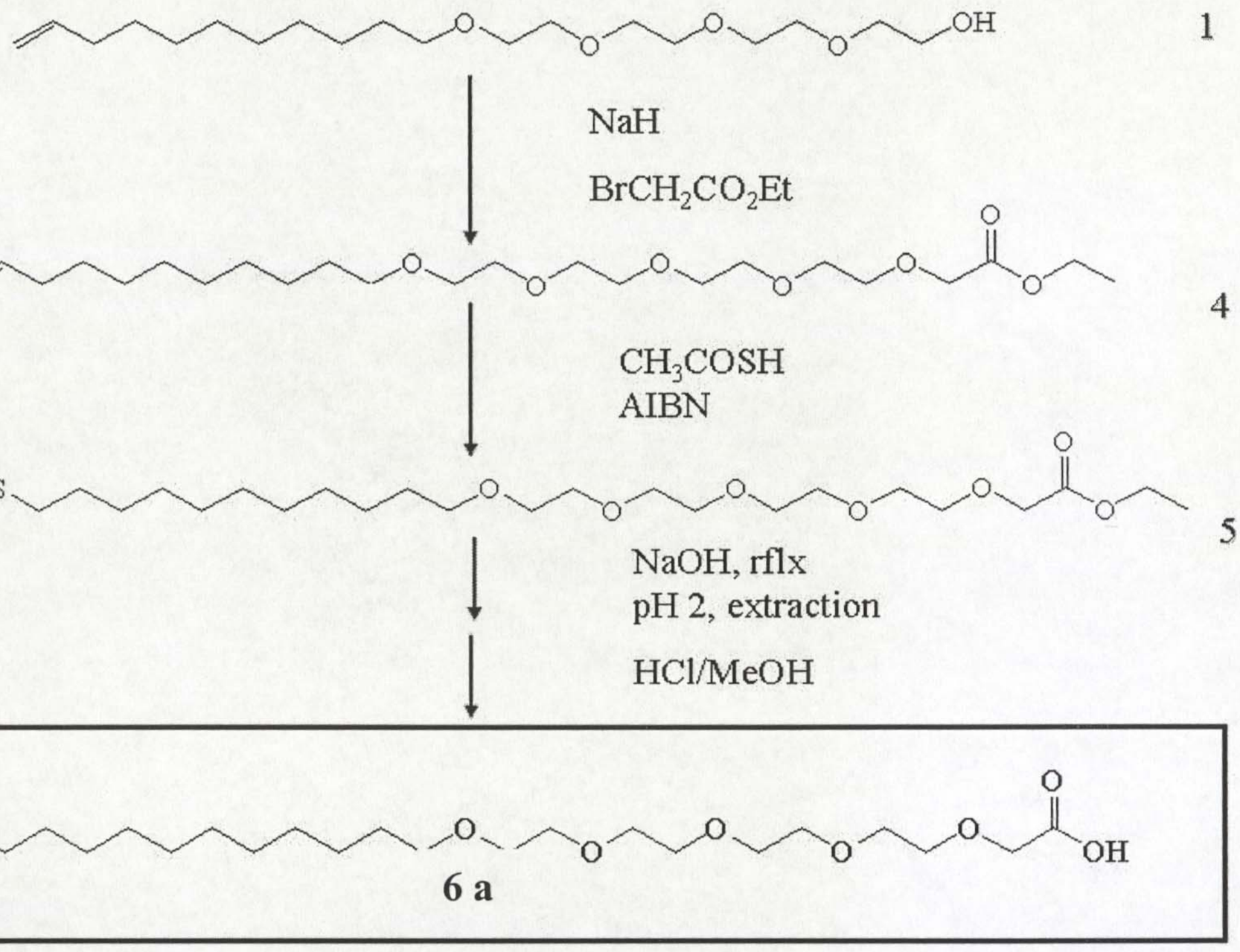

Figure 3. Synthetic scheme for the preparation of carboxylated thioalkylated PEG ligand (PEG-COOH 6)

2.4.2.2.2 Synthesis of precursor 5

To a stirred solution of compound **4** (0.7g, 1.6 mmol) in dry methanol (5 ml) was added a catalytic amount of azobis (isobutyronitrile) (AIBN) (21 mg, 0.12 mmol) and the mixture was purged with argon for 30 min at room temperature. Then, thiol acetic acid (1.6g, 21 mmol) was added and the reaction mixture was refluxed for 6h under nitrogen. Completeness of the reaction was followed by monitoring the disappearance of vinylic protons at 4.90 and 5.80 ppm from the ^{1}H NMR. After 6h, the reaction was cooled to room temperature and the crude product was concentrated under reduced pressure and work up on flash chromatography [elution: (hexane: ethyl acetate) (1:1)] to yield 42% of a thioacetate PEG (**5**).

^{1}H NMR ($CDCl_3$; 400 MHz, ppm): 1.25-1.28 (m, 15H), 1.57 (m, 2H), 2.32 (s, 3H), 2.86 (t, 2H, J = 6.70 Hz), 3.45(t, 2H, J = 6.0), 3.57-3.69 (m, 16 H), 4.15 (q, 2H, J = 7Hz), 4.16 (s, 2H).

2.4.2.2.3 Synthesis of target ligand 6

Hydrolysis and acid methanolysis of thioacetate ester **5** was carried out in situ, thus fresh aqueous 1M NaOH (20 ml) was added to compound **5** (0.4g, 0.7 mmol) and the mixture was stirred for 2hrs and cooled to room temperature. The solution was acidified to a pH 2 with 1M HCl and extracted with chloroform (2 x 30 ml). The organic extract was dried over sodium sulfate and then concentrated *in vacuo*. Subsequently, 0.1M HCl in MeOH (50 ml) was added and the mixture was refluxed for 7hrs under argon. Concentration of the reaction mixture by rotary evaporation was followed by work up by flash chromatography (pure ethyl acetate), however purification of the resulting products was found challenging. An alternative approach described by Rotello's group[40] was also followed, however, in both approaches the yield for compound **6a** was disappointingly low, < 20 %. Unless otherwise stated, an alternative ligand (hexaethylene glycol spacer) was used either obtained from Dr F. S. Kamounah of Copenhagen University (Denmark), or purchased from Prochimia Ltd (Poland).

^{1}H NMR ($CDCl_3$; 400 MHz, ppm): 1.27-1.43 (m, 14H), 1.57 (m, 2H), 1.67 (m, 2H), 2.67 (t, 2H, J = 6.7 Hz), 3.50 (t, 2H, J = 6.0), 3.57-3.69 (m, 16 H), 4.15 (s, 2H).

2.4.2.3 Synthesis of amine functionalized thioalkylated PEG (PEG-NH_2 11) target ligand [41]

2.4.2.3.1 Synthesis of precursor 7

A schematic illustration of the synthesis of PEG-NH_2 is shown in Figure 4 and synthesis of the compound **7** was carried out as follows;- to a solution of alcohol **1** (14.0g, 40 mmol) in chloroform (100 ml) under argon atmosphere was added an equimolar ratio 6ml of triethyl amine (Et_3N) (4.4 g, 43 mmol) and para-toluenesulfonyl chloride (*p*-TsCl) (8.0 g, 42.0 mmol) plus a catalytic amount of 4-dimethylaminopyridine (DMAP) and the reaction was stirred for 2 hrs. After two hrs, volatiles were rotary evaporated and the crude product extracted with hexane. Hexane extracts were concentrated *in vacuo*, to give a colourless crude oil which was purified by flash chromatography [elution: (hexane: ethyl acetate) (1:1)] to obtain compound **7** as clear oil (88 % yield).

^{1}H NMR ($CDCl_3$; 400 MHz, ppm): 1.26 (br s, 12H), 1.57 (qui, 2H, J = 7Hz), 2.04 (q, 2H, J = 7.6Hz), 2.44 (s, 3H), 3.44 (t, 2H, J = 6.79 Hz), 3.56-3.69 (m, 14H), 4.16 (t, 2H, J = 4.97 Hz), 4.94-5.01 (m, 2H), 5.78-5.82 (m, 1H), 7.33 (d, 2H, J = 8.01), 7.81 (d, 2H, J = 8.24). **^{13}C NMR** ($CDCl_3$, 75 MHz, ppm): 21.98, 26.46, 29.30, 29.49, 29.80, 29.84, 29.90, 30.02, 34.16, 69.08, 69.59, 70.45, 70.93, 70.98, 71.03, 71.16, 71.96, 114.47, 128.36, 130.17, 133.55, 139.59, 145.11.

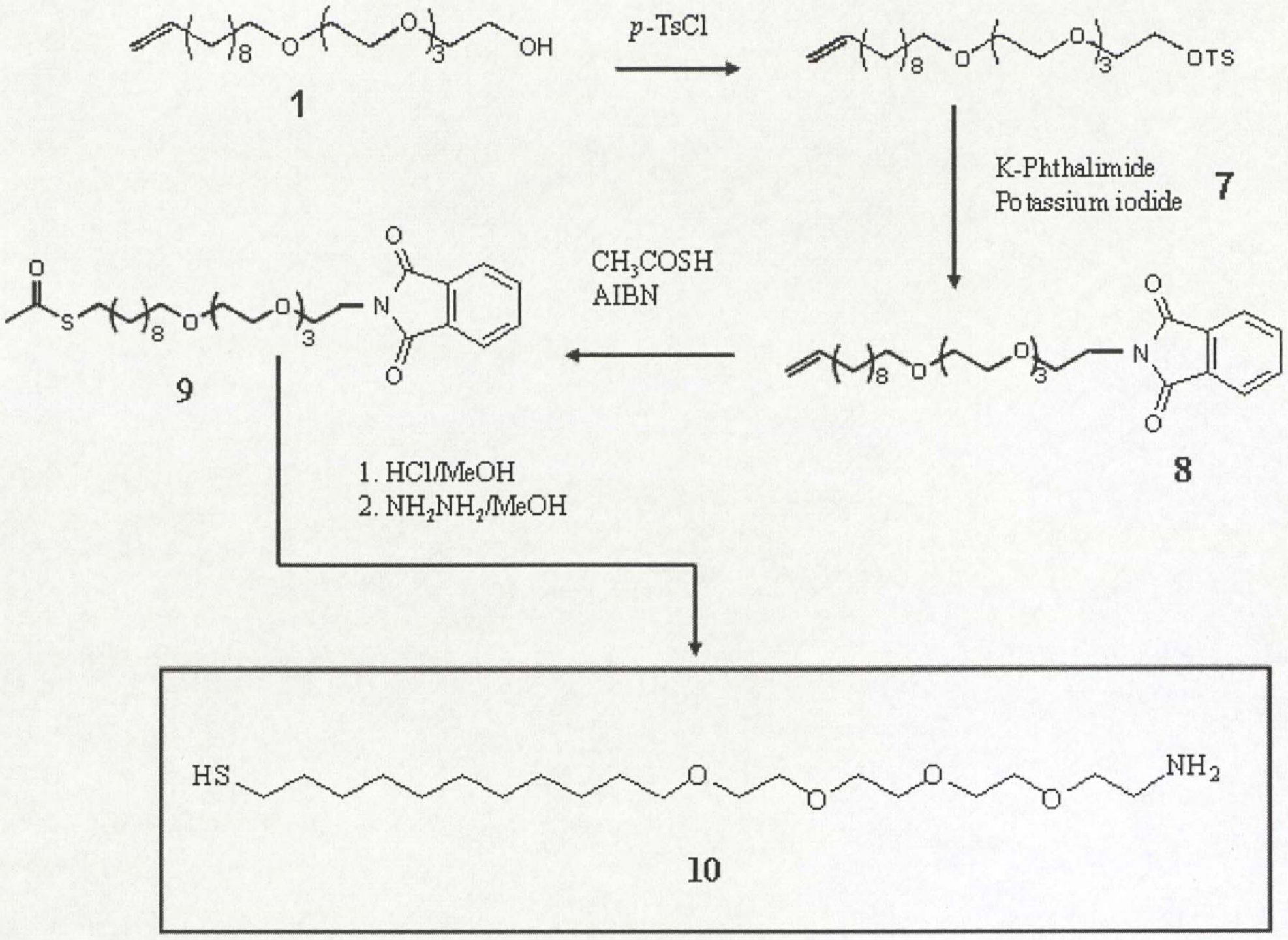

Figure 4. Synthetic scheme for the preparation of amine functionalized thioalkylated PEG (PEG-NH_2 10). [41]

2.4.2.3.2 Synthesis of precursor 8

The tosylated PEG terminated alkene **7** was converted to the phthalimide terminated derivative by adding potassium phthalimide (2.5 g, 13 mmol) and potassium iodide (1.0g, 6mmol) to a stirred solution of alkene terminated tosylated PEG **7** (2.5g, 5mmol) in dry THF (45 ml) under argon. The reaction mixture was then refluxed for 6hrs and allowed to cool to room temperature. The crude product was extracted with dichloromethane and dried over sodium sulfate and then concentrated in *vacuo*. The residual material was chromatographed [flash chromatography on silica gel: elution with ethylacetate] to obtain compound **8** as light oil in 76 % yield.

^{1}H NMR ($CDCl_3$; 400 MHz, ppm): 1.28 (br s, 12 H), 1.55 (qui, 2H, *J* = 7 Hz), 2.03 (q, 2H, *J* =7.6 Hz), 3.43 (t, 2H, *J* = 6.79 Hz), 3.55-3.72 (m, 14H), 3.90 (t, 2H, *J* = 4.97 Hz), 4.85-5.00 (m, 2H), 5.75-5.90 (m, 1H), 7.68, 7.82 (dd each, ArH (4H), *J* = 5.53, 8.49). **^{13}C NMR** ($CDCl_3$, 75 MHz, ppm): 14.46, 23.01, 26.46, 29.31, 29.49, 29.80, 29.84, 29.90, 30.03, 31.95, 34.16, 37.71, 68.30, 70.44, 70.54, 70.78, 70.96, 71.00, 71.03, 71.90, 114.46, 123.59, 132.69, 134.25, 139.58, 168.58.

2.4.2.3.3 Synthesis of precursor 9

Thiolacetic acid (5ml, 40 mmol) was added to the solution of alkene terminated phthalimide PEG **8** (3.2g, 6mmol) in dry MeOH (90 ml) and the mixture was purged with argon for 30 min at room temperature, Then, a catalytic amount of AIBN was added and the reaction mixture was refluxed for 6 hrs under N_2. After cooling to room temperature the resulting solution was concentrated in *vacuo* and then purified by flash chromatography to obtain 70 % of compound **9** as light yellow oil.

^{1}H NMR ($CDCl_3$; 400 MHz, ppm): 1.25 (br s, 14 H), 1.56 (m, 4H,), 2.31 (s, 3H), 2.85 (t, 2H, J = 7.4), 3.44 (t, 2H, *J* = 6.80 Hz), 3.53-3.78 (m, 14H), 3.90 (t, 2H, *J* = 6.0 Hz), 7.68, 7.82 (dd each, ArH (4H), *J* = 8.50, 8.48).

2.4.2.3.4 Synthesis of target ligand 10

To obtain the target ligand **10**, the thioacetate moiety of compound **9** was first hydrolysed by concentrated HCl in methanol under reflux followed by hydrolyzing the phthalimide part with hydrazine *in situ* under inert argon environment. Briefly, a mixture of compound **9** (2g, 3.5 mmol) and concentrated HCl (4 ml) in MeOH (90 ml) was stirred vigorously at room temperature for 20 min and then refluxed for 6 hrs. Then the mixture was cooled to room temperature, and a 5 ml of hydrazine hydrate (5.1 g, 103 mmol) was added. The reaction mixture was then refluxed for 3hrs under argon and then cooled to room temperature. The mixture was filtered and the filtrate was concentrated in *vacuo* prior to extraction with chloform (3 x 30 ml) and dried over anhydrous $MgSO_4$ to obtain the crude product which was purified by flash chromatography [silica gel: elution 10 % MeOH/3 % Et_3N, ethylacetate] to give

compound **10** as a light yellowish product in 72 % yield.

^{1}H NMR ($CDCl_3$; 400 MHz, ppm): 1.27 (br s, 14 H), 1.55 (m, 2H), 1.62 (m, 2H), 2.68 (t, 2H, J = 7.2), 2.87 (t, 2H, J = 5.4), 2.90 (t, 2H, J = 7.2), 3.43 – 3.74 (m, 14 H).
^{13}C NMR ($CDCl_3$, 75 MHz, ppm): 26.48, 27.16, 28.93, 29.63, 29.87, 29.99, 30.04, 39.62, 42.19, 70.47, 70.74, 70.98, 71.02, 71.94, 73.69.

2.5 References

[1] a) Qiu, B., Stefanos, S., Ma, J., Laloo, A., Perry, B. A., Leibowitz, M. J., Sinko, P. J and Stein, S., *Biomaterials*, 2003, **24**, 11. b) Novel methods for Site-directed Drug delivery. http://drugdeliverytech.com/cgi-bin/articles.cgi?idArticle=111 (13/06/2003)

[2] Novikova, L. N., Novikov, L. N and Kellerth, J., *Current Opinion in Neurology,* 2003, **16**, 711

[3] a) Minato, S., Iwanaga, K., Kakami, M., Yamashita, S and Oku, N., *Journal of controlled release,* 2003, **89,** 189. b) Borgens, R. B., Shi, R and Bohnert, D., *The journal of experimental biology*, 2002, **205**, 1

[4] Zalipsky, S., *Advanced Drug Delivery Reviews*, 1995, **16**, 157

[5] Torchilini, V. P and Trubetskoy, V. S., *Advanced Drug Delivery Reviews*, 1995, **16**, 141

[6] Kim, I., Jang, M. D., Ryu, Y. K., Cho, E. H., Lee, Y. K and Park, J. H., *Analytical Sciences,* 2002, **18**, 1357

[7] Roberts, M. J., Bently, M. D and Harris, J. M., *Advanced Drud Delivery Reviews*, 2002, **54**, 459

[8] Li, J., *BME*, 2001, 430

[9] Yamamoto, Y., Nakao, W., Atago, Y., Ito, K and Yagci, Y., *European Polymer Journal*, 2003, **39**, 545

[10] Akiyama, Y., Otsuka, K., Nagasaki, Y., Kato, M and Kataoka, M, *Bioconjugate. Chem*., 2000, **947**, 234

[11] Yokoyama, M., Okano, T and Yasuhisa, S., *Bioconjugate Chem*., 1992, **3**, 275.

[12] Li, J and Kao, W. J., *Biomacromolecules*, 2003, **252,** 3582

[13] Abuchowki A, McCoy, J. R., Palczuk, N. C., Es, T and Davies, F. F., *The Journal of Biological Chemistry,* 1977, **252,** 3582

[14] Miron, T and Wilchek, M., *Bioconjugate Chem.,* 1993, **4,** 568

[15] Manjula, B. N., Tsai, A., Upadhya, R., Perumalsamy, Smith, P. K, Malavalli, A., Vanderiff, K., Winslow, R. M., Intaglieta, M., Prabhakaran, M., Friedman, J. M and Archarya, A. S., *Bioconjugate Chem.,* 2003, **14**, 46

[16] Olivier, J., Huertas, R., Lee, H. J., Calon, F and Pardridge, W. M, *Pharmaceutical Research,* 2002, **19**, 1137

[17] Svedhem, S., Hollander, C., Shi, J., Konradsson, P., Liedberg, B and Svensson, S.C.T., *J. Org. Chem.,* 2001, **66**, 4494

[18] Yang, Z., Galloway, J. A and Yu, H., *Langmuir,* 1999, **15,** 8405

[19] Sagara, K and Kim, S. W., *Journal of Controlled Released*, 2002, **79**, 271

[20] Yanic, C., Bredenkamp, M. W., Jacobs, E.P and Swart, P., *Bioorganic & Medical Chemistry Letters*, 2003, **13**, 138

[21] Garrett, S.W., Davies, O.R., Milroy, D. A., Wood, P. J., Pouton, C. W and Threadgill, M. D., *Bioorganic & Medicinal Chemistry*, 2000, **8**, 1779

[22] Plaisance, C. B., Jean, M and Lux, F., *European Polymer Journal*, 2003, **39**, 863

[23] Yuan, M and Deng, X., *European Polymer Journal*, 2001, **37**, 1907

[24] Harris, J. M and Chess, R. B., *Nature Reviews Drug Discovery,* 2003, **2**, 214

[25] Goodson, R. J and Katre, N. V., *Biotechnology,* 1990, **8**, 343

[26] Prime, K. L and Whitesides, G. M., *J. Am. Chem. Soc.*, 1993, **115,** 10714

[27] Choi, J. H., Choi, J. S., Suh, H and Park, J. S., *Bull. Korean, Chem. Soc*., 2001, **22**, 47

[28] Henglein, A., *Chem. Rev*., 1989, **89**, 1861

[29] Rechberger, W., Hohenau, A., Leitner, A., Krenn, J. R., Lamprecht, B and Aussenegg, F. R., *Optics Communications*, 2003, **220,** 137

[30] Akerman, M. E., Chan, W. C. W., Laakkonen, P., Bhatia, S. N and Ruoslahti, E., *Proc. Natl. Acad. Sci*., 2002, **99**, 12617

[31] Templeton, A. C., Wuelfing, P. W and Murray, R. W., *Acc. Chem. Res*., 2000, **33**, 27

[32] Hostetler, M. J., Templeton, A. C and Murray, R. W., *Langmuir*, 1999, **15**, 3782

[33] Templeton, A. C., Hostetler, M. J., Warmoth, E. K., Hartshorn, C. M., Krishnamurphy, V. M., Forbes, M. E and Murray, R. W., *J. Am. Chem. Soc*., 1998, **120**, 484

[34] Wuelfing, W. P., Gross, S. M., Miles, D.T and Murray, R. W., *J. Am. Chem. Soc*. 1998, **120**, 12696

[35] Foos, E. E., Snow, A. W., Twigg, M. E and Ancona, M. G., *Chem. Mater*., 2002, **14**, 2401

[36] Zheng, M., Davidson, F and Huang, X., *J. Am. Chem. Soc*., 2003, **45**, 456

[37] Kanaras, A. G., Kamounah, F. S., Schaumburg, K., Kiely, C. J and Brust, M., *Chem Commun.,* 2002, 2294

[38] Otsuka, H., Nagasaki, Y and Kataoka, K., *Advanced Drug Delivery Reviews,* 2003, **55**, 403

[39] Grosdemange, C. P., Simon, E. S., Prime, K. L and Whitesides, G. M., *J. Am. Chem. Soc.,* 1991, **113**, 12

[40] Hong, R., Fischer, N.O., Verma, A., Goodman, C. M., Emrick, T and Rotello, V.M., *J. Am. Chem. Soc.,* 2004, **46**, 567

[41] Chirakul, P., Perez-Luna, V. H., Owen, H and Lopez, G. P., *Langmuir*, 2002, **18**, 4324

CHAPTER 3

SYNTHESIS OF GOLD AND SILVER MPCS

3 Synthesis of Gold and Silver MPCs

In this chapter we explore the use of rationally designed thioalkylated PEG ligands and peptides for the stabilization of gold and Ag nanoparticles to evaluate the usefulness of these ligands as potential stabilizing scaffolds to address biological and bio-medical applications. This is important for the development of bioconjugation strategies discussed in chapter 5.

3.1 Introduction

The preparation of metal nanoparticles (in particular those of gold and silver) has become an area of considerable interest both in applied and fundamental research largely due to their fascinating properties and attractive potential applications in electronics[1] optics [2-6] biomedical and bioanalytical areas *etc.*[7-10] Gold colloids have a long history[11] and are particularly well known for their aesthetic appeal and their therapeutic properties.[12] Ever since Faraday [13] published a report on the synthesis and properties of colloidal gold, a reasonable insight into the nature of gold sols (nucleation, growth and kinetics of coagulation) was developed.[14] Considerable attention has been drawn during the last few decades to develop and optimise methods for the preparation of gold [15-18] and silver [19, 20] nanoparticles.

Ongoing research in this field has primarily been focused on developing stable monodisperse particles of controllable size and shape, as it is generally believed that current and novel potential applications of nanostructured materials are dependent on these properties. The terms colloids and clusters are often used interchangeably in the literature. The criteria to distinguish clusters (particles described herein as ligand-stabilised or monolayer protected clusters MPCs) from colloids (electrostatically-stabilised *note* this can be confusing since others prefer this as "charge and ligand stabilised") are based on the notion that clusters are isolable, reproducible molecules

with a precise composition and structure, while colloids are much less defined and typically have a distribution of size.[21] Basically the preparation of ligand-stabilised nanoclusters dates back to 1981 to the work that was carried out at the University of Essen in Germany by Schmid *et al.* for the preparation and characterization of $Au_{55}(PPh_3)_{12}Cl_6$ nanoclusters.[22] These findings have led to the development and exploitation of ligand stabilized metal nanoclusters in diverse areas including catalysis,[23] electronics[1] *etc.* This approach had some drawbacks and limitations including lack of stability. However, it was later realized that organic sulfur compounds form stable self-assembled monolayers on gold surfaces [24] and interestingly it was also discovered that thiols can be used to stabilize gold colloids.[25]

In 1994, the first facile synthesis of very stable, isolable gold clusters was developed in Liverpool.[26] The evolution of this work has led to the preparation of metal nanoparticles of defined size and shape and has been exploited in diverse applications.

This approach takes advantage of using tetraoctyl ammonium bromide as a phase transfer catalyst, to transfer aqueous chloroauric acid to the organic phase (toluene) to form an intensely orange Au(III) complex (tetraoctylammonium tetrabromoaurate). Reducing this complex in the presence of thiols ligands, mostly alkanethiols, by $NaBH_4$ allows the formation of small clusters (1-5 nm) the diameter of which is influenced by a number of factors such as the thiols:gold ratio. It was found that the use of a larger thiols:gold molar ratio produces very small clusters [27] which are characterised by their unique dark brown colour and damped plasmon absorption band in the UV-vis spectrum. This plasmon absorption band even disappears completely when very small clusters are formed. Fast addition of the reducing agent and cooling the reaction mixture again leads to the formation of small clusters, with improved monodispersity.[27, 28] In order to isolate a high yield of very small clusters (~ 2nm) it was realized that this is achievable by carefully terminating the reaction immediately after reduction.[29, 30]

Murray *et al*, demonstrated the usefulness of this method, by carrying out extensive investigations particularly to show that this method tolerates various modification to include straight-chain alkanethiols, glutathione, tiopronin, thiolated PEG, *p*-mercaptophenol, aromatic alkane thiol, phenyl alkane thiol and mercaptopropyl trimethoxysilane as stabilising agents.[31] As stated in chapter 1, Murray's group also characterised these materials, to gain insight into their physical and chemical properties.

Upon understanding the 3D self assembly process of these materials in contrast to the 2D SAMs on the surface, Murray coined the name monolayer protected clusters (MPCs) to distinguish them from 2D SAMs. Many laboratories today employ this original protocol for the size selective formation of MPCs by varying the ratio between Au:HS-R including the preparation of very small Au MPCs.[32] Of particular importance again has been the ability to control the size distribution of these MPCs since it is known that their optical properties depend on size and shape. This has been achieved by using a number of techniques such as solvent fractionation [28] continuous free-flow electrophoresis [28, 33] size exclusion chromatography [34] and high performance liquid chromatography (HPLC).[35, 36] Successive fractionation appears to be a reliable means of obtaining narrow size distributions by taking advantage of allowing bigger particles to aggregate first due to the stronger van der Waals interaction between the larger spheres.[37] The use of chromatographic techniques for the separation of MPCs appears more attractive since it is practically not possible using TEM to distinguish the size of the ligand shell, but size exclusion chromatography does.[34]

The scope of MPC synthesis is not limited to the 1-5 nm regime, since it was realized that the basic two-phase protocol in the absence of thiols leads to the formation of somewhat larger stable nanoparticles. The stability of these particles is provided by the bromides and tetraoctyl ammonium ions which adsorb to the surface of the particles. These tetraoctyl ammonium bromides (TOABr) stabilised particles are in the 5-8 nm size regime. Increasing the dielectric constant of the medium, *e.g.* by adding alcohols to the particles leads to the formation of irreversible aggregates,

however, they have been used as readily available starting materials for the construction of self assembled mono- and multilayers on different substrates since the ionic capping can be easily removed by thiols and amine functionalities.[38]

Apart from the two phase solution synthesis, single phase methods have also been developed, to obtain MPCs of comparable sizes, including the use of $NaBH_4$ to reduce gold in alcoholic solution containing thiols.[39] However, this is only applicable when thiols to be used are soluble in alcohols. In essence, particles with both hydrophobic and hydrophilic characteristics are obtainable as was demonstrated using mercaptoundecanoic acid (MUA) as a stabilizing/capping agent.[40]

Again, the 5-8 nm particles are not limited to the two-phase approach; MPCs of about 6 nm can also be prepared by first preparing borohydride stabilized particles which can be directly converted to the desired MPCs. Even larger particles (10-40 nm) can be prepared following the classical Frens method [15] of using citrate as the reducing and stabilizing agent. By this widely used approach, gold and silver MPCs of different size and shapes can be prepared. The adsorption of citrate ions to the cluster surface is essential to electrostatically overcome the van der Waals attraction and hence to preserve the stability of the metal nanoparticles. These particles can be easily converted to MPCs by a self assembly process as demonstrated by Whitesides *et al.*[41]

Since the ultimate goal in preparing Au and Ag MPCs is to explore their unique properties [42-48] in biological applications, these materials require more than water solubility. Key issues such as functionality, stability and biocompatibility have to be addressed in particular silver known for its propensity to oxidatively corrode [49-51] and aggregate in electrolytic solution.

In order to address these challenges, ligand design strategies discussed in chapter one have been extended to include the incorporation of peptide to investigate its efficiency in stabilising Ag nanoparticles. The use of the peptide CALNN has been applied to Ag nanoparticles after it was found that the same pentapeptide is suitable for the stabilization of gold nanoparticles. Levy *et al.*[52] have shown that CALNN is indeed an alternative ligand providing stable gold nanoparticles which are amenable to

modification. They can be centrifuged, freeze-dried, chromatographed and separated by electrophoresis.

Stabilisation of silver nanoparticles using both PEG ligands and peptides to be discussed later in this chapter was carried out in collaboration with Dr Christopher Doty of the University of Liverpool to examine the use of these ligands as potential stabilizing scaffolds to address biological and bio-medical applications. [53, 54]

3.2 Results and Discussion

To develop the desired gold and silver MPCs, several common synthetic methods were followed and modified with the aim to produce size selective, stable aqueous gold and silver nanoparticles stabilised by readily functionalised PEG or peptide ligands. Thioalkylated PEG and CALNN peptide ligands used were; monohydroxy thioalkylated PEG ligands (PEG-OH), carboxylated thioalkylated PEG ligands (PEG-COOH), amine functionalized thioalkylated PEG ligand (PEG-NH_2) and penta-peptide CALNN. These ligands are shown in the experimental section (page 105) for their structural identification. In the first section the synthesis of Au-MPCs and Ag-MPCs is discussed.

Methods used for the preparation of gold and silver nanoparticles are summerised in Table 1 and 2. They are given respective codes [**RT-1 to RT-11** for gold particles (Table 1) and **RT-12 to RT-21** for silver particles (Table 2)]. The RT code represents naked or ligand stabilised particles. Synthesis of each particle is briefly discussed.

3.2.1 Synthesis of Au Nanoparticles (AuNPs)

3.2.1.1 Preparation of Au-MPCs (RT-1)

Gold nanoparticles (~ 3nm) can be prepared by a single-phase reduction method which encompasses reducing a gold salt by $NaBH_4$ in the presence of thiols in acidic alcoholic solution (to prevent any possible thiol de-protonation). This method was followed here using functionalised PEGylated ligands to investigate their capabilities as future ligands for the stabilization of small gold clusters. In fact, earlier work in our group [55] showed that it is possible to use ligand **3a** (chapter 2 and experimental section page 105), to produce stable Au-MPCs by a single phase reduction method. For the synthesis of carboxylic acid functionalized PEGylated MPCs, the same protocol was followed, in this case using ligands **6a-c** (experimental section page 105) thus; by adding an aqueous solution of $NaBH_4$ to an alcoholic

solution of tetrachloauric acid and the carboxylated thiol, we observed an immediate colour change from yellow (Au (III)) to dark brown (Au (0)) which is indicative of the formation of small gold clusters (mostly with diameters less than 3 nm). It is important to use a freshly prepared sodium borohydride solution to ensure complete reduction since borohydride degenerates with time in aqueous solution.

The particles were easily isolated by precipitating them out with hexane followed by washing with diethyl ether and ethyl acetate. They could be dried and stored as solids and re-dissolved in water without loss of material. Importantly, these particles require either ultracentrifugation for purification (due to their small size), or, alternatively, they can be purified by size exclusion chromatography. The latter was achieved using sephacryl 100HR or sephadex-G25 as supports materials and water as the mobile phase. It was found that both supports allow easy purification of these MPCs without loss of material. These particles were characterized by transmission electron microscopy (TEM) and UV-vis spectroscopy. Their broad plasmon absorption band from the UV-vis (Figure 1, RT-1) clearly shows that the particles are mostly less than 5 nm, since larger particles would show a more intense and sharper plasmon absorption band.[57]

NPs Code	Size/ nm	Ligand	Method	Stabilisation
RT-**1**	3.5 ± 0.8	PEG-COOH **6b**	Single-phase- reduction	Ligand
RT-**2**	6.2 ± 1.9	TOABr	Two phase-reduction	Electrostatic
RT-**3**	6.3 ± 1.5	PEG-COOH **6a or 6b**	Two-phase transfer -ligand exchange	Ligand
RT-**4**	3.0 ± 1.0	PEG-COOH **6a**	Two-phase transfer -ligand exchange	Ligand
RT-**5**	6.2 ± 1.8	BH_4^-	Borohydride reduction	Electrostatic
RT-**6**	7.4 ± 1.5	PEG-COOH **6b**	Ligand exchange	Ligand
RT-**7**	13.9 ± 0.6	Citrate	Citrate reduction	Electrostatic
RT-**8**	14.0 ± 1.5	PEG-COOH **6a or 6b**	Ligand exchange	Ligand
RT-**9**	17.6 ± 2.3	PEG-COOH **6b**	Simultaneous addition	Ligand
RT-**10**	14.1 ± 1.8	PEG-OH/NH_2 **3a/10**	Ligand exchange	Ligand
RT-**11**	50.8 ± 8.5	PEG-COOH **6c**	Propanol reduction	Ligand

Table 1. Different methods employed for the preparation of size selective aqueous gold nanoparticles.

NPs Code	**Size/ nm**	**Ligand**	**Method**	**Stabilisation**
RT-**12**	8.1 ± 1.6	Citrate	Citrate reduction	Electrostatic
RT-**13**	8.2 ± 2.0	CALNN	Ligand exchange	Ligand
RT-**14**	15.3 ± 6.4	Citrate	Citrate reduction	Electrostatic
RT-**15**	16.3 ± 4.5	CALNN or CCALNN	Ligand exchange	Ligand
RT-**16**	8.2 ± 2.4	CALNN	Two-phase transfer reduction	Ligand
RT-**17**	5.5 ± 0.9	Decane-or Dodecanethiol	Two phase transfer -reduction	Ligand
RT-**18**	5.3 ± 1.0	PEG-OH **3a**	Ligand -exchange	Ligand
RT-**19**	5.3 ± 1.0	PEG-NH_2 **10**	Ligand exchange	Ligand
RT-**20**	4.5 ± 0.9	PEG-OH **3a**	Two-phase-AgBr	Ligand
RT-**21**	4.5 ± 0.9	PEG-NH_2 **10**	Two-phase-AgBr	Ligand

Table 2. Different methods employed for the preparation of size selective aqueous silver nanoparticles.

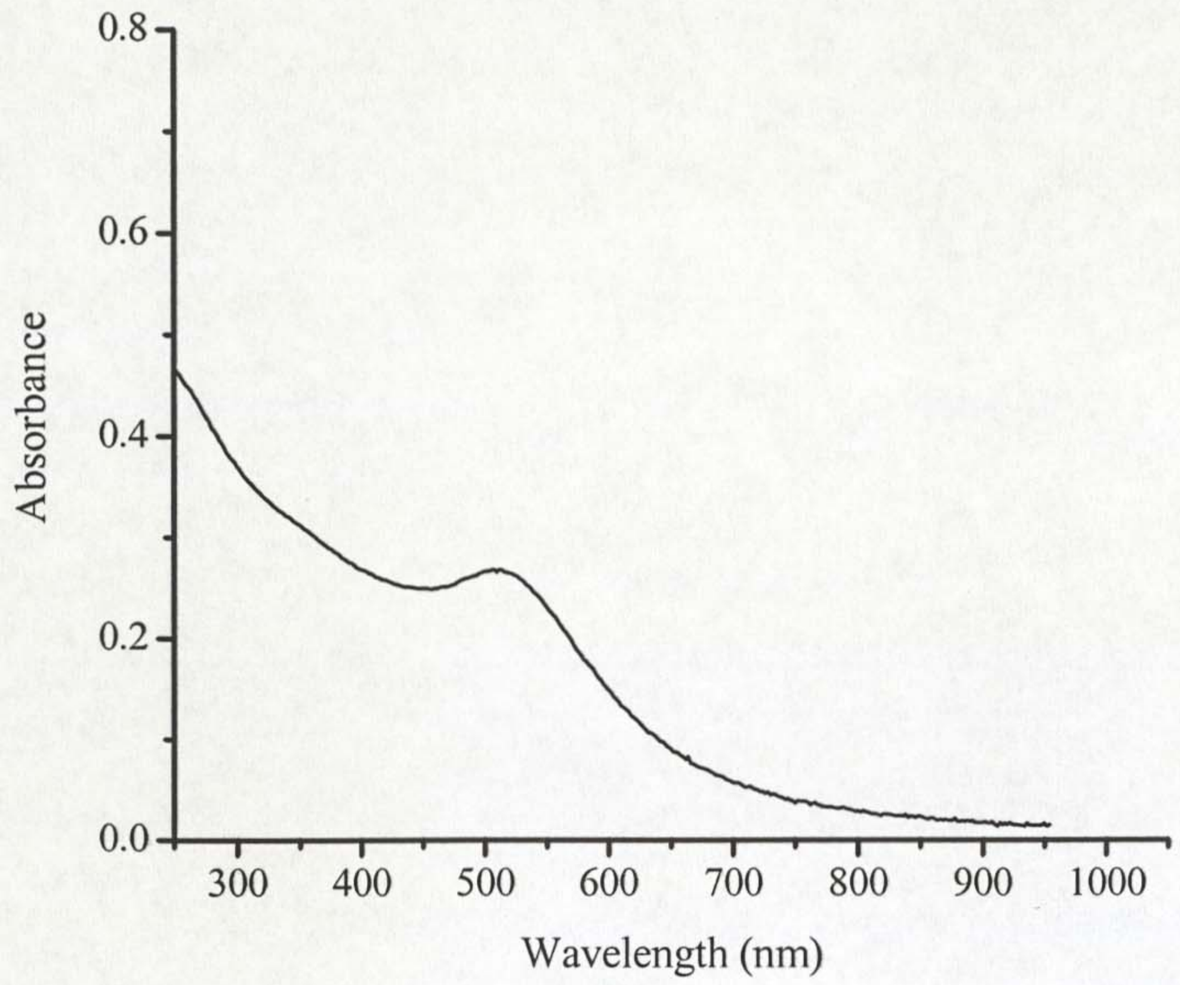

Figure 1. UV-vis absorption spectrum of the RT-1 (3.5 ± 0.8 nm) carboxylic acid functionalized (PEG-COOH 6b) Au-MPCs prepared via single-phase method.

Figure 2 shows a TEM micrograph (image a) of the particles obtained when PEG-COOH **6b** was used as the passivating ligand. The particles are uniform, measuring about 3.5 ± 0.8 nm and irrespective of the thioalkylated PEG ligand length used no detectable changes with respect to particles size, shape and stability occurs. A histogram of these particles is presented in Figure 3 and shows that about 75% of the particles prepared in this approach are about 3.5 nm.

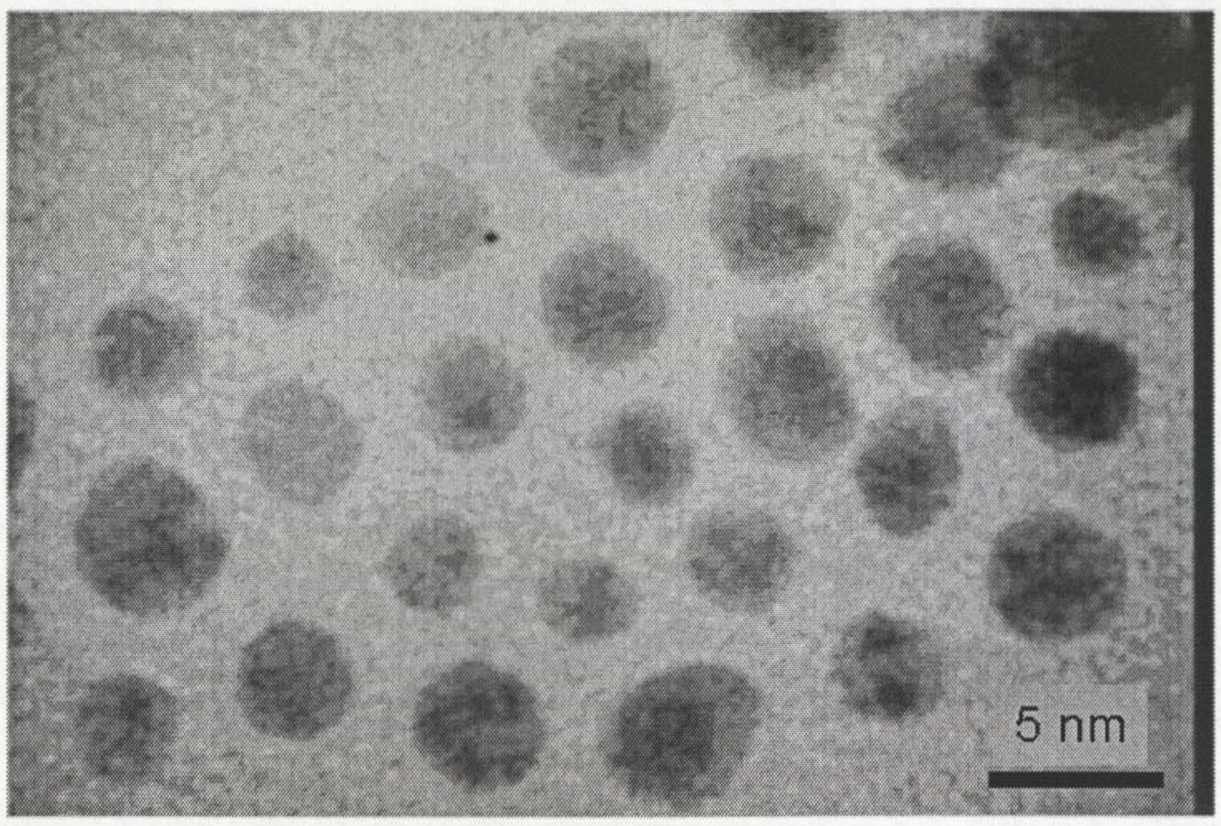

Figure 2. TEM micrograph of (RT-1) MPCs (3.5 ± 0.8, Table 1) produced via single-phase reduction method using PEG-COOH 6b ligand.

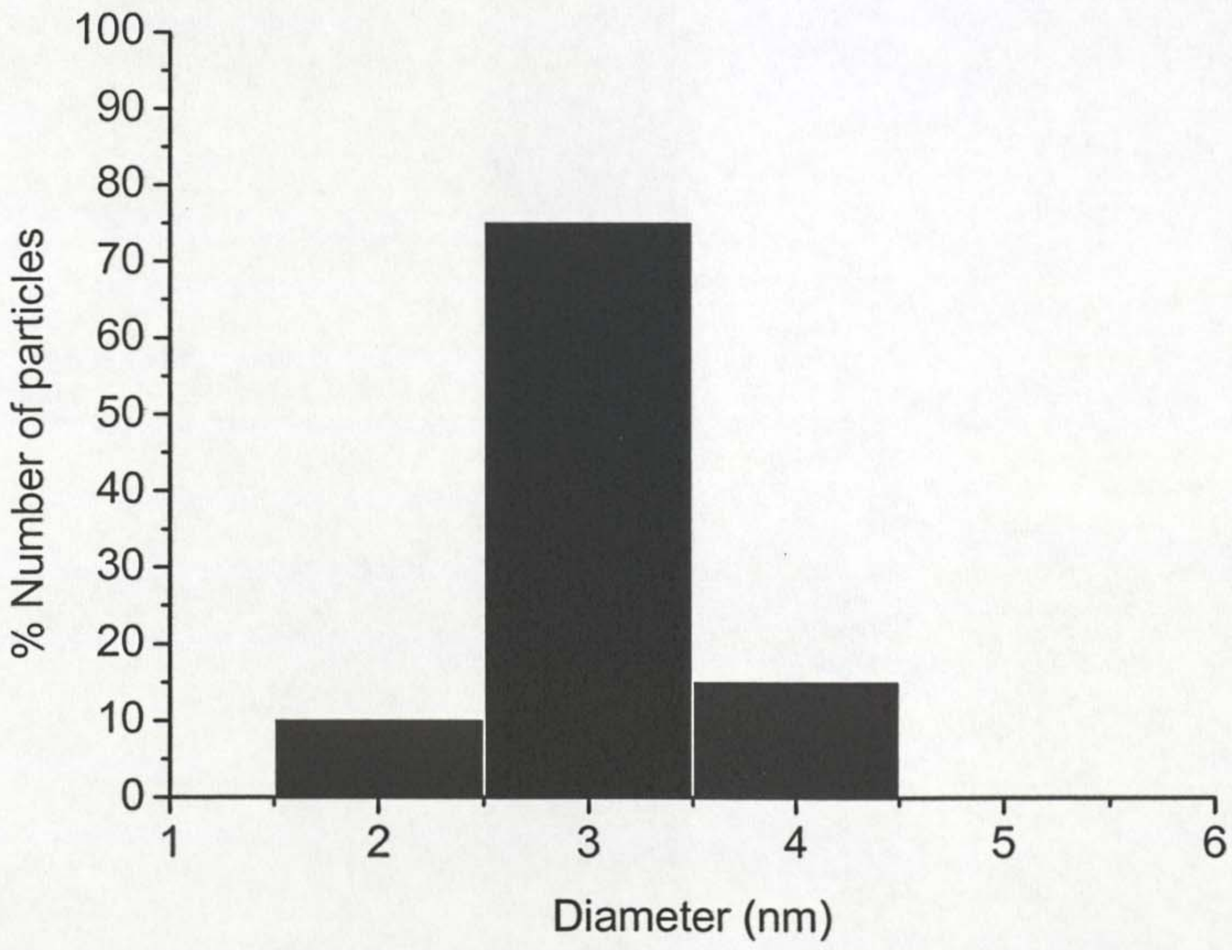

Figure 3. Histogram for the size distribution of PEGylated Au-MPCs (RT-1, Table1).

3.2.1.2 Two phase (water-toluene) solution system (RT-2, 3 and 4)[26]

Two-phase solution synthesis is used for the preparation of isolable metal clusters normally in the 1-10 nm regime. Basically, aqueous tetrachloroaurate is transferred to an organic phase (toluene) using a phase transfer agent (tetraoctylammonium bromide (TOABr)) to give an intense orange Au (III) complex (tetraoctylammonium tetrabromoaurate, a simple schematic illustration is given in Figure 4). Once this complex is formed, two approaches can be followed for the formation of gold clusters of different sizes; i) reducing the complex with $NaBH_4$ gives rise to the formation of ruby red TOABr stabilized particles (Figure 4 route a). Since the resulting electrostatically stabilized particles are not stable enough when isolated from solution, TOABr stabilised particles are treated with thiol ligands to give stable Au-MPCs in the 5-8 nm regime. ii) Thiols are added to the complex before, followed by reduction with $NaBH_4$ yielding very small particles of which their size is influenced and controlled to some extent by the ratio of Au: HS-R employed.

Addition of thiols in organic phase (toluene) serves two purposes, first, they reduce Au (III) ions to form a polymeric Au (I) intermediate while they are themselves oxidized to disulfides. Secondly, they provide stability to the resulting gold clusters accompanying the reduction of Au (I) intermediate by a suitable reducing agent ($NaHB_4$) according to equation (ii). During reduction, an intense orange colour of Au (I) changes to dark brown, which is a characteristic colour of the formation of small gold clusters. As stated above, the literature is replete with the modification of this basic two-phase protocol to produce desirable size controlled metal nanoparticles.[31]

In the case of transferring the TOABr stabilised particles (Figure 4 a) to water, an alcoholic solution of thioalkylated PEG ligands (**3a,b** and **6a-c**) were employed to treat TOABr capped gold nanoparticles in toluene. Attachment of PEG thiols to the surface of gold clusters is evidenced by a slight colour change from wine red towards blue. This occurs because particles begin to aggregate upon replacing the adsorbed TOABr ions on clusters surface by PEG thiols. After 3h of stirring at room temperature, clusters were transferred to the aqueous phase, washed with diethyl ether (3 times) and were further purified by repeated centrifugation (25000g) (Figure 4a).

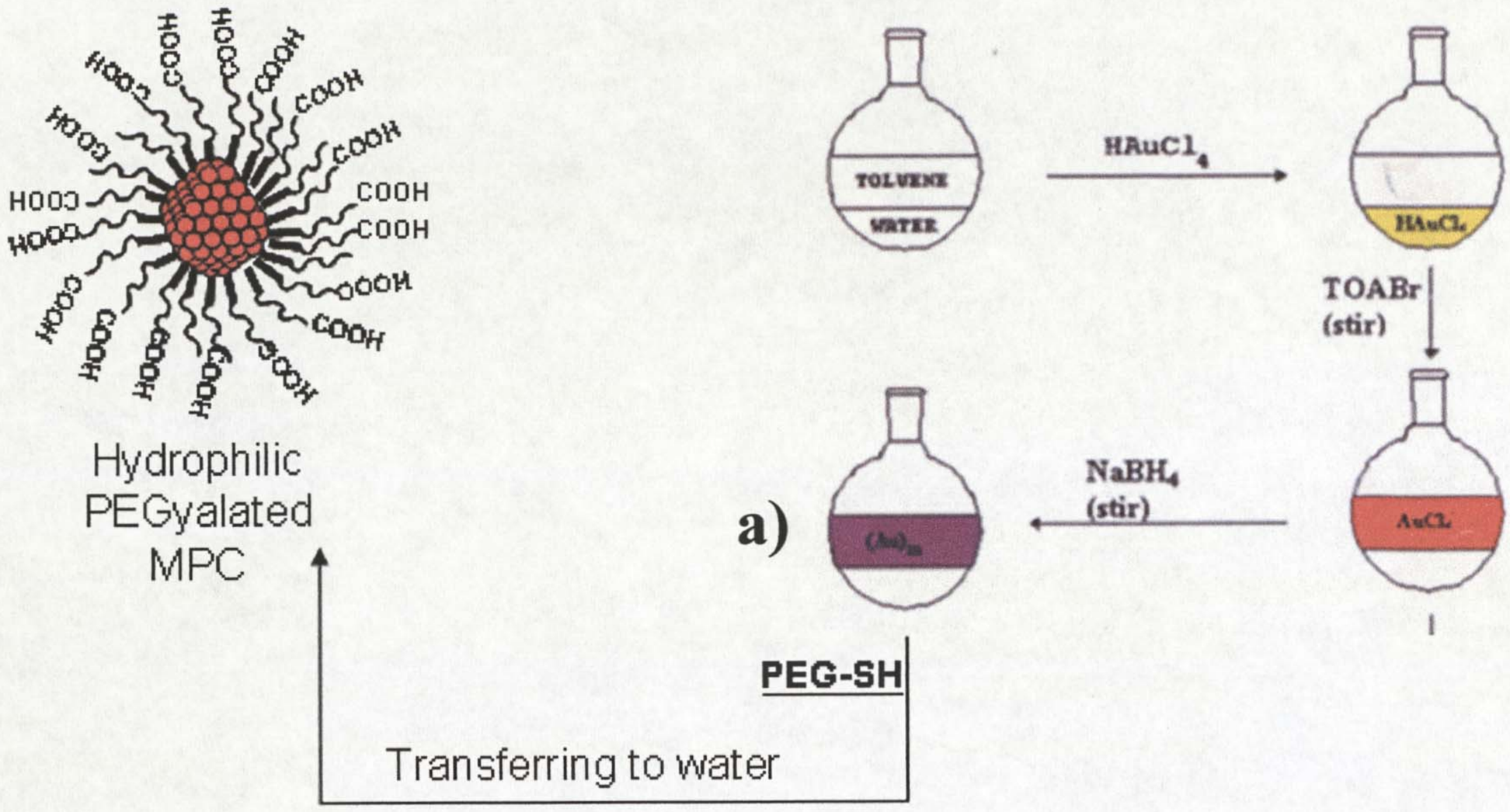

Figure 4. **A schematic illustration for the formation of Au-MPCs via a two phase liquid/liquid system. In route a, the ruby red TOABr stabilised particles are formed (RT-2, 6.3 ± 1.9 nm) and thiol PEG addition leads to the formation of Au-MPCs (RT-3, route a).**

The resulting PEGylated gold MPCs were characterised by UV-vis and TEM. Figure 5b shows the typical UV-vis absorption spectrum of electrostatically stabilised particles in toluene (RT-2). These particles measure 6.2 ± 1.9 nm and their TEM image is shown in Figure 5a. They were used as precursors for the production of hydrophilic MPCs. Figure 6 shows the TEM images of the resulting hydrophilic MPCs (RT-3) in which PEG-COOH **6b** (image a), PEG-COOH **6c** (image b) and PEG-COOH **6a** (image c) were used to transfer the particles from toluene to water. Their representative UV-vis absorption spectrum is shown in Figure 6d. Irrespective of the size of the PEG ligand used the particles can be easily transferred from toluene to water by simply adding water to the toluene particles and shake them vigorously, allowing a complete transfer to water. Their morphology resembles that of the conventional TOABr stabilised particles (RT-2) and the average size of the carboxylated MPCs shown in the TEM in Figure 6 measure (~ 6.3 ± 1.5 nm).

Following the most common two phase route, where gold is reduced in the presence alkane thiols, yielded small clusters which were comparable in size to those prepared by the single phase method described above (RT-1), and they could easily be transferred to water, purified and manipulated without loss of their properties.

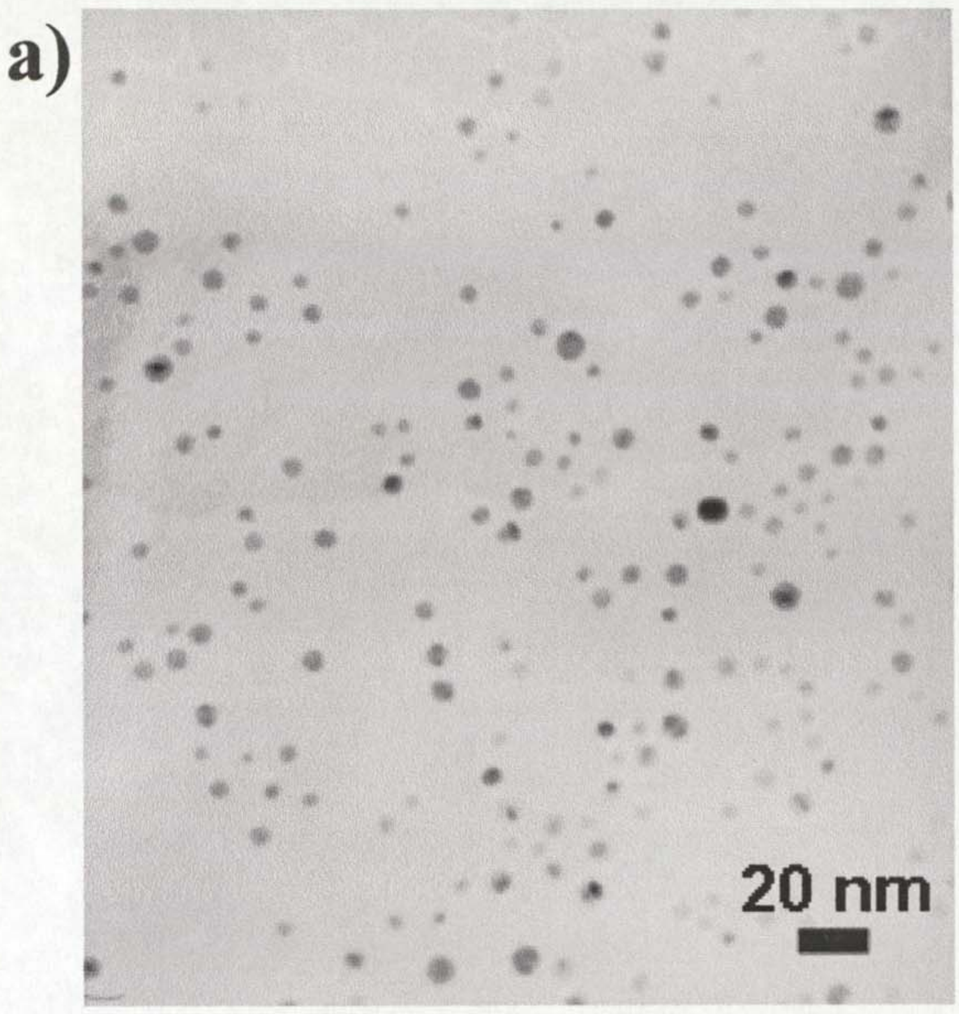

Figure 5. TEM image of a) TOABr stabilised particles and b) their UV-vis spectrum in toluene. (RT-2, Table 1)

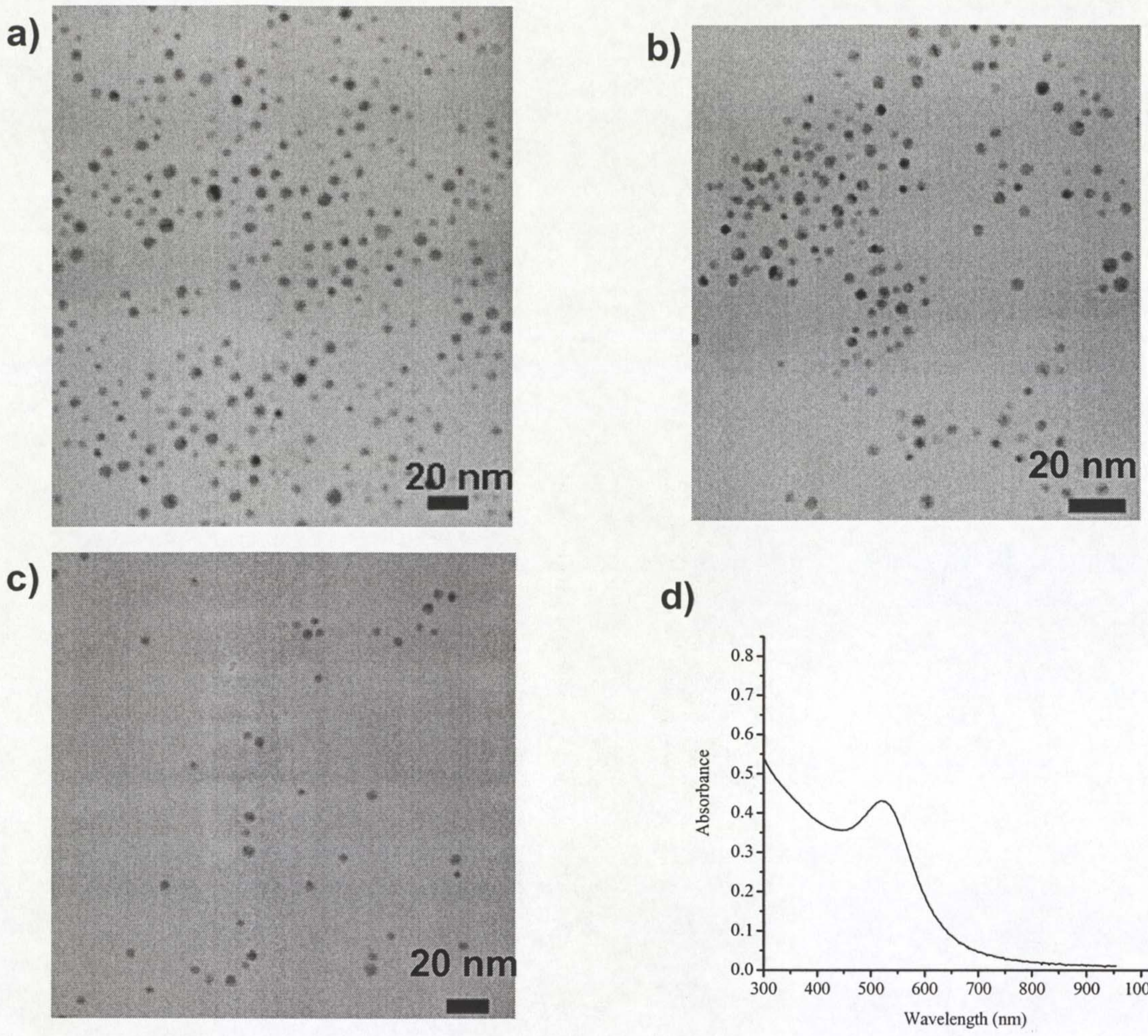

Figure 6. TEM images of a) PEG-COOH 6b stabilised particles b) PEG-COOH 6c stabilised and c) PEG-COOH 6a stabilised MPCs prepared via the two-phase route (Figure 4a, RT-3).

3.2.1.3 Reduction with borohydride in water (RT-5 and RT-6) [58]

In aqueous solution, sodium borohydride can be used as a reducing and stabilizing agent for the preparation of uniform particles by controlling the reaction parameters such as temperature and pH during preparation. [58] The most important step in the preparation of these electrostatically stabilised particles is to carefully add portions of the reducing agent ($NaBH_4$) to an aqueous solution of chloroauric acid and K_2CO_3 at low temperature (*ca.* 0 °C). The resulting particles are electrostatically stabilised by borohydride ions and a narrow size distribution can be achieved by fast addition of borohydride to the reaction mixture. We have prepared these particles (RT-5) by adding 1 ml aliquots of $NaBH_4$ 5 times to the stirred aqueous solution of chloroauric acid on ice. Addition of $NaBH_4$ aliquots should be successively performed until all 5 ml are added to obtain small uniform particles. Otherwise, bigger particles (~ 12 nm) are produced. The particles obtained by reduction with borohydride were converted to the desired MPCs (RT-6) by addition of carboxylated thioalkylated PEG ligands. Unlike their precursors, the Au-MPCs (RT-6) can be purified by centrifugation or size exclusion chromatography (Sephacryl 100HR) and are amenable to further chemical modification.

The TEM images of RT-5 and RT-6 gold nanoparticles are shown in Figure 7a and Figure 7b respectively, with their size distribution in Figure 7c and 7d, while their UV-vis spectra are shown in Figure 8. Generally, the borohydride stabilised particles (Figure 7a) are uniform with a moderately narrow size distribution and they measure 6.2 ± 1.8 nm. A histogram of their size distribution (Figure 7c) indicated that a large number of these particles are within 6-7 nm. Their MPCs derivatives (RT-6) shown in Figure 7b were also obtained within a good size distribution measuring 7.4 ± 1.5 nm and after purification over 80% of these particles are within 6-8 nm as depicted on their histogram in Figure 7d. The UV-vis spectra of both RT-5 and RT-6 in Figure 8 show that there is a significant shift of the plasmon absorption band of the RT-5 particles from 512 nm to 524 nm upon functionalizing borohydrides hydrosols with PEG-COOH **6b** ligand and this is generally expected due to the change in the refractive index induced by ligand shell composition.

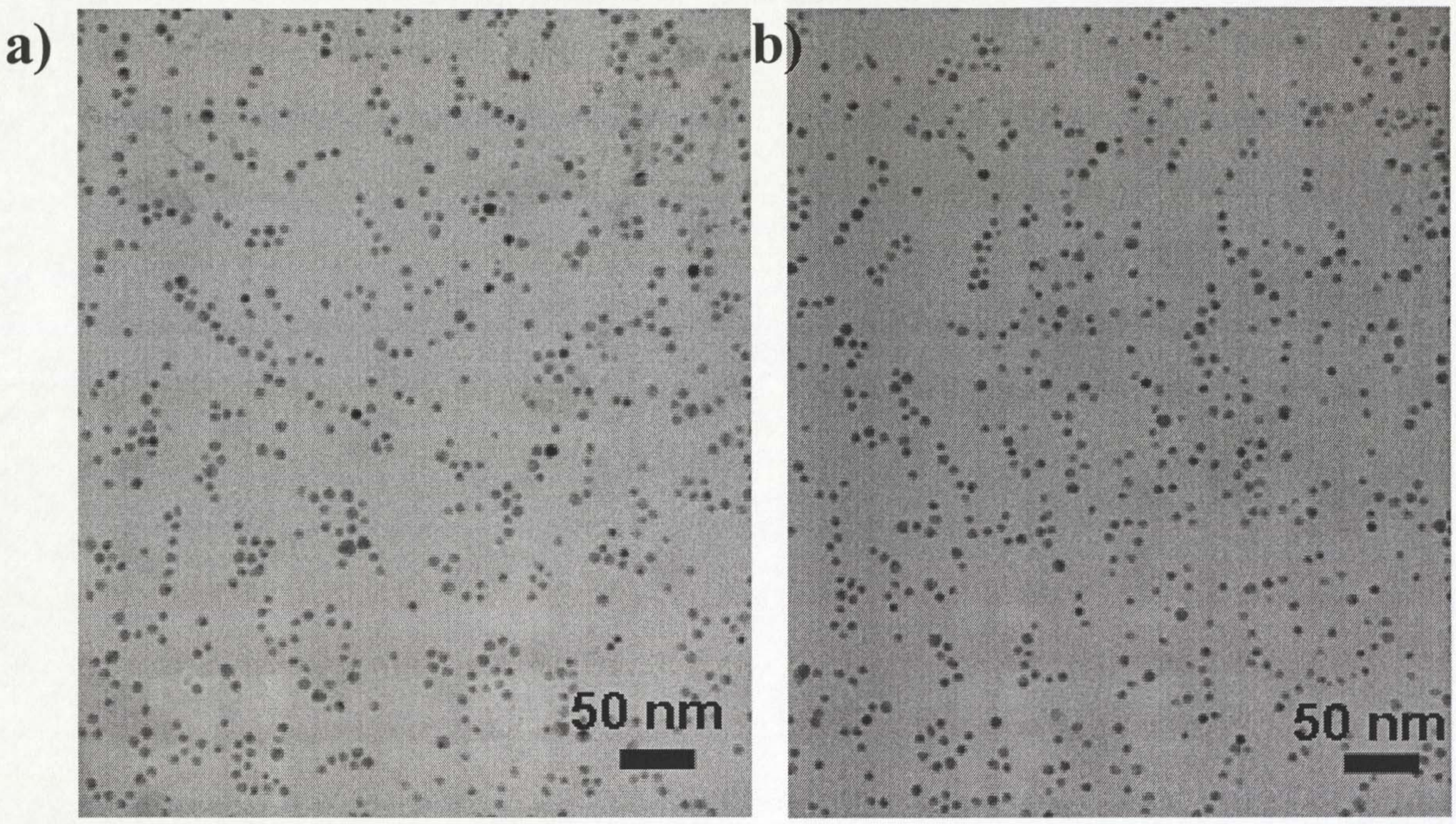

Figure 7. TEM image of a) RT-5 gold particles, b) RT-6 Au-MPCs particles and the histograms of c) RT-5 and RT-6 particles (Table 1).

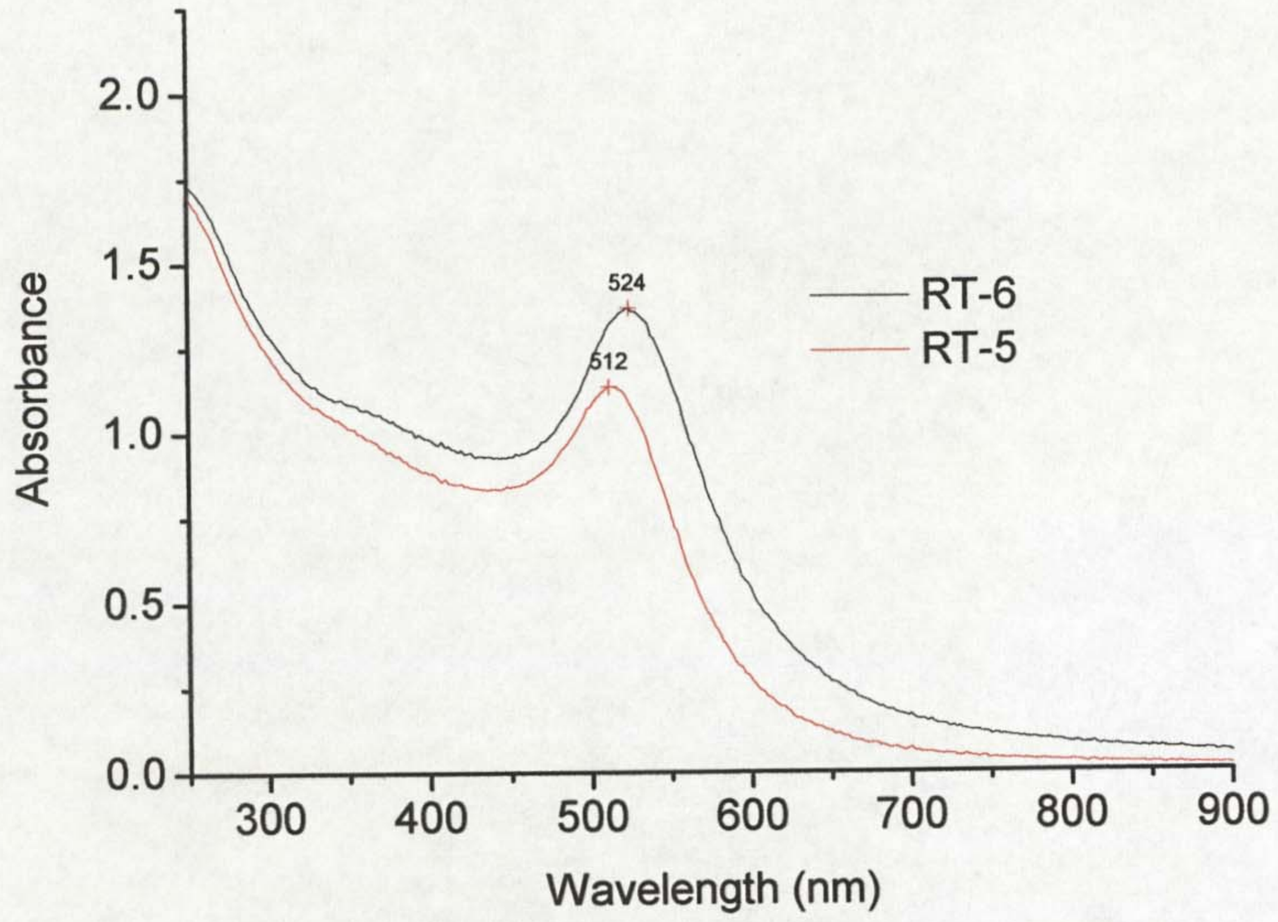

Figure 8. UV-vis spectra of borohydride stabilised particles (RT-5) and carboxylated PEGylated Au-MPCs RT-6 particles in water.

3.2.1.4 Citrate reduction routes (preparation of RT-7, 8 and 9)

Citrate stabilized nanoparticles were prepared as precursors to MPCs of larger sizes. The use of tri-sodium citrate as a reducing and stabilising agent provides uniform, charge stabilised gold nanoparticles, and it is possible to control their size (ranging from 10 – 100 nm) by changing the citrate/gold molar ratio.[15] This method was used here to prepare citrate stabilised gold nanoparticles of various sizes mostly between 12-40 nm. To functionalise citrate stabilized gold nanoparticles with carboxylic acid functionalized thioalkylated PEG ligands **6a-c,** different synthetic routes were explored as schematically shown in Figure 9.

In the first case, citrate-stabilized particles (RT-7 particles) were prepared by the standard Frens method [15] in which citrate is used as a reducing and stabilizing agent. This is achieved by adding tri-sodium citrate to a boiling chloroauric acid solution. The resulting electrostatically stabilised particles are uniform, can be filtered and remain stable for a long time in pure water. The TEM of these particles is shown in Figure 10a (~ 13.9 ± 0.6 nm) and their UV-vis spectra is presented in Figure 10b.

The plasmon absorption band at around 520 nm is typical of the classical citrate particles measuring around 14 nm.[14,15] These particles were subsequently treated with thioalkylated PEG ligands to give PEGylated Au-MPCs retaining the size and shape of the original particles, as expected. This is shown in Figure 9 route A in which PEG-COOH **6b** was used as the capping ligand to produce the desired PEGylated Au-MPCs (RT-8) measuring (14.0 ± 1.5 nm). Their TEM image is shown in Figure 10c and the UV-vis is shown in Figure 10d. A higher magnified image of the carboxylated Au-MPCs (PEG-COOH **6a**, RT-8) is shown in Figure 11a.

On the other hand route B in Figure 9 shows the preparation of Au-MPCs by simultaneous addition of both citrate and PEG-COOH ligand after refluxing the aqueous chloroauric acid solution. Figure 11b shows the TEM image of the particles produced in this route and their corresponding UV-vis spectrum is shown in Figure 11c. Noteworthy is that a red shifted plasmon absorption band ($\lambda \sim 28$ nm) of particles prepared following the simultaneous addition of PEG was observed (Figure 11c) as compared to the standard citrate approach discussed above. This is due to the larger Au-MPCs (measuring 17.6 ± 2.3 nm) obtained by this route as shown in Figure 11b with some of the particles adopting different shapes. In fact, it is generally known that larger particles (~ 30 nm) tend to deviate from spherical.

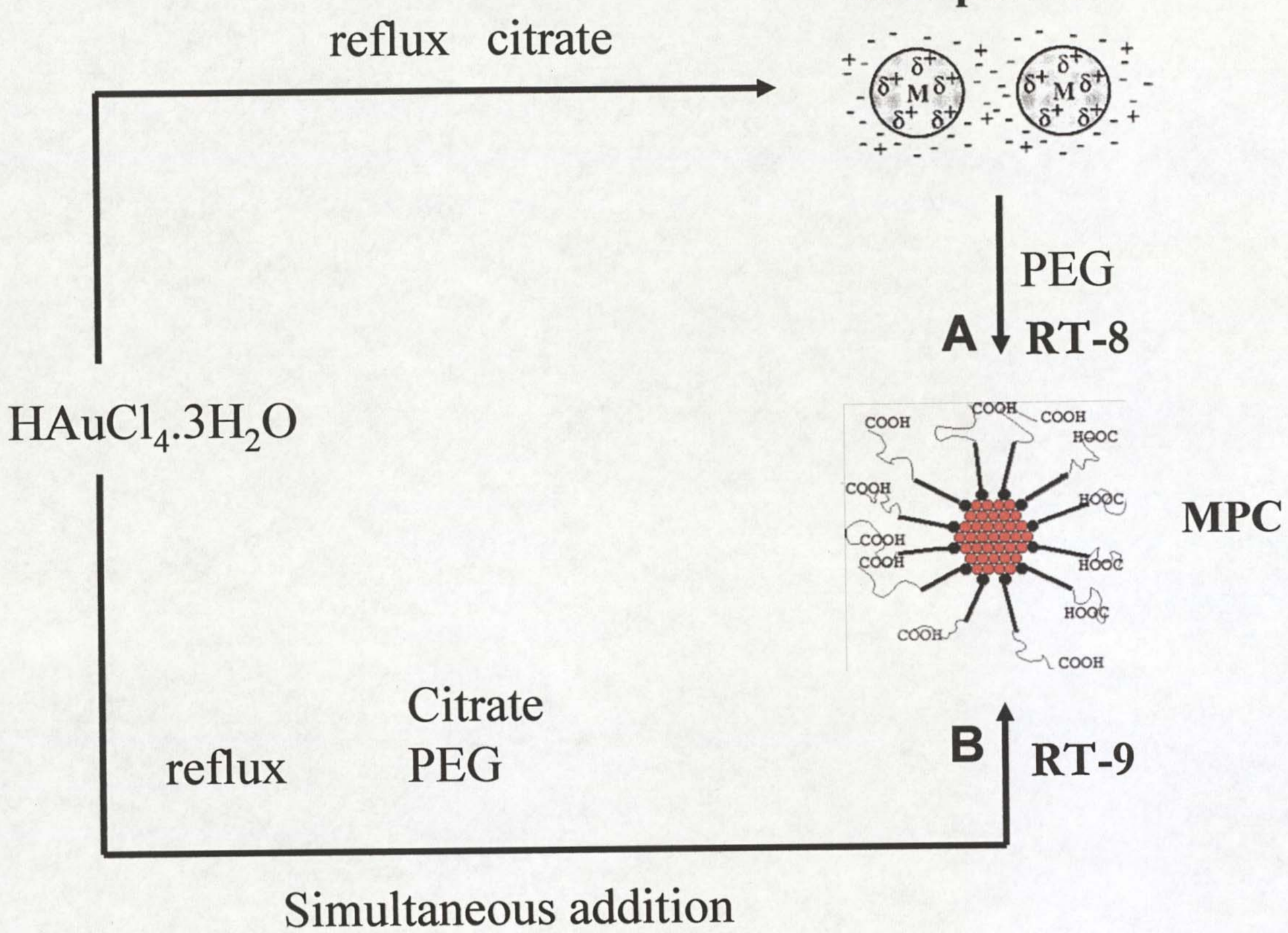

Figure 9. Schematic illustration for the preparation of (RT-7 particles), leading to RT-8 MPCs (route A) and route B shows the preparation of RT-9 MPCs (Table 1).

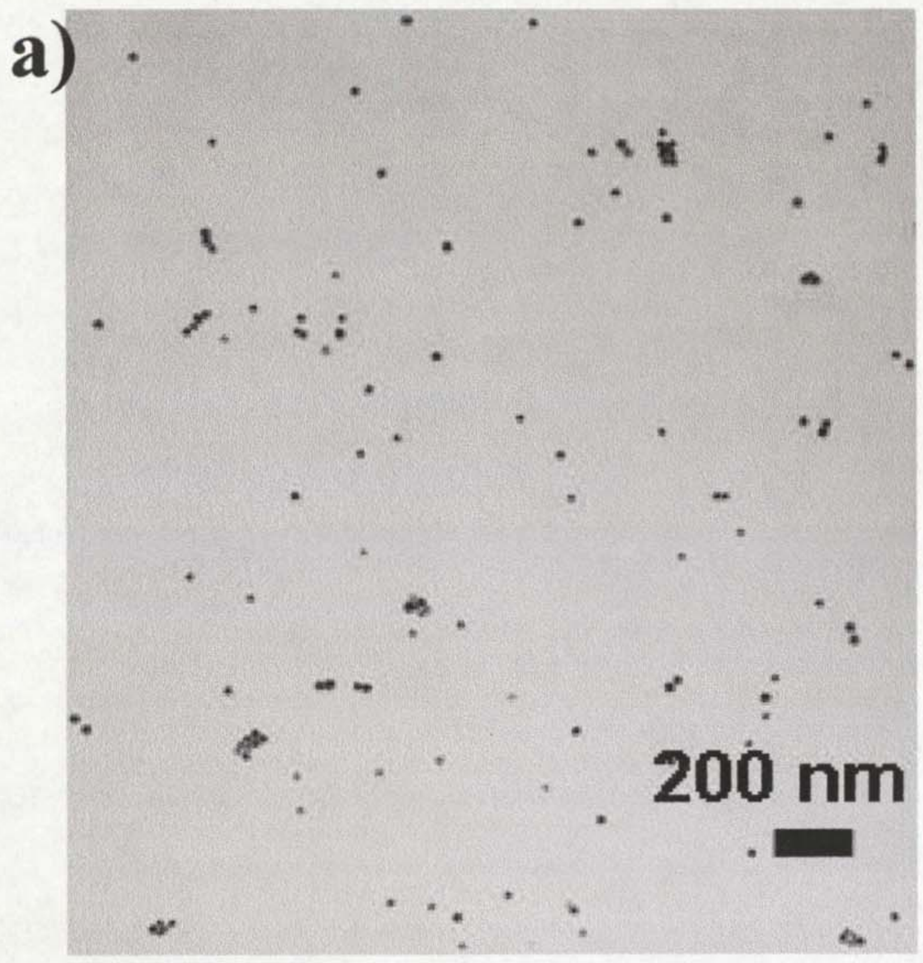

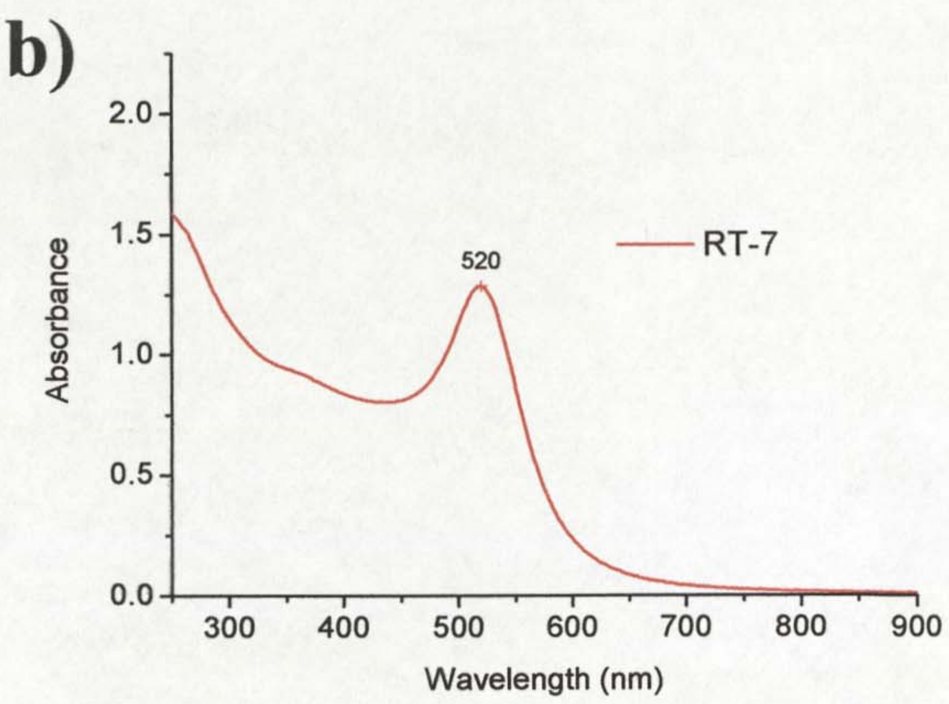

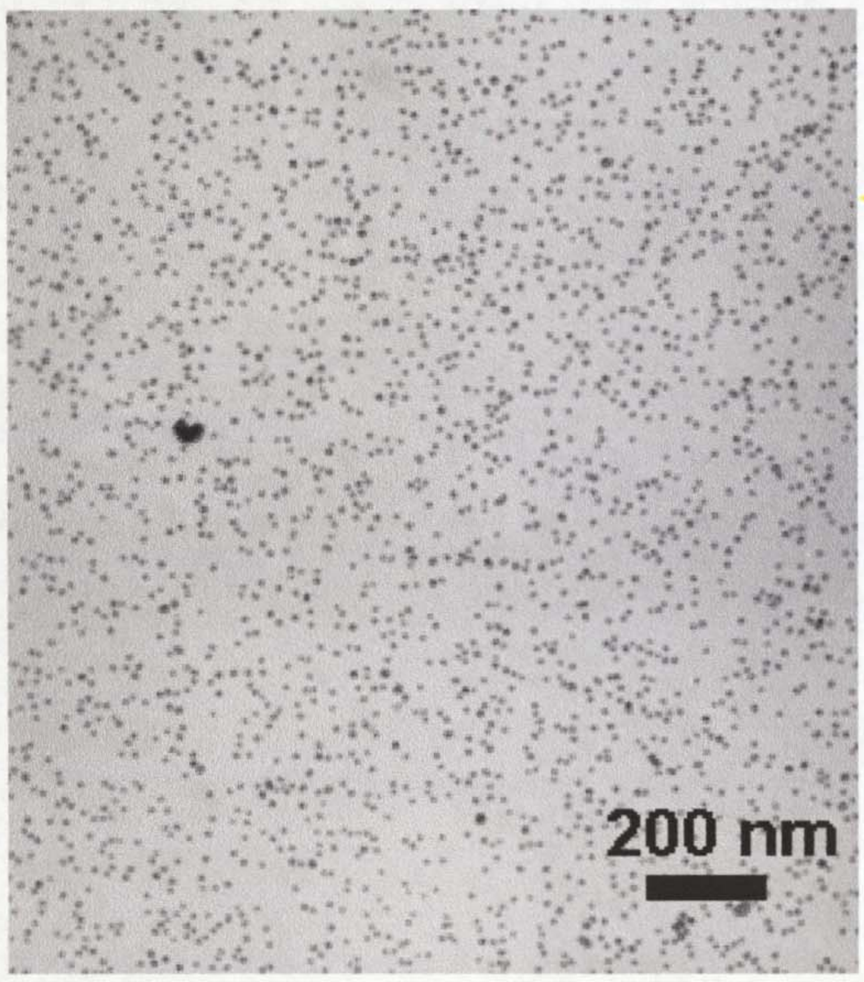

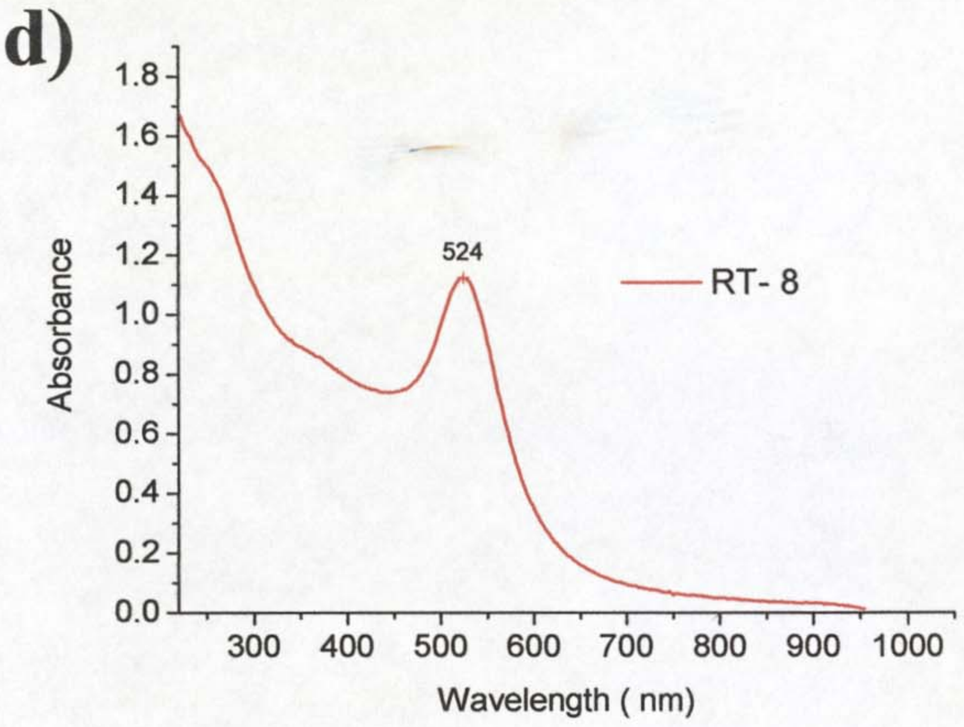

Figure 10. TEM images of a) RT-7 nanoparticles and b) their UV-vis spectrum while c) shows the TEM image of RT-8 MPCs and their corresponding d) UV-vis spectra in water (Table 1).

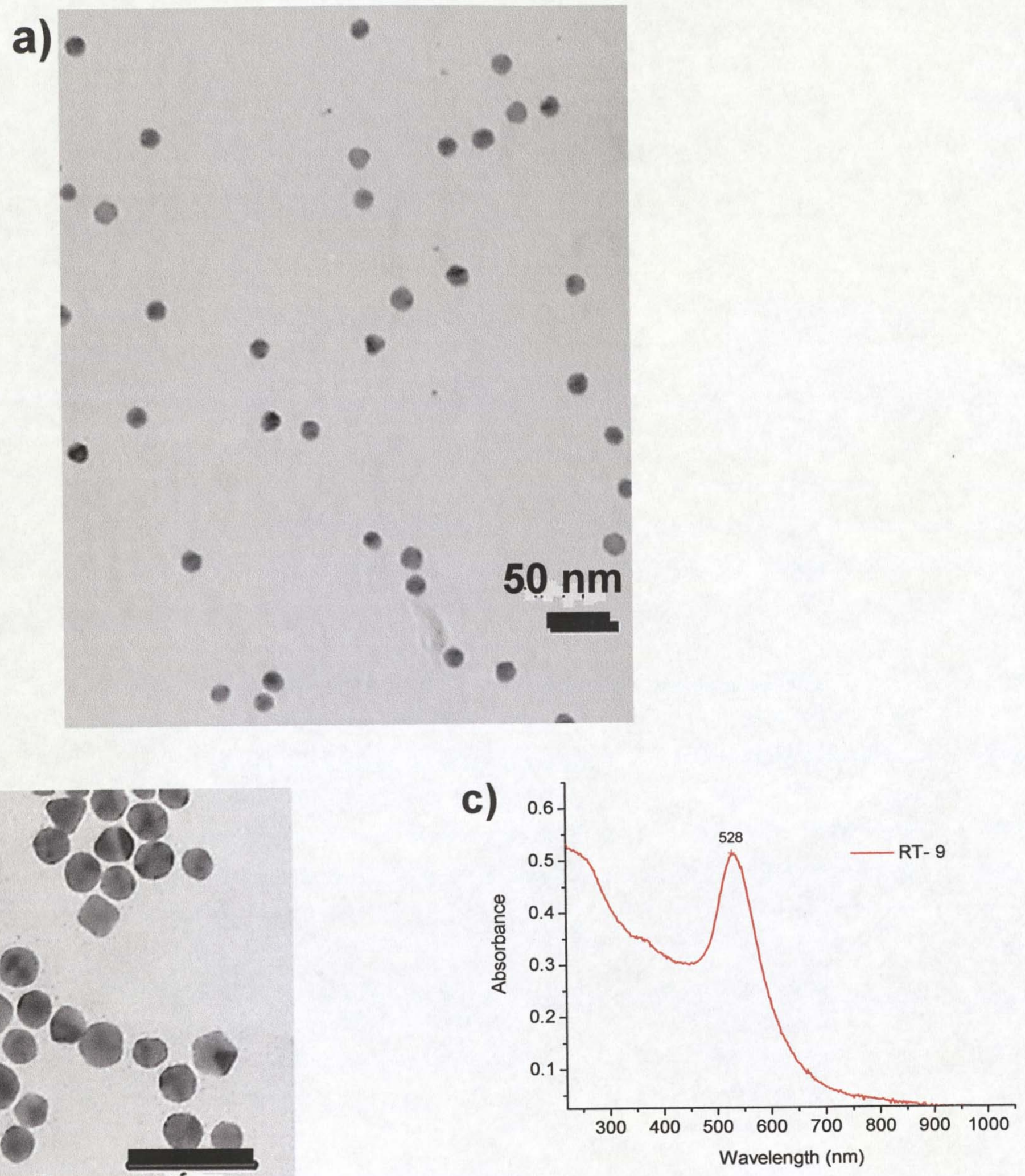

Figure 11. TEM image of a) RT-8 MPCs (PEG-COOH 6) prepared in route A (Figure 9) and b)PEGylated Au-MPCs prepared via synthetic route B in Figure 9 (RT-9) and c) the UV-vis spectrum of RT-9 MPCs (Table 1).

3.2.1.5 Amine functionalized PEGylated Au-MPCs (RT-10)

Addition of amine terminated PEG ligand **10**, following the methods described above proved unsuccessful. This is because the ligand contains thiol and amine groups both having affinity for gold. When added to gold nanoparticles, the ligand links nanoparticles together resulting in irreversible nanoparticles aggregation. To address this challenge, we have developed a simple protocol which takes advantage of using the monohydroxy thioalkylated ligand **3a** as a co-stabilizer for the formation of amine functionalized particles of which the density of amine functionality can easily be controlled such that up to 70 % amine functionalisation is achievable. A scheme for the preparation of amine functionalized Au-MPCs is shown in Figure 12.

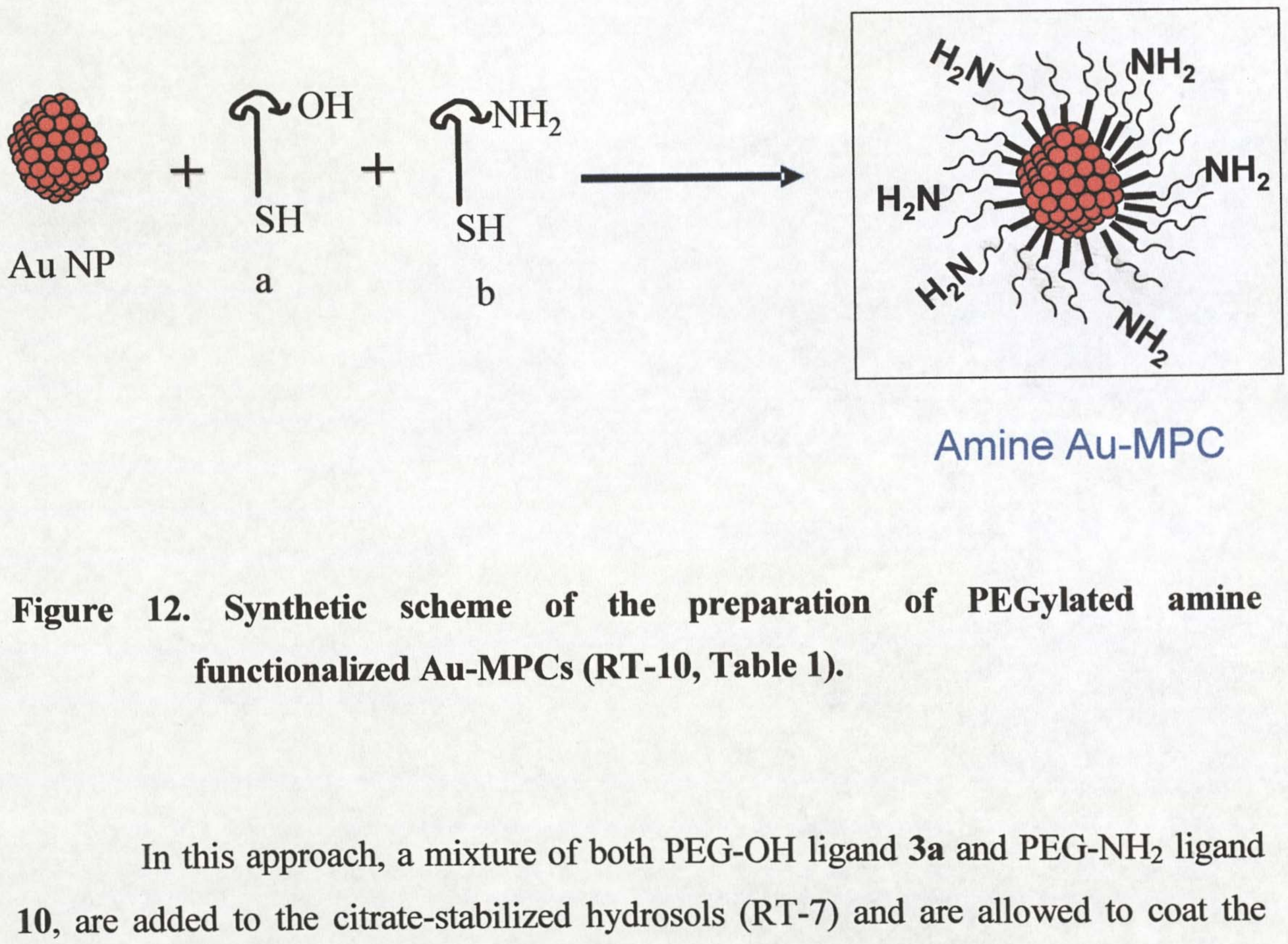

Figure 12. Synthetic scheme of the preparation of PEGylated amine functionalized Au-MPCs (RT-10, Table 1).

In this approach, a mixture of both PEG-OH ligand **3a** and PEG-NH_2 ligand **10**, are added to the citrate-stabilized hydrosols (RT-7) and are allowed to coat the particles in such a way that PEG-OH molecules significantly stabilize the particles in comparison to using PEG-NH_2 alone. Through this strategy it is possible to selectively attach a defined proportion of amine functionalities to the nanoparticles surface by varying the ratio of PEG-OH to PEG-NH_2.

The resulting amine particles can be easily purified, dried and manipulated. These particles have to be stored in suitable vials to minimize their non specific interaction with Eppendorf tube walls. However, particles with less amine loading (~ 30 % amine) do not show any non-specific interaction and are potential candidates for use in conjugation experiments to be discussed in chapter 5. This approach not only opens a simple functionalisation route to these special hydrophilic Au-MPCs but also leads to particles that are stable in biological environment and harsh conditions. The TEM of these particles is shown in Figure 13a and they measure 14.1 ± 1.8 nm. Their UV-vis spectrum with a sharp plasmon absorption band (λ = 528 nm) is shown in Figure 13b. Generally, the particles are uniform and reasonably monodisperse.

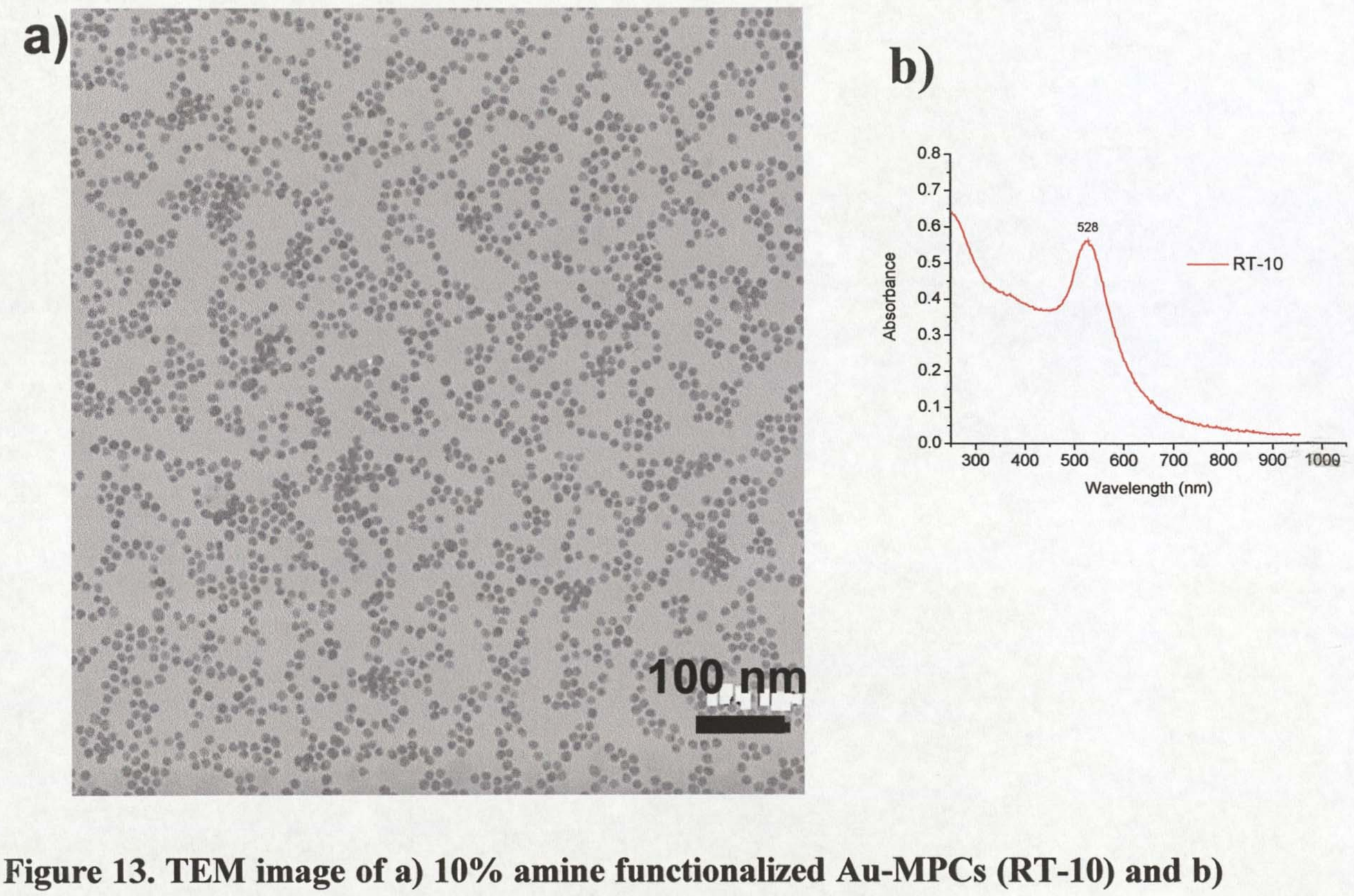

Figure 13. TEM image of a) 10% amine functionalized Au-MPCs (RT-10) and b) the corresponding UV-vis spectrum.

3.2.1.6 Reduction with propanol (RT-11)

A synthetic scheme for the preparation of Au-MPCs (RT-11) via propanol reduction route is given in Figure 14 below.

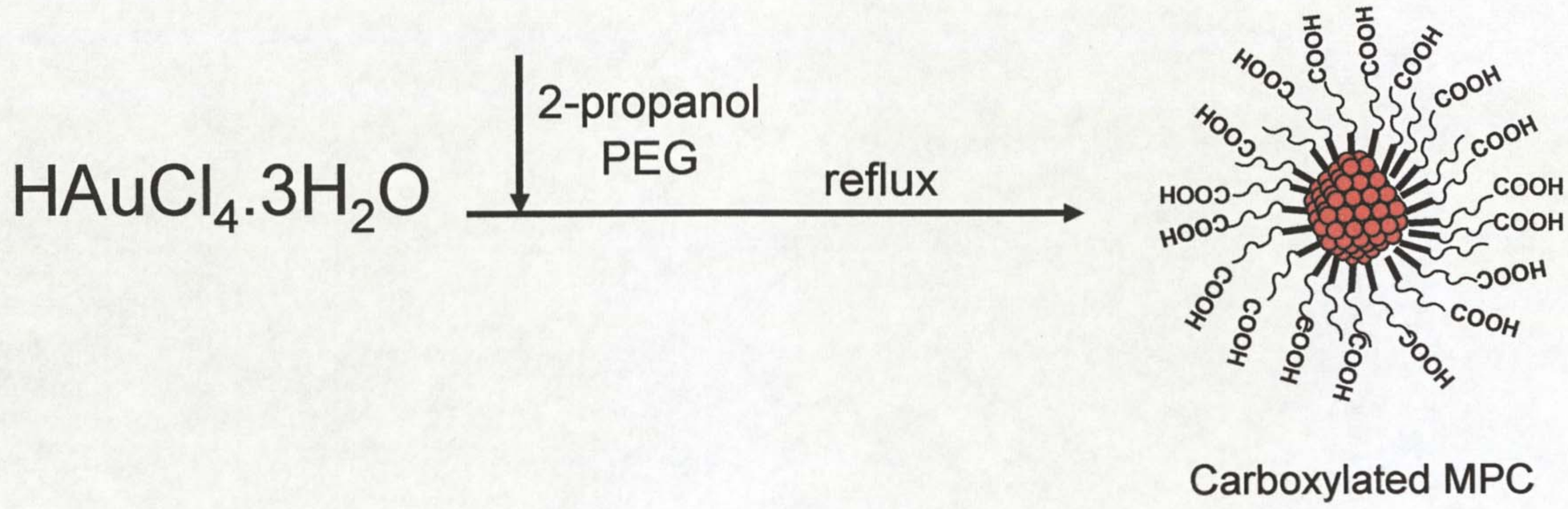

Figure 14. Reaction scheme for the preparation of carboxylated Au-MPCs (RT-11) via propanol reduction route.

Alcohols are commonly used as reducing agents for the formation of metal nanoparticles.[53] We attempted to use propanol as a reducing agent for the formation of PEGylated Au-MPCs as outlined in Figure 14. To achieve this, a mixture of chloroauric acid and PEG ligand **6c** (experimental section page 105) in iso-propanol was heated under reflux for 10 min. The resulting particles showed a red shifted sharp plasmon absorption band at around 540 nm in the UV-vis spectrum (Figure 15a) which clearly indicated the formation of larger nanoparticles. TEM analysis of these particles revealed the formation of particles measuring 50.8 ± 8.5 nm. These particles had different morphologies as shown in Figure 15b and isolated shapes are shown in Figure 15c. As discussed before, it is known that as the particle size increases above 30 nm, particles tend to deviate from spherical to adopt different shapes, and reaction parameters can be varied to obtain shape controlled synthesis of metal nanoparticles.[62] Even though the spherical particles account for bigger ratio, triangular, hexagons, rectangular shapes were produced which are easily identifiable.

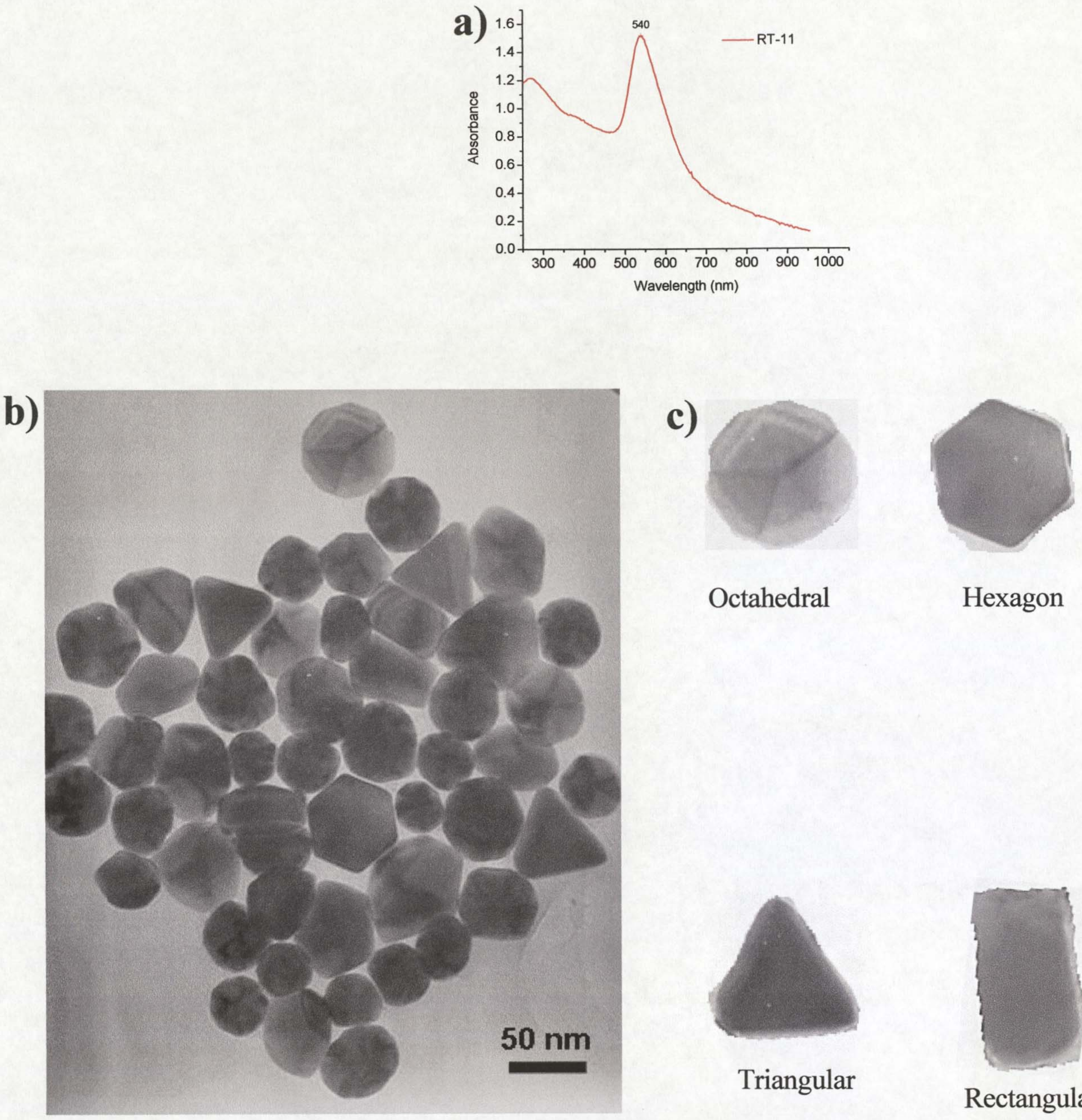

Figure 15. UV-vis absorption spectrum of gold nanoparticles produced via propanol reduction route (RT-11) (a) and the TEM image of the RT-11 (50.8 ± 8.5 nm) (b) selected shapes prepared by the propanol reduction approach (c) (Table 1).

3.2.1.7 Optical properties of PEGylated Au-MPCs

Generally there are many literature methodologies, as discussed in the introduction, leading to the formation of Au nanoparticles of different size and shapes. Of particular importance for this study is to exploit the optical properties of Au/Ag nanoparticles for number of biological applications to be discussed in chapter 5. These properties are strongly dependent on the particles' size and shape. As shown above, functionalized PEGylated MPCs can be easily prepared exhibiting different surface plasmon resonance (SPR) bands. Size dependant optical properties of Au-MPCs prepared in this study are presented in Figure 16 ranging from small particles with a plasmon absorption band at around 512 nm to those prepared by propanol reduction route with an absorption band at around 540 nm.

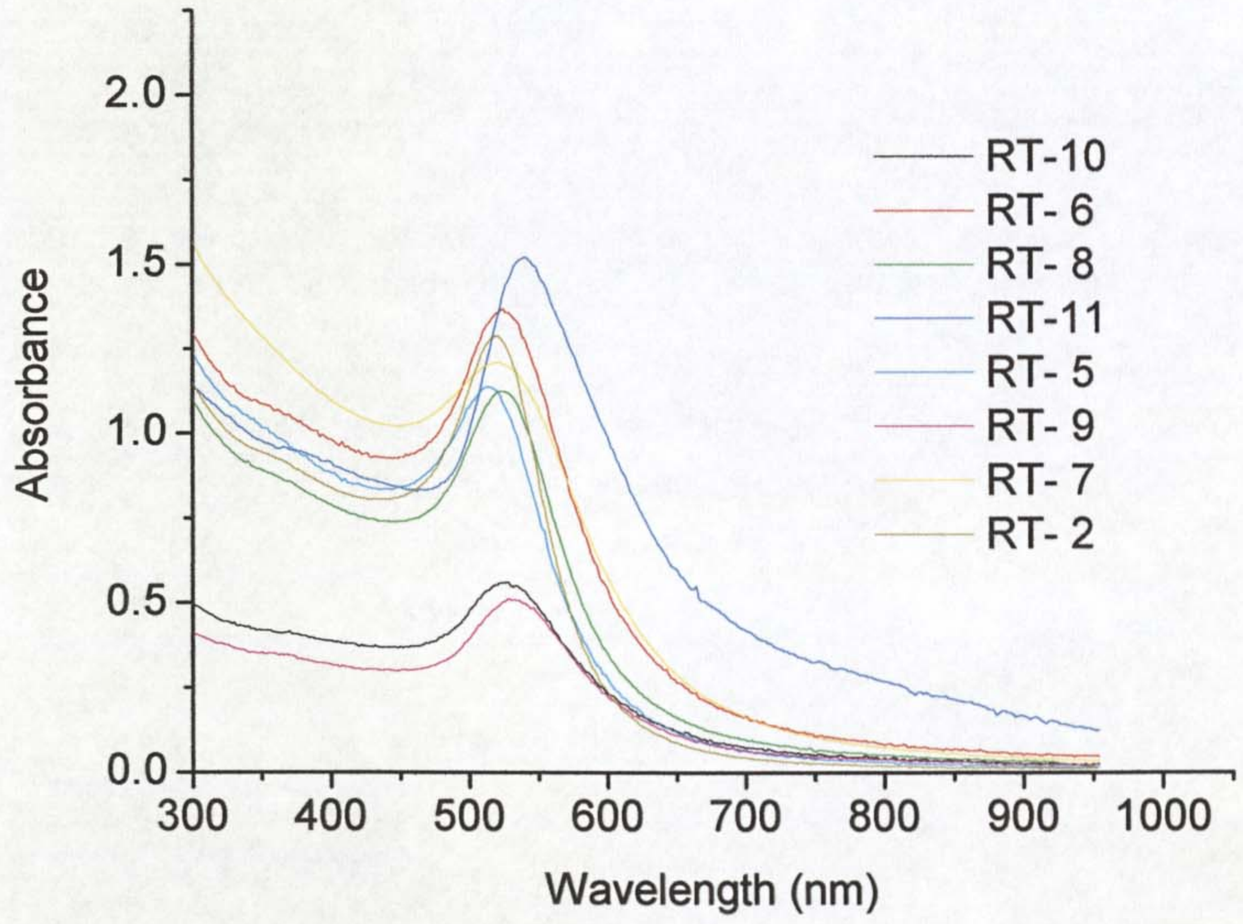

Figure 16. UV-vis absorption spectra of PEGylated Au MPCs based on different synthetic protocols showing size dependant surface plasmon resonance (SPR).

It should be pointed out however, that, the optical properties of citrate stabilized Au hydrosols can be fine tuned across the spectrum, simply by changing the citrate to Au molar ratio during reduction and hence their size. Thus, PEGylated Au-NPs having unique optical properties can be manufactured. Apart from using citrate particles which are difficult to prepare with diameters less than 10 nm, borohydride reduced particles of about 5 nm can be prepared in the same fashion in aqueous solution.

3.2.1.8 PEGylated Au-MPCs summary

We needed to develop functionalized particles, which could easily be manipulated and further functionalized without loss of stability and solubility since this is very important if biological applications are envisaged. We have tested the stability of all PEGylated Au-MPCs (presented in Table 1, quantitative results not shown) under conditions likely to be encountered in a physiological environment (such as high electrolyte concentrations, varied pH ranges) and these MPCs are very stable at high NaCl (>3M) concentration and at pH ranging from 1-14 irrespective of the length of the ligand used. These particles are particularly attractive, easily manipulated and can be used under extremely hash conditions, even at conditions requiring the use of organic solvents. As an overview, we have exploited different synthetic methodologies leading to the formation of size-selective Au-MPCs. The smaller particles (~ 3nm) were prepared by either single-phase reduction method (RT-1) or by common two-phase solution approach (RT-4). The two-phase approach employing TOABr stabilised precursor particles allows the production of particles with diameters of around 6 nm (RT-3) and they are generally smaller than MPCs derived from the borohydride precursors which allow the production of MPCs with diameters of about 7 nm (RT-6). It was noted that to obtain a narrow size distribution for the production of these MPCs (RT-3 or RT-6), it is essential that their precursors are practically uniform, even though size separation by centrifugation or using chromatographic techniques can be performed. The need for precursor particles with narrow size distribution was also a prerequisite for the citrate derived MPCs (RT-8). The propanol reduction approach (RT-11) is particularly attractive for the preparation of aqueous MPCs of varied

morphologies and centrifugation or chromatographic techniques can be applied for separation.

The reactivity of MPCs depends on monolayer packing density and for many applications, it is important to control the functional moieties on the cluster surface. However, this is generally a great challenge since the attachment of ligands to the cluster surface depends on many factors such as ligand type, size and the nature of MPCs core diameter. Nevertheless, place-exchange reactions [63] and *in-situ* preparation [64] of functionalised mixed monolayer clusters can be achieved. In particular, a well defined number of capping ligands per nanoparticle was achieved by Alivisatos *et al.* [65] in which nanoparticles with a defined number of DNA strands are separated using gel electrophoresis [66] while Levy *et al.* [67] recently reported a generic approach to monofunctionalisation of peptide capped gold nanoparticles based on immobilized metal ion affinity chromatography.

To estimate the average number of thioalkylated PEG-ligands on MPCs clusters, an elemental analysis was performed using ICP-AES. For a typical preparation of PEGylated MPCs (RT-7) a composition of gold = 85% and sulphur = 0.5% was found to give an estimation of 3000 PEG ligands per particle. A complete analysis was extracted from the following references. [68-70]

To prepare amine functionalized MPCs (RT-10), the molar ratio of both PEG-OH and PEG-NH_2 was varied to obtain stable mixed monolayer MPCs. In general, we have developed facile functionalisation approach to Au-MPCs either by two-phase transfer approach or by direct addition of PEGylated thiols to bare particles (borohydride or citrate stabilised) for the formation of the desired MPCs. The mixed monolayer strategy developed for amine functionalisation is particularly attractive, and was later applied to the introduction of water insoluble species to the MPCs ligand shell such as calixarene, to be discussed in chapter 4. [71]

The rationale in the design of the PEGylated system was also designed to address in particular the stability and functionality of silver nanoparticles, since Ag is known for its propensity to oxidatively corrode and aggregate [49,51] in electrolyte solution. In the next section such experiments which have been carried out to address the stability issues related to Ag-MPCs are discussed.[54]

3.2.2 Synthesis of Ag-MPCs [54]

To prepare Ag-MPCs and hence to address the question of stability and functionality, PEG-OH **3a**, PEG-NH_2 **10** and penta-peptide CALNN **11** ligands (chapter 2 and in experimental section) were used modifying common literature methods for the preparation of Ag nanoparticles of different size. To compare the properties of both CALNN and PEG for their ability to produce stable Ag-MPCs, first of all, both molecules possess a terminal thiol that chemisorbs to the Ag surface. In the case of the peptide, the positive charge of the N-terminal amino group may facilitate attachment to the negatively charged nanoparticle surface. Secondly, interchain interactions play an important role in maintaining a compact ligand shell. For the peptide this is accomplished by hydrophobic interactions between the side chains of alanine and leucine and hydrogen-bonding between the backbone amides. Combinatorial work shows that hydrogen-bonding between the hydrophilic side chains of the terminal asparagines may also be necessary to maintain the integrity of the ligand shell. [52] For the thioalkylated polyethylene glycol we have discussed in chapter 2 that this is accomplished by hydrophobic interactions between the undecane chains. Finally, water solubility is provided by the outer surface of the ligand shell. For the peptide this consists of the hydrophilic side chains of the asparagines and the C-terminal carboxylic acid. Thioalkylated polyethylene glycol-stabilized particles are made water-soluble by the tetraethylene oxide region and the terminal hydroxyl or amino groups.

Synthesis of Ag nanoparticles using these ligands is discussed briefly prior to stability studies. Silver nanoparticles prepared are listed in Table 2.

3.2.2.1 General Preparation of Ag nanoparticles (RT-12 to 20)

Citrate can be used to stabilize silver nanoparticles in aqueous solution by reducing $AgNO_3$ salt with $NaBH_4$ in the presence of tri-sodium citrate to give yellow aqueous silver nanoparticles, with core diameters controllable by varying the reaction parameters such as mixing rate, temperature and activity of the borohydride solution. We have followed the literature protocol [72] for the synthesis of electrostatically stabilised silver nanoparticles of two different sizes (8 nm for RT-12 and 14 nm for RT-14). These particles were used as building blocks for the construction of Ag-MPCs (RT-13 and RT-15) by simply adding an aqueous solution of CALNN ligand to the citrate stabilised Ag particles and allowing the mixture to sit to room temperature and particles were purified from excess CALNN by centrifugation to provide stable Ag-MPCs (RT-13 and RT-15) (Table 2).

Apart from using citrate stabilised particles, we have also employed a common two-phase approach similar to the synthesis of Au-MPCs. In this case, Ag^+ ions are transferred to the organic phase (toluene) by phase transfer catalyst (TOABr) followed by reduction with aqueous borohydride in organic phase. In this transfer reaction, there is no precipitation of insoluble AgBr formed and it is believed that first the aqueous negatively charged AgBr is formed at the initial stage of the reaction then followed by its transfer by TOABr to organic phase, where the colloid (AgBr) is further stabilised by excess bromide ions followed by reduction with aqueous BH_4^-.

The common two-phase approach was followed, to stabilize the particles with CALNN. This was achieved by combining an aqueous solution of $AgNO_3$ and a toluene solution of phase transfer TOABr to establish a two-phase solution system, followed by CALNN addition to the two phase mixture. This is then followed by silver ion reduction in the presence of CALNN by addition of aqueous BH_4^-. The Ag nanoparticles are initially stabilised by phase transfer catalyst and upon shaking, they are then allowed to interact with CALNN and then followed by transferring Ag nanoparticles to water by phase separation and filtering the particles to remove any insoluble material and further purified by centrifugation to obtain Ag-MPCs (RT-16).

The above two phase approach was also applied for the preparation of decane- or dodecane thiol stabilised Ag-MPCs (RT-17). In this case Ag^+ ions are transferred to the organic phase in the two-phase (water-chloroformic) solution mixture by TOABr and then separated from aqueous solution. Aqueous BH_4^- is then added to the organic phase in the presence of decane-or dodecanethiols to reduce Ag(I) to metallic Ag(0) yielding the desired Ag-MPCs (RT-17).

The decane-or dodecanethiol stabilised Ag-MPCs, (RT-17) were later used to explore place-exchange reaction for the generation of RT-18, and 19 Ag-MPCs (Table 2). This was achieved in particular by treating hexane solution of dodecanethiol stabilised particles with a methanolic solution of PEG-OH **3a** (chapter 2 and in experimental section). By shaking the mixture simply allows an exchange reaction to take place within minutes and the particles tend to precipitate out of the solution. Assuming that a complete exchange reaction took place, the particles were then centrifuged allowing the alkanethiols to remain in the supernatant. At the end, the centrifuged particles are transferred to buffer solution and further filtered to remove any insoluble material to obtain PEGylated Ag-MPCs (RT-18). The amine functionalized PEGylated Ag-MPCs (RT-19) were obtained in a similar fashion to PEG-OH only that instead of dodecanethiol stabilised particles, decane-stabilised particles were exchanged with PEG-NH_2 **10** and both RT-18 and RT-19 particles were further purified by size-exclusion chromatography using Sepharose-CL-6B as stationary phase and water as mobile phase to remove any excess PEG ligands.

Two-phase solution synthesis using negatively charged AgBr hydrosols approach [73] was explored to prepare Ag-MPCs (RT-20). This approach takes advantage of synthesizing stable negatively charged AgBr hydrosol by adding excess of bromide to a dilute aqueous solution of silver nitrate and the resulting negatively charged AgBr hydrosols is transferred to organic phase (toluene) by TOA^+ cations. The Ag (I) ions are then reduced by aqueous BH_4^- in the presence of passivating ligands PEG-OH or PEG-NH_2 to yield Ag-MPCs (RT-20 and RT-21 respectively). In the previous two phase system discussed above, the aqueous AgBr colloid is transferred by TOABr to the organic phase where it is stabilised in organic phase by

adsorption of excess bromide ions and then followed by aqueous BH_4^- reduction. In this case, the aqueous AgBr colloid is "uncoupled" from its transfer to organic phase to generate first stable aqueous negatively charged AgBr colloids, which are then transferred to organic phase by TOA^+ and then reduced. Schiffrin's group developed this strategy so that each synthetic step can be easily controlled.[73]

TEM images of water-soluble peptide-and PEG-stabilized Ag-MPCs prepared as described above are shown in Figures 17 and 18. Figures 17A and B show CALNN-stabilized Ag nanoparticles derived from citrate-stabilized nanoparticles. [73] The citrate-stabilized nanoparticles were synthesized under slightly different reaction conditions to give two different sizes. The particles in Figure 17A (RT-13) measure 8.2 ± 2.0 nm in diameter and are derived from citrate-stabilized nanoparticles (RT-12) measuring 8.1 ± 1.6 nm in diameter. The particles in Fig. 17B (RT-15) measure 16.3 ± 4.5 nm in diameter, and their citrate-stabilized precursors (RT-14) measured 15.3 ± 6.4 nm in diameter. While it appears that the addition of CALNN to 15.3 nm citrate-stabilized particles has tuned the size distribution (standard deviation 28% of mean compared to 42%), this is merely a result of the centrifugation process used to purify the particles from excess peptide. A number of particles less than 10 nm in diameter remained in solution after a 30 minute spin at 10000 g, and, as a result, the peptide-stabilized nanoparticles appear to have a smaller size distribution than the citrate-stabilized particles which cannot be centrifuged without inducing irreversible aggregation. It is, however, an indication that the rather broad size distribution, at least compared to Au, can be focused by varying the centrifugation conditions. The particles in Fig. 17A are well-separated and spherical in shape. The particles in Figure 17B are also well-separated but there is not the same uniformity in shape. After the initial nucleation of 1-2 nm Ag clusters, the mechanism for particle growth is aggregation.[74] As the particles get larger the collisions are more likely to result in ellipsoids than spheres as discussed for Au nanoparticles.

The particles in Figure 17C (RT-16) are stabilized by CALNN and were produced in a two-phase synthesis. They measure 8.2 ± 2.4 nm in diameter. The particles are well-separated and, much like the RT-13 CALNN-stabilized particles in

Figure 17A, are predominantly spherical in shape. Figure 17D (RT-17) shows an array of nanoparticles assembled from an organic solution of dodecanethiol-capped Ag nanoparticles with a diameter of 5.5 ± 0.9 nm. The water-soluble particles produced by ligand-exchange of the alkanethiol with PEG-OH **3a** are shown in Figure 17E. The particles measure 5.3 ± 1.0 nm in diameter, are well-separated, and retain the spherical shape of the alkanethiol-capped nanoparticles. Ligand-exchange of decane-and dodecanethiol for PEG-NH_2 and PEG-OH, respectively, does not affect the particle size or size distribution and the same trend was observed when the two-phase approach was employed for gold MPCs. Ag MPCs stabilized by PEG can also be obtained with a very small size distribution (<10%) by narrowing the size distribution of either decane- or dodecanethiol stabilised particles in organic phase prior to ligand exchange.

A representative TEM for the PEGylated Ag-MPCs (RT-19 and RT-20) prepared via two-phase stable negatively charged AgBr route are shown in Figure 18. The particles are very uniform measuring 4.5 ± 0.9 nm particles after multiple centrifugation steps, to obtain MPCs with narrow size distribution. The PEG-OH and PEG-NH_2 particles are generally indistinguishable in size.

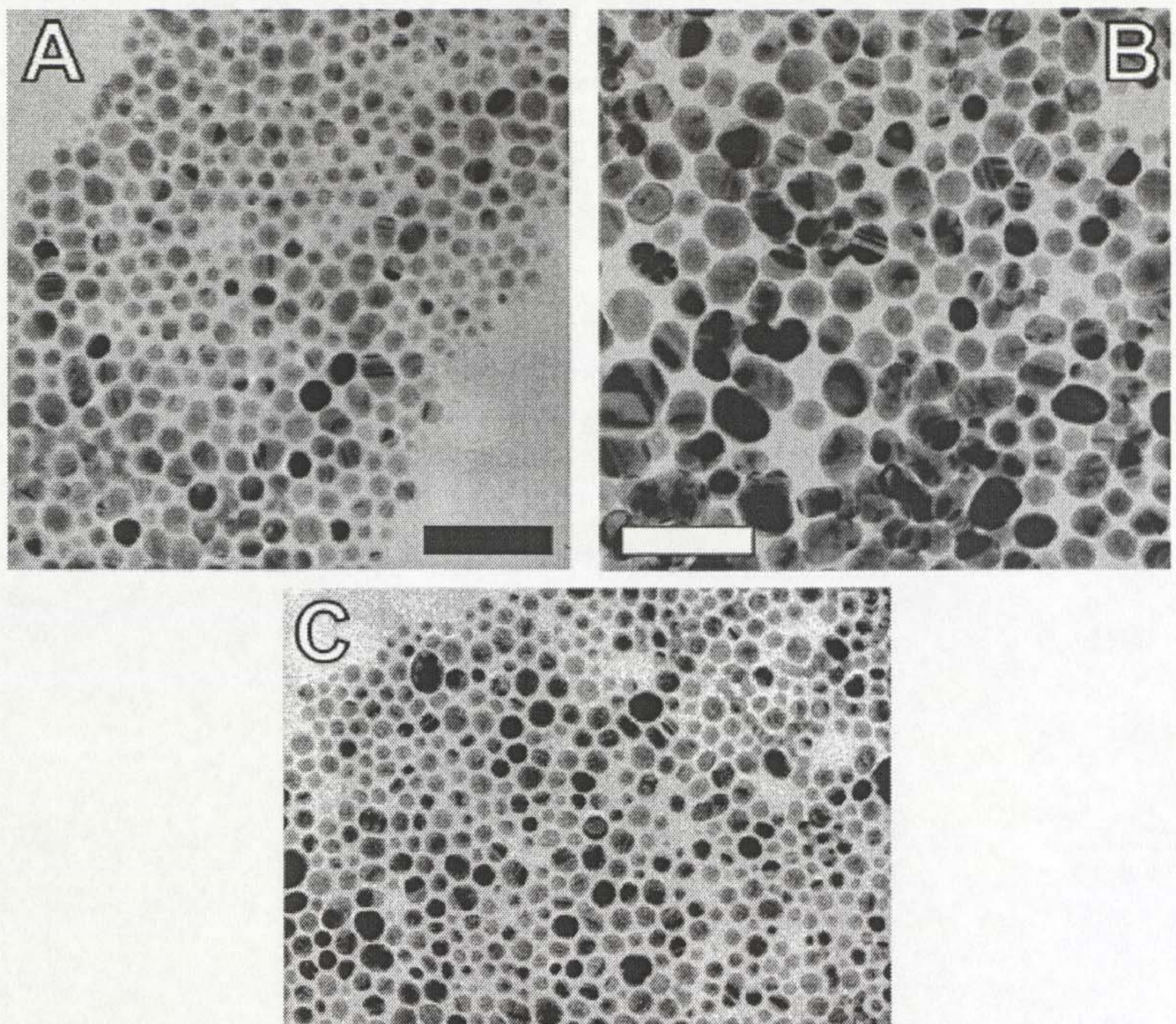

Figure 17. Transmission electron micrographs of (A) RT-13 (8.2 ± 2.0 nm) and (B) RT-15 (16.3 ± 4.5 nm) CALNN-stabilised Ag nanoparticles derived from citrate-stabilised Ag nanoparticles, (C) RT-16 (8.2 ± 2.4 nm) CALNN-stabilised Ag nanoparticles produced in a two phase synthesis, (D) RT-17 (5.5 ± 0.9 nm) dodecanethiol-stabilised Ag nanoparticles, and (E) RT-18 (5.3 ± 1.0 nm) PEG-OH stabilized Ag nanoparticles derived from the RT-17 nanoparticles via ligand exchange. PEG-NH_2 nanoparticles are not distinguishable by TEM from the PEG-OH nanoparticles shown. All scale bars are 50 nm (Table 2).

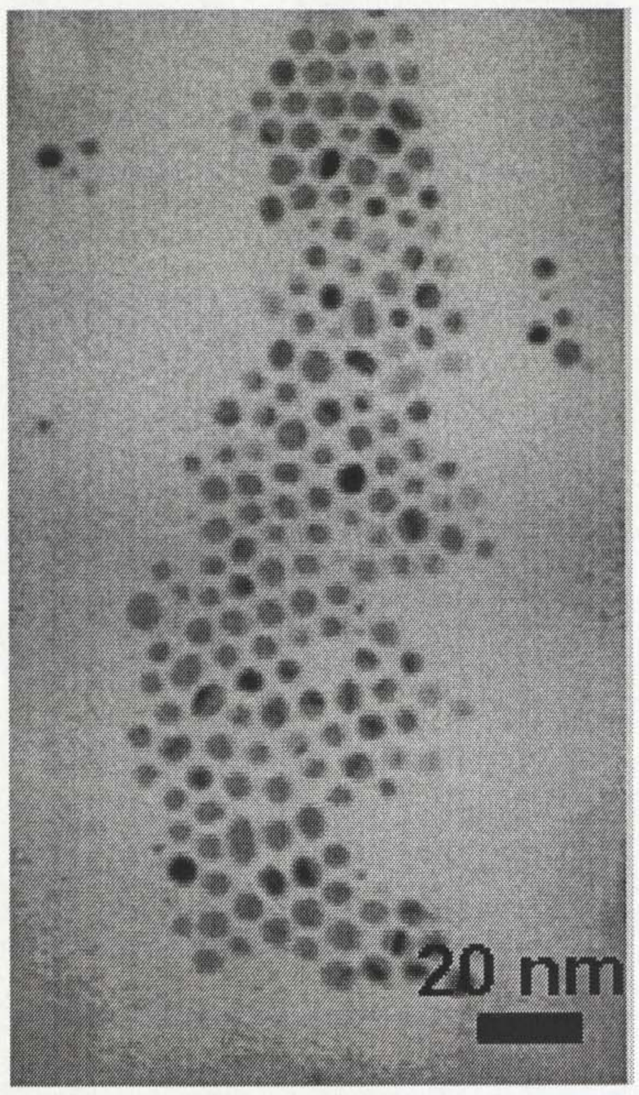

Figure 18. A representative TEM image of RT-20 and 21 Ag-MPCs prepared via the two-phase AgBr route measuring 4.5 ± 0.9 nm (Table 2).

3.2.2.2 Stability Studies of Ag-MPCs

The stability studies of silver nanoparticles were carried out to determine the usefulness of these particles in biological applications in addition to their water solubility. For that purpose, 1.5 ml solutions of CALNN-stabilized nanoparticles were centrifuged at 18000 g for 90 minutes and the supernatant was removed. To determine nanoparticle stability with respect to the concentration of NaCl, the particles were re-dispersed in 1.5 ml of 10 mM Tris buffer at pH 8. Purified PEG-OH-stabilized Ag nanoparticles were used without further processing steps. The desired NaCl concentrations were achieved by adding aliquots of 2.5 M NaCl in ultrapure water to 100 μL of the buffered nanoparticle solution. To determine nanoparticles stability with respect to pH, the particles were re-dispersed in 150 μL of ultrapure water. A 10 μL aliquot of the concentrated nanoparticle solution was diluted in 90 μL of different buffer solutions at pH 2 through 12.

The pH of purified PEG-OH- and PEG-NH_2-stabilized Ag nanoparticle solutions was adjusted by adding concentrated HCl and NaOH. The short-term stability of the particles was evaluated by taking absorption spectra 10 minutes after the pH and NaCl concentration of the nanoparticle solution was adjusted. The long-term stability was evaluated by taking additional spectra after 24 hours.

Their stability in high ionic strength environments is shown in Figure 19. The normalized absorbance spectra of 16.3 nm (RT-15) CALNN-stabilized nanoparticles at various concentrations of NaCl are shown in Figure 19A, displaying the characteristic plasmon band of Ag nanoparticles at 420 nm. Up to a NaCl concentration of 500 mM, the spectra are indistinguishable. At 1 M NaCl there is a slight increase in the absorbance between 500 and 700 nm in specific cases. This absorbance feature is indicative of the onset of particle aggregation and is a result of plasmon coupling between aggregated nanoparticles. The aggregation could be caused by screening of the nanoparticle surface charge. Reduction of the electrostatic repulsion allows the attractive van der Waal's forces to induce particle aggregation. The slight increase in the absorbance feature between 500 and 700 after 24hrs disappeared and its loss is accompanied by a slight decrease in absorbance. This behavior can be explained as aggregation of the largest particles in solution (15% of the particles are greater than 20 nm in diameter). As the NaCl concentration increases, so does the degree of electrostatic screening. Since the van der Waal's forces are a function of size, the largest particles aggregate first, similar to the size-selective precipitation procedure used to isolate fractions of monodisperse nanocrystals in non-polar organic solvents. Thus, the size distribution of water-soluble Ag nanoparticles can be narrowed by salting-out the largest particles. In combination with the above mentioned separation of the smallest nanoparticles via centrifugation, the size distribution of CALNN-stabilized Ag nanoparticles can be considerably narrowed. For 16.3 nm CCALNN-stabilized nanoparticles there is no indication of particle aggregation at NaCl concentrations up to 1 M, as shown in Figure 19B. While the second cysteine was intended to increase particle stability by making it more difficult for the peptide to detach from the nanoparticle surface, in this case it may have been the added length that provided an increased steric barrier to particle aggregation.

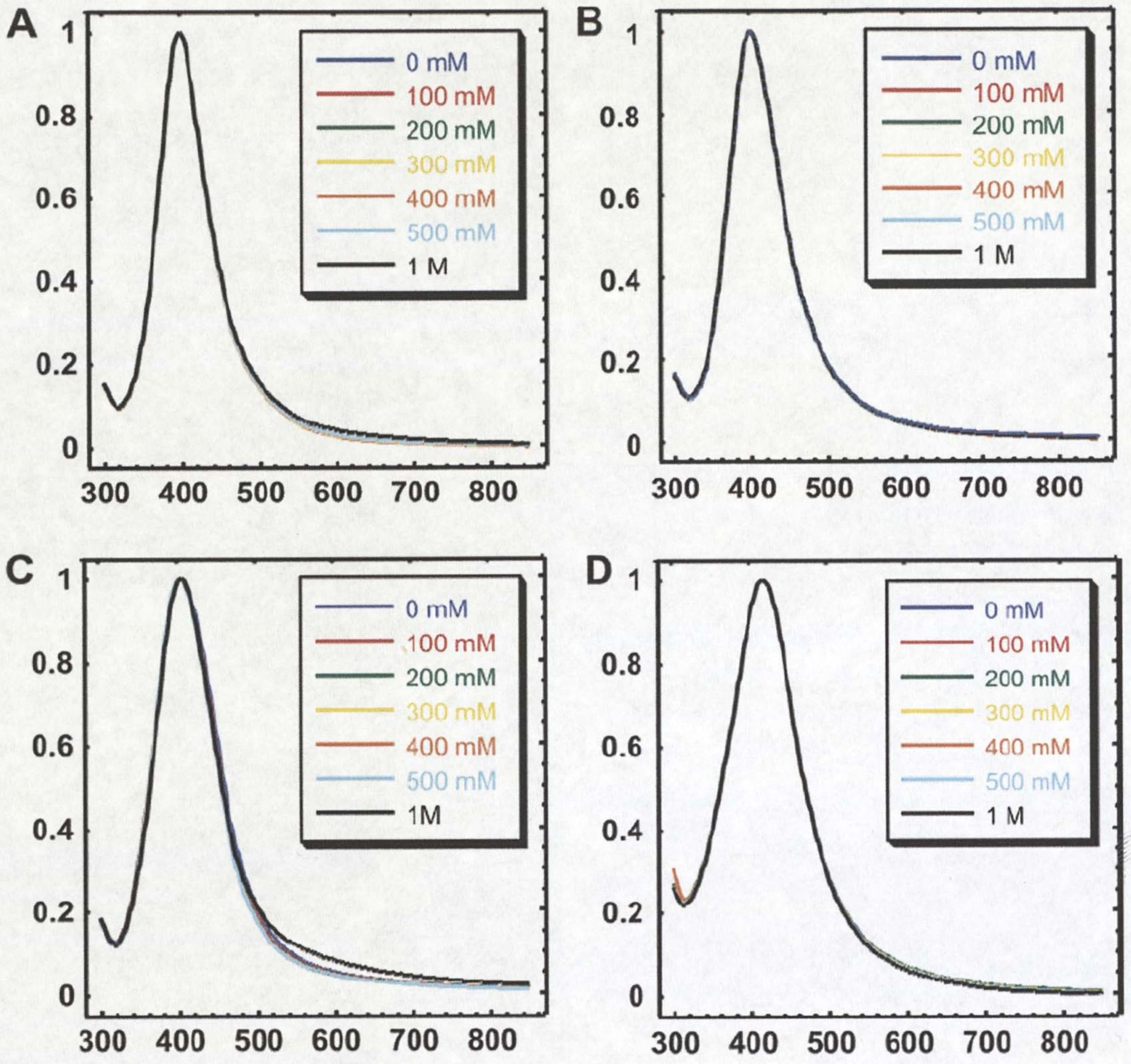

Figure 19. UV-vis study of nanoparticle stability as a function of NaCl concentration for (A) 16.3 nm CALNN-stabilised Ag nanoparticles (RT-15), (B) 16.3 nm CCALNN-stabilised particles (RT-15), (C) 8.2 nm CALNN-stabilised particles (RT-16) and (D) 5.3 nm PEG-OH-stabilised particles (RT-18), PEG-NH_2, particles exhibit the same behavior (Table 2).

The 8.2 nm CALNN-stabilized particles (RT-16) produced in a two-phase synthesis also show increased absorbance between 500 and 700 nm (Figure 19C). It is proposed that the aggregation in this case is not based on the particles size salting-out since the particles are small (8.2 nm) and have narrow size distribution. In this case it is likely that the nanoparticles are insufficiently stabilized with peptides. Upon introduction of the reducing agent to the two-phase mixture, the Ag nanoparticles are initially present in the organic phase and stabilized by the phase-transfer catalyst. Vigorous mixing brings the nanoparticles into contact with the peptide, and they are eventually transferred into the aqueous phase. This does not guarantee a complete ligand shell of peptide around the nanoparticles but simply a sufficient number of peptides to make them water-soluble. Attempts to fill-in any gaps on the particle surface by incubating purified particles with excess peptide did not have a noticeable effect on particle stability.

For 5.3 nm PEG-OH-stabilized nanoparticles (RT- 18), there is no indication of particle aggregation at NaCl concentrations up to 1 M, as shown in Figure 19D. Purified PEG-NH_2 stabilized particles (RT-19) were stable in a 2 M NaCl buffer used for size-exclusion chromatography. Not only that the thioalkylated polyethylene glycol act as an excellent protecting ligand but the small size of these particles (5 nm) also results in a relatively weak attractive force. PEG-OH- and PEG-NH_2 stabilized nanoparticles (RT-18 and 19) are stable at any pH between 1 and 14.

Nanoparticle stability as a function of pH is shown in Figure. 20. Evidence of particle aggregation is present in the UV-vis spectra of both CALNN- and CCALNN-stabilized Ag nanoparticles at pH 2 and 3, as shown in Figures 20A and B, respectively. The spectrum of CALNN-stabilized nanoparticles contains the slight increase in absorbance between 500 and 700 nm that was seen at 1 M NaCl, while the initial spectrum of the CCALNN particles shows extensive aggregation, as evidenced by peak shifting and large shoulders centered between 500 and 600 nm. After 24 hours the particles have completely precipitated out of solution. At pH 4 and above, however, the particles are stable over a 24 hour period. The pK_a of the terminal carboxylic acid of the peptide is 4, and as the pH drops below that the nanoparticles lose their charge, and, hence, their electrostatic repulsion.

Van der Waal's attractions lead to extensive aggregation of all the particles in solution. The differing aggregation kinetics of the two sets of nanoparticles may be a result of differences in peptide packing around the nanoparticle. It is not currently known how the peptides are aligned on the nanoparticle surface, and whether or not an additional cysteine disrupts the potentially efficient packing of CALNN peptides, rendering them slightly less stable at low pH (despite the observation that they appear slightly more stable at high concentrations of NaCl).

UV-vis spectra of the 8.2 nm CALNN-stabilized nanoparticles (RT-16) produced in a two-phase synthesis show a 100 nm red-shift and slightly line broadening at pH 2 and 3 indicative of extensive particle aggregation (Fig. 20 C). There is also increased absorbance between 500 and 700 nm at pH 4 and 5. Over the course of 24 hours all of the particles between pH 2 and 5 precipitated out of solution. For reasons discussed above, the aggregation at pH 2 and 3 is expected. The aggregation at pH 4 and 5 is further evidence that the two-phase synthesis does not provide a sufficient peptide ligand shell to stabilize the particles in adverse conditions. It is likely that some of the phase-transfer catalyst (TOAB) is still associated with the nanoparticle surface and the ligand shell.[75] This could result in a reduced number of peptides attached to the nanoparticle surface, or a reduction in the overall charge of the ligand shell if the positively charged ammonium groups are able to orient themselves such that they interact with the negatively charged C-terminal carboxylic acid. Nevertheless, PEG-OH **3a** and PEG-NH_2 **10** ligands provided nanoparticles of extreme stability at any pH between 1 and 14. This is particularly attractive since the amine functionality is readily available for further functionalisation of these Ag-MPCs.

In summary, stable water-soluble peptide-stabilised Ag nanoparticles were produced by the addition of CALNN or CCALNN peptide to citrate-stabilised Ag nanoparticles. Both sets of peptide-stabilised particles are stable in 1M NaCl and between pH 4 and pH 12, with only slight differences in the aggregation at low pH and some aggregation of the largest CALNN-stabilised particles in 1M NaCl solution. CALNN-stabilised particles were also synthesized in a two-phase reaction. These particles were stable between pH 6 and pH 12 and up to 1 M NaCl. Particle aggregation at pH 4 and 5 and slight aggregation in 1 M NaCl was believed to be a result of incomplete peptide coverage inherent in the two phase synthesis.

Thioalkylated PEG-OH and amine functionalized thioalkylated PEG-NH_2- stabilised Ag MPCs were produced by ligand exchange of alkanethiol molecules. Both PEG-OH and PEG-NH_2 stabilised Ag-MPCs were also prepared via the negatively charged AgBr route and a proof of a concept was demonstrated that these PEGylated Ag-MPCs are extremely stable in high NaCl concentrations (> 2 M) and between pH 1 and pH 14. This is particularly attractive in view of exploiting the use of Ag nanoparticles for biological applications. These are the key issues needed to be addressed, thus compatibility in biological environment (conferred by CALNN and PEG chains), solubility in water and above all unprecedented extreme stability, which PEGylated Ag-MPCs, allow them to be employed in extreme harsh conditions.

To this end we have manufactured functionalized gold and silver MPCs. Their applications as useful tools in biology will be the subject of chapter 5. In the next chapter, we explore the versatility of PEGylated system to incorporate a non biological recognition motif to the MPCs ligand shell.

3.3 Experimental

3.3.1 Materials

Unless stated otherwise, all reagents were purchased from Sigma-Aldrich (UK) and used without further purification. PEG-OH **3a**, PEG-COOH **6a-c** and PEG-Amine **10** were either prepared following literature methods[53] or purchased from Prochimia (Poland). PEG-OH **3b** and PEG-COOH **6c** were obtained from Dr F. S Kamounah in Copenhagen University (Denmark). CALNN **11** and CCALNN peptides were purchased from Pepsyn Ltd. (Liverpool, UK). The following is a list of the ligands used;

i) Monohydroxy thioalkylated PEG analogs (PEG-OH)

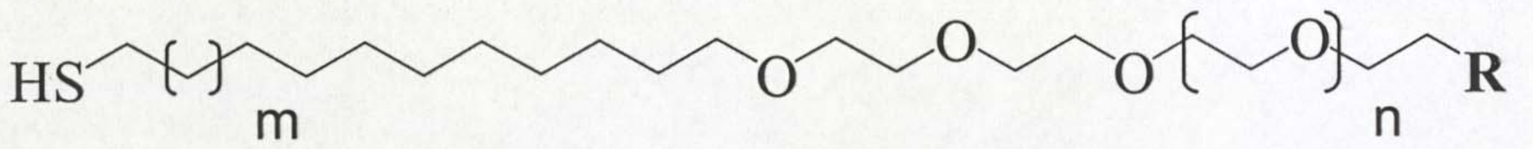

3a (R = OH, m and n = 1)

3b (R = OH, m = 6 and n = 3)

ii) Carboxylated thioalkylated PEG analogs (PEG-COOH)

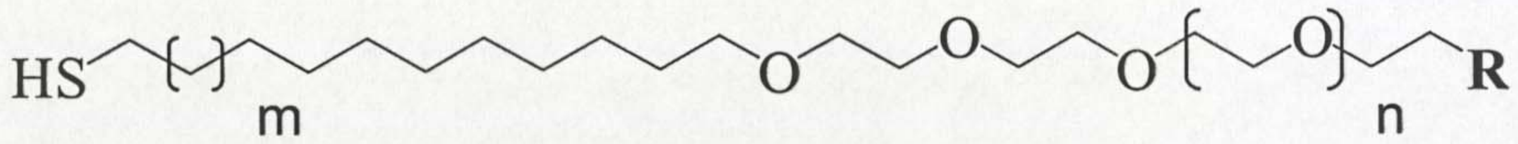

6a (R = OCH_2CO_2H, m = 1 and n = 1)

6b (R = OCH_2CO_2H, m = 1 and n = 3)

6c (R = OCH_2CO_2H, m = 1 and n = 20)

iii) Amine functionalized thioalkylated PEG ligand (PEG-amine)

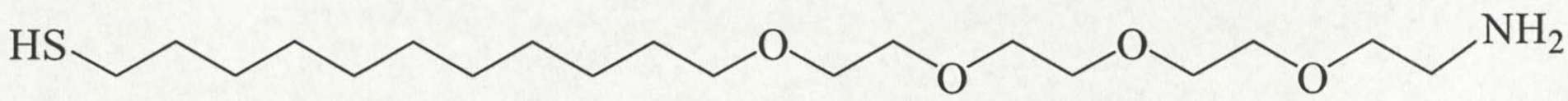

10

iv) Pentapeptide CALNN

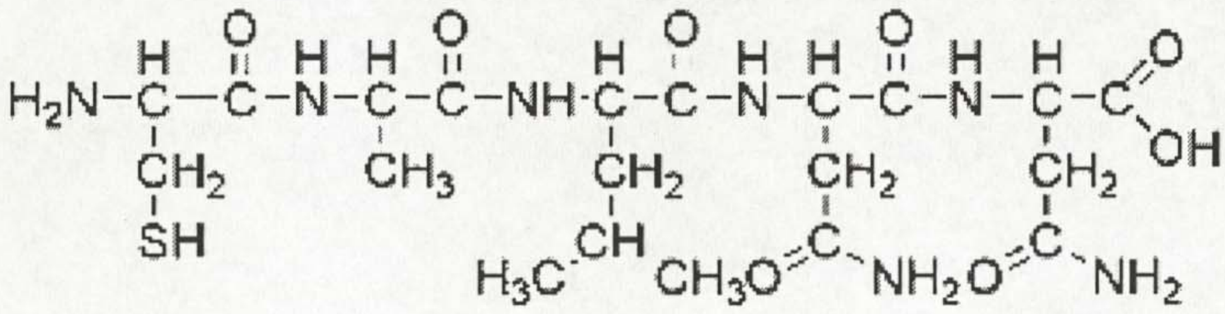

C A L N N

11

C = Cystine, **A** = Alanine, **L** = Leucine, **N** = asparagine

3.3.2 Synthetic procedures

3.3.2.1 Preparation of Au-MPCs (RT-1)

Generally, 35 mg of hydrogentetrachloroaurate trihydrate (chloroauric acid) were dissolved in 2-propanol (50ml) and a small amount of glacial acetic acid (0.5 ml) was also added to prevent thiols from de-protonation. To the stirred solution, was added an alcoholic solution of PEG-COOH thiol **6b** (10mg, 19μmol) and the solution was stirred for a few minutes. A freshly prepared $NaBH_4$ solution (5ml, 0.5M) in methanol was quickly added to the stirred mixture. Upon addition of the reducing

agent, an immediate colour change from yellow to dark brown was observed, and the reaction mixture was stirred for 3h. Then, particles were precipitated by adding excess hexane (200 ml) to the reaction mixture. The supernatant was decanted and the solid product was washed (2 times) with diethyl ether (20 ml) and ethyl acetate (20 ml). The product was re-dissolved in water and further purified by size exclusion chromatography (either Sephadex G-25 or Sephacryl S100HR (Amersham Biosciences) as the stationary phase and milliQ water as the mobile phase).

3.3.2.2 Two-phase (water-toluene) system (RT-2, 3 and 4) [26]

A well established two-phase procedure [26] was followed for the synthesis of these Au nanoparticles. Two approaches were followed; i) an aqueous solution of chloroauric acid (30 ml, 30 mM) was mixed with a tetraoctylammonium bromide solution (80 ml, 50 mM) in toluene to give a two-phase liquid/liquid system. The resulting two-phase mixture was vigorously stirred, allowing a complete transfer of tetrachloroaurate into the organic phase. A freshly prepared aqueous solution of sodium borohydride (25 ml, 0.4 M) was added slowly with vigorous stirring to give a ruby red 5-8 nm TOABr stabilized particles and the mixture was stirred for 3 hrs (RT-2). Then the organic phase was separated and washed once with 0.1M H_2SO_4 (30 ml), 0.1 M NaOH (30 ml) and 5 times with water (50 ml). 7 mg (13 μmol) of PEG-COOH **6b** dissolved in methanol (2 ml) was added to the TOABr solution (20 ml) and stirred for 3 hrs. During stirring, a slight colour change (from wine red to purple) of the solution was noted, which is a clear indication of a beginning aggregation and hence of thiol attachment to the surface of the Au clusters. After 3 hrs, water (10ml) was added and the mixture was shaken vigorously. Consequently, the organic phase became completely colourless while the aqueous phase became deep wine red indicating that gold clusters have been transferred to the aqueous phase (RT-3). The aqueous phase was separated, washed with diethyl ether (3 times, 10 ml) and the particles were further purified by centrifugation (25000g) and re-dispersion of the pellets in water using a refrigerated MIKRO 22 R centrifuge.

ii) For the preparation of small clusters (~ 3nm) (RT-4), the PEG-COOH **6** ligand (7 mg, 16μmol) was added to the intensely orange Au (III) complex (tetraoctylammonium tetrabromoaurate) stirred for 30 min, then followed by fresh $NaBH_4$ (25 ml, 0.5M) addition and the mixture was further stirred for at least 3h. After 3hr, water (15 ml) was added to the mixture and vigorously stirred to allow a complete transfer. The aqueous phase was separated and washed as described for single phase and then purified by size exclusion chromatography.

3.3.2.3 Reduction with borohydride in water (RT-5 and RT-6)[58]

About 375 μL of aqueous 0.1M $HAuCl_4$ plus 500 μL of aqueous 0.2 M K_2CO_3 was added to 100 ml water and the mixture was cooled on ice (4 ^{0}C) and mixed well for 5 minutes. Then 5 ml of $NaBH_4$ (0.5mg/ml) was added in 1ml steps with rapid stirring. A colour change from yellow to reddish-orange was noted during the $NaBH_4$ additions. After complete addition of $NaBH_4$ the mixture was further stirred for 1h on ice. The particles were then filtered (0.45 μm filter Millipore) (RT-5). The resulting particles were converted to PEGylated MPCs by addition of 5mg (9 μmol) of PEG ligand **6b** or other ligands in methanolic solutions and stirring for an additional 3hrs. Then the particles (RT-6) were centrifuged (25000g, 90 min, using a refrigerated MIKRO 22 R centrifuge.

3.3.2.4 Citrate reduction routes (RT-7, 8 and 9)[15,53]

The classical citrate reduction method was followed in two different routes; In route A, an aqueous solution of sodium citrate (10 ml, 17 mM) was added to the boiling aqueous solution of $HAuCl_4$ (180 ml, 0.3 mM) and the reaction mixture was heated under reflux for 30 min. It was then allowed to cool to room temperature, stirred overnight and filtered before use (0.45 μm, Millipore filter). To the resulting citrate stabilized particles (20 ml, 1.8 nM) (RT-7) was directly added an alcoholic solution (200μL) of PEG-COOH ligand *e.g* ligand **6b** (5mg, 9 μmol) and the solution was stirred at room temperature for 3h. Particles were purified by repeated centrifugation (11000 rpm, 12 min) using a refrigerated MIKRO 22 R centrifuge and

further purified by size exclusion chromatography (S-100HR support) to give RT-8 Au-MPCs. Following route A, citrate and gold nanoparticle ratios were varied to obtain the desired gold nanoparticles sizes, *e.g.* using 0.13 ml of 38.8 mM citrate and 5 ml of chloroauric acid yielded 30-40 nm particles.

In route B, the procedure described for the synthesis of Au-MPCs (RT-8) in route A was followed, however, PEG-COOH **6b** legend (5mg, 9 μmol) and citrate (10 ml, 17 mM) were added simultaneously to the refluxing aqueous solution of $HAuCl_4$ (180 ml, 0.3 mM) and the particles were allowed to cool to room temperature and purified as described in route A (RT-9).

3.3.2.5 Amine functionalized PEGylated Au-MPCs (RT-10)

The standard citrate method was followed as described above. To the resulting filtered particles (20 ml, 1.8 nM) was added mixture of PEG-OH **3** (4.5 mg, 12 μmol) and PEG-NH_2 **10** (0.5 mg, 1.3 μmol) in methanol (100 μL) for 10 % amine functionalisation. After stirring for 3h, particles were repeatedly centrifuged 3 times at 11000 rpm for 12 min and re-dispersed in water. To change the amine density, molar ratio of PEG-OH **3** and PEG-NH_2 **10** was varied.

3.3.2.6 Propanol reduction approach (RT-11)

To a solution of chloroauric acid (35 mg, 10 ml iso-propanol) was added PEG-COOH **6b** ligand (2 mg, 3.8 μmol) and the mixture was refluxed for 10 min. The particles formed immediately and were cooled to room temperature and centrifuged at 5000 rpm (using Sigma (1-13) bench top centrifuge) for 10 min and re-dispersed in water.

3.3.2.7 Citrate-stabilised Ag nanoparticles (RT-12 and RT 14)

Citrate-stabilized Ag nanoparticles were synthesized according to a modified version of the procedure published by Jana *et al.* [72] An aqueous solution of $NaBH_4$ (6 ml, 10 mM) was added to 200 ml of a solution of $AgNO_3$ (0.25 mM) and tri-sodium citrate (0.25 mM). The mixture was stirred for 30 minutes, resulting in a yellow colloidal silver solution, and was then left overnight. The average particle size can vary upon slight modifications of the reaction conditions, such as mixing rate, temperature and activity of the borohydride solution. In this case AgNPs with 8 nm size (RT-12) and 16.3 nm (RT-14) were prepared.

3.3.2.8 Peptide-stabilised Ag-MPCs (RT-13, 15 and 16)[54]

Peptide-stabilized Ag nanoparticles were prepared by two different methods. In the first, 1 ml of the citrate-stabilized Ag nanoparticle solution was mixed with a 250 μL aliquot of peptide (CALNN or CCALNN, 2 mg/ml in phosphate buffer) and left to sit for a minimum of 24 hours. The nanoparticles were purified from excess peptide and other reactants by multiple cycles of centrifugation at 18000 g for 90 minutes to obtain AgMPCs (RT-13 and 15). In the second, peptide-stabilized silver nanoparticles were synthesized according to a modified version of the common two-phase synthesis. About 9 ml of an aqueous solution of $AgNO_3$ (0.03 M) was combined with 6 ml of a toluene solution of phase transfer catalyst (0.2 M TOAB) and vigorously stirred for 1 hour. One ml of peptide (2 mg/ml in phosphate buffer) was then added to the two-phase mixture. After stirring for 1 hour, the silver ions were reduced by introduction of 7 ml of an aqueous solution of $NaBH_4$ (0.44 M). This solution was stirred for approximately 12 hours to allow the reaction to reach completion. The aqueous phase was isolated from the organic phase by phase separation and passed through filter paper to remove any insoluble material. The particles were purified from excess peptide and other reactants by multiple cycles of centrifugation at 18000 g for 90 minutes to obtain Ag-MPCs (RT-16).

3.3.2.9 Alkane thiol stabilised Ag-MPCs (RT-17)

Decanethiol-and dodecanethiol-stabilized silver nanoparticles were synthesized according to a modified version of the common two-phase synthesis. 9 ml of an aqueous solution of $AgNO_3$ (0.03 M) was combined with 6 ml of a chloroformic solution of phase transfer catalyst (0.2 M TOAB) and vigorously stirred for 1 h. The organic phase, which now contained the silver ions, was isolated from the aqueous phase by phase separation and 0.25 mmol of decane- (50 μL) or dodecanethiol (60 μL) was added. After stirring for 15 min, the silver ions were reduced by introduction of 7 ml of an aqueous solution of $NaBH_4$ (0.44 M). This solution was stirred for approximately 12 hours to allow the reaction to reach completion. The organic phase was isolated from the aqueous phase by phase separation. The nanoparticles were then washed in excess ethanol (4:1) to remove any phase transfer catalyst and unbound thiols in the organic phase. After centrifugation at 25000 g for 10 min, the nanoparticle pellet was re-dispersed in 10 ml of hexane and repeatedly centrifuged to remove insufficiently passivated nanoparticles.

3.3.2.10 PEGylated Ag-MPCs (RT-18 and 19)

PEG-OH **3a** stabilized Ag nanoparticles were produced via ligand exchange with dodecanethiol-stabilized Ag nanoparticles. 400 μL of a methanolic solution of PEG-OH **3a** (12.5 mg/ml) was added to 4 ml of dodecanethiol-stabilized Ag nanoparticles in hexane and the mixture was gently shaken. Within minutes the nanoparticles began to precipitate out of solution. Once the ligand-exchange was complete, the solution was centrifuged for 30 minutes at 10000 g and the supernatant was removed. The nanoparticles were re-dispersed in phosphate buffer and passed through a 0.22 μm filter to remove any insoluble material. PEG-NH_2 **10** stabilized Ag nanoparticles were produced via ligand exchange with decanethiol-stabilized Ag nanoparticles. 400 μL of a methanolic solution of PEG-NH_2 (15 mg/ml) was added to 1 ml of decanethiol-stabilized Ag nanoparticles in hexane. The solution was gently shaken and left undisturbed for 24 hours, at which point 1 ml of phosphate buffer was

added and the 2-phase mixture was violently shaken. Upon repartitioning of the two phases the nanoparticles transferred into the aqueous/methanolic phase. This phase was isolated by phase separation. PEG-OH-stabilized Ag nanoparticles were purified from excess PEG-OH by size-exclusion chromatography using Sepharose CL-6B (Amersham Biosciences) as the stationary phase and ultrapure water at pH 10 as the mobile phase. PEG-NH_2-stabilized Ag nanoparticles were also purified from excess PEG-NH_2 by size-exclusion chromatography using Sepharose CL-6B with ultrapure water at pH 10 and a NaCl concentration of 2 M as the mobile phase.

PEG-OH **3a** and PEG-NH_2 **10** functionalized Ag nanoparticles were also synthesized via a AgBr route.[73] Briefly, for PEG-OH **3a** stabilized MPCs, a negatively charged AgBr hydrosol was prepared by dropwise addition of $AgNO_3$ (50 ml, 0.02 M) to a solution of KBr (50 ml, 0.022 M) under vigorous stirring. After 20 minutes a toluene solution of TOABr (100 mL, 0.020 M) was added, and the reaction mixture was stirred overnight. PEG-OH **3a** (75 mg, 0.0197 mmol) in methanol (10 ml) was then added to the mixture and stirred for 20 min. Upon addition of freshly prepared, aqueous $NaBH_4$ (50 ml, 0.24 M) the toluene phase changed to dark brown in color and the reaction mixture was vigorously stirred for 1.5hrs. Then the mixture was vigorously shaken and the particles transferred completely to the aqueous phase which was then separated from toluene phase. They were further purified by washing with ethyl acetate and chromatographed through gel filtration chromatography (G-25, Amersham Biosciences UK).

For PEG-amine **10** functionalisation, the procedure described for the preparation of Ag bromide hydrosol was followed, and the reaction mixture was scaled down to about 50 ml total volume. For 10 % amine, mixture of PEG-OH **3a** (9 mg, 24 μmol) and PEG-NH_2 **10** (1mg, 2.6 μmol) in methanol was added to the two-phase AgBr hydrosol (50 ml) and the reaction mixture was stirred for 20 min, followed by fresh $NaBH_4$ (10 ml, 0.24M) addition. The reaction mixture was further stirred for an additional 2hr and worked up as described for PEG-OH.

3.3.3 Characterisation

3.3.3.1 UV-vis spectroscopy

UV-vis absorption spectra were recorded either on a Spectra Max Plus microplate reader (Molecular Devices, Wokingham, UK) or Genesys 10-S spectrophotometer (Thermospectronic USA).

3.3.3.2 Transmission electron microscopy (TEM)

Images of nanoparticles were acquired on a JEOL 2000 FX and EX TEM both operating at 200 kV. Specimens were prepared by evaporating a diluted 10 μL drop of sample on a 400 mesh carbon-coated copper grid (Agar Scientific Ltd., Essex, UK). Image J image processing and analysis software (http://rsb.info.nih.gov/ij/) was used for measurement of particle size.

3.4 References

[1] Feldheim, D. L and Keating, C. D., *Chem. Soc. Rev.*, 1998, **27**, 1

[2] Henglein, A., *Chem. Rev.*, 1989, **89**, 1861

[3] Schmid, G., *Chem. Rev.*, 1992, **92**, 1709

[4] Rechberger, W., Hohenau, A., Leitner, A., Krenn, J. R., Lamprecht, B and Aussenegg, F. R., *Optics Communications.*, 2003, **220**, 137

[5] Qu, S., Du, C., Song, Y., Wang, Y., Gao, Y., Liu, S., Li, Y and Zhu, D., *Chem. Phys. Lett.*, 2002, **356**, 403

[6] Prodan, E., Nordlander, P and Halas, N. J., *Nano Lett.,* 2003, **3** 1411

[7] Niemeyer, C. M., *Angew. Chem. Int. Ed.*, 2001, **40**, 4128

[8] Raschke, G., Kowarik, S., Franzi, T., Sonnichsen, C., Klar, T.A and Fieldmann, J., *Nano Lett.,* 2003, **3**, 935

[9] Katz, E and Willner I., *Angew. Chem. Int. Ed.*, 2004, **43**, 6042

[10] Parak, W. J., Gerion, D., Pellegrino, T., Zanchet, D., Michael, C., Larabell, C. A and Alivisatos, A. P., *Nanotechnology*, 2003, **14**, 15

[11] Turkevich, J., *Gold Bull.*, 1985, **18**, 86

[12] Marie-Christine, D and Astruc, D., *Chem. Rev.*, 2004, **104**, 293

[13] Faraday, M., *Phil. Trans. Roy. Soc.*, 1857, **147**, 145

[14] Turkevich, J and Enustun, B. V., *J. Am. Chem. Soc.*, 1963, **85**, 3317

[15] Frens, G., *Nature (London), Phys. Sci.*, 1973, **241**, 20

[16] Morris, R. H and Milligan, W. O., *Morphology of colloidal gold*, 1964, 3461

[17] Duff, D. D and Baiker, A. *Langmuir*., 1993, **9**, 2301

[18] Brust, M., Bethell, D., Schriffrin, D. J and Kiely, C. J., *Adv. Mater*., 1995, **7**(9), 795

[19] Heath, J. R., Knobler, C. M and Leff, D. V., *J. Phys. Chem. B,* 1997, **101**, 189

[20] Korgel, B. A., Fullam, S., Connolly, S and Fitzmaurice, D., *J. Phys. Chem, B*, 1998, **102**, 8379

[21] Schmid, G and Peschel, S., *New J. Chem*., 1998, **22**, 669

[22] Schmid, G., Pfeil, R., Boese, R., Bandeman, F., Meyer, S., Calis, G.H.M and van der Felden, J. W. A., *Chem. Ber*., 1981, **114**, 3634

[23] Haruta, M., Yamada, N., Kobayashi, T and Lijima, S., *Catalysis*, 1989, **115**, 301

[24] Nuzzo, R. G and Allara, D. L., *J. Am. Chem. Soc.,* 1983, **105,** 4481

[25] Giersig, M and Mulvaney, P., *Langmuir*, 1993, **9**, 3408

[26] Brust, M., Walker, M., Bethell, D., Schiffrin, D. J and Whyman, R., *J. Chem. Soc., Chem. Commun.,* 1994, 801

[27] Hostetler, M. J., Wingate, J. E., Zhong, C. J., Harries, J. E., Vachet, R. W., Clark, M. R., London, J. D., Green, S. J., Stokes, S. J., Wignal, G. D., Glish, G. L., Porter, M. D., Evans, N. D and Murray, R. W., *Langmuir*, 1998, **14**, 17

[28] Wetten, R. L., Khoury, J. L., Alvarez, M. M., Murthy, S., Vezmar, I., Wang, Z. L., Stephan, P. W., Cleverland, C. L., Luedtke, W. D and Landman U., *Adv. Mater.,* 1996, **8**, 428

[29] Schaaff, T. G., Shafigullin, M. N., Khoury, J. T., Vezmar, I., Whetten, R. L., Cullen, W., First, P. N., Gutierrez-Wing, C., Ascensio, J and Jose-Yacaman, M. J., *J. Phys. Chem*. **B**, 1997, **101**, 7885

[30] Alvarez, M. M., Khoury, J. T., Schaaff, T. G., Shafigullin, M. N., Vezmar, I and Whetten, R. L., *Chem. Phys. Lett*., 1997, **266**, 91

[31] Templeton, A. C., Wuelfing, W. P and Murray, R. W., *Acc. Chem. Res*., 2000, **33**, 27

[32] Jimenez, V. L., Georganopoulou, D. G., White, R. J., Harper, A. S., Mills, A. J., Lee, D and Murray, R. W., *Langmuir,* 2004, **20**, 6864

[33] Hicks, J. F., Templeton, A. C., Chen, S., Sheran, K. M., Jasti, R., Murray, R. W., Debord, J., Scaaff, T. G and Whetten, R. L., *Anal. Chem*., 1999, **71**, 3703

[34] Wilcoxon, J. P., Martin, J. E and Provencio, P., *Langmuir*, 2000, **16**, 9912

[35] Jimenez, V. L., Leopold, M. C., Mazzitelli, C., Jorgenson, J. W and Murray, R. W., *Langmuir*, 2004, **20**, 6864

[36] Song, Y., Jiminez, V., McKinney, C., Donkers, R and Murray, R. W., *Anal. Chem*., 2003, **75**, 5088

[37] Ohara, P. C., Leff, D. V., Heath, J. R and Gelbart, W. M., *Phys. Rev. Lett.,* 1995, **75**, 3466

[38] Fink, J., Kiely, C.J., Bethell, D and Schiffrin, D. J., *Chem, Mater.,* 1998, **10**, 922

[39] Brust, M., Fink, J., Bethel, D., Schiffrin, D. J and Kiely, C. J., *J. Chem. Soc., Chem. Commun.,* 1995, 1655

[40] Kim, Y., Johnson, R. C and Hupp, J. T., *Nano Lett.,* 2001, **1** 166

[41] Weisbecker, C. S., Merritt, M. V and Whitesides, G. W., *Langmuir*, 1996, **12**, 3763

[42] Yguerabide, J and Yguerabide, E. E., *Anal. Biochem.,* 1998, **262**, 137

[43] Yguerabide, J and Yguerabide, E. E., *Anal. Biochem.*, 1998, **262**, 157

[44] Vlckova, B, Tsai, D., Gu, X., Moskovits, M., *J. Phys. Chem.*, 1996, **100**, 3169

[45] Cao, Y. C., Jin, R and Mirkin, C. A., *Science*, 2002, **297**, 1536

[46] Nie, S and Emory, S. R., *Science,* 1997, **275**, 1102

[47] Lee, P. C and Mesisel, D., *J. Phys. Chem.*, 1982, **86**, 3391

[48] Zhang, J and Lakowicz, J. R., *J. Phys. Chem. B.*, 2005, **109**, 8701

[49] Mulvaney, P., Linnert, T., Henglein, A., *J. Chem. Phys.*, 1991, **95**, 7843

[50] Henglein, A., *J. Phys. Chem.*, 1993, **97**, 5457

[51] Henglein, A., *Chem. Mater.*, 1998, **10**, 444

[52] Levy, R., Thanh, N. T. K., Doty, R. C., Hussain, I., Nichols, R. J., Schiffrin, D. J., Brust, M and Fernig, D. G., *J. Am. Chem. Soc.*, 2004, **126**, 10078

[53] Tshikhudo, T. R., Wang, Z and Brust, M., *Materials Science & Technology*, 2004, **20**, 980

[54] Doty, R. C., Tshikhudo, T. R., Brust, M and Fernig, D. G., *Chem. Mater.*, 2005, **17**, 4630

[55] Kanaras, A. G., Kamounah, F. S., Schaumburg, K., Kiely, C. J and Brust, M., *Chem. Commun.*, 2002, 2294

[56] Lz-Marzan, L. M., *Langmuir,* 2006, **22**, 32

[57] Mulvaney, P., *Langmuir*,1996, **12,** 788

[58] Hermanson, G. T., *Bioconjugate techniques,* Academic press, Elsevier, London, p597

[59] Hirai, H., Nakan, Y and Toshima, M., *J. Macromol. Science. Chem.*, 1979, **A13**, 727.

[60] Hirai, H., *J. Macromol. Science. Chem.,* 1978, **A13**, 633

[61] Tan, C. K., Newberry, V., Webb, T. R and McAuhffe, A. C., *J. Am. Chem. Soc. Dalton Trans.*, 1987, 1299

[62] Sun, Y and Xia, Y., *Science*, 2002, **298**, 2176

[63] Hostetler, M. J., Templeton, A. C and Murray, R. W., *Langmuir*, 1999, **15,** 3782

[64] Pasquato, L., Pengo, P and Scrimin, P., *J. Mater. Chem.*, 2004, **14**, 3481

[65] Fu, A., Micheel, C. M., Cha, J., Chang, H., Yang, H and Alivisatos, A. P., *J. Am. Chem. Soc.,* 2004, **126,** 10832

[66] Ackerson, C. J., Sykes, M. T and Kornberg, R. D., *Proc. Natl. Acad. Sci .*, 2005, **102**, 13383

[67] Levy, R., Wang, Z., Duchesne, L., Doty, R. C., Cooper, A. I., Brust, M and Fernig, D. G., *ChemBioChem*, 2006, **7**, 592

[68] Yang, W., Chen, M., Knoll, W and Deng, H., *Langmuir*, 2002, **18**, 4142

[69] Sloane, N. J. A and Teo, B. K., *Inorg. Chem.,* 1985, **24**, 4545

[70] Love, J. C., Estroff, L. A., Kriebel, J. K., Nuzzo, R. G and Whitesides, G. M., *Chem. Rev.,* 2005, **105**, 1103

[71] Tshikhudo, T. R., Demuru, D. Wang, Z., Brust, M., Secchi, A., Arduini, A and Pochini, A., *Angwew. Chem. Int. Ed.*, 2005, **44,** 2293

[72] Jana, N. R., Gearheart, L and Murphy, C. J., *Chem. Commun.,* 2001, 617

[73] Lahtinen, R. M., Mertens, S. F. L., East, E., Kiely, C. J and Schifrin, D. J., *Langmuir*, 2004, **20**, 3289

[74] van Hyning, D. L., Klemperer, W. G., Zukoski, C. F., *Langmuir*, 2001, **17**, 3120

[75] Waters, C. A., Mills, A. J., Johnsson, K. A., Schiffrin, D. J., *Chem. Commun.*, 2003, 540

[76] Pale-Grosdemange, C., Simon, E. S., Prime, K. L and Whitesides, G. M., *J. Am. Chem. Commun.*, 1991, **113**, 12

[77] Chirakul, P., Perez-Luna, V. H., Owen, H., Lopez, G. P and Hampton, P. D., *Langmuir,* 2002, **18**, 4324

CHAPTER 4

CALIX[N]ARENE MODIFIED GOLD MPCS

4 Calix[n]arene modified gold MPCs

4.1 Introduction

4.1.1 General Overview

In this chapter, the versatility of PEGylated MPCs is demonstrated by introducing supramolecular chemistry.[1] This is diagrammatically illustrated in Figure 1, in which a water insoluble supramolecular host calix[4]arene is introduced to the MPCs ligand shell and thus transferred into an aqueous environment. Importantly, it is demonstrated that the calix[4]arene moiety retains its molecular recognition properties in aqueous solution. Specific recognition of immobilised cationic pyridinium moieties by the calix[4]arene-modified MPCs in aqueous solution is demonstrated by a simple colour test and by atomic force microscopy (AFM). A facile protocol which allows the incorporation of the calixarene moiety to the MPCs ligand shell is described.

In addition to demonstrating the molecular recognition properties of calix[4]arene moiety in water, we show that in an organic phase calix[6]arene can be used as an alternative wheel for the construction of calixarene-based rotaxane on gold nanoparticles.

This work was carried out in collaboration with Dr F. Domenico Demuru from the Univerity of Parma in Italy. Dr Demuru prepared and characterized the calix[n]arene ligands which were used here for the development of water-soluble calixarene modified AuMPCs and for the construction of calixarene-based rotaxane on gold nanoparticles.

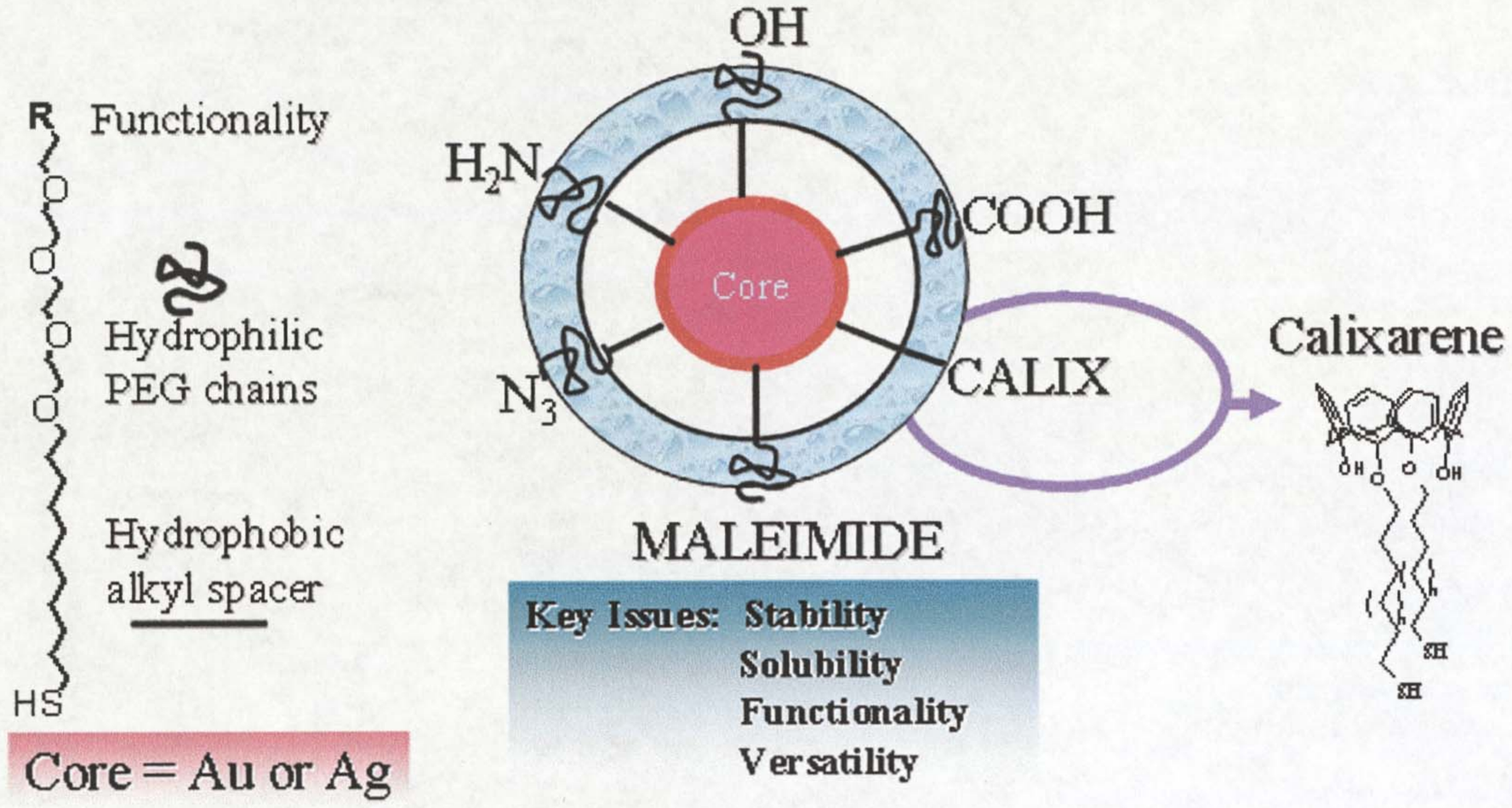

Figure 1. Diagrammatic illustration of the specific functional groups introduced to the PEGylated MPCs ligand shell, in which PEG-OH acts as a stabiliser and solubiliser.

4.1.2 Calix[n]arene -Introduction

Calix[n]arenes are a class of macrocyclic compounds discovered by Gutsche in the 1970´s.[2] They are well known for their host-guest properties[3] in supramolecular chemistry.[4] These cyclooligomers shown in Figure 2a are often obtained *via* base catalysed condensation of *p*-alkyl-phenol and formaldehyde to yield repeated phenolic units bridged by methylene spacers which function as points in which phenolic units rotate to adapt different conformers.[5] Of the resulting phenolic units, studies show that tetramers (4 phenolic units) are suited for analytical purposes while hexamers (6 phenolic units) have received less attention. The resulting cyclic structures can be functionalised on the *para*-position of the aromatic rings or on the phenolic OH position commonly known as the upper-and the lower-rim, respectively (Figure 2b). Of particular importance is that these cup-shaped structures (Figure 2c) are very electron rich and have thus been widely used for the recognition of metal ions and quaternary ammonium ions.[6]

For characterization, NMR spectroscopy is the most commonly applied technique particularly to gain insight into the conformational dynamics that calixarenes undergo. These are influenced by the substituents either on the upper or lower rims. It was found that the *cone* conformer (in which the cavity is in position to host the guest on the upper rim) is the most stable form both in solution and in the solid phase. Conformational interconversions,[7-9] and the complexation abilities of calixarenes have also been studied using simulation techniques such as molecular mechanics, dynamics *etc*. to support the experimental observations.[10, 11]

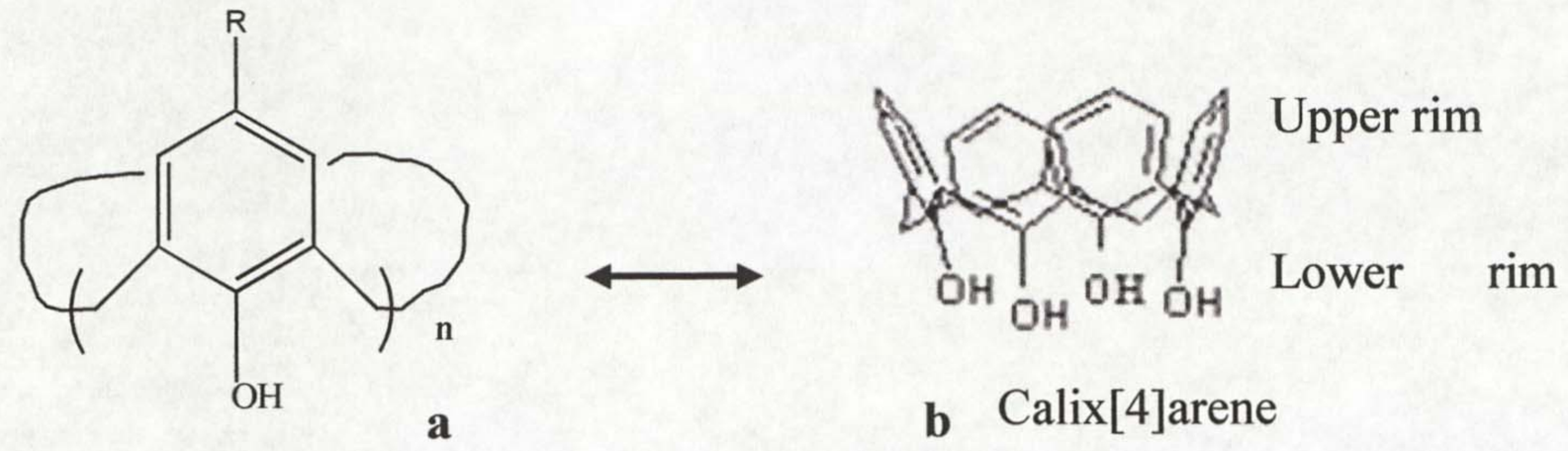

Figure 2. Schematic illustration of a) calixarene cyclooligomers formed by base condensation of *p*-alkyl-phenols and formaldehyde, b) Calix[4]arene in cone conformer and c) Cup-shape like structure of calixarene, d) Alkylated calix[4]arene (host) encapsulating a guest species.

An important goal of the synthesis of these macromolecules is to examine their complexation abilities towards specific guest molecules. Many synthetic strategies in which calixarene receptors have been functionalized or derivatised on the upper or lower rims in order to control their complexation/binding efficiencies towards neutral organic molecules,[12] metal cations and also quaternary ammonium salts[13] have been reported. In fact any group that can be attached on the upper or lower rim will affect the binding constants of the calixarene cavity towards a particular guest species.

In addition to their host-guest properties, calixarenes and other related macrocycles such as resorcinarenes have received attention as new materials in thin films, chromatography supports, polymers and catalysis. In thin films, deposition techniques such as Langmuir Blodgett (LB), self-assembly and evaporative techniques have been applied to generate ordered calixarene mono-and multilayers.[14] These thin films when deposited on suitable substrates, demonstrated high sensitivities towards a range of metal ions,[17] molecular ions[18] and neutral organic molecules.[19] In addition, some calixarene thin films have been reported to show pyroeletric[20] and semiconductor type properties.[21]As a result there is a growing interest in calixarene thin films for the development of new sensing devices and for biological applications.

4.1.3 Rotaxane-Introduction

Rotaxanes [22] represent a class of compounds that consist of linear and cyclic species bound together non-covalently as shown in Figure 3. The insertion of an acyclic molecule (axle) into the cavity of a macrocyclic compound (wheel) leads to pseudorotaxanes. The variation of free energy of the complexation process (molecular recognition) governs the equilibrium between the species. Introduction of groups (stoppers) that are dimensionally bigger than the cavity of the macrocyclic compound, on the ends of the axle, leads to the formation of a non-dissociable complex called rotaxane as illustrated in Figure 3.[23, 24] The geometry and the relative position of the components of the complex are controlled by non-covalent interaction. Several macrocycles such as crown ethers or cyclodextrins are used as wheels.[23-28]

Recently, calix[6]arene containing 1,3,5-trimethoxy-2,4,6-trioctyloxy groups on the lower rim and three phenylureido moieties on the upper rim (called tri-phenylureido-calix[6]arene (Figure 4)) has been used as a wheel together with dialkylviologen derivatives (as axle) for the formation of pseudorotaxane and rotaxane complexes. [9, 29]

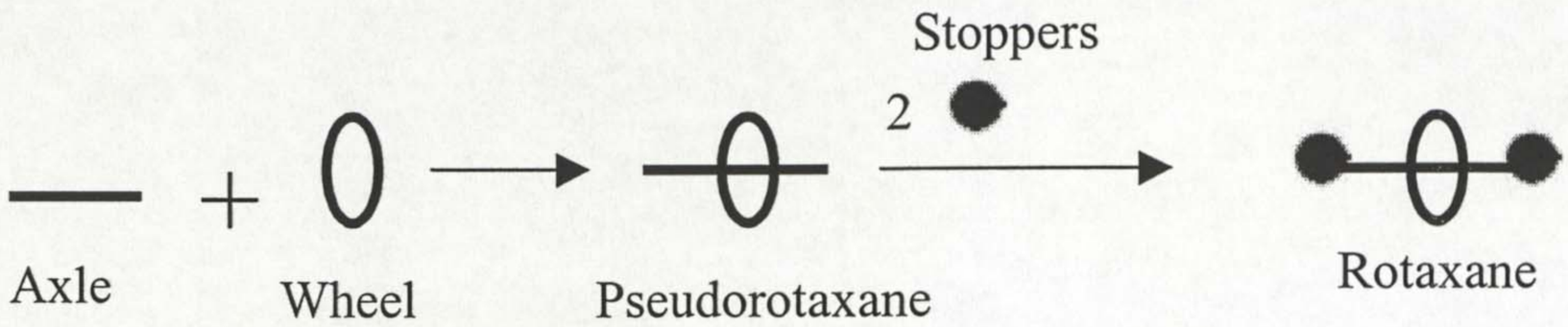

Figure 3. Schematic illustration of the formation of pseudorotaxane and rotaxane complexes.

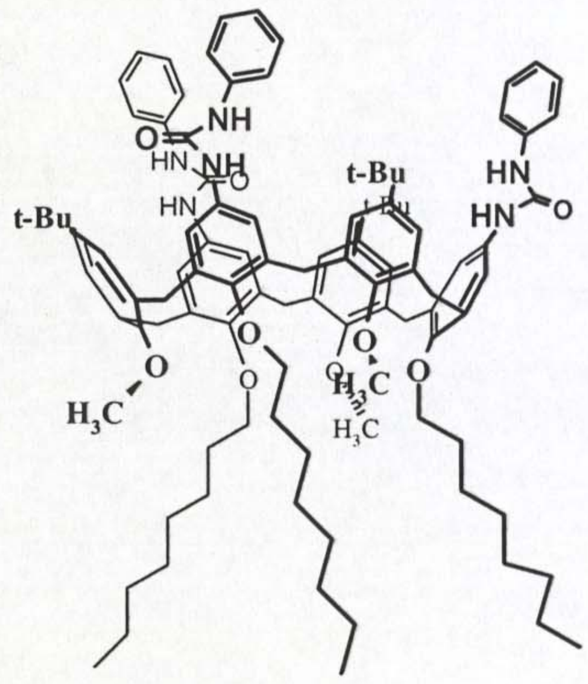

Figure 4. The structure of tri-phenylureido-calix[6]arene

Some interesting features regarding the assembly in an apolar solvent have been identified;[29] i) The steric effects induced by the strong ion pairs from *N,N''*-dialchylic bipyridinyl salts(axle) prevent its entrance into the calix aromatic cavity.

ii) The presence of three methoxy groups on the lower rim which are oriented towards the cavity of the calix allows the axle to be inserted only from the upper rim due to the steric effects iii) The functional groups from the phenyl ureido on the upper rim are capable of dividing the ion pairs and then allow the threading only from the top of the calix.[29] These phenylureido groups play a significant role in the orientation of the threading of the axle's cationic parts through the upper rim of the wheels. Introduction of another stopper on the axle gives the oriented rotaxane. Of particular interest to us is to investigate the effects of molecular orientation of the resulting pseudorotaxane or rotaxane assemblies in which, gold nanoparticles are used as alternative stoppers. This will be discussed by identifying different strategies for the formation of calixarene mediated pseudo/rotaxane systems.

Molecular recognition studies by calix[4]arene modified gold nanoparticles will be discussed prior to calixarene-mediated rotaxane assemblies.

4.2 Results and Discussion

4.2.1 Molecular recognition by calix[4]arene modified Au-MPCs in in water [1]

Unmodified calixarenes are completely insoluble in water, which significantly limits their potential applications as molecular recognition units. In non-aqueous systems, the incorporation of calixarenes in 1.5-4 nm MPCs is known to enhance their affinity to guest molecules.[30] To demonstrate molecular recognition properties of unmodified calixarene in an MPC ligand shell in aqueous environment, we have developed a protocol for the preparation of water soluble, calixarene-modified Au-MPCs. The preparative method is briefly discussed below.

4.2.1.1 Preparation of water soluble calixarene modified AuMPCs

The preparation of calixarene-modified nanoparticles is schematically illustrated in Figure 5. Citrate-stabilised gold hydrosols (RT-7, chapter 3) were reacted with a 2:1 mixture of the stabilising ligand (1-mercaptoundec-11-yl) tetraethylene glycol **1** and 25, 27-bis(11-thio-1-oxy-undecan)-26,28-dihydroxy-calix[4]arene **2** in a water/THF solvent system to directly give the modified particles **3**, which were isolated from excess ligand material by centrifugation. Given the conformation of the relatively rigid **2** it is reasonable to assume that both thiol functionalities of **2** bind to the surface of the same gold particle. Otherwise, cross-linking of particles *via* bis-thiol bridges and precipitation of aggregates could be expected.[31] This has not been observed in this case. On the contrary, the particles are extremely stable and can be centrifuged, dried and re-suspended in aqueous solution several times without loss of material. The ruby red suspensions are very robust against non-specific aggregation. For example, unlike their precursor hydrosols (RT-7), the particles do not aggregate even in a 2M sodium chloride solution.

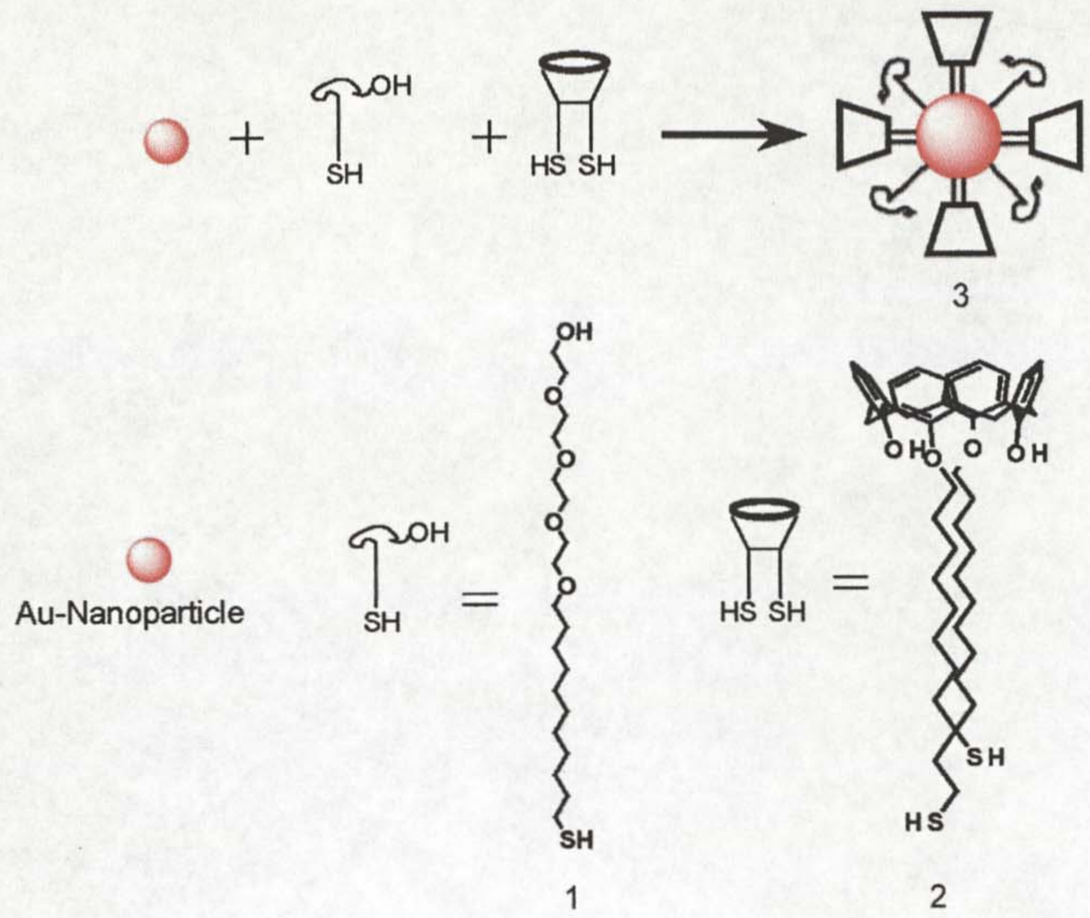

Figure 5. Reaction scheme illustrating the one-step stabilisation and functionalisation of gold nanoparticles with (1-mercaptoundec-11-yl) tetraethylene glycol 1 and 25,27-bis(11-thio-1-oxy-undecan)-26,28-dihydroxy-calix[4]arene 2 carried out in a THF/water mixture.

The particles exhibit a characteristic plasmon absorption band in the UV-visible spectrum at 526 nm. They have been further characterized by TEM and by NMR spectroscopy Their size as confirmed by TEM analysis in Figure 6 is that of the original citrate-stabilised particles (14 ± 1 nm).

The molecular composition of the ligand shell has been studied by ^{1}H NMR spectroscopy. Figure 7 shows the NMR spectra of the pure ligands **1** and **2** in $CDCl_3$ and that of the particles **3** in D_2O. As expected, the spectrum of the particles shows significant peak broadening, in particular of the methylene protons adjacent or close to the sulphur atom that binds to the surface of the particle. This is probably chiefly due

to the lack of mobility of the closely packed molecules in the ligand shell, which on the nanometer scale resembles a solid-state material. Several other factors contributing to line broadening in NMR spectra of MPCs have also been suggested, and the phenomenon is still subject to some debate. Although the broadening of the features impedes a more detailed interpretation, it is apparent that all characteristic main features of the two different ligands are also present in the spectrum of the particles. Importantly, slightly broadened peaks between 6.6 and 7.2 ppm characteristic of the aromatic protons of the calixarene cavity are clearly present in the spectrum of the particles. This gives evidence for the inclusion of **2** in the ligand shell. Since it was found that in MPCs of **1** of the same size there are approximately 3000 thiol ligands per particle (chapter 3), it can be estimated that here each gold particle carries on the order of 960 molecules of **2**.

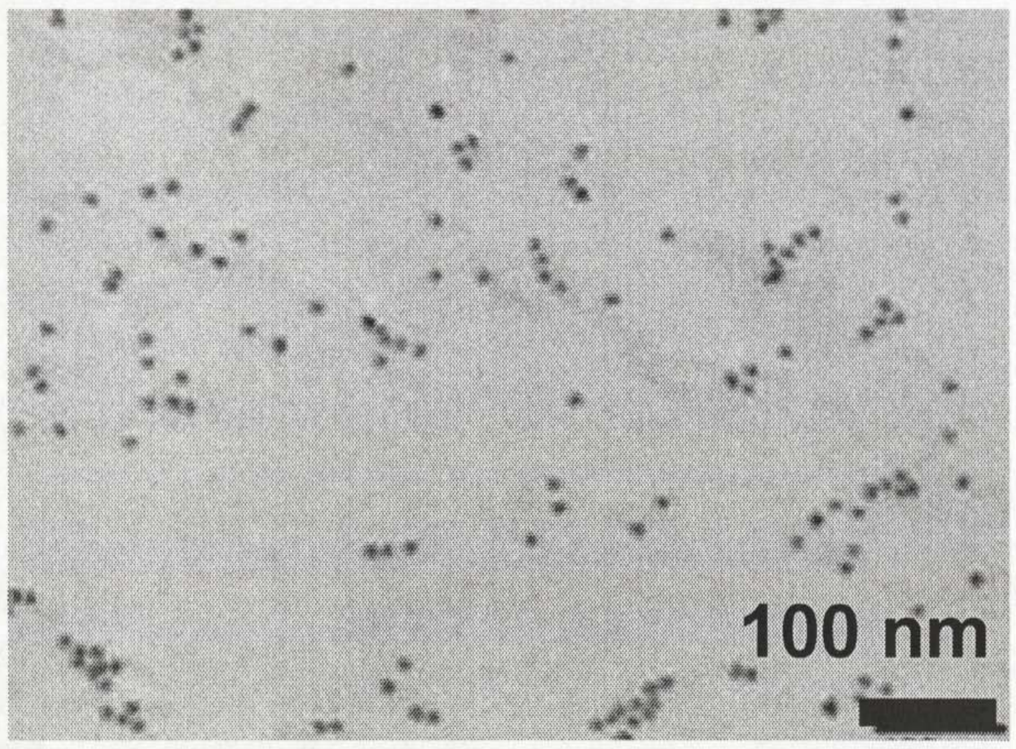

Figure 6. TEM image of 14 nm gold nanoparticles, 3, stabilised and functionalised with 1 and 2.

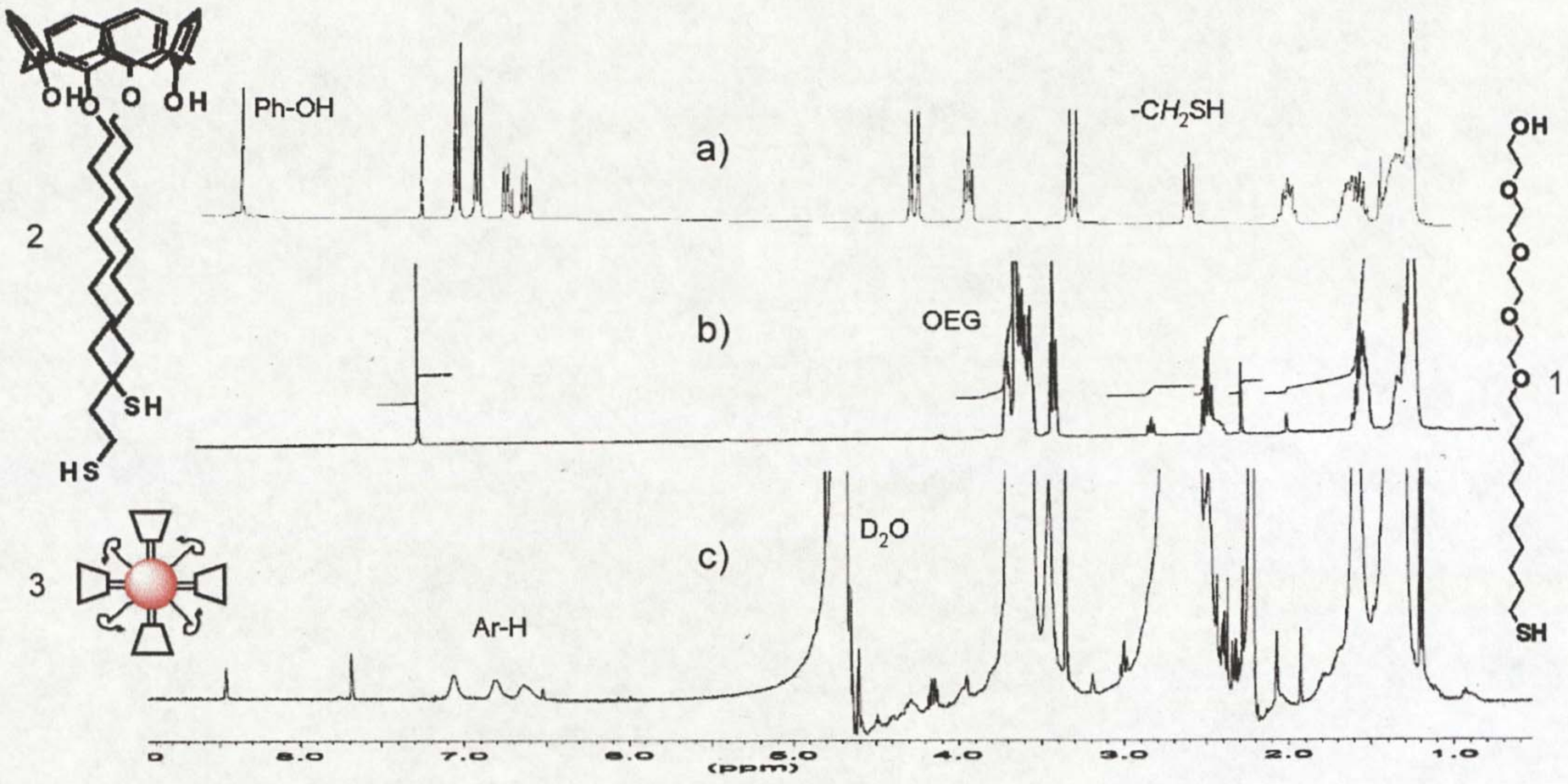

Figure 7. ^{1}H NMR spectra of 2 (a) and 1 (b) in $CDCl_3$ and of 3 (c) in D_2O showing that 1 and 2 have been attached to the gold nanoparticles (methylene protons adjacent to the thiol and oligoethylene glycol protons are marked). In particular, the aromatic protons (Ar-H) in (c) indicate the presence of the calixarene cavity in the ligand shell of the particles.

The binding properties of a solution free water soluble model calix[4]arene derivative towards *N*-alkyl pyridinium salts in D_2O are given quantitatively in the experimental section. In order to demonstrate qualitatively the molecular recognition properties of the particle-bound calixarene in water, specific binding studies were carried out using two different chemically modified substrates as illustrated in Figure 5. In the simplest case the substrate was prepared by the non-specific adsorption of 1-[thio acid S-11-(toluene-4-sulfonyloxy)-undecyl]pyridine-1-ium (pyridinium tosylate thiol) **4** to white molecular sieve beads. For non-aqueous media it is known that the cationic pyridinium moiety is specifically recognised by calix[4]arenes.[31]

It was found that the nanoparticles **3** bind specifically from aqueous solution to the molecular sieve beads primed with **4** indicating that the calixarene cavity of **2** exhibits its characteristic cation binding properties also in aqueous media and when immobilised in the ligand shell of the MPCs.

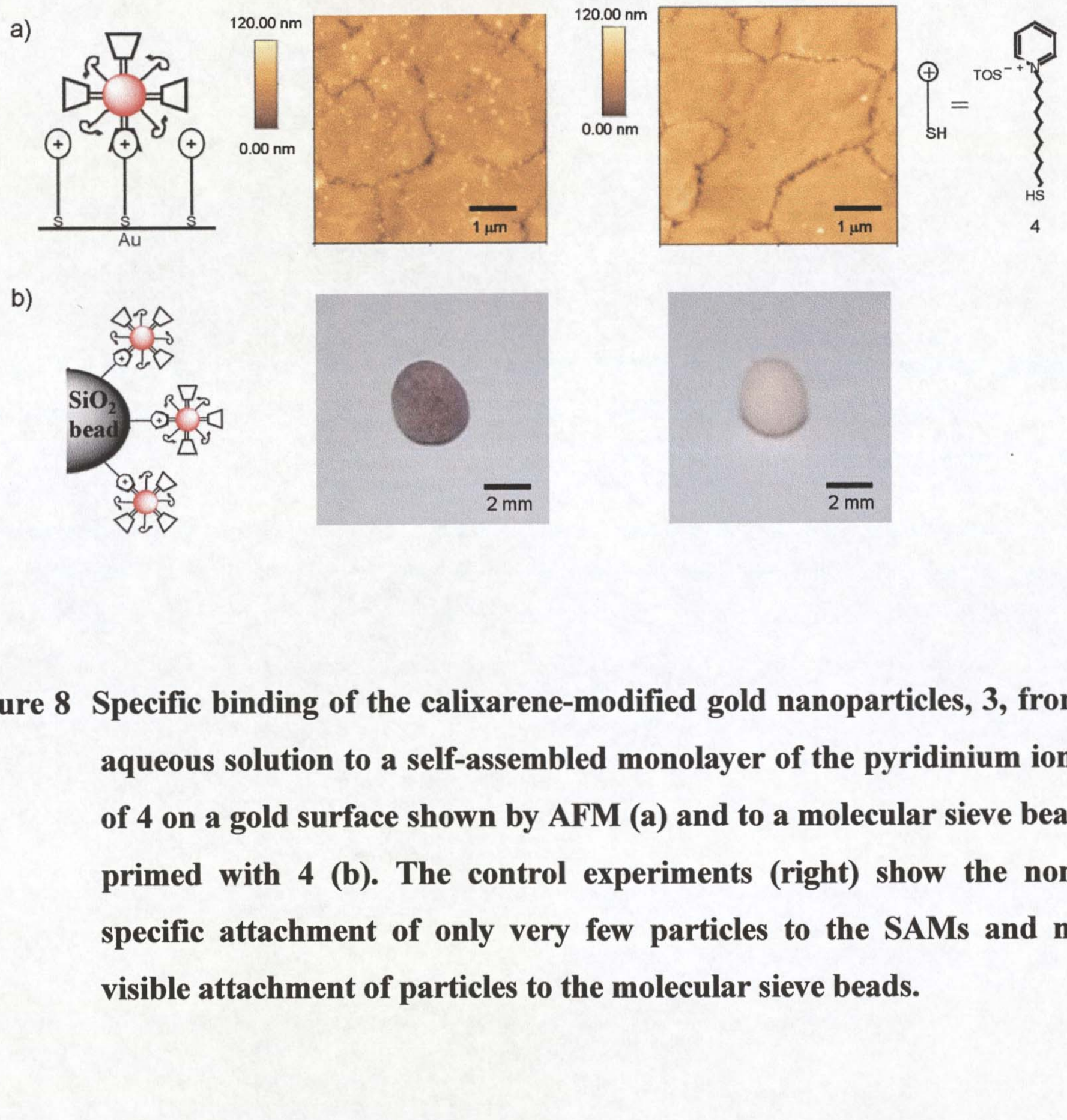

Figure 8 Specific binding of the calixarene-modified gold nanoparticles, 3, from aqueous solution to a self-assembled monolayer of the pyridinium ions of 4 on a gold surface shown by AFM (a) and to a molecular sieve bead primed with 4 (b). The control experiments (right) show the non-specific attachment of only very few particles to the SAMs and no visible attachment of particles to the molecular sieve beads.

This binding interaction is easily observed with the naked eye due to the intense red colour of the gold nanoparticles. A number of control experiments clearly confirmed that both the pyridinium and the calixarene moieties have to be present to achieve any attachment of MPCs to the molecular sieve beads. Further binding studies were carried

out by AFM using a self-assembled monolayer (SAM) of **4** on a flat gold surface as the substrate. As demonstrated in the AFM images in Figure 5 the calixarene-modified nanoparticles **3** were found to bind selectively to this SAM from aqueous solution, while binding to clean gold surfaces occurred only as a non-specific minority event. MPCs without calixarene in their ligand shell did not show any significant binding to the SAMs nor to clean gold surfaces.

In summary, we have introduced a very simple route for the preparation of water-soluble calixarene-functionalised MPCs of gold. Importantly, it has been demonstrated that in an aqueous environment the calixarene retains its molecular recognition properties, which have been utilised here to bind the MPCs selectively to chemically modified substrates. The MPCs also act as readily detectable markers of the specific recognition events demonstrating a high potential for simple, colour based diagnostic tests, for example, those required for many routine bioanalytical applications. The preparative method is very general and can readily be adapted to other artificial molecular recognition systems. Particularly attractive is the opportunity demonstrated here, to make totally water insoluble recognition systems amenable to aqueous solutions, which again is of great interest in the context of future bioanalytical applications of MPCs.

In the next section, the use of tris-phenylureido as an alternative wheel for the construction of calixarene- based rotaxane is discussed.

4.2.2 Calixarene-based rotaxane on gold nanoparticles

The formation of calix[6]arene mediated pseudorotaxane or rotaxane assemblies in which gold nanoparticles are used as alternative stoppers is discussed. The reagents used during the synthesis are shown in Figure 9. The calix[6]arene used here (the wheel) is derivatised on the upper rim to contain three phenylureido moieties and on the lower rim to contain 1,3,5-trimethoxy-2,4,6-trioctyloxy groups (Figure 9b) (or ethoxy groups instead of octyl group). The wheel is called tri-phenylureido-calix[6]arene (introduction)]. The wheel has been complexed with dialkylviologen derivatives (the axle, Figure 9a) to establish two isomeric pseudorotaxane products shown in Figure 9d (with octyl group) and Figure 9e (with ethoxy group).

In addition, the wheel has been complexed with an axle containing a molecular stopper (Figure 9c) to obtain oriented pseudorotaxane shown in Figure 9f (with octyl group) and Figure 9g (with ethoxy group). The isomeric pseudorotaxane (d,e) and oriented pseudorotaxane (f, g) complexes were prepared in organic solvents (toluene or chloroform) and characterised at the University of Parma in Italy and used as received.

The effects of molecular orientation on assembling these complexes with gold nanoparticles on the formation of gold based oriented pseudorotaxane or rotaxane products have been investigated and the observations are summarised in Table 1.

Tetraoctyl ammonium bromide (TOABr) stabilised particles (RT-2, 6 nm, chapter 3) were used for the formation of each product. Generally, the capping agents (Figure 9a, d, e, f and g) were treated with a toluene solution of electrostatically stabilised particles for some time (approximately 3hrs). The products were purified by centrifugation (25 000g, 90 mins) and re-suspended in either toluene or chloroform.

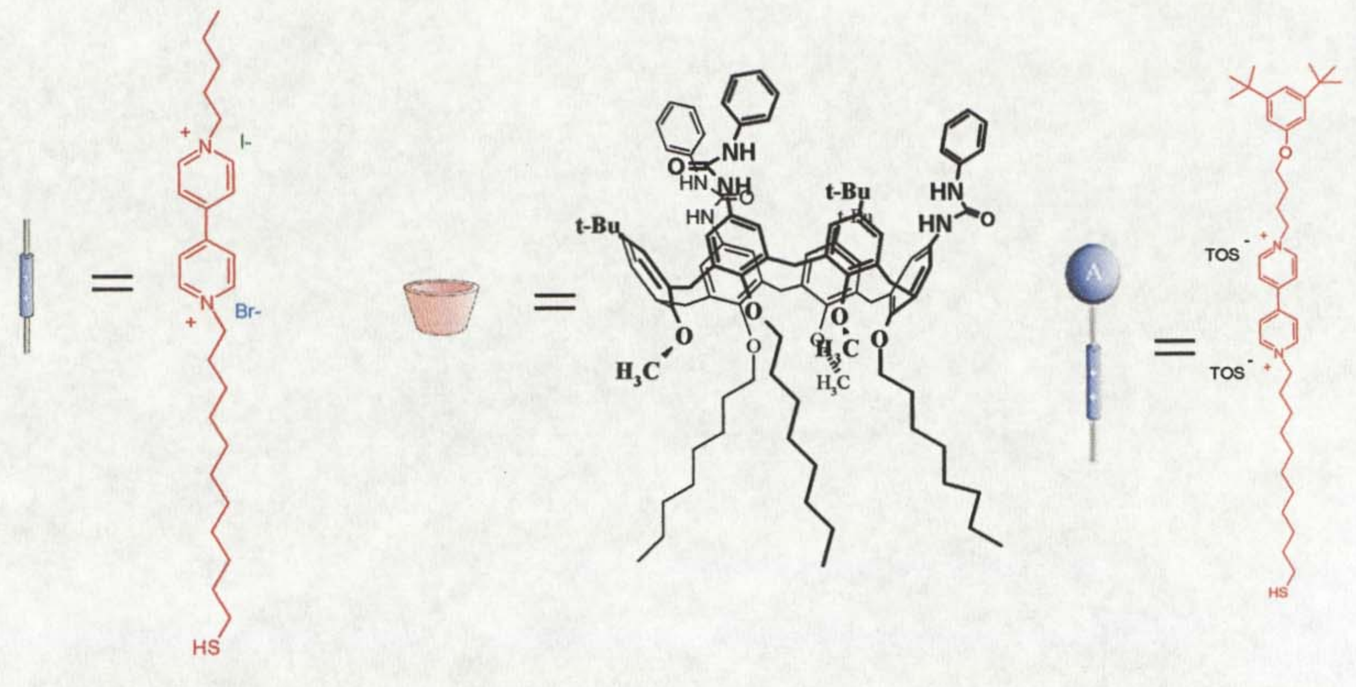

Figure 9. Units used for the assembly of pseudo rotaxane a) an axle without a stopper, b) calix[6]arene receptor, c) stoppered axle, d) Octyl isomer a and b mixture, e) Ethoxy isomer a and b mixture, f) Oriented pseudorotaxane b and c complex.

Experiment no.	**Nanoparticles stabiliser**	**Additional stabilizer Dodecanethiol**	**Product**	**Observation during nanoparticles preparation**
1	Octyl isomer (**d**)	No	Not isolated	Aggregation (precipitates)
2	Octyl isomer (**d**)	Yes	Oriented pseudorotaxane	Stable particles
3	Ethoxy isomer (**e**)	No	Not isolated	Aggregation (precipitates)
4	Ethoxy isomer (**e**)	Yes	Oriented pseudorotaxane	Stable particles
5	Axle (**a**)	No	Not isolated	Aggregation (precipitates)
6	Axle (**a**)	Yes	Axle-stabilised MPCs	Stable particles
7	Ethoxy oriented Pseudorotaxane (**g**)	No	Rotaxane	Stable particles
8	Octyl oriented Pseudorotaxane (**f**)	No	Rotaxane	Stables particles

Table 1. List of the pseudorotaxane and rotaxane products formed using gold nanoparticles (RT-2, 6 nm) as alternative stopper.

At first, attempts were made to stabilize gold nanoparticles using isomer (d) or (e) with no success (experiment 1 and 3, Table 1). When these isomers were added to the TOABr stabilised particles, they immediately aggregated and precipitated out of the solution. This suggests that isomers are capable of linking gold nanoparticles together leading to the formation of nanoparticle aggregates. It is unclear what actually causes this aggregation. However, stable solutions were obtained by addition of dodecane thiols (~ 10 %) as additional stabilizing ligands during mixing (expt. 2 and 4). The stability of nanoparticles was pronounced when an isomer (d) with an octyl spacer was used. A scheme illustrating the formation of oriented octyl pseudorotaxane (with ~10% of dodecane thiol as an additional stabiliser) complex is shown in Figure 10a. The resulting particles were analysed by TEM shown in Figure 10b.

The TEM image shown in Figure 10b reveals that in general, particles are aggregated, however, by examining the images carefully, it can be seen that these are ordered aggregates of particles. This ordering behavior raised a few questions. (i) Are the ordered aggregates due to the additional stabilizer (dodecane thiol)? (ii) is it due to the octyl spacer? or (iii) is it the direction in which the calixarene cavities are oriented (in which the other wheel is facing gold nanoparticles or the opposite)?.

To investigate weather the orientation of the calixarene cavity has a significant effect on the ordering behavior of the nanoparticles, it was reasoned that by generating axle-stabilised particles first, it is possible to direct the orientation of the calixarene moiety. This is achievable since the insertion of the un-stoppered axle fixed on gold particles into the calixarene cavity can be accomplished in one direction, that is, the axle cannot be inserted on the lower rim due to the steric effects incurred by methoxy groups and hence the only possible way is the formation of oriented pseurorotaxane in which the calixarene cavity is facing gold nanoparticles. This is schematically shown in Figure 11a.

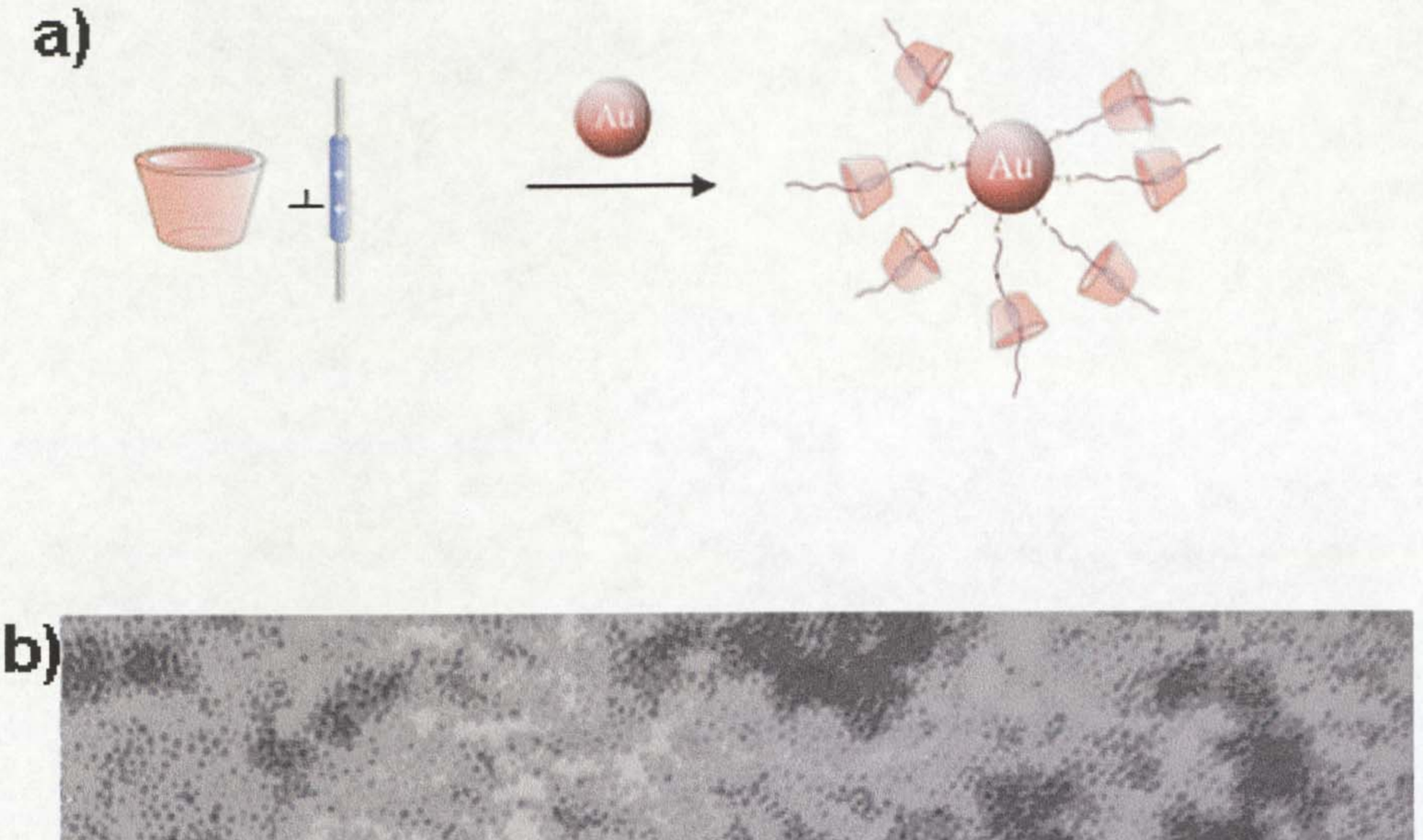

Figure 10. Schematic illustration for the synthesis of oriented pseudorotaxane using octyl isomer as a stabiliser with atleast 10% dodecane thiol added during particles preparation (a) and the corresponding TEM image (b).

Attempts to stabilize gold nanoparticles with an axle (a) proved unsuccessful. Aggregates are formed when axle (a) is added to the TOABr particles (expt. 5). Nevertheless, addition of an additional stabilizer (dodecanethiol, 10 %) led to the formation of stable particles. The axle-stabilised particles were treated with the wheel (b) under conditions used to form pseudorotaxane complexes and the TEM image of the particles formed with 10% dodecanethiol is given in Figure 11b (expt. 6). As shown in Figure 11b, particles are dispersed compared to those prepared by the mixture of isomers shown in Figure 10b, but it is difficult to distinguish weather the resulting oriented pseudorotaxane with a wheel's cavity pointing towards gold nanoparicles largely contribute to any ordering behavior observed in Figure 10b.

To gain insight in the ordering behavior of these particles, we decided to stabilize gold nanoparticles with readily prepared oriented pseudorotaxane containing both octyl and ethoxy chains at the lower rim. The rationale in this case was to observe a critical contributing factor leading to these nanoscopic ordering. In this case thioalkylated axle (c) with a molecular stopper (3,5-di-tert-butyl-phenoxy) on one end was inserted into the calixarene cavity (b) in chloroform. It is important to prepare this complex in chloroform to maintain the integrity and stability of the complex.[29] The resulting oriented pseudorotaxane complexes with either an octyl group (Figure 9f) or an ethoxy group (Figure 9g) were prepared and characterised at Parma in Italy. They were used to stabilize gold nanoparticles for the formation of octyl or ethoxy rotaxane assemblies as schematically shown in Figure 12. The particles prepared in this way were very stable, and un-reacted capping ligands were purified by repeated centrifugation (25000g, 90 mins), re-suspending them in chloroform until the supernatant did not contain any ligands.

The TEM image of ethoxy calixarene mediated rotaxane is presented in Figure 13 and shows that particles are generally dispersed and comparatively not different from their original TOABr stabilised particles. This indicates that the stability and dispersity of the resulting particles are influenced by the presence of a molecular stopper on the axle, which significantly enhances MPCs stability.

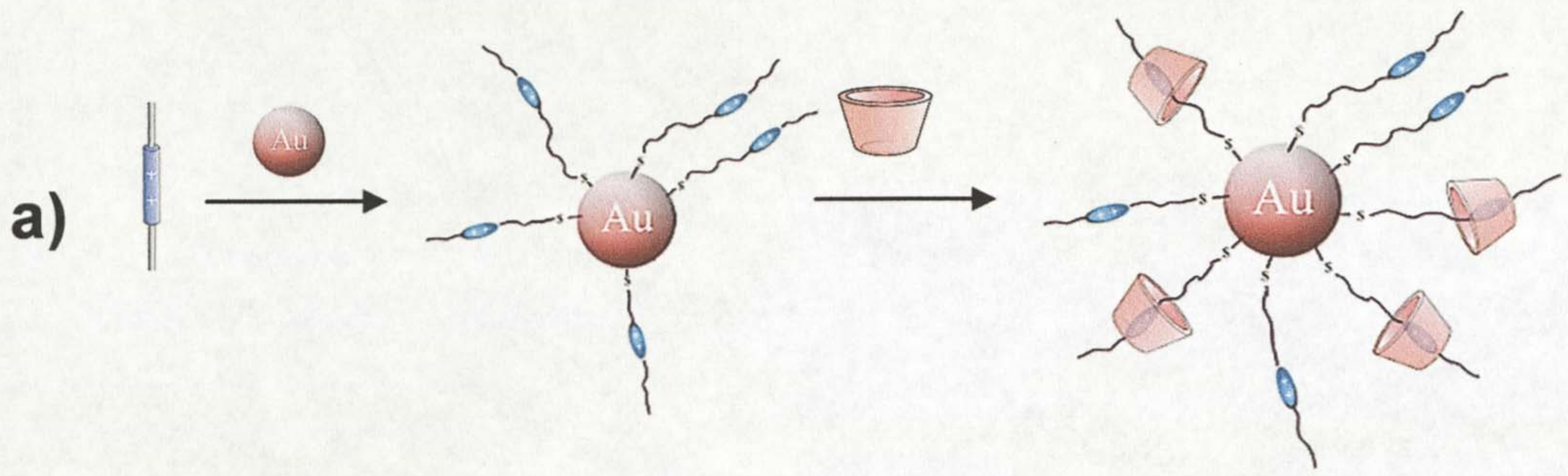

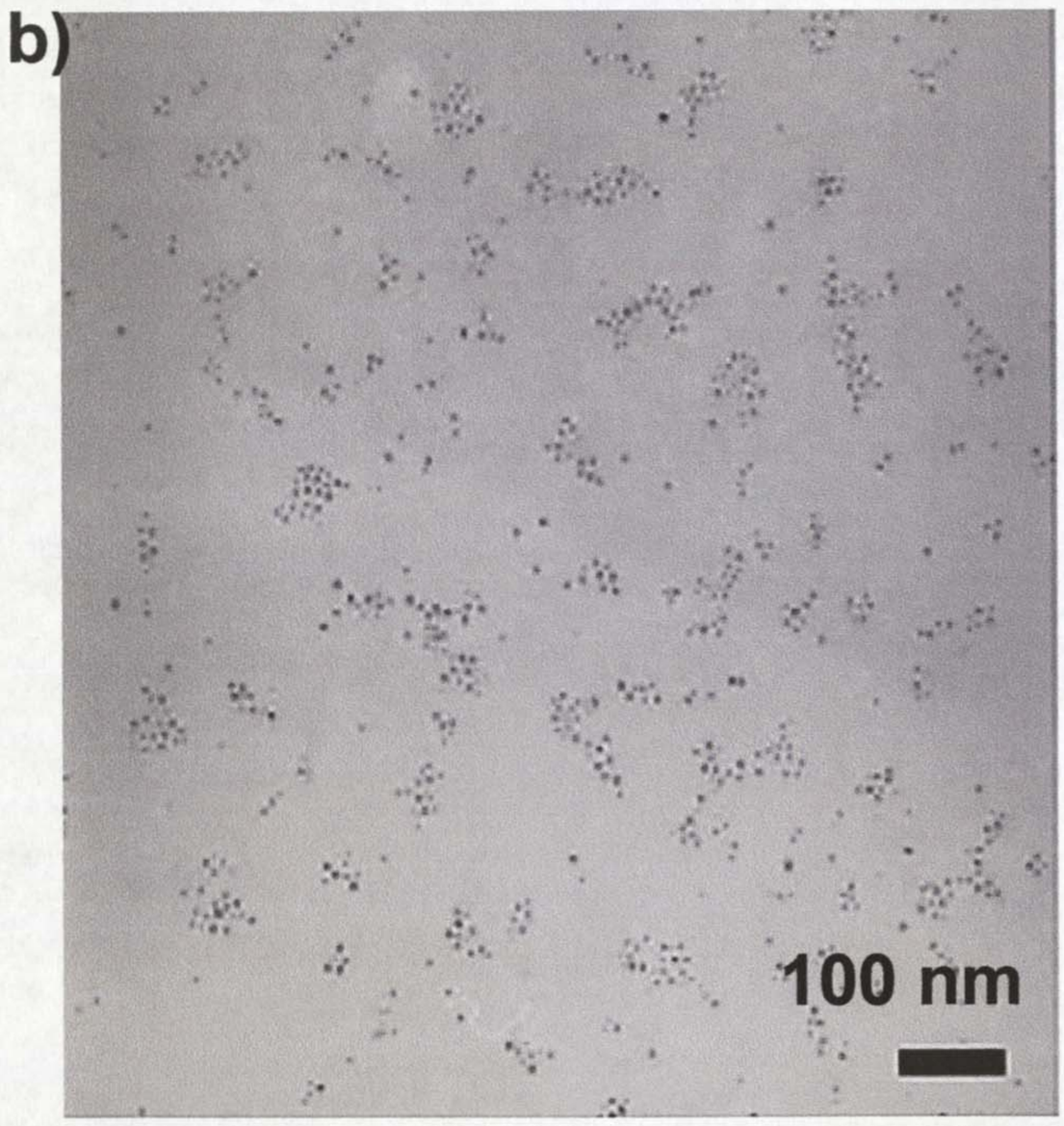

Figure 11. Schematic representation for the synthesis of a) oriented pseudorotaxane complex on gold MPCs using axle (a) in Figure 7, and b) the resulting TEM image.

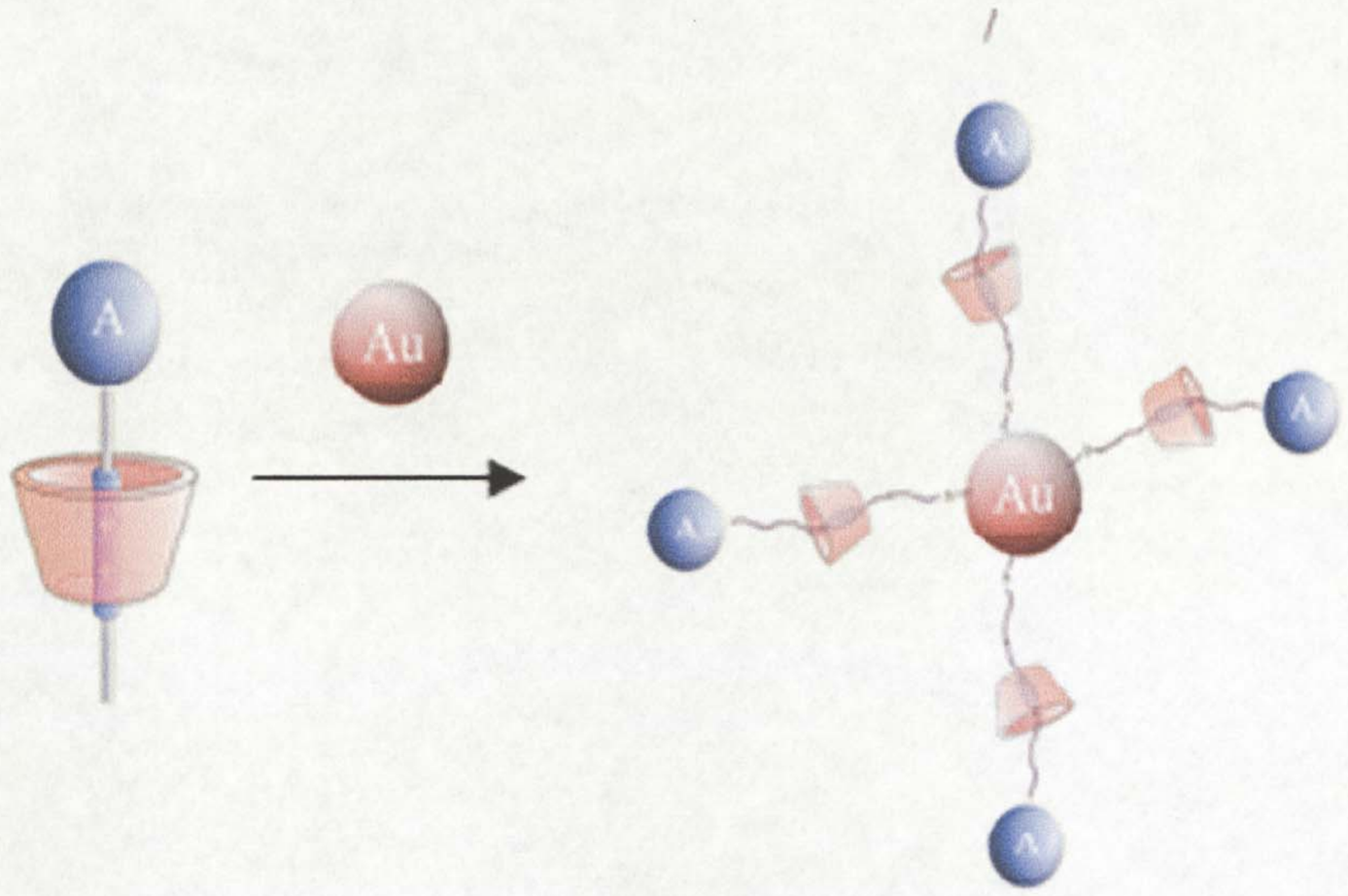

Figure 12. Schematic illustration for the formation of calixarene mediated rotaxane assembly on gold nanoparticles.

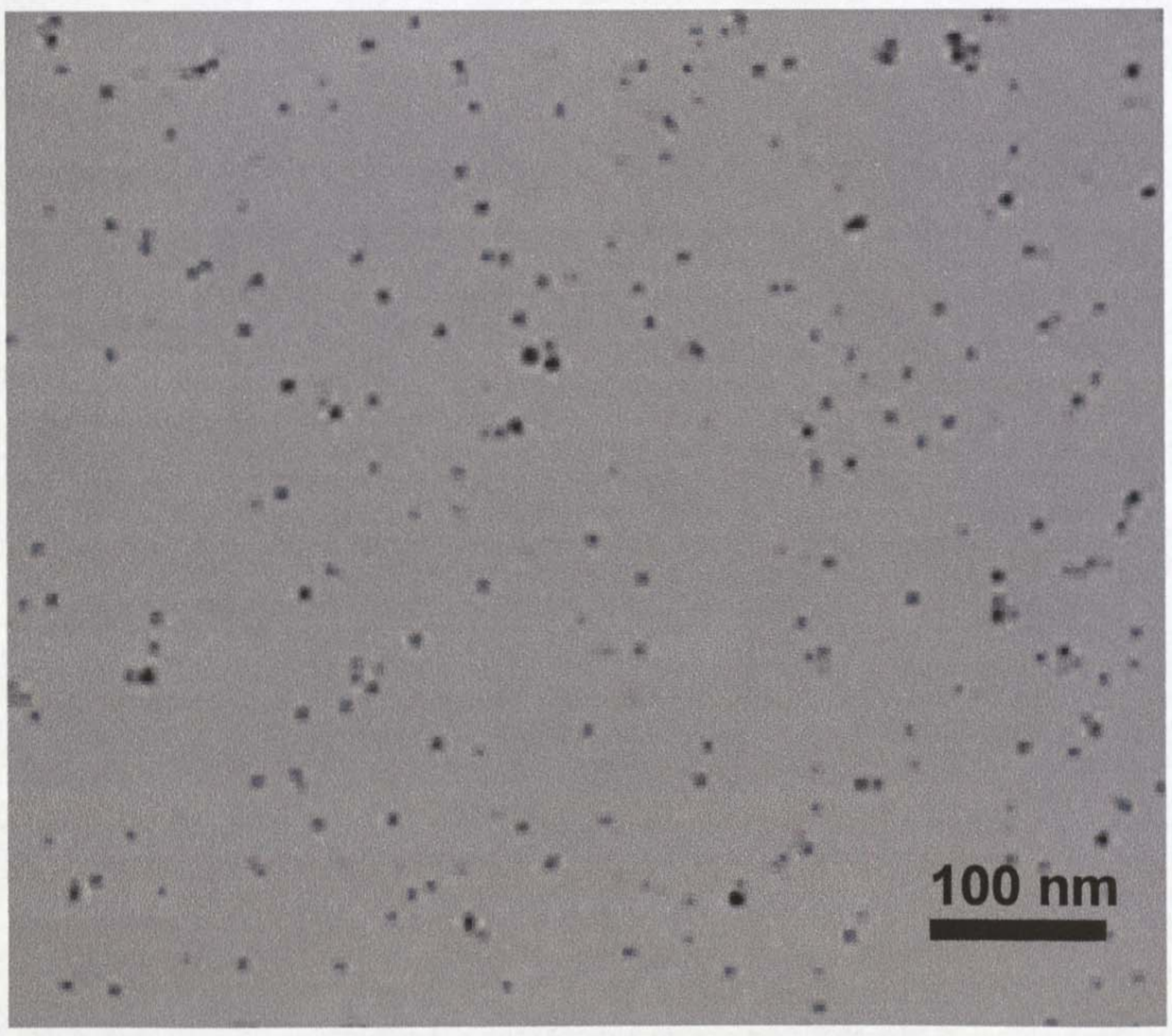

Figure 13. TEM images of ethoxy calixarene mediated rotaxane.

Apart from using ethoxy oriented pseudorotaxane, we explored the use of octyl oriented pseudorotaxane. The octyl oriented pseudorotaxane was used as capping agent to establish a rigidified oriented complex also shown in Figure 12. The complex led to the formation of stable MPCs. Moreover, inspection of the TEM results of this octyl calixarene mediated rotaxane Au-MPCs revealed the formation of stable and to some extent ordered MPCs. This is shown in Figure 14a (for a low magnified image) and high magnified image (Figure 14b). This is rather interesting bearing in mind that the other counterpart (in which calixarene is derivatised with ethoxy group, Figure 11b) doesn't form any ordering behavior observed in this case. The ordering behavior is highly reproducible and the materials were extensively purified, to ensure that the ordering is not caused by any impurities.

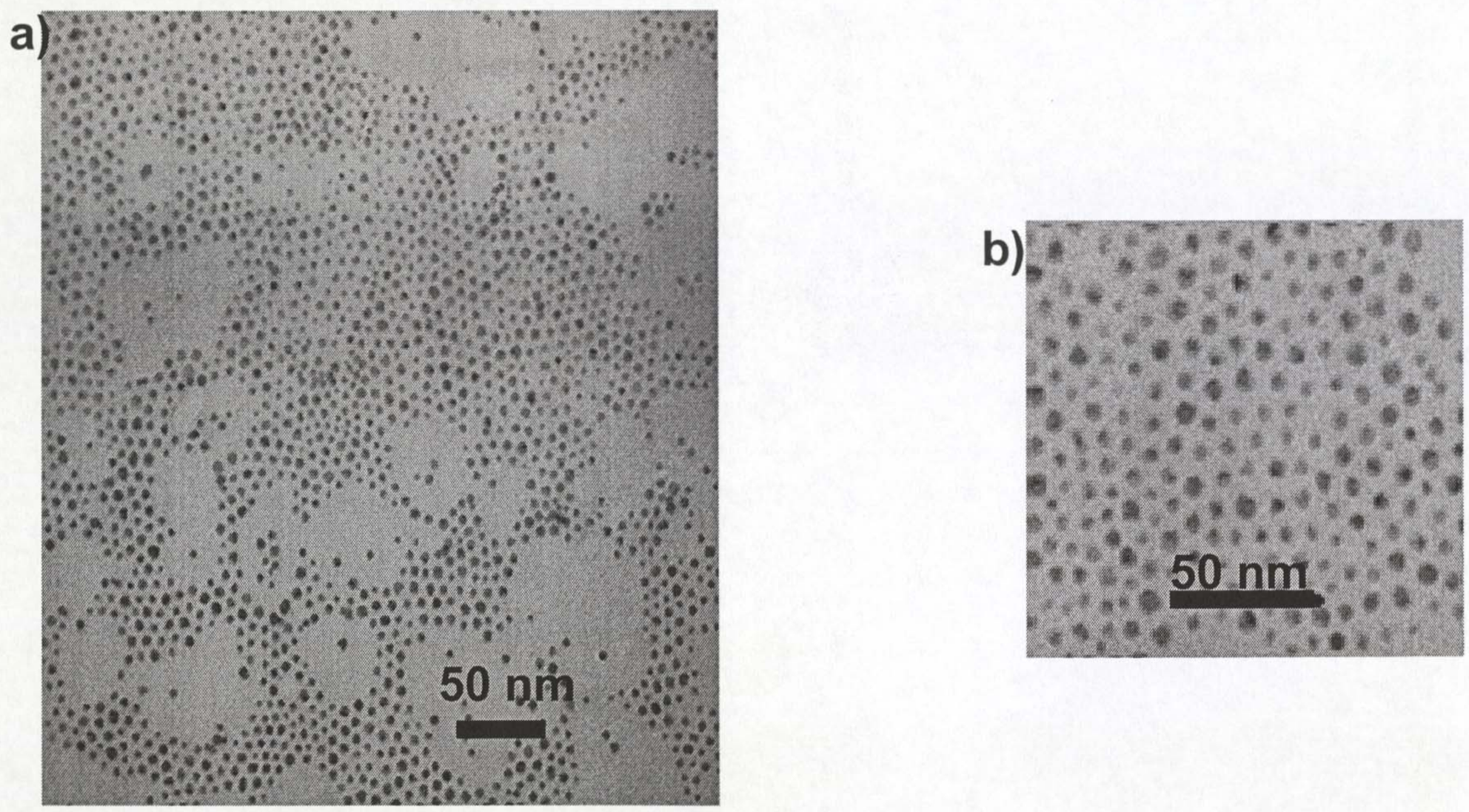

Figure 14. TEM images of a) octyl calixarene mediated rotaxane and b) the higher magnification.

Therefore it can be concluded that, the ordering is due to the formation of rotaxane based gold MPCs enhanced by the octyl spacer on the calixarene and the molecular stopper attached to the axle. The ordering behaviour occurs only when the alkyl (octyl) spacer on calixarene's cavity and molecular stopper attached to the axle are rigidified and then assembled with gold nanopartilces in either chloroform or toluene. An elemental analysis of the pure calixarene mediated rotaxane Au-MPCs showed that at least 63% of the ligand monolayers are the oriented pseudorotaxane passivated on gold nanoparticles and hence this shows that the rotaxane assembly on gold nanoparticles does not dissociate and both the axle and the wheel are present on the surface of gold nanoparticles.

It is hypothesized that the calixarene cavity has to be oriented away from the gold core to establish nanoscopic ordering observed here. However, this should be further validated by additional experiments which allow the formation of oriented pseudorotaxane with the calixarene cavity facing to the opposite side of the molecular stopper. Our attempt to achieve that proved unsuccessful since it was not possible to orientate the calixarene cavity towards the gold core in the absence of an additional stabilizer (dodecanethiol). Importantly, it was found that it is essential to have an alkyl spacer such as octyl to exhit such a nanoscopic ordering. This implies that the alkyl spacer imparts additional stability and rigidifies the resulting conformation and hence leads to ordering of MPCs. The ethoxy group is highly mobile in solution and doesn't provide any additional stability to the entire complex and hence the MPCs are not showing any ordering behavior. Of particular importance in this study is to demonstrate that molecular orientation can potentially lead to nanoscopic ordering.

4.3 Experimental

4.3.1 General materials

Unless specified, chemicals were purchased from Sigma and used as received. Solvents were dried prior to use following standard methods. Flash chromatography was used for purification using standard flash grade silica gel, while thin layer chromatography (TLC) was carried out on silica gel plates (SiO_2, MN ALUGRAM® SIL G/UV_{254}). ^{1}H and ^{13}C NMR spectra were recorded on Bruker AMX-300 or 400 and chemical shifts are quoted relative to the solvent peaks as δ values in ppm. Mass spectra were recorded on VG Auto Spec mass spectrometer. Elemental analysis was obtained using Perkin Elmer 2400 CHN analyser. Melting points were obtained on a Gallenkamp apparatus. UV-vis spectra were obtained from Genesys 10-S spectrophotometer using 1cm quartz cells. For TEM examinations, a single drop of diluted aqueous solution was placed onto a carbon coated copper grid. The grid was left drying on air for several hrs at room temperature. TEM analysis was carried out in a JEOL 2000FX or 2000EX operating at 200keV. Synthesis of (1-mercaptoundec-11-yl) tetraethylene glycol (**1**) was carried out as described elsewhere [31-33] and the synthesis of the host ligand **25,27-bis(11-thio-1-oxy-undecan)-26,28-dihydroxy-calix[4]arene (2)** was also described in detail elsewhere.[32] AFM characterization was carried out by Prof. Zhenxin Wang in Liverpool using AFM (Thermo Explorer ^{TM}) with SPMLab NT Ver. 5.01.

4.3.2 Synthesis

4.3.2.1 Synthesis of Calix[4]arene modified Au MPCs (3)

Compound **1** was synthesized as described in [31] Compound **2** was synthesized as described in. [30] THF (12.5 ml) was added to an aqueous solution of citrate-stabilised gold nanoparticles (RT-7, Chapter 3) (12.5 ml, 2.9 nM).[34-35] To this mixture, solutions of **1** (10 mg, 0.025 mmol, 0.5 ml) and **2** (10 mg, 0.012 mmol, 0.5 ml) in THF were added simultaneously under stirring. It was stirred for 3 hours and filtered (0.45 μm millipore filter).

The particles were purified by repeated centrifugation (3 times) at 11000 rpm (Sigma 1-13 model) and re-dispersion in water. A molar absorption coefficient of 4.2×10^8 $M^{-1}cm^{-1}$ (at 526 nm) based on gold nanoparticles of 15 ± 1.2 nm diameter was used to calculate a final concentration of 1.5 nM (12.5 ml).[36] For ^1H NMR spectroscopy pellets of centrifuged particles were dried under vacuum overnight and re-dissolved in D_2O.

4.3.2.2 Synthesis of 1-[Thio acid S-11-(toluene-4-sulfonyloxy)-undecyl]pyridine-1-ium (4)

Synthesis of compounds **4b-d** and section **4.3.2.2.3** were performed by Dr D. F. Demuru, (Parma, Italy) and are presented as follows;

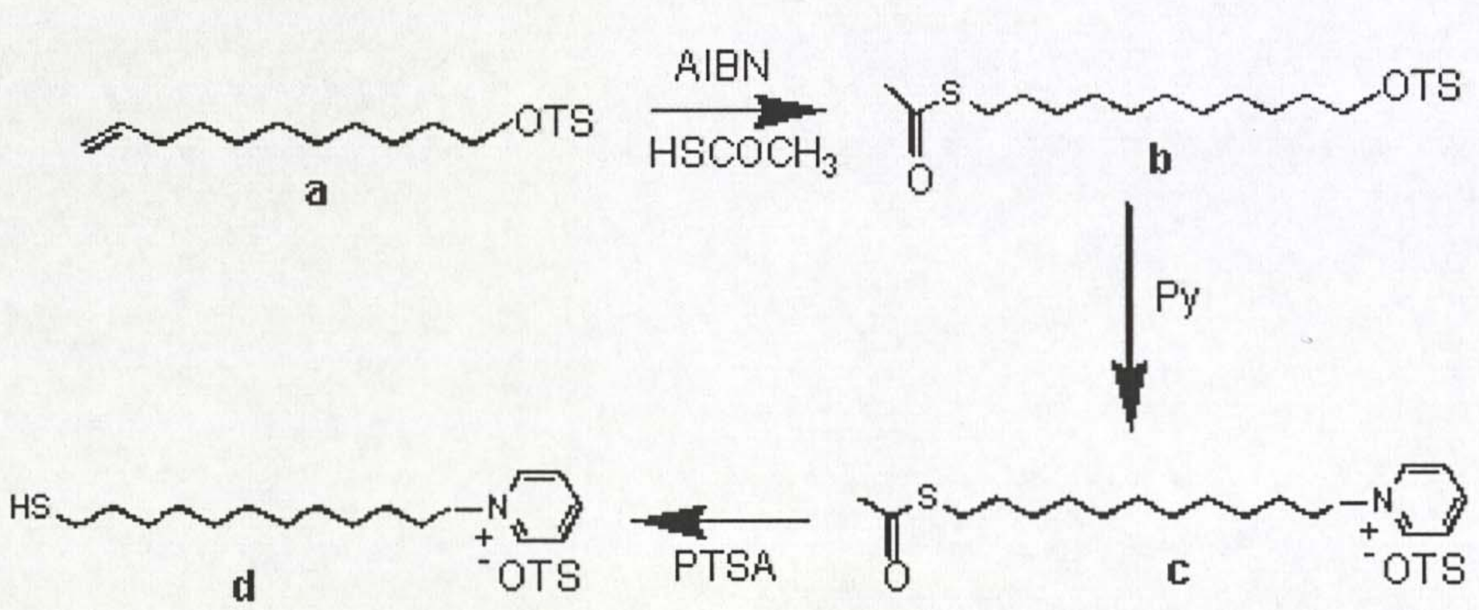

Figure 15. Synthetic scheme for the preparation of 1-[Thio acid S-11-(toluene-4-sulfonyloxy)-undecyl]pyridine-1-ium (4).

4.3.2.2.1 Synthesis of thioacetic acid S-[11-(toluene-4-sulfonyloxy)-undecyl]ester (4b)

Toluene-4-sulfonic acid undec-10-enyl ester (**a**) (5 g, 15.4 mmol) and thioacetic acid (2.3 g, 31 mmol) were dissolved in toluene (200 ml) and purged with argon for 30 mins. A catalytic amount of AIBN was then added to the solution and heated under reflux for three hrs. After three hrs, solvent evaporation was carried out under vacuum and the resulting crude solid material was dissolved in methylene chloride and washed with water and sodium hydrogen carbonate. The product was purified by column chromatography (silica gel, hexane 90%- ethyl acetate 10%) to give a yellowish viscous solid (90% yield). **^{1}H NMR** ($CDCl_3$, 300 MHz, ppm): δ 1.18-1.30 (14H, m), 1.48-1.70(4H, m), 2.32(3H, s), 2.45(3H, s), 2.85(2H, J=6 Hz, t), 4.00(2H, J=6 Hz, t), 7.32(2H, J=6 Hz, d), 7.78(2H, J=6 Hz, d). **^{13}C NMR** ($CDCl_3$, 75 MHz, ppm): δ 22.0, 25.7, 29.2, 29.25, 29.3, 29.4, 29.5, 29.6, 29.7, 29.9, 31.1, 71.1, 128.3, 130.2, 133.8, 144.9, 196.3. **EI-MS** (m/z): 400(M^+). **Elemental analysis:** C_{20}: 59.94%, H_{32}: 8.05%, S_2: 8.10%; found C_{20}: 60.20%, H_{32}: 8.20%, S_2: 8.42%.

1-[Thioacetic acid S-11-(toluene-4-sulfonyloxy)-undecyl ester]-pyridine-1-ium (4c)

To the solution of thioacetic acid S-[11-(toluene-4-sulfonyloxy)-undecyl]ester (**4b**) (2 g, 5 mmol, in acetonitrile (100 ml) was added pyridine (0.5 g, 5 mmol) and the mixture was refluxed for 24 hrs. Solvent was evaporated under vacuum and the pure white solid product was obtained by precipitation in ethyl acetate/acetone in good yield 80%. **^{1}H NMR** (DMSO-d_6, 300 MHz, ppm): δ 1.21-1.30(14H, m), 1.5(2H, m), 1.9(2H, m), 2.28(3H, s), 2.32(3H, s), 2.75(2H, J=5.5 Hz, t), 4.60(2H, J=5.5 Hz, t), 7.11(2H, J=5.5 Hz, d), 7.48(2H, J=6 Hz, d), 8.15(2H, J=5.5 Hz, t), 8.60(1H, J=6 Hz, t), 9.06(2H, J=4 Hz, d). **^{13}C NMR** (DMSO-d_6, 75 MHz, ppm): δ 21.1, 25.7, 28.5, 28.7, 28.8, 29.0, 29.1, 29.5, 30.9, 31.0, 61.2, 125.9, 128.4, 128.5, 137.9, 145.1, 145.8, 146.2, 195.7. **EI-MS** (m/z): 308(M^+). **m.p.**: 166-168 °C. **Elemental analysis:** C_{25}: 62.58%, H_{37}: 7.78%, N: 2.90%, S_2: 13.38%; found C_{25}: 62.79%, H_{37}: 8.10%, N: 3.10%, S_2: 13.00%.

1-[Thio acid S-11-(toluene-4-sulfonyloxy)-undecyl]pyridine-1-ium (4d)

1-[Thioacetic acid S-11-(toluene-4-sulfonyloxy)-undecyl ester]-pyridine-1-ium (**4c**) (2 g, 4 mmol) and para-toluene sulphonic acid (1 g, 7 mmol) were dissolved in methanol. The mixture was stirred and refluxed overnight followed by solvent evaporation under vacuum. Precipitation of the resulting mixture in methylene chloride afforded a pure white sticky solid product (75 % yield). **^{1}H NMR** (DMSO-d_6, 300 MHz, ppm): δ 1.23-1.32(14H, m), 1.52(2H, m), 1.91(2H, m), 2.29(3H, s), 2.55(2H, *J*=6 Hz, t), 4.59(2H, *J*=5.5 Hz, t), 7.10(2H, *J*=5.5 Hz, d), 7.49(2H, *J*=6 Hz, d), 8.15(2H, *J*=5.5 Hz, t), 8.60(1H, *J*=6 Hz, t), 9.07(2H, *J*=4 Hz, d). **^{13}C NMR** (DMSO-d_6, 75 MHz, ppm): δ 21.1, 22.3, 25.8, 28.7, 28.9, 29.0, 29.1, 29.2, 29.8, 31.0, 31.1, 55.7, 61.2, 125.9, 128.4, 128.5, 138.0, 145.1, 145.8, 146.2. **EI-MS** (m/z): 266(M^+). **m.p.**: 186-188 °C. **Elemental analysis:** C_{23}: 63.10%, H_{35}: 8.06%, N: 3.20%, S_2: 14.66%; found C_{23}: 62.80%, H_{35}: 8.20%, N: 3.42%, S_2: 14.33%.

4.3.2.2.3 Determination of the binding abilities of the model calix[4]arene derivative toward N-alkyl pyridinium salts in aqueous solution

The salt ***5*** was obtained by titration with 0.01 M NaOH solution the 25,27-Bis[carboxymethoxy]-26,28-dihydroxycalix[4]arene, synthesized according to known procedures.[37]

The *Critical Association Concentration* (CAC) of **5** was then estimated by ^{1}H NMR spectroscopy recording the chemical shift variation of the phenolic OH proton signal upon dilution with D_2O. No significant chemical shift variation was observed for solutions of **5** from 10^{-3} to 10^{-4} M concentration interval. Several titration experiments were performed with calix[4]arene **5** toward *N*-methyl pyridinium tosylate **6** and *N*-propyl pyridinium iodide **7** in D_2O by ^{1}H NMR spectroscopy. All NMR spectra showed time-averaged signals for the free and complexed species, hence the association constants (K_{as}) were determined using methods previously described[38] having verified a 1:1 stoichiometry through "continuous variation" methods, by adding increasing amounts of the appropriate host solution (c = 1.0 x 10^{-3} M) to a solution

of the guest (c = 1.7 x 10^{-2} M), and monitoring the shift of the NC<u>H</u>$_3$ or NC<u>H</u>$_2$- signals that, because of their endo cavity inclusion, are upfield shifted. The results obtained for the two guests are reported in the following table:

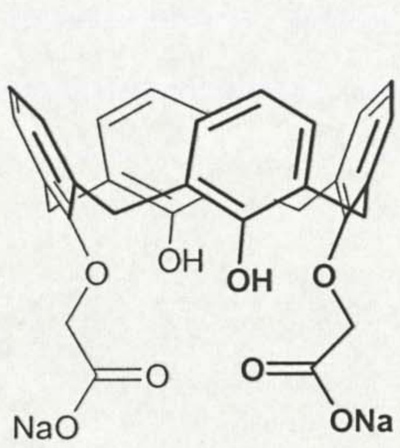

5

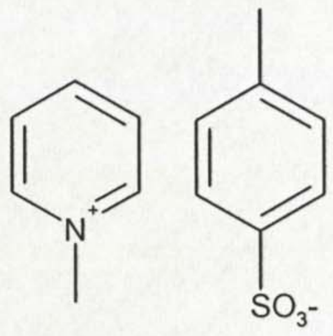

6

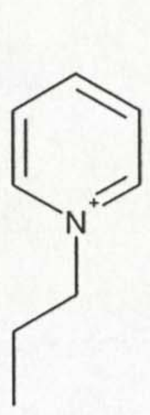

7

Salts	**6**	**7**
K_{as} (M^{-1})	600 ± 100	260 ± 50

4.3.3 Preparation of self assembled monolayers (SAMs) of 4

SAMs of **4** on gold (gold films of *ca*. 250 nm thickness on quartz glass, Arrandee, Germany) were prepared by overnight immersion of the cleaned and flame annealed substrates in a solution of **4** in chloroform (5 ml, 1.2 x 10^{-4} M) followed by thorough rinsing with chloroform and drying in a stream of nitrogen. Single molecular sieve beads (4A type, Aldrich, UK) were modified by overnight immersion in solutions of **4** (2.5 ml, 1.2 x 10^{-4} M) in chloroform. After removal from the solution, the beads were washed thoroughly with chloroform and allowed to dry at room temperature.

4.3.4 Specific recognition

Specific recognition experiments were carried out by overnight immersion of the substrates (SAMs and beads) in a solution of **3** (0.034 nM, 2.5 ml for SAMs and 1.2 nM, 1.5 ml for beads). Adequate control experiments were performed to exclude the possibility of non-specific binding.

4.3.5 General preparation of calixarene-based rotaxane on gold nanoparticles

4.3.5.1 Synthesis of tetraoctyl ammonium bromide stabilised particles

Synthesis of TOABr stabilised particles was carried out as discussed in chapter 3 (RT- 2) briefly; an aqueous solution of chloroauric acid (*ca*. 30 ml, 30 mM) was mixed with tetraoctylammonium bromide solution (80 ml, 50 mM in toluene). The resulting two-phase mixture was vigorously stirred, allowing a complete transfer of tetrachloroaurate into an organic phase. A freshly prepared aqueous solution of sodium borohydride (25 ml, 400 mM) was added slowly with vigorous stirring and the mixture was stirred for 3 hrs. After 3 hrs, the organic phase was separated and washed once with 0.1M H_2SO_4, 0.1 M NaOH and 5 times with water, to give 5-8 nm TOABr stabilized particles

A general procedure for the preparation of calixarene-based rotaxane gold nanopartlces was carried out as follows: To the tetraoctyl ammonium bromide stabilised particles (6 ml) was added toluene solution (0.5 ml) of oriented pseudorotaxane complex (3.9 mg/ml) and the reaction mixture was stirred for 2hrs and then repeatedly centrifuged (2 times, at 25000g, 90 min), re-suspending particles in either toluene or chloroform.

For the preparation of oriented pseudorotaxane mediated gold nanoparticles the experimental procedure described for the preparation of calixarene-based rotaxane gold nanoparticles was followed using caping ligand (3.9 mg/ml) added to RT-2 particles (6 ml) and where necessary 10% of dodecane thiol was added. The same procedure was followed using octyl (5mg/ml) or ethoxy (5mg/ml) isomers or axle (4.2mg/ml) for the stabilization of gold nanoparticles (6 ml).

4.4 References

[1] Tshikhudo, T. R., Demuru, D. Wang, Z., Brust, M., Secchi, A., Arduini, A and Pochini, A., *Angew. Chem. Int. Ed.*, 2005, **44,** 2293

[2] Bohmer, V., *Angew. Chem. Int. Ed.,* 1995, **34**, 713

[3] Ashton, P. R., Boyd, S. E., Brindle, A., Langford, S. J., Menzer, S., Pere-Garcia, L., Preece, J. A., Raymo, F. M., Spencer, N., Stoddart, J. F., White, A. J. P and Williams, D. J., *New J. Chem.*, 1999, **23**, 587

[4] Fitzmaurice, D., Rao, S. N., Preece, J. A., Stoddart, J. F., Wenger, S and Zaccheroni, N., *Angwew. Chem. Int. Ed.* 1999, **38**, 1147

[5] Casnati, A., Ferdani, R and Pochini, A., *J. Org. Chem*., 1997, **62**, 6236

[6] Mandolini, L and Ungaro, R., *Calixarenes in actions*, Imperial College Press, London, 2000

[7] Bohmer, V., Merkel, L and Kunz, U., *J. Chem. Soc. Chem. Commun*., 1987, 896.

[8] Shinkai, S., *Tetrahedron*, 1993, **49**, 8933.

[9] Kanamathareddy, S and Gutsche, C. D., *J. Am. Chem. Soc*., 1993, **115**, *6572*

[10] van Hoorn, W. P., Morshuis, M. G. H, van Veggel, F. C. J. M and Reinhoudt, D. N. *J. Chem. Phys. A*., 1998, **102**, 1130

[11] Briels, W. J and van Duynhoven, J. P. M., *J. Org. Chem*., 1998, **63**, 1299

[12] Arduini, A., McGregor, M. W., Pochini, A., Secchi, A., Ugozzoli, F., Húngaro, R., *J. Org. Chem*. 1996, **61**, 6881

[13] Koh, K. N., Araki, k., Ikeda, A., Otsuka, H and Shinkai, S., *J. Am. Chem. Soc*. 1996, **118**, 755

[14] Conner, M., Janout, V and Regen, S. J., *J. Am. Chem. Soc*., 1993, **115**, 1178

[15] Dedek, P., Webber, A. S., Janout, V., Hendel, R. A and Regen, S. J., *Langmuir*, 1994, **10**, 3943

[16] Hendel, R. A., Janout, V and Regen, S. J., *Langmuir*, 1996, **12**, 5745

[17] Dei, L., Casnati, A., Lonostro, P and Baglioni, P., *Langmuir*, 1995, **11**, 1268

[18] Tyson, J. C., Moore, J. L., Hughes, K. D and Collard, D. M., *Langmuir*, 1997, **13**, 2068

[19] Kurihara, K., Ohto, K., Tanaka, Y., Aoyama, Y and Kunikate, T., *J. Am. Chem. Soc*., 1991, **113**, 444

[20] Richardson, T., Greenwood, M. B., Davis, F and Stirling, C. J. M., *Langmuir*, 1995, **11**, 4623

[21] Nabok, A. V., Richrdson, T., Greenwood, M. B., Davis, F and Stirling, C. J. M., *Langmuir*, 1997, **13**, 3198

[22] Lo, PK., Chen, D. Z., Meng, O. W and Wong, M. S., *Chem.. Mater*. 2006, **18**, 3924

[23] Abou-Hamdan, A., Bugnon, P., Saudan, C., Lye, P.G and Merbach, A. E., *J. Am. Chem. Soc*., 2000, **112**, 592

[24] Saudan, P., Dunand, F. A., Abou-Hamdan, A., Bugnon, C., Lye, P and Merbach, G., *J. Am. Chem. Soc*., 2001, **123**, 10290

[25] Loeb, S. J., Tiburcio, J., Vella, S. J and Wisner, J. M., *Org. Biomol. Chem*., 2006, **4**, 667

[26] Skinner, P. J., Blair, S., Kataky, R and Parker, D., *New J. Chem*., 2000, **24**, 265

[27] Nepogodiev, S. A and Stoddart, J. F., *Chem. Rev*., 1998, **98**, 1959

[28] Zhao, Y., Chen, Y., Wang, M and Liu, Y., *Organic Lett.*, 2006, **8,** 1267

[29] Arduni, A., Ferdani, R., Pochini, A., Secchi, A and Ugozzoli, F., *Angew. Chem. Int. Ed.*, 2000, **39**, 3453

[30] Ardunini, A., Demuru, D., Pochini, A and Secchi, A *Chem. Commun.*, 2005, 645

[31] Pale-Grosdemange, C., Simon, E. S., Prime, K. L., Whitesides, G. M., *J. Am. Chem. Soc.*, 1991, **113**, 12

[32] Tshikhudo, T.R., Wang, Z., Brust, M., *J. Mater. Science & Technol.*, 2004, **20** (8), 980

[33] Kanaras, A. G., Kamounah, F. S., Schaumburg, C., Kiely, C. J and Brust, M., *Chem. Commun.*, 2002, 2294

[34] Turkevich, J.,Stevenson, P. J and Hillier, J., *Discuss. Faraday Soc.*, 1951, **11**, 55

[35] Frens, G., *Nature Physical Science,* 1973, **241**, 20

[36] Demers, L. M., Mirkin, C. A., Mucic, R. C., Reynolds, R. A., Letsinger, R. L., Elghnian, R., Viswanadham, G., *Anal. Chem.,* 2000, **72**, 5535

[37] Arena, G., Casnati, A.,Mirone, L., Sciotto, D and Ungaro, R *Tetrahedron Lett.,* 1997, **38**, 1999

[38] Arduini, A., McGregor, W. M., Paganuzzi, D., Pochini, A., Secchi, A., Ugozzoli F., and Ungaro, R., *J. Chem. Soc, Perkin Trans., 2* 1996, 839

CHAPTER 5

BIOMOLECULAR FUNCTIONALISATION OF GOLD AND SILVER MPCS

5 Biomolecular Functionalisation of Gold and Silver MPCs

5.1 Introduction

Proteins are major components of cells and they are in the size domain (~ 5 nm) of nanoparticles. This similarity in size provides a rationale for the use of nanoparticles as probes to investigate biological and intra-cellular processes. Many applications of nanoparticles in biology and medicine have been reviewed by Salata [1] including:-

i) Biodetection of pathogens

ii) Detection of proteins

iii) Drug and gene delivery

iv) Tumor destruction via heating (hyperthermia)

v) Probing DNA structure

vi) Fluorescent biological labels *etc*.

All these applications require the attachment of a biomolecule of interest to the nanoparticle. This bioconjugation step must be performed under mild conditions to retain the biological activity of the resulting nanohybrid material. Many strategies have been attempted and utilized to date to attach biomolecules to nanoparticles. Reviews by Kumar, [2] Katz and Willner,[3] outlined relevant bioconjugation strategies which can be categorised as electrostatic binding, [4] covalent coupling [5-8] and specific recognition. [9-11]Some of these strategies are shown in Figure 1.

Adsorption of biomolecules to the nanoparticles by electrostatic interaction is illustrated in Figure 1A and B. Gold and silver hydrosols prepared by the citrate reduction method for instance are negatively charged allowing simple adsorption of positively charged proteins [4] (Figure 1A). This has been commonly used to prepare bioconjugates for immunolabeling since the 1960s. [12] Multilayer assemblies of proteins as shown in Figure 1B can be constructed by attaching a polyelectrolyte polymer to the protein-coated nanoparticles, which then allows the deposition of a second protein layer. [5, 6] The major drawbacks of protein adsorption by electrostatic interaction are (i) that it is very difficult to control the number of biomolecules attached (ii) that the particles lack stability and (iii) that the activity of biomolecules generally decreases gradually with time.

Chemisorption of biomolecules to nanoparticles is shown in Figure 1C and D. In the simplest case, proteins can be chemisorbed to the nanoparticles through thiol or amine groups that can be engineered [13, 14] or are already present in the protein. [15, 16] In either way, the biological activity of the resulting bioconjugates usually decreases dramatically due to conformational change upon adsorption. [3, 17] In addition, it has been shown that proteins are often denatured leading to the loss of their biological activity. To avoid some of these problems, bifunctional linkers containing a thiol group to link to the particle and functional groups such as carboxylic acid to link to the protein have been used [8, 18, 19] (Figure 1C). Particles engineered in this way are stable, however, site specific attachment of biomolecules by covalent means is generally a substantial synthetic challenge.[20] Nucleic acids have been widely used following the approach illustrated in Figure 1D. Since they can be synthesized terminated with alkane thiol groups, they have been used to directly stabilize gold nanoparticles.[21-23]

Figure 1E, shows physisorption of biomolecules to nanoparticles and the immobilization of other biomolecules by the biotin-avidin system. Avidin and or antibodies can be adsorbed to nanoparticles, which are then used to bind to biotinylated functionalities and antigens, respectively. This is an attractive and frequently used strategy, however, the particles often lack stability. [24,25]

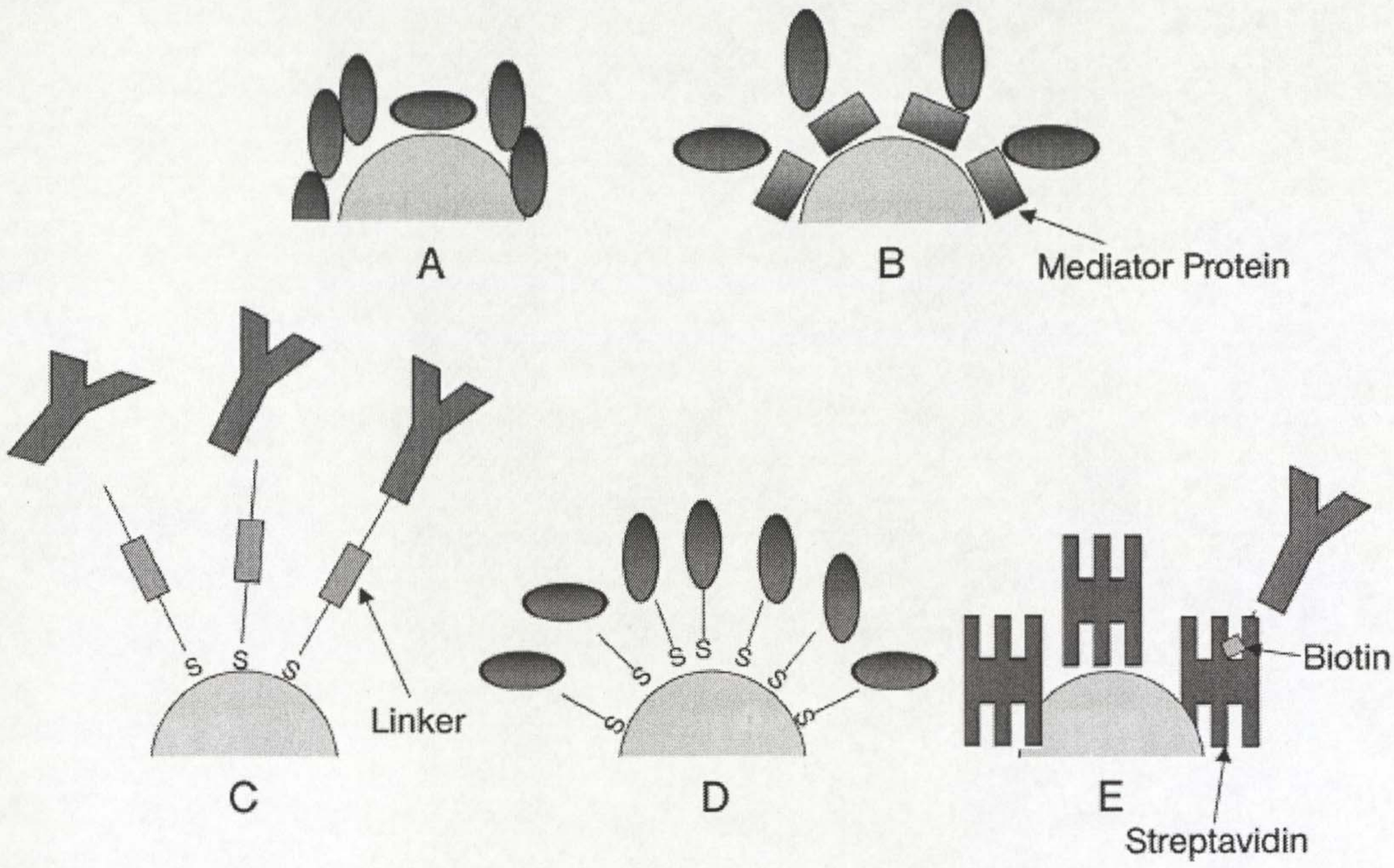

Figure 1. Strategies commonly used for biomolecular functionalisation, A) direct physisorption of biomolecules to nanoparticles. B) Assisted physisorption using pre-bound biomolecule, C) Bioconjugation via cross-linkers on the chemisorbed functional ligand on nanoparticles. D) Direct conjugation of thiolated biomolecules to nanoparticles. E) Attaching biotinylated molecules to avidin physisorbed on nanoparticles. [2]

5.2 Results and Discussion

Generally, biomolecular functionalisation was achieved by two different approaches, *i.e.* covalent linkage employing either carbodiimide chemistry or "click" chemistry, and non-covalent attachment via the biotin-avidin-biotin (BAB) system. These approaches are diagrammatically illustrated in Figure 2. For simplicity, a modular annotation is introduced here to clearly describe and identify each biomolecularly functionalized particle produced in this chapter. Familiarity with this system is essential in order to understand the material presented. The annotation consists of five modules, (i) type of metal, (ii) size of particle in nm, (iii) percentage of functional ligand within the PEG ligand shell, (iv)attachment type of biomolecular functionality and (v) biomolecular functionality. A generic example is given below.

[Au, 5, 1%, BAB, IgG]

This example refers to gold nanoparticles of 5 nm diameter, with 1% of functional ligand in the PEG ligand shell. The attachment strategy is non-covalent *via* the biotin-avidin-biotin system "BAB" (Figure 2), and the biomolecular functionality used is IgG. From now on, this annotation will be used consistently to fully describe all particles prepared and used in this chapter. Table 1 gives an overview of all modules employed in this work. Partially assembled particles, for example, precursors of a final product, are annotated with "_" to indicate missing modules (see below).

[Au, 5, 1%, B, -]

Non-covalent biomolecular functionalisation will be discussed first followed by covalent approaches.

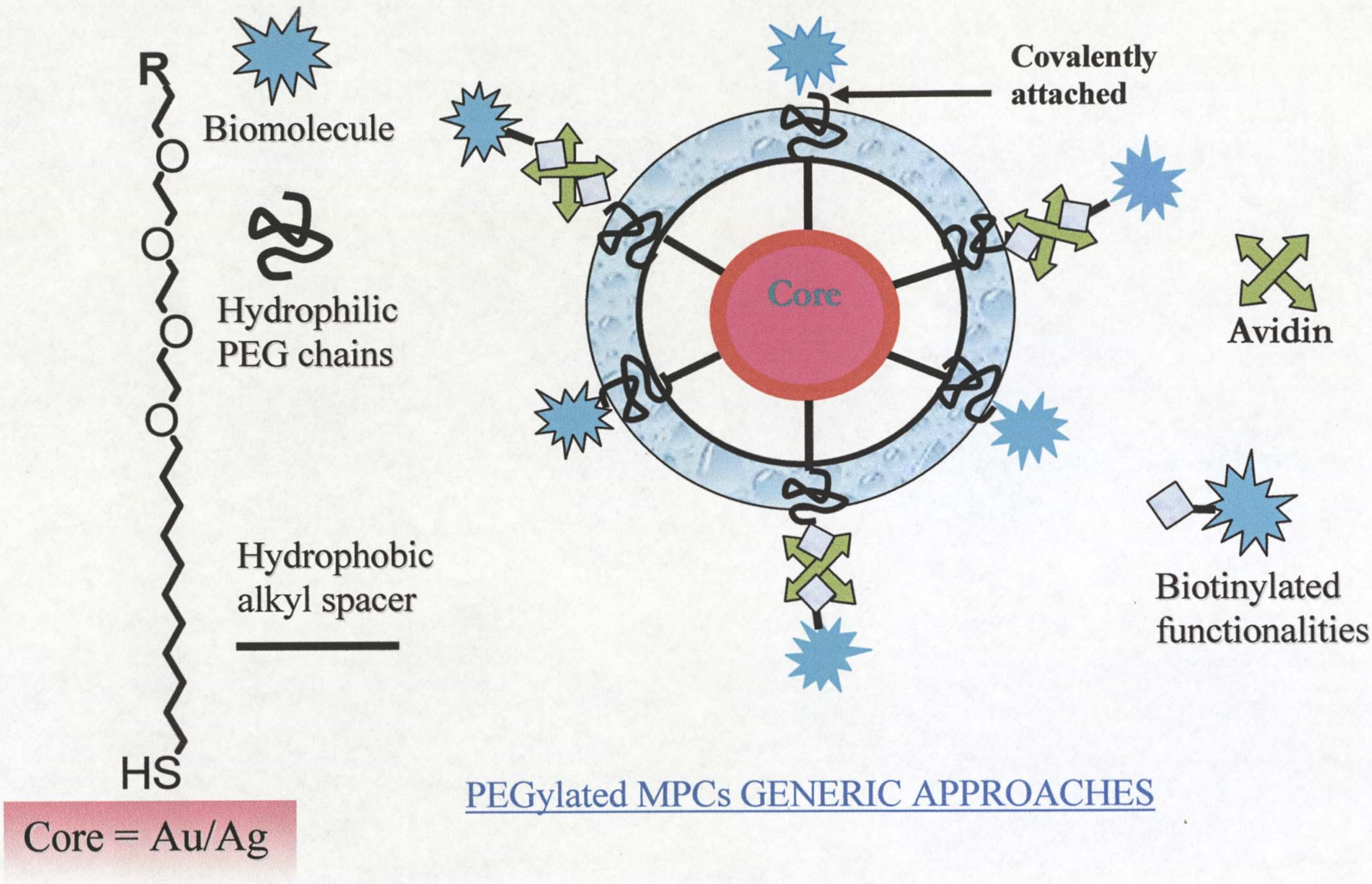

Figure 2. Diagrammatic illustration of the two generic approaches for the development of biomolecular functionalized MPCs, *i.e.* covalent and non-covalent chemistry.

Metal	**Size/ nm**	**% Function**	**Attachment type**	**Biomolecular functionality**
Au	~ 5	1	B	IgG
Ag	~ 6	5	BA	Sugar
	~ 14	10	BAB	Dye
		70	EDC	Lipase
		100	Click	DNA
				BSA
				Avidin*
				Biotin

Table 1. Overview of all modules used to construct biomolecularly functionalized nanoparticles. B = biotin, BA = Biotin-Avidin*, BAB = Biotin-Avidin*-Biotin, Click = conjugation via click chemistry, EDC = conjugation via 1-ethyl-3-(3-dimethylaminopropyl)carbodiimide hydrochloride (EDC) cross-linker.

* or streptavidin, or neutravidin

5.2.1 Non-covalent bioconjugation

5.2.1.1 The biotin-avidin-biotin system (BAB)

This approach was chosen to take advantage of the well-established affinity between biotin and avidin (or its analogs, *i.e.* neutravidin and streptavidin) to develop the desired biomolecularly functionalized MPCs. The aim of this study is to first prepare biotin-functionalised hydrophilic MPCs (see 5.2.1.2), and then saturate them with avidin to obtain avidin functionalised MPCs (5.2.1.3). The avidin particles can then be used as readily available bio-gold products to bind to any biotinylated functionality of choice, which can be made or purchased. The overall picture is shown in Figure 3 demonstrating the development of a kit for biomolecularly functionalized MPCs by the BAB-type method, *e.g.* MPCs with antibodies attached for diagnostic purposes *etc.*

5.2.1.2 Preparation of biotin modified MPCs

[Au, 14, 1%, B, -], [Au, 14, 10%, B, -], [Au, 6, 1%, B, -], [Au, 6, 10%, B, -]

A schematic diagram for the preparation of biotin modified PEGylated MPCs is shown in Figure 4. Biotin modified MPCs were prepared by taking advantage of using readily available thioalkylated PEG-biotin. This ligand was attached to the nanoparticles surface by using the monohydroxy PEG ligand (PEG-OH) as a stabiliser and solubiliser similar to the approach described for the introduction of calix[4]arene to Au MPCs (chapter 4). In this case, a mixture of PEG-OH and PEG-biotin ligands (1 or 10% biotinylated species) in alcohol was incubated with citrate stabilised particles [(RT-7, 14 nm), chapter 3] and stirred overnight to obtain the desired biotin modified MPCs. The biotinylated MPCs of smaller Au core [Au, 6, 1%, B, -], [Au, 6, 10%, B, -] were also prepared in the same way using borohydride stabilised particles (RT-5, chapter 3). The resulting biotin modified MPCs were generally purified by size-exclusion chromatography (Sephacryl 100HR) and stored in phosphate buffer.

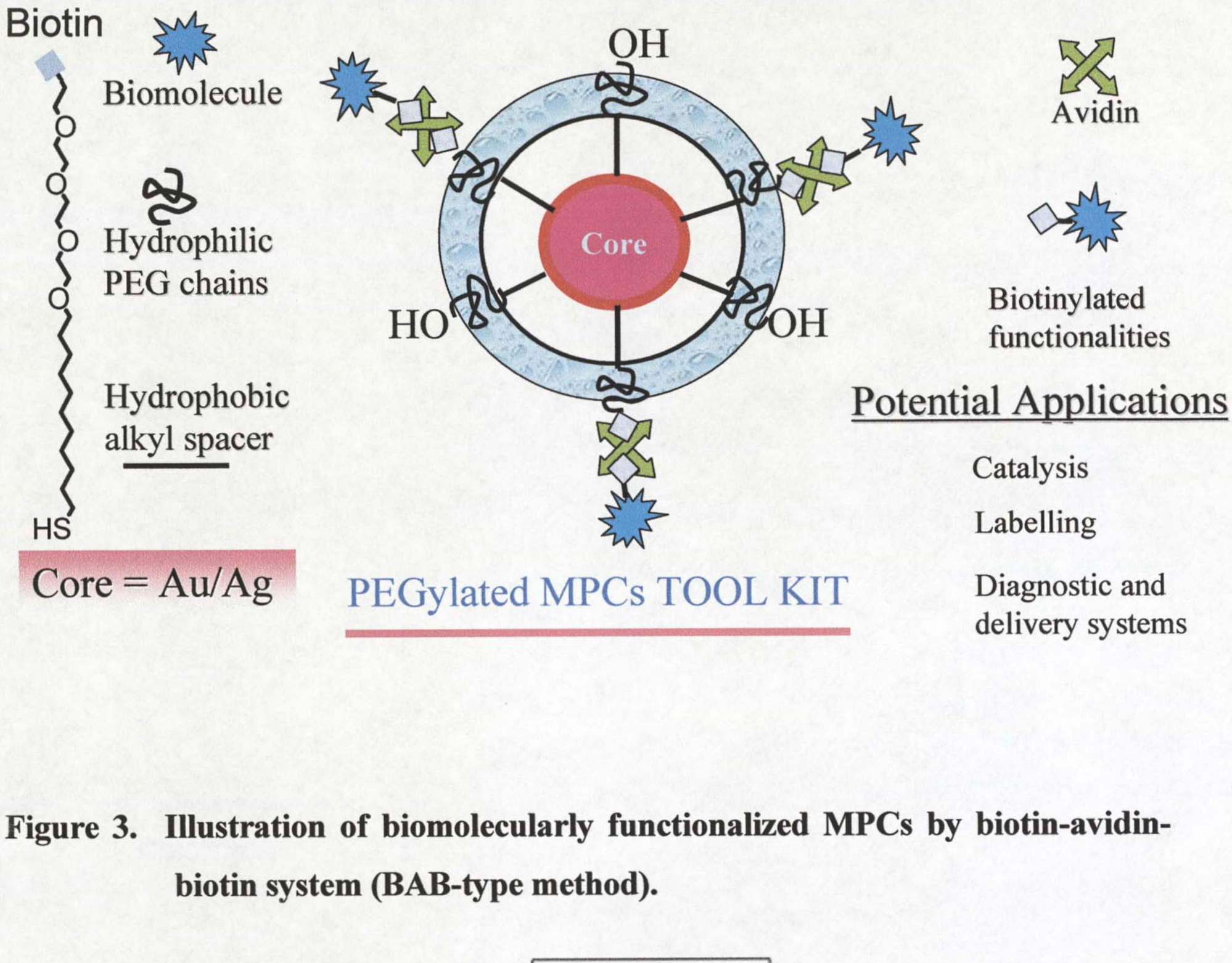

Figure 3. Illustration of biomolecularly functionalized MPCs by biotin-avidin-biotin system (BAB-type method).

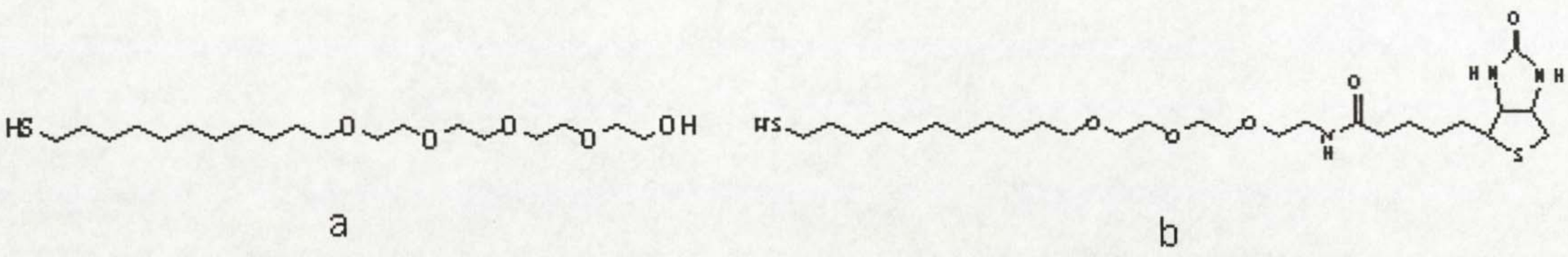

Figure 4. Schematic for the preparation of biotin modified MPCs using thioalkylated PEG-OH (a) and PEG-biotin (b) ligands.

Unlike their precursor particles (RT-7 and RT-5, chapter 3), the PEGylated and biotin modified MPCs are extremely stable in high electrolyte concentration (> 2M NaCl) and at pH ranging from 1-14 and can be manipulated easily without the loss of material. They were characterized by gel electrophoresis and TEM. Figure 5 shows the TEM images of biotin modified MPCs of, (a) [Au, 6, 10%, B, -], (b) [Au, 14, 1%, B, -] and (c) [Au, 14, 10%, B, -]. Noteworthy is the fact that in addition to the stability of these MPCs, they are very uniform and resemble the respective precursor particles.

Gel electrophoresis is a useful technique providing important information on the success of the conjugation reaction. We have compared the electrophoretic mobility of larger biotin modified MPCs in agarose gel electrophoresis (2 % (wt/v)) using TBE buffer. The results are shown in Figure 6, in which lane 1 shows the migration of [Au, 14, 1 %, B, -], lane 2 band carries [Au, 14, 10 %, B, -]. Generally, particles move towards the positive pole indicating negative charge at neutral pH. This makes MPCs with more biotin [Au, 14, 10%, B, -] in lane 2, to migrate faster than those with less biotin [Au, 14, 1%, B, -] in lane 1, towards the anode. Based on the elemental analysis presented in chapter 3 for PEG-OH, it is reasonable to estimate that, there are approximately 30 and 300 biotin molecules per particle for [Au, 14, 1%, B, -] and [Au, 14, 10%, B, -] respectively. Detailed saturation experiments are described later.

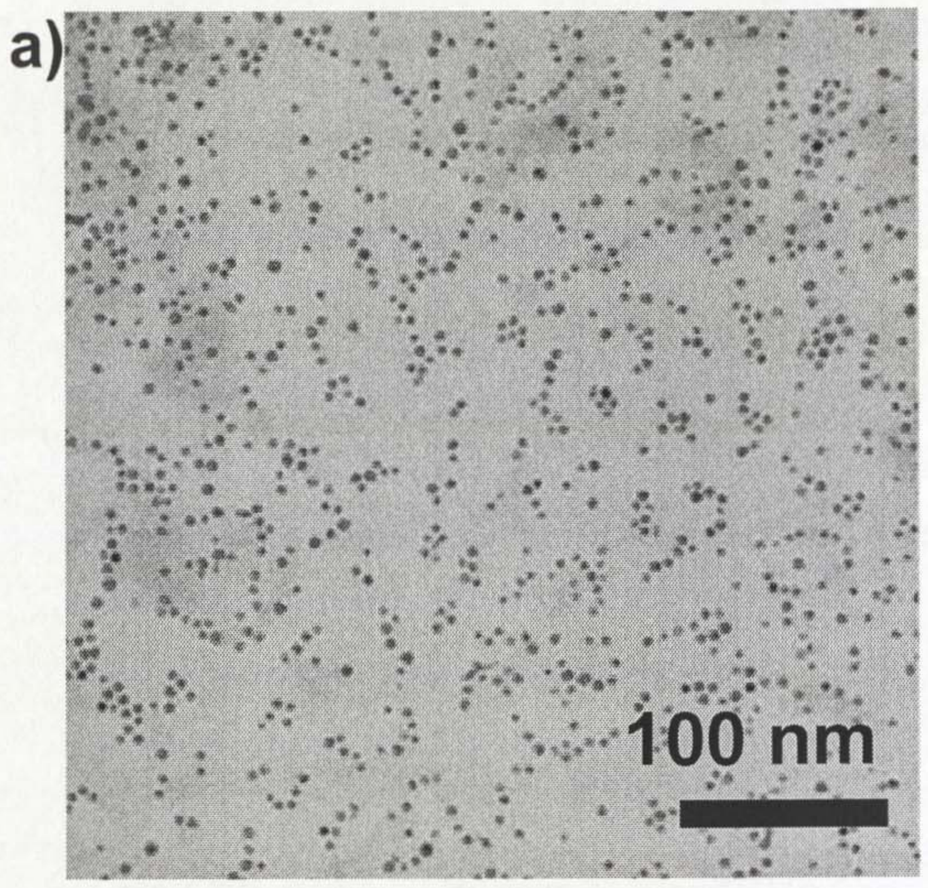

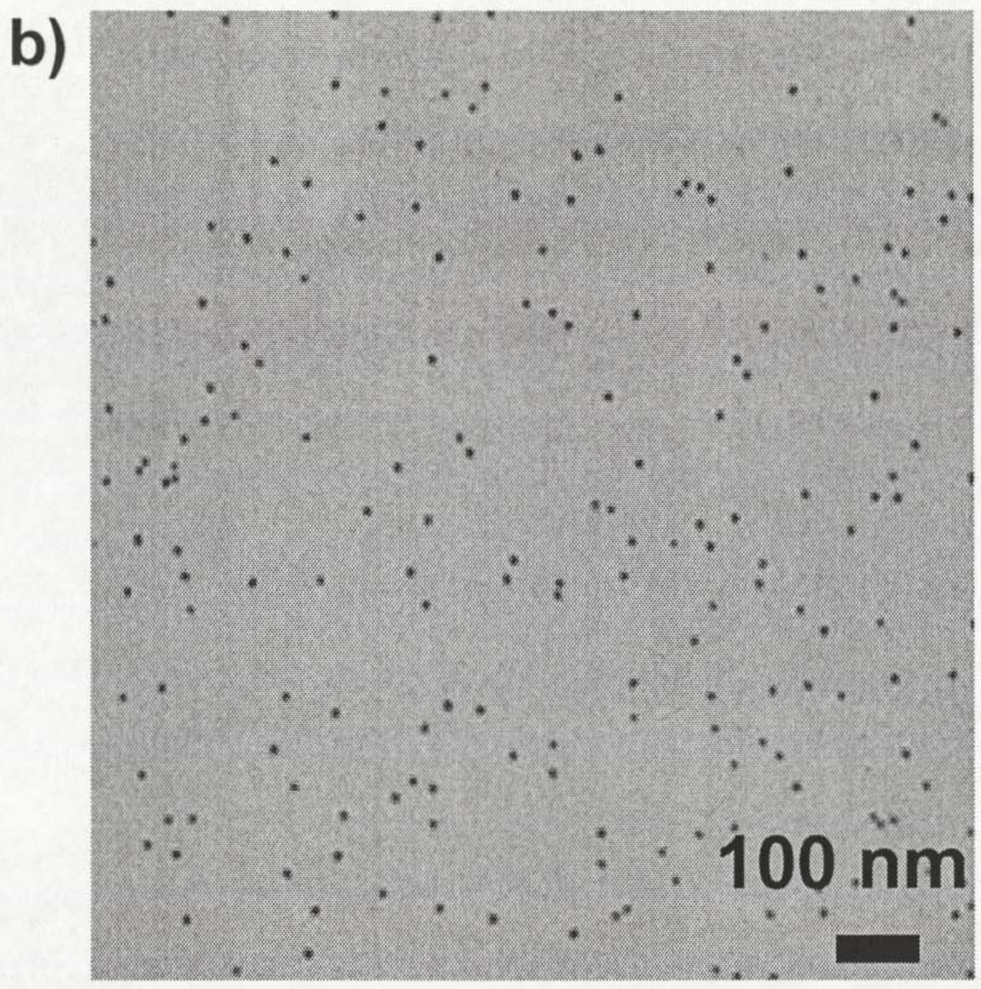

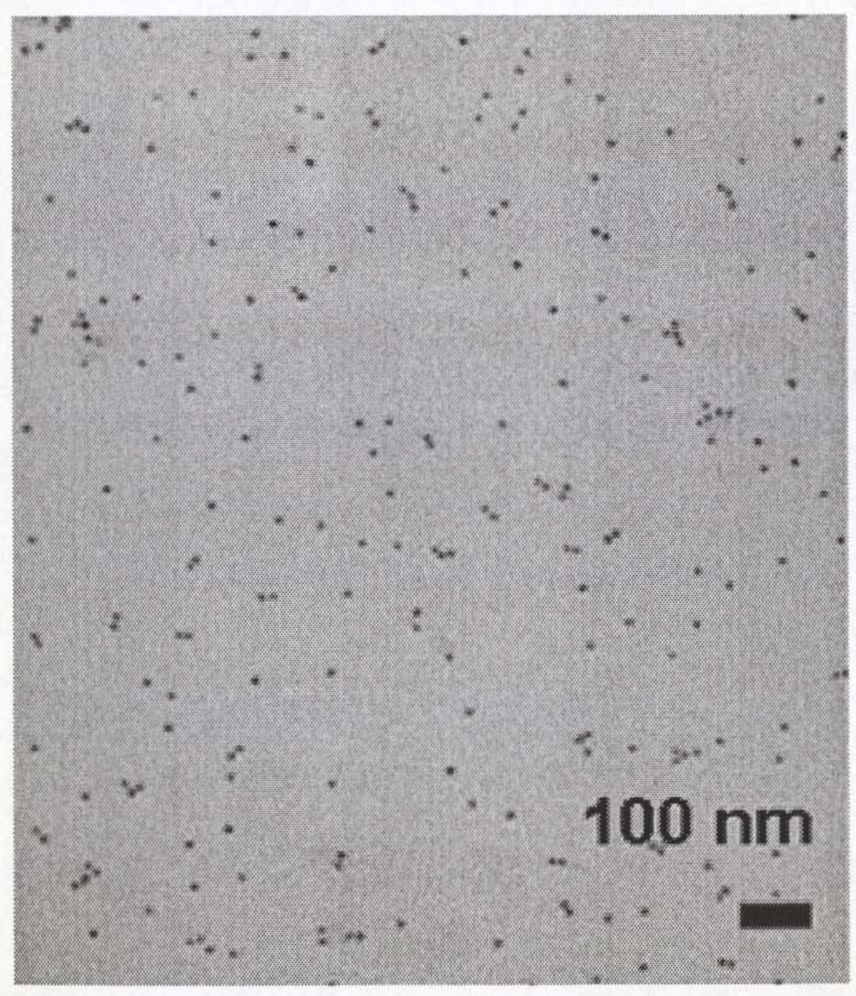

Figure 5. TEM images of biotin modified MPCs a) [Au, 6, 10%, B, -], b) [Au, 14, 1%, B, -], c) [Au, 14, 10%, B, -].

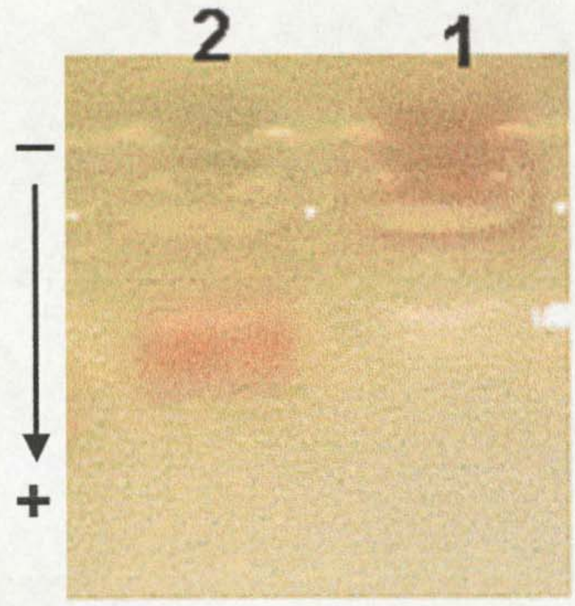

Figure 6. Agarose gel electrophoresis (Gels) of biotin modified MPCs, [Au, 14, 1%, B, -] (lane 1), [Au, 14, 10%, B, -] (lane 2).

5.2.1.3 Preparation of avidin modified MPCs

[Au, 14, 1%, BA, -], [Au, 14, 10%, BA, -], [Au, 6, 1%, BA, -], [Au, 6, 10%, BA, -]

Addition of avidin to biotinylated particles under certain biotin/avidin molar ratios leads to particles aggregation. This is due to the fact that avidin molecules can connect (*via* avidin bridges) the biotin molecules of different particles, generating inter-particle biotin-avidin-biotin complexes and hence leading to particles aggregation. It is very important that this cross-linking phenomenon be overcome in order to obtain individual avidin modified particles. This can be achieved by saturating biotinylated particles with avidin.

Purified biotin modified MPCs were used for saturation experiments. Basically, [Au, 14, 1%, B, -] were incubated with excess avidin overnight. The resulting [Au, 14, 1%, BA, -] were centrifuged and redispersed several times until the avidin absorption peak in the supernatant at ~ 282 nm was undetectable by UV-vis spectroscopy.

Alternatively, particles were purified by size-exclusion chromatography. [Au, 14, 1%, BA, -] are stable, however, they are generally difficult to handle and manipulate, since they non-specifically bind to the walls of the Eppendorf tubes which leads to a significant decrease in nanoparticles concentration. The use of special protein handling tubes from commercial sources did not improve the non-specific binding. Avidin is a basic glycoprotein (pl ~ 10), glycosylated at 17-asparagine, and well known to non-specifically bind.

To minimize non-specific binding, neutravidin, a de-glycosylated form of avidin with neutral isoelectric point (pl ~ 6.3) and streptavidin a bacterial analog isolable from *streptomyces avidinii* having a mildy acidic pl ~ 5, were used for the preparation of streptavidin or neutravidin modified MPCs here also referred to as [Au, 14, 1%, BA, -]. These did not show any significant non-specific binding.

To find the conditions under which the neutravidin or streptavidin modified MPCs were stable and did not cross-link, aggregation studies were performed (a scheme illustrating saturation experiments is shown in Figure 7). To carry out an aggregation study, a small amount of native avidin was first added to [Au, 14, 1%, B, -] in a molar ratio of biotin/avidin of 2: 1. After a while, we observed red aggregates shown in Figure 7, which disappear upon shaking the particles. A complete aggregation study was carried out using streptavidin as an avidin analog. To conduct the study, the concentration of [Au, 14, 1%, B, -] was kept constant while different amounts of streptavidin were added to each sample as presented in Table 2. The ratio of [Au, 14, 1%, B, -]/streptavidin (A) was varied from 1:0.033 to 1:333 respectively.

The resulting particles to which streptavidin had been added were left to stand at room temperature for several hours and then subjected to TEM analysis. The TEM images are presented in Figure 8, ranging from biotin modified MPCs to particles with excess streptavidin added. Figure 8a shows an image of [Au, 14, 1%, B, -]. These particles are generally uniform, monodisperse and show no signs of aggregation.

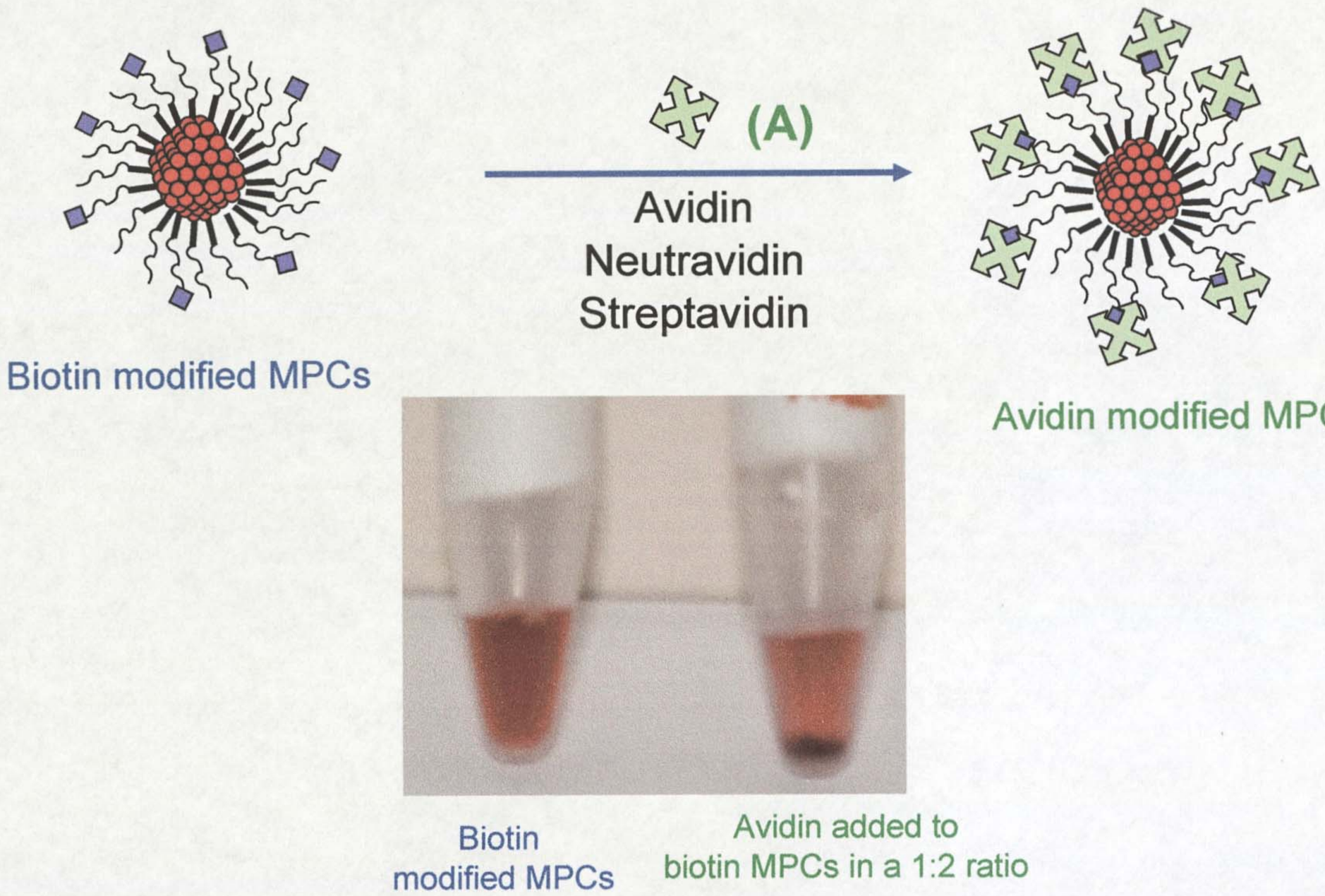

Figure 7. Saturating [Au, 14, 1%, B, -] with avidin for the generation of [Au, 14, 1%, BA, -]. Red aggregates formed when avidin was added to [Au, 14, 1%, B, -] in a molar ratio of avidin/biotin (1:2).

When a small amount of streptavidin was added to [Au, 14, 1%, B, -] in a ratio of (1:0.033, Table 2b) particles get organized in a certain way. In particular, we observed linear clustering of MPCs (Figure 8b) but they do not precipitate from solution. This suggests that the added streptavidin is insufficient to link all the biotinylated MPCs in solution.

Aggregation study experimental no.	**Streptavidin concentration (nM)**	**Biotin/streptavidin molar ratio**	**Observation of the MPCs morphology by TEM**
a	0.0	-	Uniform monodisperse MPCs
b	3.5	1:0.03	Linear clustering of MPCs
c	35	1:0.33	3-D aggregates
d	70	1:0.6	Monodisperse dimers and trimers of MPCs
e	350	1:3.33	Monodisperse MPCs
f	3500	1:33.3	Monodisperse MPCs
g	35000	1:333	Highly ordered MPCs

Table 2. Aggregation studies leading to the formation of stable streptavidin modified MPCs. The biotin concentration (105 nM) was kept constant in each experiment (from a – g) while different amounts of streptavidin were added (from 3.5 – 35000 nM).

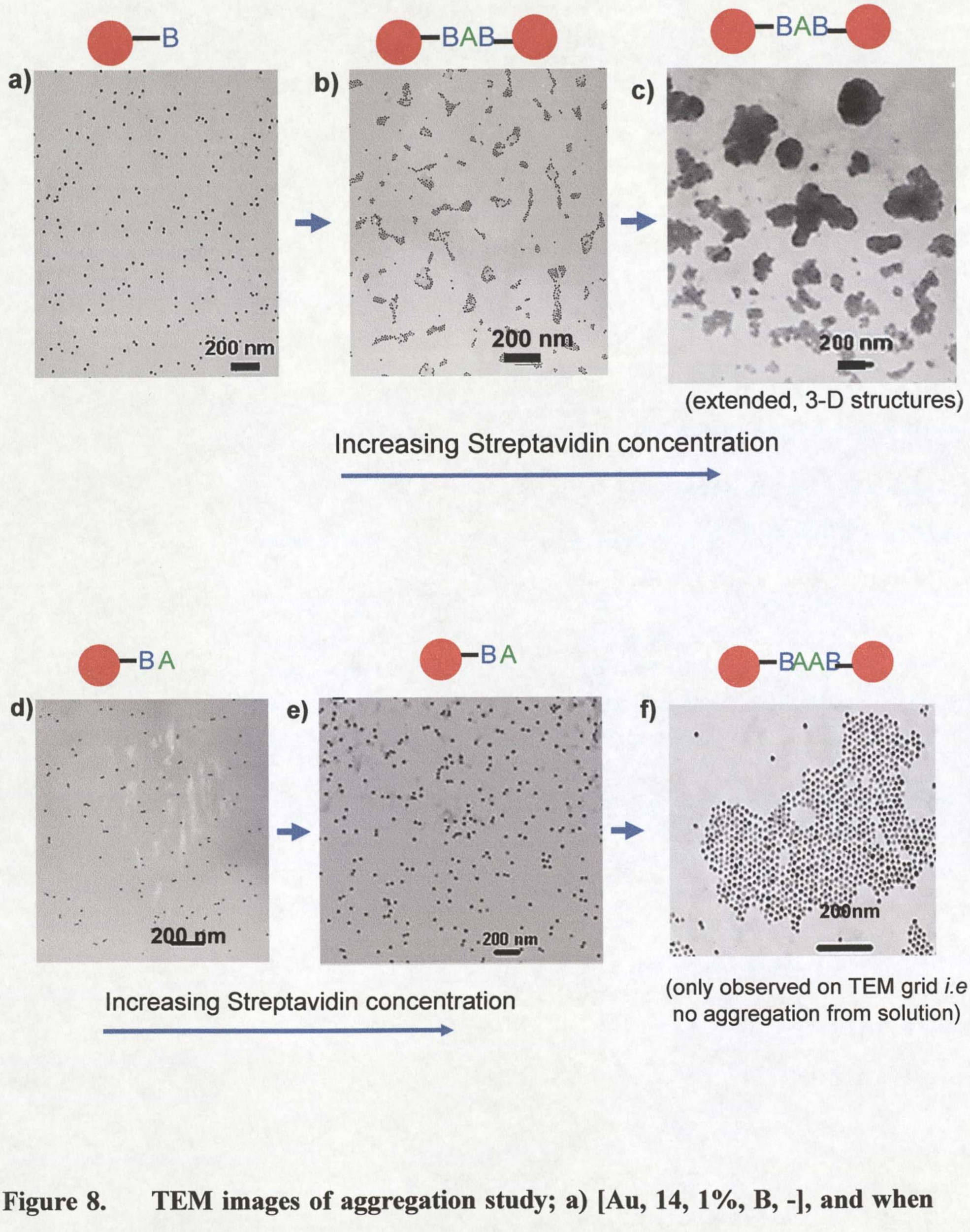

Figure 8. **TEM images of aggregation study; a) [Au, 14, 1%, B, -], and when streptavidin (A) was added at ratio of; b) (1:0.03), c) (1:0.33), d) (1:0.6), e) (1:3.3) and f) (1:333) (Table 2).**

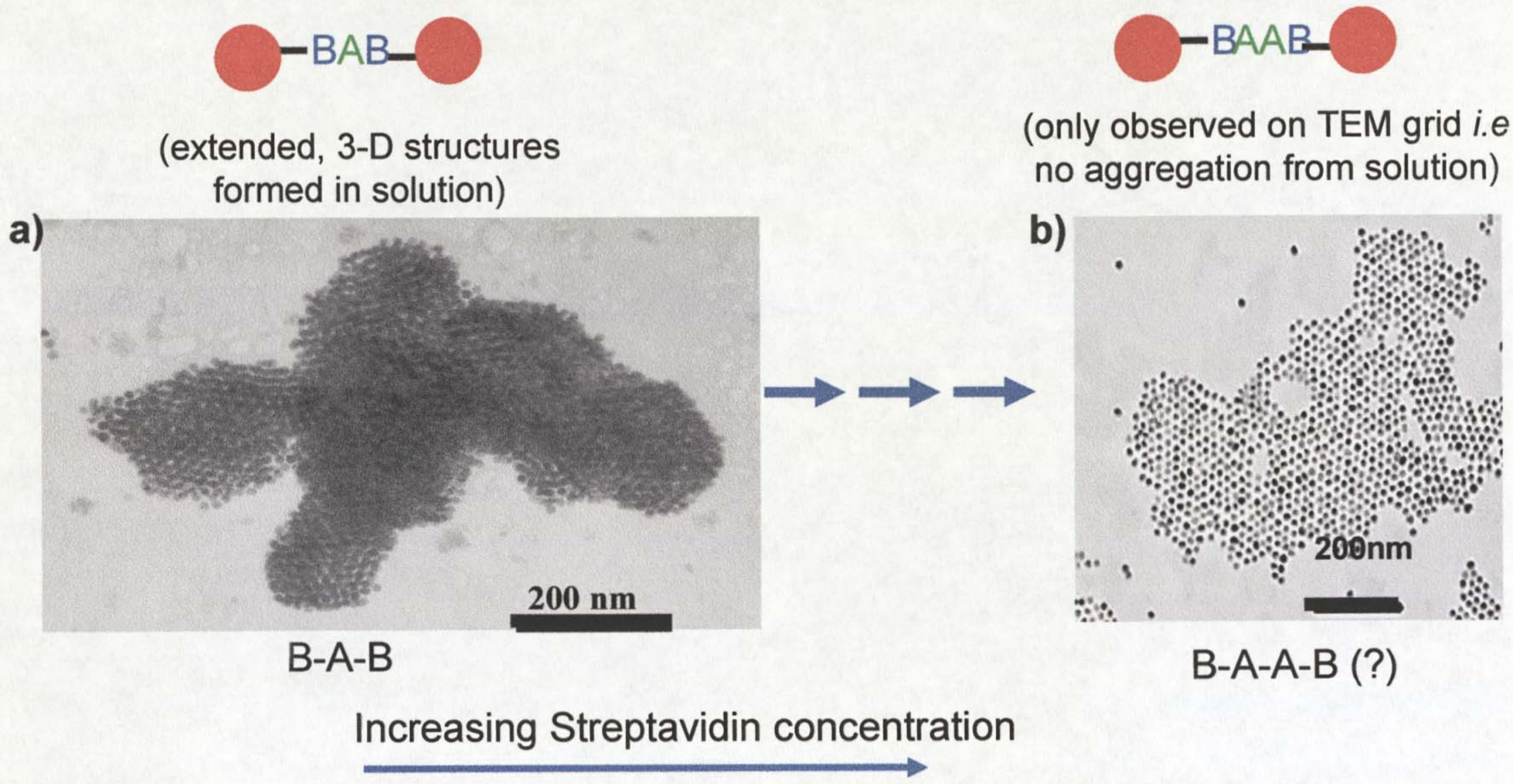

Figure 9. TEM images comparing the aggregation phenomena resulting from the addition of less streptavidin (A) to biotin modified nanoparticles forming 3-D nanostructures (B-A-B) (a) and when a large excess of A is added to biotinylated MPCs possibly to form ordered MPCs (B-A-A-B) (b)The latter are formed on the TEM grid.

It is noteworthy that at certain biotin/streptavidin molar ratio complete aggregation occurs. The resulting 3-D aggregates are shown in Figure 8c. These architectures were observed when the ratio of biotin particles [Au, 14, 1%, B, -]/A (1:0.33) was used respectively. This shows that there are sufficient streptavidin (A) molecules just to link biotinylated MPCs leading to the formation of biotin-avidin-biotin (BAB) 3-D multilayer assemblies.

By increasing (double) the concentration of A we produced again well dispersed particles. The TEM images of the resulting avidin MPCs are shown in Figure 8d, however, some of these particles are still intact as dimers or trimers.

We found that this situation can be overcome by increasing the biotin/A ratio even further 1:3.33 (Table 2e, Figure 8e). At this point, a complete saturation of [Au, 14, 1%, B, -] by A is achieved, allowing the development of uniform well dispersed [Au, 14, 1%, BA, -].

Addition of an even larger excess of A (biotin/A 1: 333, Table 1g), leads to the formation of highly ordered two dimensional assemblies on the TEM grid but not in solution as shown in Figure 8f. In Figure 9 we compare the 3D aggregates and the ordered MPCs. The aggregates are formed due to the formation of biotin-avidin-biotin (B-A-B) interaction however the most likely contributing factor leading to the formation of ordered particles may be the formation of a biotin-avidin-avidin-biotin (B-A-A-B) assembly. This requires further studies in order to elucidate what types of structures are formed.

In addition to the formation of [Au, 14, 1%, BA, -], discussed above, using [Au, 14, 10%, B, -], [Au, 6, 1%, B, -], [Au, 6, 10%, B, -], as precursors [Au, 14, 10%, BA, -], [Au, 6, 1%, BA, -] and [Au, 6, 10%, BA, -] were successfully obtained. Generally, all the avidin (referring to streptavidin or neutravidin analogs) modified MPCs are stable and resemble their precursor MPCs. They can be centrifuged without compromising their stability. They can be purified by centrifugation or by size-exclusion chromatography (Sephacryl 100HR) and do not non-specifically bind to surfaces. Like their precursor MPCs they do not aggregate at high electrolyte concentration (> 2 M NaCl) and at varied pH ranges.

Aggregation studies carried out here were very crucial giving an insight into the development of stable avidin modified MPCs. These particles are a prerequisite for the attachment of a biomolecular functionality of choice by the BAB type strategy (Table 1). In the next section, a generic BAB linking method is introduced.

5.2.1.4 Attachment of biomolecular functionality by the BAB type

The generic reaction master scheme for the attachment of biotinylated biomolecular functionalities to MPCs of the type [Au, 14, 1%, BA, -] is shown in Figure 10. Generally, purified [Au, 14, 1%, BA, -] were incubated with excess biotinylated functionalities (B-F) overnight in buffer or water. The resulting [Au, 14, 1%, BAB, F], bioconjugates were isolated from excess biomolecules by centrifugation or size exclusion chromatography (Sephacryl 100HR). Selected biotinylated functionalities employed include:- bovine serum albumin (BSA), Gal α1-3Gal (Sugar), fluorescein (dye) and anti-horse immunoglobulin G (IgG, antibody). Purified bioconjugates were characterised by TEM and agarose gel electrophoresis.

Gel electrophoresis provides visual identification of the conjugated systems based on the differences in their electrophoretic mobility, compared to the precursor particles. The results obtained are presented in Figure 11a for [Au, 14, 1%, BAB, BSA], while Figure 11b presents [Au, 14, 1%, BAB, Sugar] and [Au, 14, 1%, BAB, dye]. In Figure 11a, a band in lane 1 shows the migration of [Au, 14, 1%, B, -], lane 2 is [Au, 14, 1%, BA, -] and lane 3 shows the migration of [Au, 14, 1%, BAB, BSA].

The high migration speed exhibited by [Au, 14, 1%, BA, -] relative to its precursor [Au, 14, 1%, B, -] in Figure 11a, generally demonstrates immobilization of streptavidin. The higher electrophoretic mobility accompanying the [Au, 14, 1%, BA,-], is attributed to its low isoelectric point (pl ~ 5) making the MPCs more negatively charged at neutral pH. Again, [Au, 14, 1%, BAB, BSA] with an acidic isoelectric point moved faster than [Au, 14, 1%, BA, -] demonstrating successful attachment of biotinylated functionality by the BAB method. In Figure 11b, lane 1 and 2 show how [Au, 14, 1%, B, -] and [Au, 14, 1%, BA, -] migrated respectively. However, [Au, 14, 1%, BAB, sugar] in lane 3 is characterized by its slow migration compared to the precursor [Au, 14, 1%, BA, -].

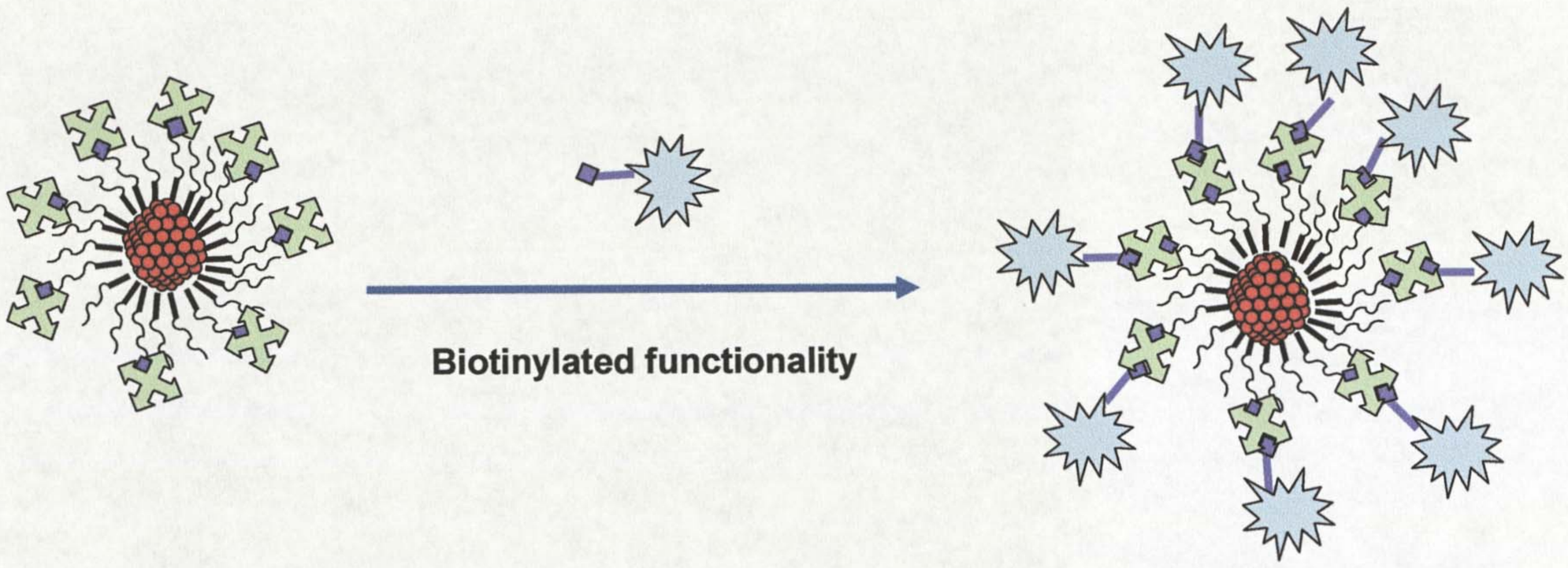

Figure 10. Generic master scheme for biofunctionalisation of nanoparticles by the BAB method.

The retarded migration could have been influenced by the basic character of the sugar, suggesting that particles are positively charged at neutral pH. The Gal α1-3Gal (Sugar) is an antigen to antibody (IgG). The attachment of [Au, 14, 1%, BAB, dye] is shown in lane 4.

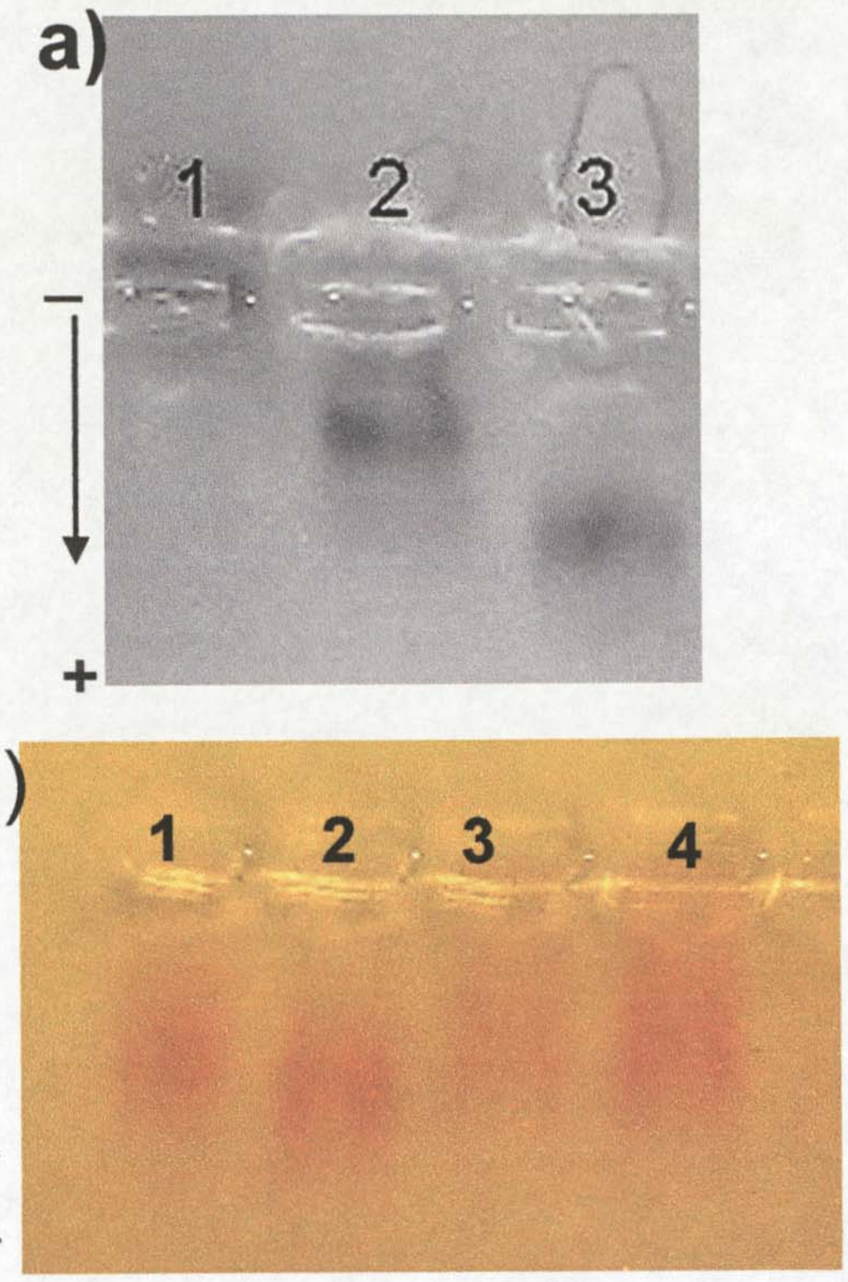

Figure 11. Gels of:- a) [Au, 14, 1%, B,-] (lane 1), [Au, 14, 1%, BA, -] (lane 2), [Au, 14, 1%, BAB, BSA] (lane 3). b) [Au, 14, 1%, B, -] (lane 1), [Au, 14, 1%, BA, -] (lane 2), [Au, 14, 1%, BAB, Sugar] (lane 3) and [Au, 14, 1%, BAB, Dye] (lane 4).

Apart from investigating biomolecular attachment by the BAB method in which streptavidin is employed, neutravidin (A) was also employed to prepare [Au, 14, 10%, BAB, Sugar] and [Au, 14, 10%, BAB, IgG] with success. Figure 12 shows TEM images of a) [Au, 14, 10%, BAB, Sugar] and b) [Au, 14, 10%, BAB, IgG].

Since TEM images alone do not provide evidence for conjugation, agarose gel electrophoresis was run to confirm the success of the conjugation reaction. Figure 13 Lane 1 shows [Au, 14, 10%, B, -], and lane 2 shows faster migration of [Au, 14, 10%, BA, -], a typical migration of neutravidin modified MPCs relative to the precursor MPCs. Successful application of the BAB method is demonstrated by retarded migration of [Au, 14, 10%, BAB, IgG] in lane 3.

Our generic approach to biomolecular functionalisation by the biotin-avidin-biotin approach is not limited to MPCs with larger core diameter (14 nm), but we also explored the use of MPCs with smaller core diameters [Au, 6, 1%, BA, -] and [Au, 6, 10%, BA, -]. As an example, [Au, 6, 1%, BAB, IgG] and [Au, 6, 1%, BAB, Sugar] were successfully prepared and characterized. Figure 14 shows representative TEM images of a) [Au, 6, 1%, BAB, IgG] and b) [Au, 6, 1%, BAB, Sugar] both derived from particles with a core diameter of around 6.2 nm (RT-5 NPs, chapter 3). As seen in Figure 14, the antibody and antigen MPCs conjugates are uniform and very stable. Particles can be purified and manipulated like the larger core MPCs (14 nm). Gel electrophoresis was run to account for successful bioconjugation.

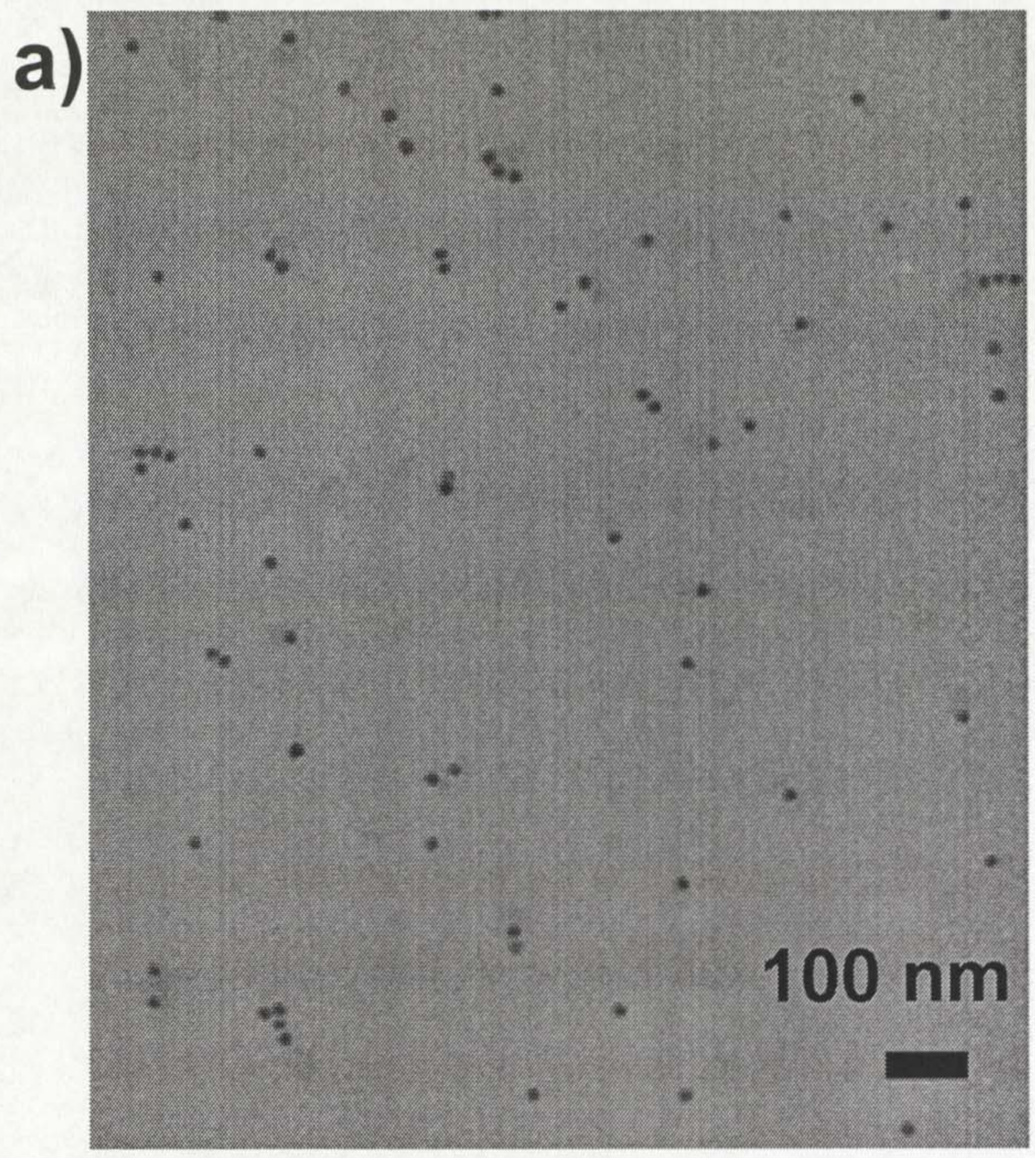

Figure 12. TEM images of a) [Au, 14, 1%, BAB, Sugar] and b) [Au, 14, 10%, BAB, IgG].

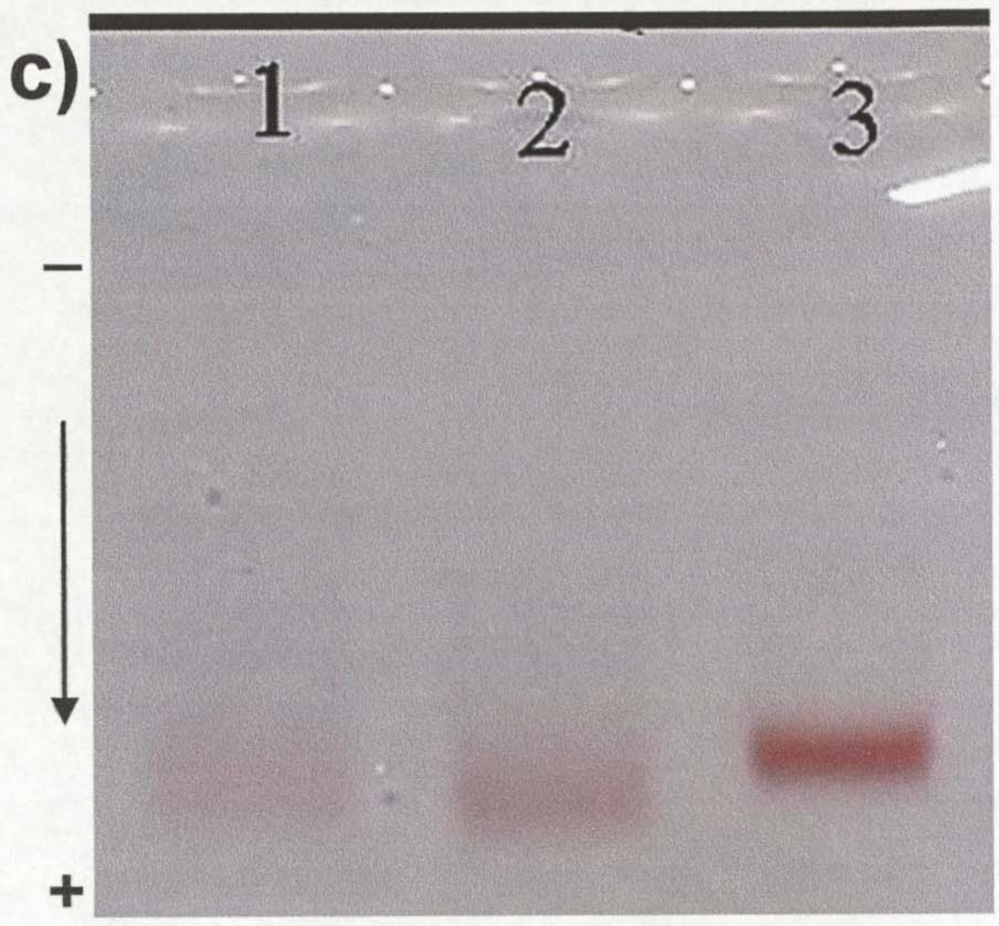

Figure 13. Gels of [Au, 14, 10%, B, -] (lane 1), [Au, 14, 10%, BA, -] (lane 2) and [Au, 14, 10%, BAB, IgG] (lane 3).

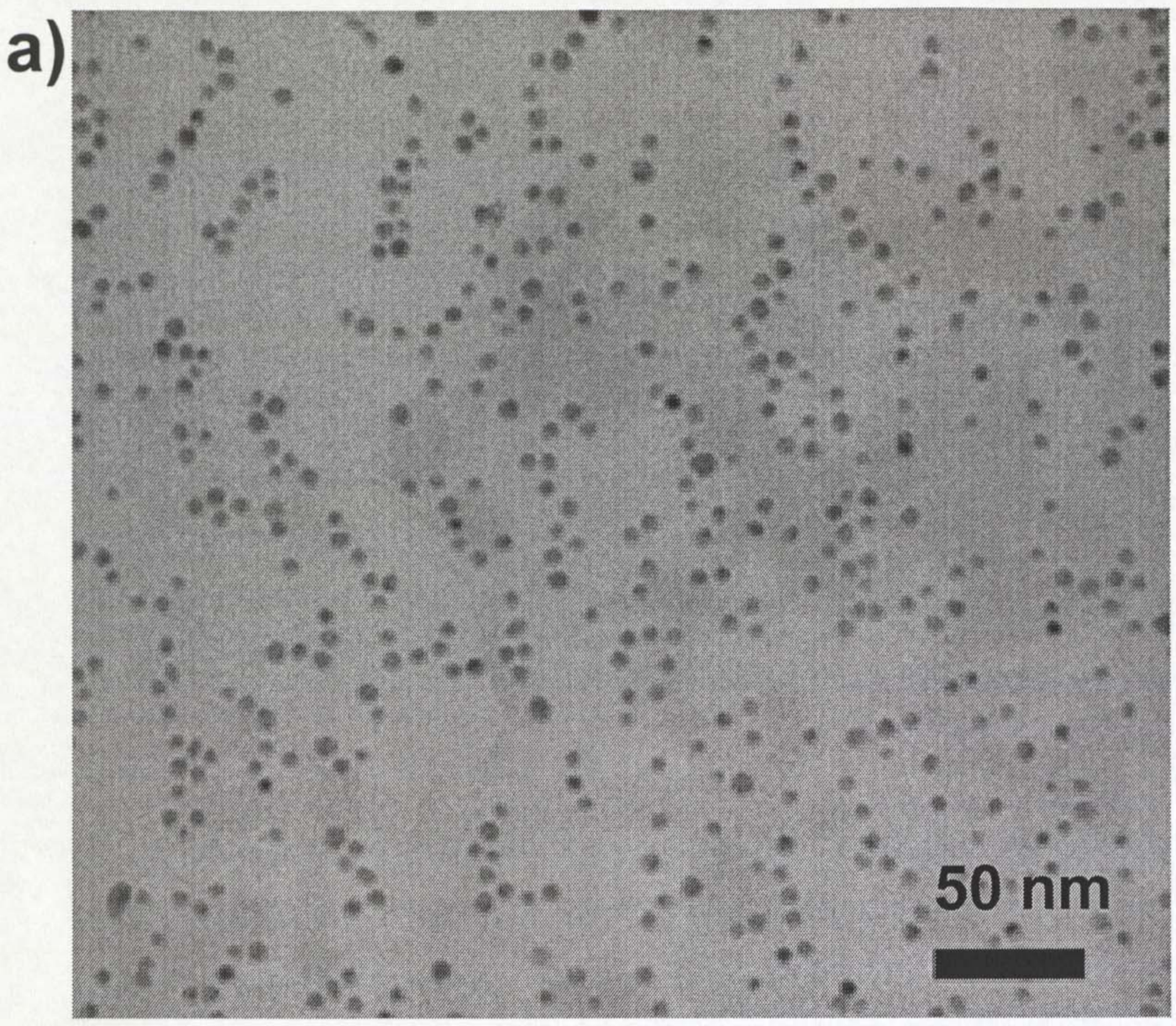

Figure 14. TEM images of a) [Au, 6, 1%, BAB, IgG] and b) [Au, 6, 1%, BAB, Sugar].

Necessary control experiments to investigate the possibility of non-specific interactions were carried out and confirmed that biomolecular attachment by the BAB method occurs only between the biotinylated functionality and avidin modified MPCs via the avidin-biotin interaction. It should be noted that proteins are amphoteric compounds and their net charge mostly is dependent on the pH of the surrounding medium. This implies that in a buffer medium with a pH above the isoelectric point (pI) proteins are negatively charged, and positively charged at pH lower than pI. In general, their electrophoretic separation under non-denaturing conditions is dependent on charge and size and varies from protein to protein. Nucleic acids on the other hand remain negatively charged at any pH used for electrophoresis since they contain a fixed negative group arising from the phosphate group at each nucleotide backbone and they are separated based on size.

In summary, all the bioMPCs [Au, X, Y%, BAB, F] were found extremely stable and could be stored, dried and centrifuged without any loss of material. The preparative methods for the construction of these special PEGylated bioMPCs were optimized and simplified and exhibit a high level of reproducibility. Both neutravidin and streptavidin can be used during saturation, and apart from the two sizes of gold nanoparticles examined, other sizes, particularly the development of bioMPCs tools with very small core size, can be achieved. While we focused primarily on using a gold core, it should be pointed out that silver bioMPCs are also constructed by the same generic approach.

5.2.2 Exploitation of biomolecular functionality by the BAB method

5.2.2.1 Specific biomolecular recognition

As it is important to investigate weather the attached biomolecules retain their biological activity we explored weather the antibody (IgG) coated bioMPCs [Au, 14, 1%, BAB, IgG] retain the ability to recognize a specific antigen. An immunoglobulin G type (IgG) is a primary divalent antibody mostly found in human serum and is widely used in diagnostic applications based on its reliability and specificity in antigen recognition properties.[26] Protein G is an antigen of interest since IgG binds specifically to it. The biomolecular recognition properties of the particle-bound IgG [Au, 14, 1%, BAB, IgG] are qualitatively demonstrated by specific binding of a protein modified substrate, *i.e.* protein G immobilized on a molecular sieve bead, as illustrated in Figure 15.

The substrate was prepared by the adsorption of Protein G to white molecular sieve beads. [Au, 14, 1%, BAB, IgG] binds specifically to the molecular sieve beads primed with protein G indicating that the [Au, 14, 1%, BAB, IgG] exhibits the characteristic molecular binding properties of IgG when immobilised in the ligand shell of the MPCs by the BAB method (Figure 15). The intense red colour of the [Au, 14, 1%, BAB, IgG] (3.6 nM) is extracted by a molecular sieve bead and this binding interaction is easily observed with the naked eye (Figure 15b). The original red solution of [Au, 14, 1%, BAB, IgG] became almost colourless (Figure 15b) indicating that almost all the particles have been extracted by the bead. Extraction of nanoparticles by the bead is in fact due to the IgG molecules attached to the AuMPCs ligand shell, which specifically binds to the protein G molecules immobilized on silica bead. This specific biomolecular interaction was confirmed by a number of control experiments, of which two are shown in Figure 15a and c. In Figure 15c, protein A primed on silica bead (protein A does not bind to IgG) remained colorless after immersed into the [Au, 14, 1%, BAB, IgG] solution.

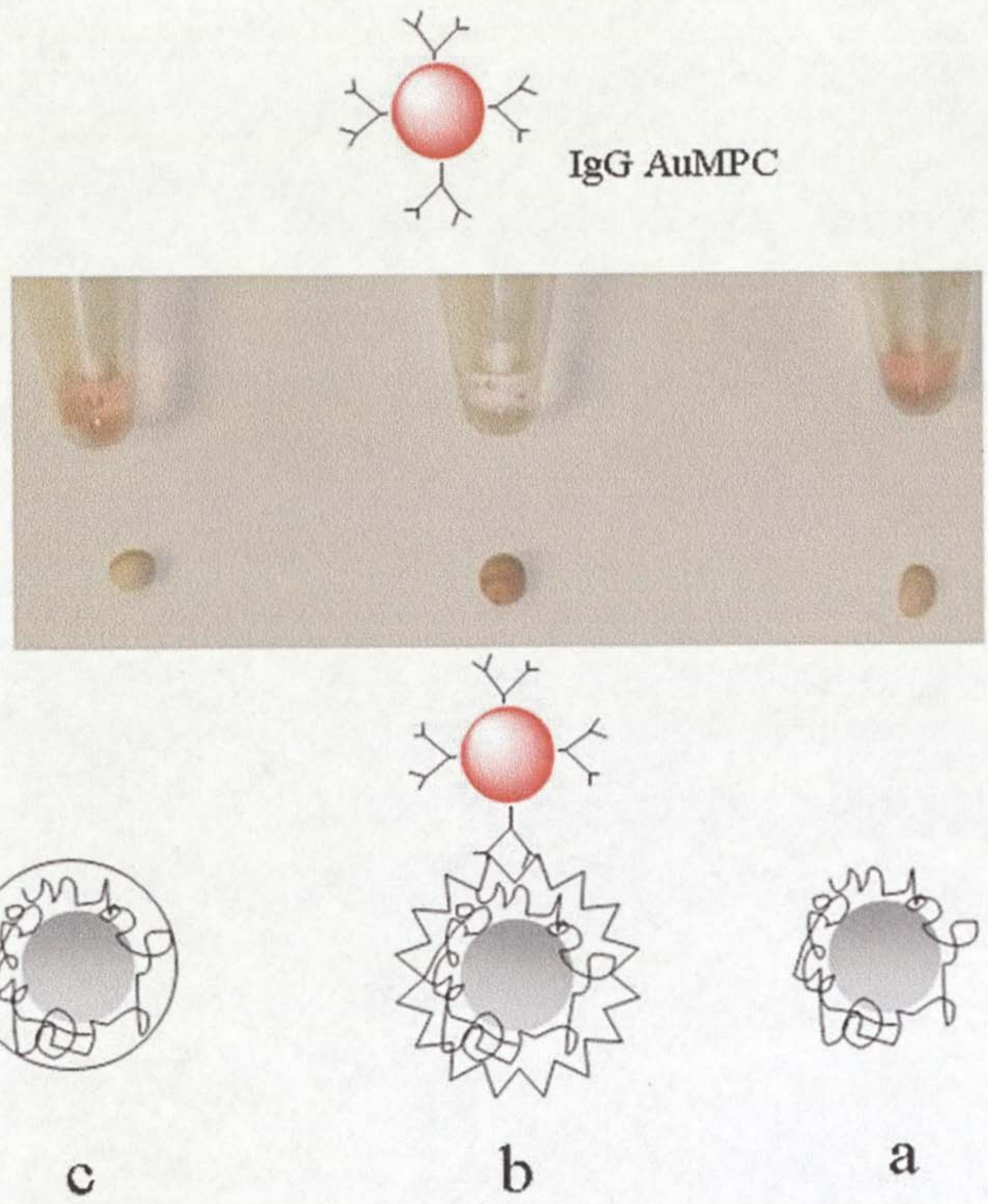

Figure 15. Specific biomolecular recognition of (b) [Au, 14, 1%, BAB, IgG] binding to protein G primed bead (bead becomes red). No interaction (*i.e.* beads remained colourless) for the control experiments (a) BSA coated bead and (c) protein A coated bead immersed into the [Au, 14, 1%, BAB, IgG] solution.

A BSA coated silica bead remained colourless even after being dipped into the red solution of [Au, 14, 1%, BAB, IgG] providing a clear demonstration that non-specific binding does not occur (Figure 15a).

Further experiments to confirm specific biomolecular recognition properties of [Au, 14, 1%, BAB, IgG] were carried out. However, minor non-specific interaction between IgG modified MPCs and the uncoated silica bead were observed.

5.2.2.2 Specific biomolecular recognition in solution

In addition to demonstrating specific bio-molecular recognition of [Au, 14, 1%, BAB, IgG] by binding to protein G primed beads, we also examined if these particles are capable of binding an antigen Galα1-3Gal (Sugar) moiety attached on MPCs *i.e.* [Au, 14, 1%, BAB, Sugar], in solution. The Galα1-3Gal (Sugar) is an antigen to IgG.[27] To determine the binding efficiency of [Au, 14, 1%, BAB, IgG] to the antigen (sugar), experiments were carried out in which the antigen was attached to smaller [Au, 6, 1%, BAB, sugar] and larger [Au, 14, 1%, BAB, Sugar] MPCs.

Firstly, MPCs of the same size were self-assembled as schematically shown in Figure 16a. Antibody [Au, 14, 1%, BAB, IgG] (B) and antigen [Au, 14, 1%, BAB, Sugar] (A) modified MPCs were incubated and allowed to react at room temperature. Particles were then analysed by TEM and the images are shown in Figure 16b. Particles generally interacted with each other and aggregated. The higher magnified images (D) clearly show that particles bind to each other but it is not possible to distinguish them. Nevertheless, this clustering is directed by the association of [Au, 14, 1%, BAB, Sugar] with [Au, 14, 1%, BAB, IgG].

Secondly, specific interaction was demonstrated by mixing particles of different sizes. [Au, 14, 1%, BAB, IgG] and [Au, 6, 1%, BAB, Sugar] were self-assembled as schematically shown in Figure 17a. Solutions of purified MPCs were mixed and allowed to react at ambient temperature. TEM images in Figure 17b show aggregated MPCs arising from the interaction between [Au, 14, 1%, BAB, IgG] and [Au, 6, 1%, BAB, Sugar] at an approximate ratio of 2:1 respectively.

The extent of aggregation is dependent on the molar ratio between the MPCs of different size, similar to the aggregation studies discussed above during saturation experiments employing the biotin-avidin system. Decreasing the molar ratio of the smaller MPCs [Au, 6, 1%, BAB, Sugar] leads to extended aggregations in which the smaller MPCs (antigen) bridge the larger ones (antibody).

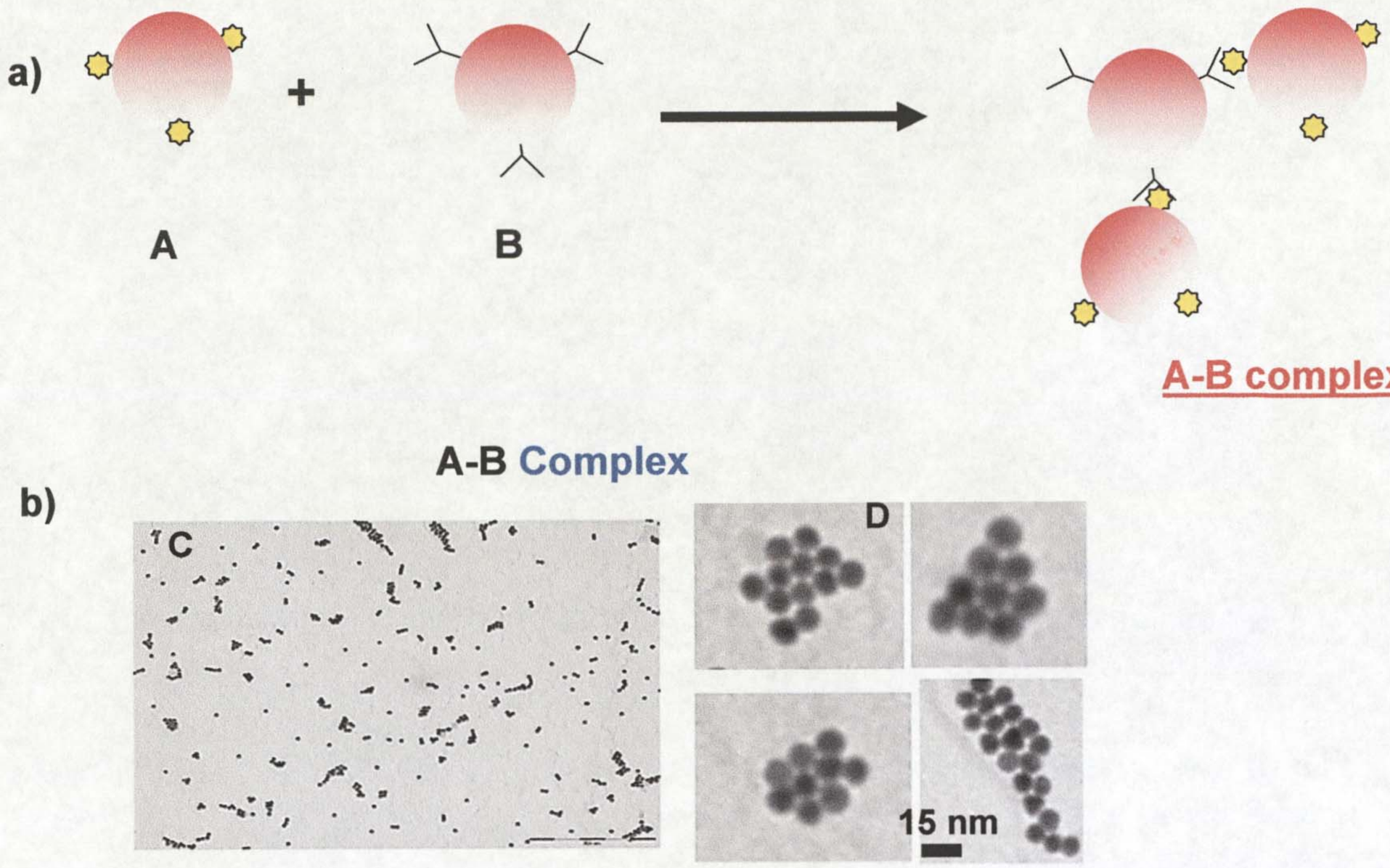

Figure 16. Schematic illustration of a) specific binding between [Au, 14, 1%, BAB, Sugar] (A) and [Au, 14, 1%, BAB, IgG] (B) and b) TEM images showing interaction between [Au, 14, 1%, BAB, Sugar] and [Au, 14, 1%, BAB, IgG] in C) low magnification and D) high magnification.

Computer simulation of selective aggregation in binary colloids has been recently reported by Pierce *et al.*[28, 29] Their results demonstrated the production of fractal structures as a function of the ratio of the number of small to larger particles. As the number ratio of smaller to larger particles was decreased, the size and structure of the binary assemblies evolved from colloidal "micelles" and colloidal aggregates/clusters into colloidal rings and chains. It was revealed that excess of smaller particles completely saturate (surround) larger particles with no indication of colloidal aggregation. However, decreasing the number ratio of smaller particles leads

to compact binary colloid clusters. Chain-like structures were produced at a very low ratio of smaller to larger particles, a consequence of larger particles being joined by one or two smaller particles.

These results are in good agreement with the experimental results of binary biocolloids [30] In Figure 17b, careful examination of TEM images in particular the magnified image inserted (C) revealed that in most cases the smaller particles surround the bigger particles in such a way that they act as glue to assemble larger conglomerates. However, attachment of single, double or even complete coverage of smaller [Au, 6, 1%, BAB, Sugar] to the larger [Au, 14, 1%, BAB, IgG] can be achieved in a one reaction vial (images in A-B complex D). Linear branched clusters of the larger core sizes [Au, 14, 1%, BAB, IgG] can be constructed by introducing a smaller amount of smaller core [Au, 6, 1%, BAB, Sugar].

Of particular importance here is the ability to demonstrate qualitative biomolecular recognition-driven assembly of MPCs. By manipulating the ratio of complementary molecules in this way (or valency of reactive sites), nanostructured materials with exciting unique properties can be constructed.

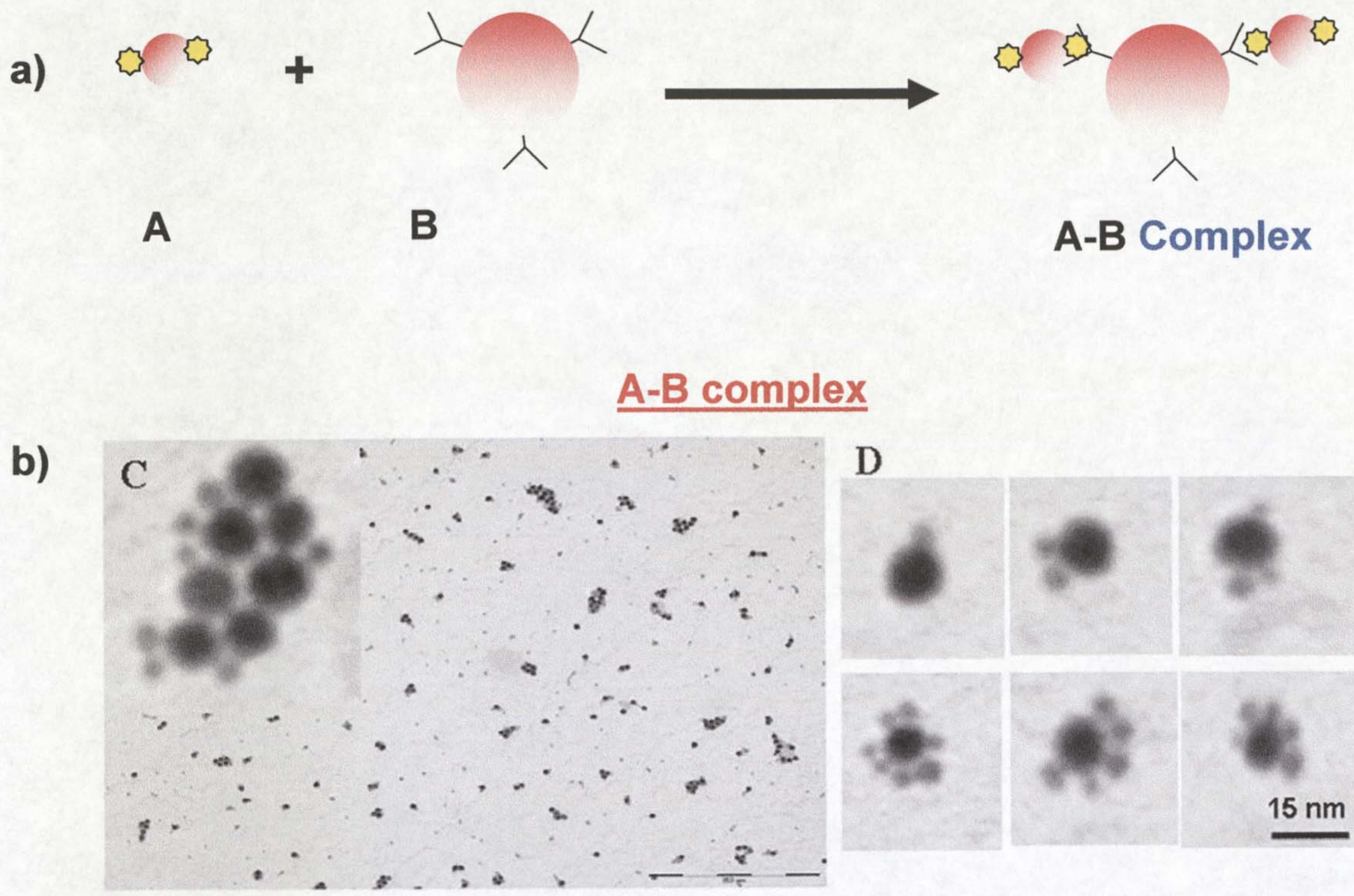

Figure 17. Schematic showing, a) specific binding between [Au, 6, 1%, BAB, Sugar] (A) and [Au, 14, 1%, BAB, IgG] (B) and b) TEM images of the resulting A-B complex in high and low magnification (C) and some selected binary interaction showing one-two and even complete coverage of larger MPC by smaller MPCs (D).

5.2.3 Covalent bioconjugation

Bioconjugation by covalent approaches will be discussed under two different strategies that we have developed for the preparation of PEGylated bioMPCs. These are carbodiimide coupling (EDC-type method) and conjugation by click chemistry (click-type method). These strategies were employed to attach biomolecules of interest such as proteins and oligonucleotides, which in most cases retain their biofunction.

5.2.3.1 Preparation of avidin modified bioMPCs [Au, 14, 100%, EDC, Avidin]

We have also developed an alternative, covalent approach to immobilise avidin on PEGylated MPCs which then acts as compatible bridge allowing the incorporation of biotinylated functionality of choice.

To prepare avidin modified MPCs, carboxylated Au-MPCs (RT-8, chapter 3) were used as precursors. These MPCs were incubated with excess avidin in a phosphate buffer solution in the presence of a water soluble cross-linker 1-ethyl-3-(3-dimethylaminopropyl) carbodiimide hydrochloride (EDC). This is schematically illustrated in Figure 18. Since avidin contains accessible reactive primary amines, it is possible to couple the amine moiety with carboxylated gold MPCs using EDC which activates the carboxylates to form a highly reactive o-acylisourea active intermediate. The active species can then react with nucleophiles, in this case primary amines to form a stable amide bond. Reaction was allowed to take place for a period of two hours in a phosphate buffer solution before the particles were purified either by repeated centrifugation until avidin is no longer detectable in the supernatant by UV-vis or by size-exclusion chromatography (Sephadex G-25).

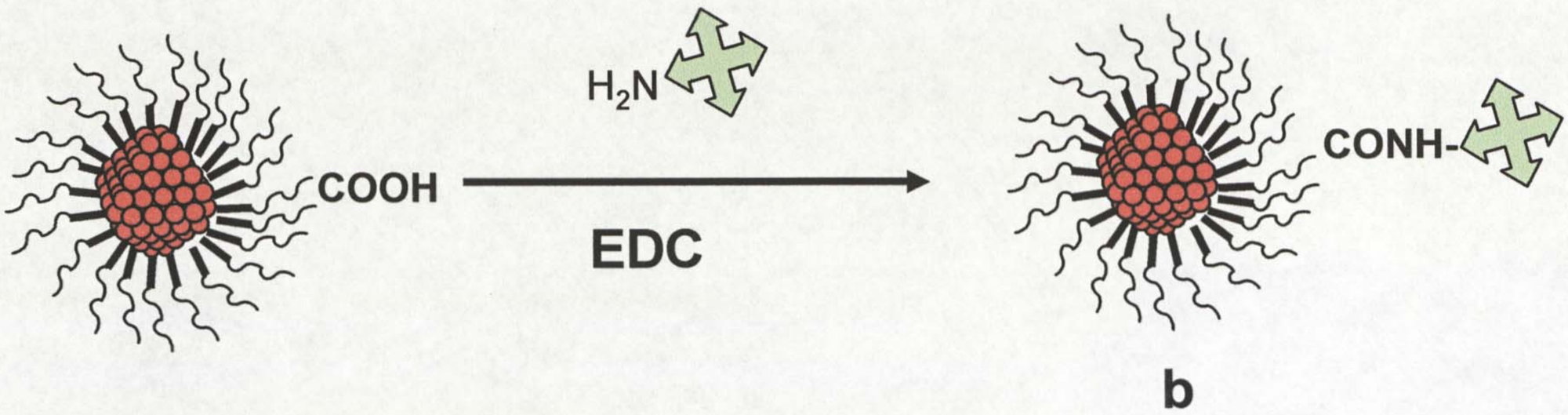

Figure 18. Scheme illustrating the covalent attachment of avidin to the carboxylated MPCs (a) for the production of avidin modified MPCs [Au, 14, 100%, EDC, Avidin] (b) by the EDC attachment method.

The success of bioconjugation was monitored by agarose gel electrophoresis (2% (wt/v)). Samples were run at 100 V for 2 hrs in a tris-borate EDTA (TBE) buffer and the results are shown in Figure 19. Lane B in Figure 19 shows high mobility of carboxylated MPCs (RT-8) towards the positive pole, while successful bioconjugation is demonstrated by retarded migration of [Au, 14, 100%, EDC, Avidin]. [Au, 14, 100%, EDC, Avidin], binds to the Eppendorf tubes. Nevertheless, other avidin analogs (neutravidin or strepavidin) could be used to minimize the non-specific binding. Since the ultimate goal is to determine their biotin binding efficiency, it was found however, that, these particles [Au, 14, 100%, EDC, Avidin] are generally unstable during biotin-binding studies. When mixed with biotinylated MPCs, particles aggregate and grow to micrometer size dimension. Attempts to optimize conditions did not yield better results and hence limiting their applications unlike the BAB method described above.

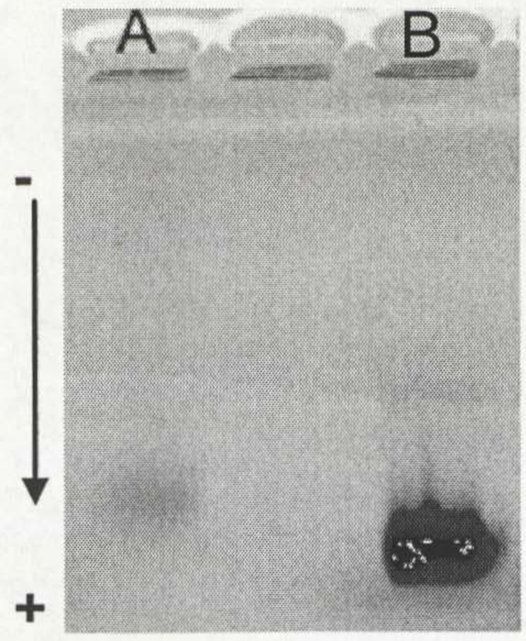

Figure 5. Gels of A) [Au, 14, 100%, EDC, Avidin] and B) carboxylated MPCs (RT-8)

5.2.3.2 Preparation of DNA-AuMPCs Conjugates (EDC method)

[Au, 14, 70%, EDC, DNA]

Assembling gold nanoparticles with DNA for programmed self assembly of nanostructures is an area that has been widely explored.[31] This is generally achieved by chemically attaching thiolated DNA molecules of defined sequences to gold nanoparticles and subsequently hybridizing the resulting single stranded DNA gold nanoparticles (due to the unique specificity of Watson-Crick base pairing) with complementary strands to create the desired programmed assembly. [31]

Since we have developed very stable PEGylated Au-MPCs (chapter 3), we were now interested in functionalizing them with DNA in such a way that they can be used as probes for the detection of complementary molecules attached to the particles in solution. To achieve this, a number of preparative steps have been developed for the

attachment of single-stranded DNA (ssDNA) to the PEGylated Au-MPCs. The strategy encompasses the use of amine functionalized MPCs (RT-10, chapter 3) as the starting materials for the preparation of maleimide activated Au-MPCs as schematically depicted in Figure 20 and described below.

5.2.3.3 Preparation of maleimide activated gold MPCs

Amine functionalized MPCs (RT-10, 70% amine) were activated for conjugation with thiolated single stranded DNA by introducing a maleimide functionality using sulfosuccinimidyl 4-[*N*-maleimidomethyl]cyclohexane-1-carboxylate (sulfo-SMCC) (Figure 20) which is a water-soluble analogue of the widely used heterobifunctional cross-linker 4-[*N*-maleimidomethyl]cyclohexane-1-carboxylate (SMCC). Amongst other bi-functional cross-linkers, of the same type, Sulfo-SMCC has the advantage that *N*-hydroxysuccinimydyl (NHS) reacts at neutral pH with primary amines to generate a stable amide bond, while the sulfonyl group imparts water solubility to the molecule. The spacer arm of this molecule, which measures 11.5 Å, contains a cyclohexane bridge, which stabilizes the maleimide functionality, which is susceptible to hydrolysis.

Maleimide activated particles were prepared as shown in Figure 20. This was carried out by coupling amine functionalized MPCs with excess sulfo-SMCC in a conjugation buffer at a pH lower than 8 to minimize any possible maleimide hydrolysis. The coupling reaction is generally complete within two hrs. Excess sulfo-SMCC was removed by repeated centrifugation, while re-suspending pellets in buffer. Alternatively, particles were purified (Sephadex G-25) and used immediately after column purification.

5.2.3.4 Preparation of DNA modified Au-MPCs

As long as the maleimide group is present on the surface of the particles, its double bond will undergo alkylation reactions (Michael-type addition) to form stable thioether bonds with the sulfhydryl group, (HS-R) of the DNA molecule. This reaction is known to proceed at a rate 1000 times faster than the equivalent reaction with

amines at pH ranges 6.5-7.5, however at pH 8, or higher cross reactivity with amine groups occurs.[32] DNA modified particles [Au, 14, 70%, EDC, DNA] were prepared (Figure 20) by incubating 5'-thiolated single strand DNA (22-bases) and maleimide activated PEGylated MPCs at room temperature. Unreacted thiolated DNA was removed by either repeated centrifugation or gel filtration chromatography (Sephadex G-25) before use during the hybridization assay.

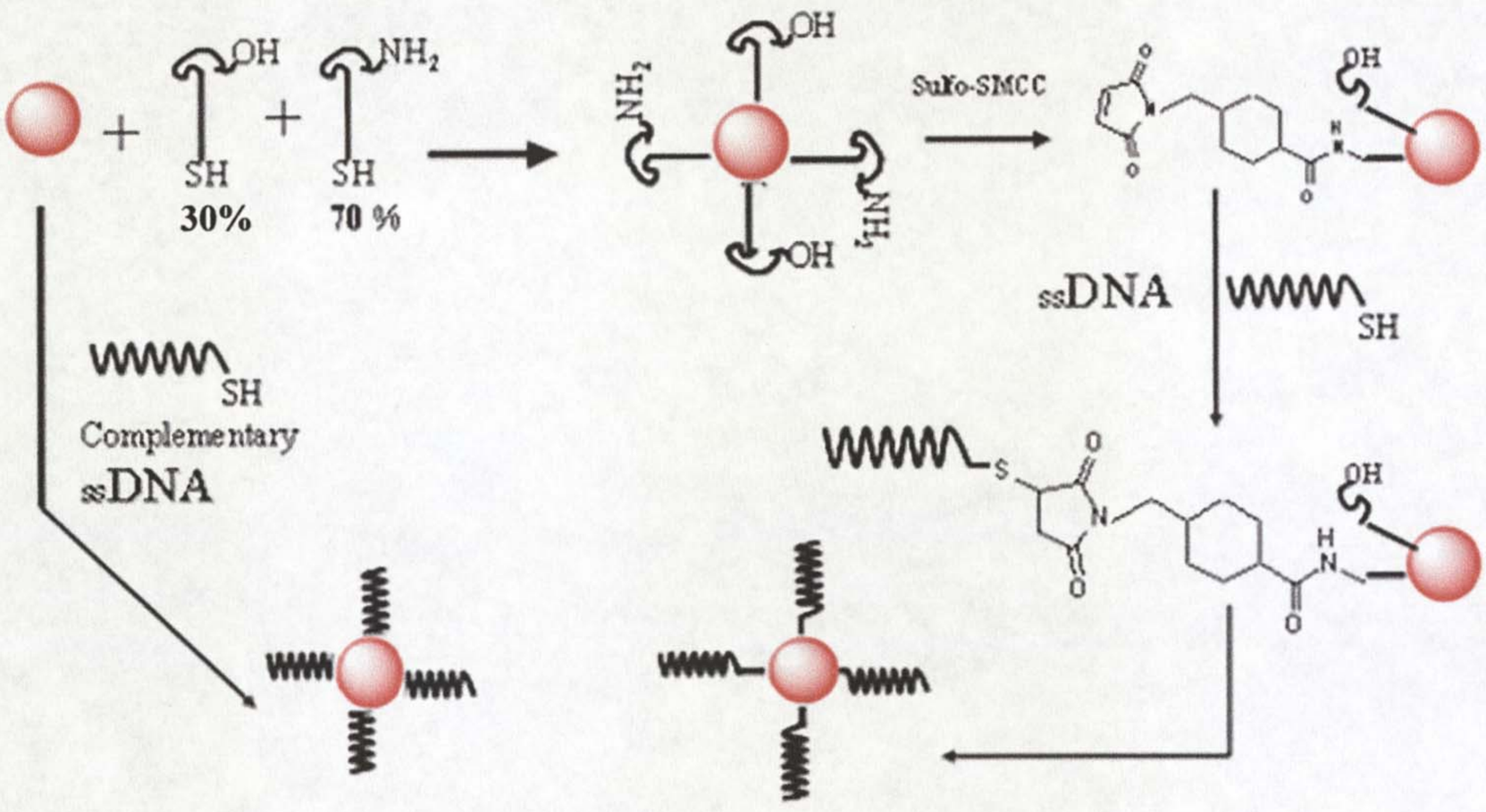

Figure 6. Reaction scheme of the preparation of maleimide activated MPCs and subsequent attachment of thiolated DNA [Au, 14, 70%, EDC, DNA]. The other route shows synthesis of particles with complementary DNA strands.

5.2.3.5 Hybridisation

Prior to hybridization, gold nanoparticles with complimentary strand DNA to the [Au, 14, 70%, EDC, DNA] were prepared as shown schematically in Figure 20. This was achieved by reacting 5'-thiol modified single-stranded DNA (22 bases) directly with citrate stabilized particles (RT-7, chapter 3) using the "slow evaporation technique" [31] This technique generally allows derivatizing gold nanoparticles with a DNA ligand shell and concentrating the sample in a vacuum centrifuge. Complementary DNA particles were purified before use following common purification protocols. [31]

A schematic representation of hybridization and de-hybdridisation is shown in Figure 21. The hybridization experiment was carried out by incubating both the complementary DNA particles and [Au, 14, 70%, EDC, DNA] in a buffer overnight. Then, the red colour of the particles became blue (Figure 21a). A red to blue colour change is a well known concept depicting an aggregation of gold nanoparticles. This aggregation phenomenon arises from the linking of both probe and target particles. Addition of the particles with complementary strand to the [Au, 14, 70%, EDC, DNA] leads to the formation of a polymeric network (a consequence of Watson-Crick base pairing, (H-bonding)) connecting the two particles together and hence inducing plasmon interparticles coupling which causes a red shift (and broadened) of the surface plasmon resonance (which accounts for the blue colour observed).

Hybridisation is a reversible process. If the temperature of the resulting aggregates is increased above the melting temperature (Tm) of duplex DNA (Tm is sequence specific), then thermally induced dissociation process can be monitored by concomitant blue to red colour change. The aggregates were heated to 90 ^{0}C leading to a colour change from blue to red (Figure 21b). The colour change of aggregates from blue to red is an indication of a reversible process, showing the detection ability of PEGylated AuMPCs [Au, 14, 70%, EDC, DNA] to the particles with complementary strand in solution. The red colour becomes blue on standing to room temperature, again demonstrating a reversible hybridization process.

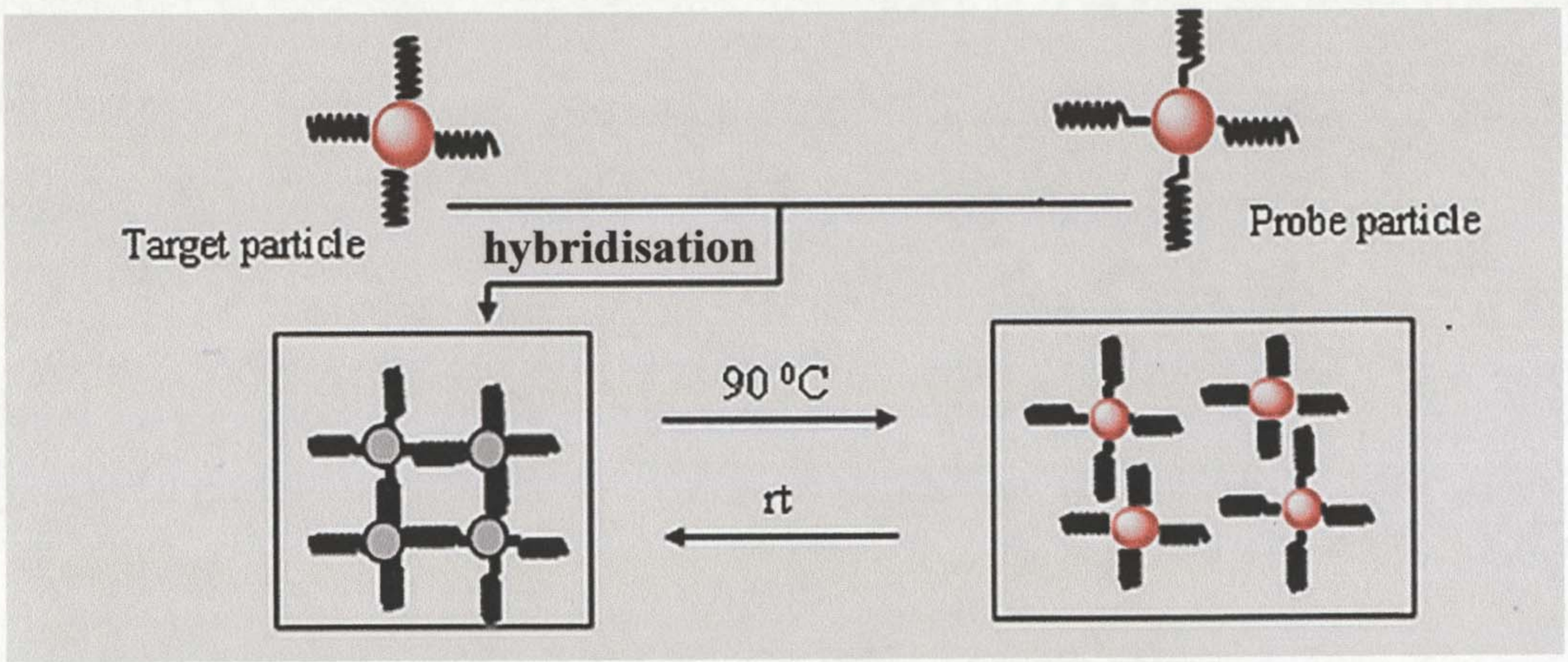

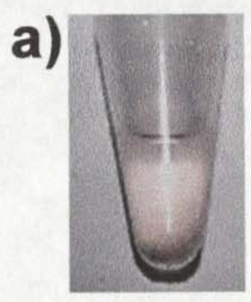

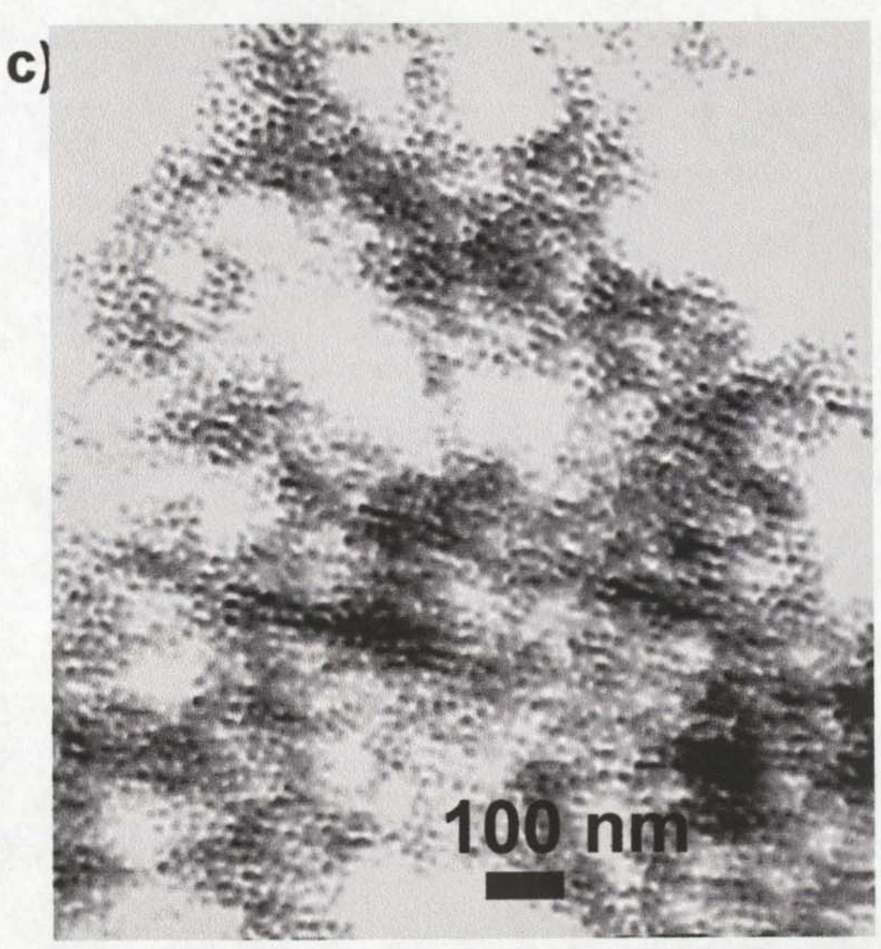

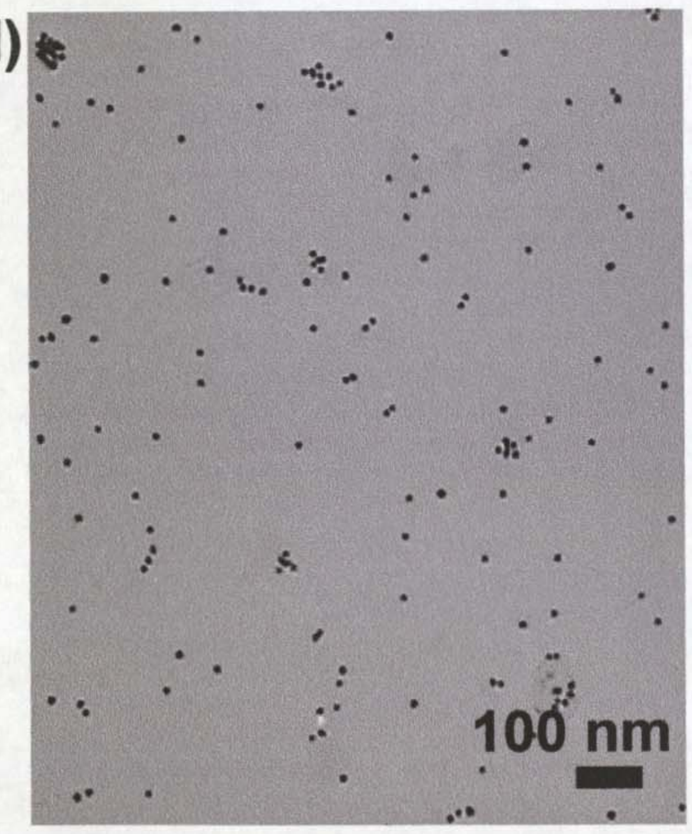

Figure 7. Hybridization and de-hybridization results showing a) a solution of [Au, 14, 70%, EDC, DNA] and particles with complementary DNA strand hybridized at room temperature, b) the same solution de-hybridisation-heating to 90 °C, c)TEM of hybridized particles in (a) and d) TEM of particles before hybridization.

To further characterize the hybridization and de-hydridisation process, TEM images of the particles after hybridization and before hybridisation were obtained. The TEM image of aggregated particles (blue colour) is shown in Figure 21c and results from the hybridization experiment while particles before hybridization are shown in Figure 21d, showing disperse particles.

Of particular importance here is to demonstrate the molecular recognition properties of PEGylated [Au, 14, 70%, EDC, DNA] binding to complementary target molecules attached to nanoparticles (DNA hybridization). The sensitivity of these MPCs was not investigated further.

It should be highlighted that stabilization and functionalisation of gold nanoparticles by thiolated DNA is a well established concept introduced by Mirkin, who developed a gold nanoparticle-bioconjugate based colorimetric assay by attaching thiolated DNA to the nanoparticle. The advantage of using PEGylated MPCs described here is that, stability of the particles is never compromised. In addition, non-specific adsorption of macromolecules is reduced by the PEG segments attached and it is possible to vary the DNA ligands on MPCs.

5.2.3.6 Preparation of biotin modified MPCs (EDC method)

[Au, 14, 10%, EDC, Biotin], [Au, 6, 10%, EDC, Biotin] and [Ag, 5, 10%, EDC, Biotin]

Biotinylation by carbodiimide coupling was carried out as schematically illustrated in Figure 22a. The amine functionalized Au or Ag (RT-10 or 21, chapter 3) were used as precursors. Biotinylation was performed by incubating the precursor MPCs and excess sulfo-NHS-LC-biotin ligand in a phosphate buffer medium. The reaction was allowed to take place for a period of two hrs. The products were purified by either centrifugation or size-exclusion chromatography. [Au, 14, 10%, EDC, Biotin], [Au, 6, 10%, EDC, Biotin] and [Ag, 5, 10%, EDC, Biotin] were derived from RT-10, RT-5 and RT-21 particles (chapter 3) respectively.

The success of biotinylation was verified by gel electrophoresis (agarose) shown in Figure 22b for AuMPCs and Figure 22c for AgMPCs. As an example, Figure 22b lane 1 shows the migration of amine functionalized MPCs (RT-10). Biotinylation is evidenced by faster migration of [Au, 14, 10%, EDC, Biotin] (lane 2). In Figure 22c, lane 1 shows the mobility of amine functionalized AgMPCs (RT-21, chapter 3) and biotinylation is characterized by faster migration of [Ag, 5, 10%, EDC, Biotin].

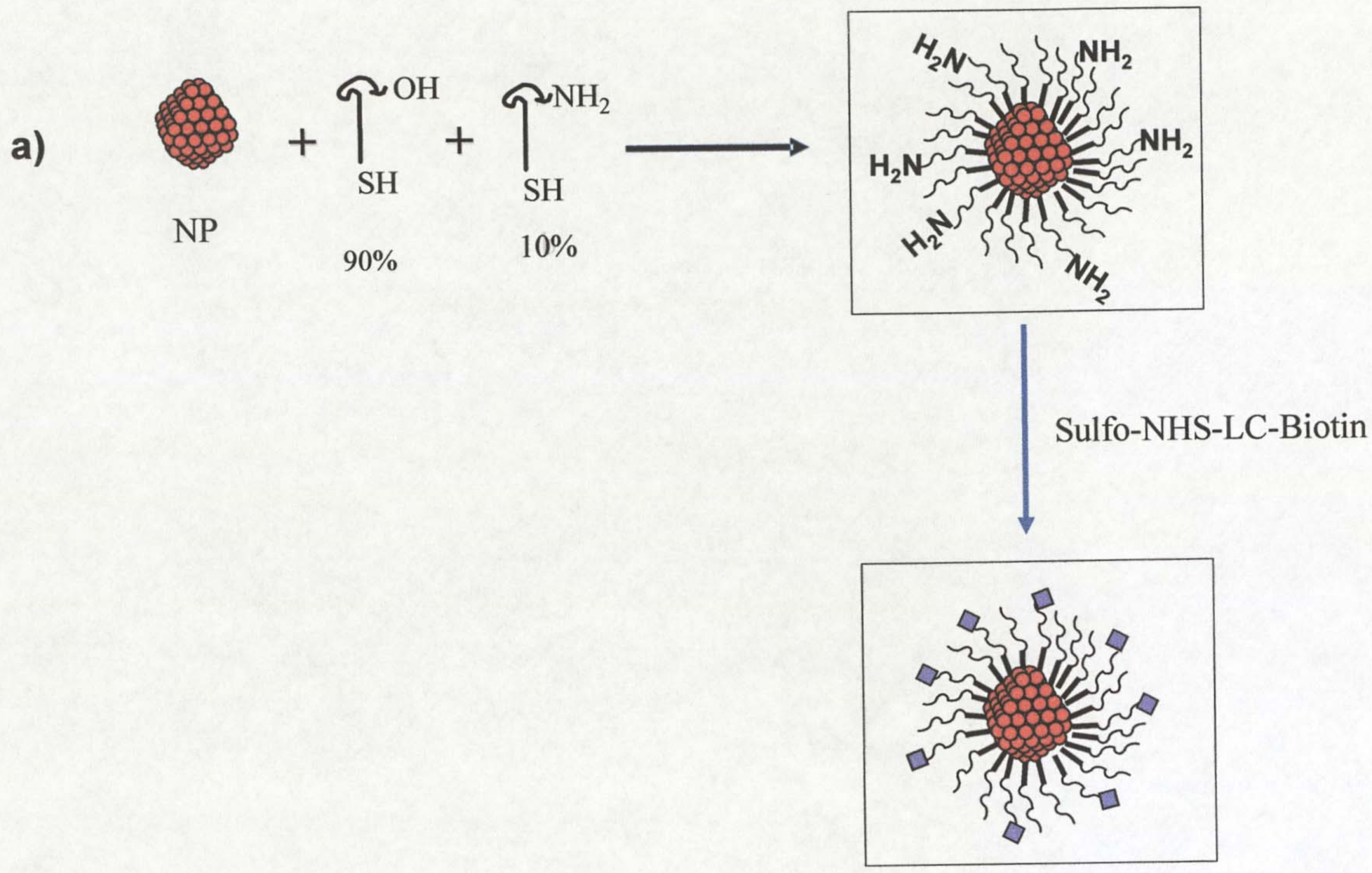

Figure 22. a) Schematic illustration of the preparation of biotin modified MPCs via amine synthetic approach. b) Gels of amine functionalized MPCs RT-10 (lane1) and [Au, 14, 10%, EDC, Biotin] (lane 2). c) Gels of amine functionalized Ag MPCs RT-19 (lane 1) and [Ag, 5, 10%, EDC, Biotin] (lane 2).

5.2.3.6 Preparation of lipase-AuMPCs conjugates (EDC)

[Au, 14, 100%, EDC, Lipase]

Two different approaches will be discussed (i) carbodiimide coupling (EDC) and (ii) click chemistry (Click). The click chemistry work was carried out in collaboration with Dr. J.L. Brennan (Liverpool University), who carried out the click reactions and lipase activity assays, while I prepared and analyzed the azide modified nanoparticles designed to undergo click reactions. This work was also carried out in collaboration with Nijmegen and Novozymes, (The Netherlands), who provided the enzymes to be coupled to the particles. These enzymes were engineered in a way that they contained a defined number of linkage functionalities *e.g.* a free amine of an extra LYS residue per protein.

Lipase from *Thermomyces lanuginosus* (30 000 daltons) was attached to carboxylated MPCs (RT-8, chapter 3) following the reaction scheme depicted in Figure 21. Basically, carboxylated MPCs were mixed with excess of lipase and EDC in a phosphate buffer medium. The mixture was vortexed for 2hrs before purified by repeated centrifugation.

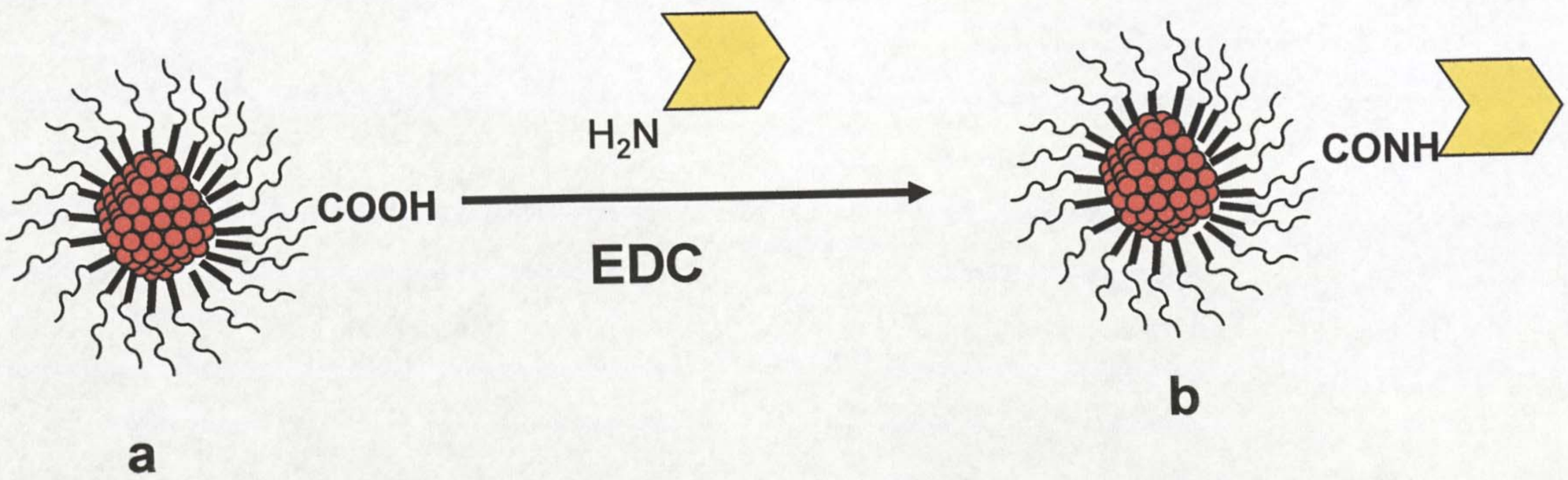

Figure 23. Reaction scheme of the preparation of (b) [Au, 14, 100%, EDC, Lipase] MPCs via the EDC method using (a) carboxylated MPCs (RT-8 NPs).

The products of the conjugation experiments, [Au, 14, 100%, EDC, Lipase], were analysed by gel electrophoresis (agarose). Figure 24 (lane 1), shows the migration of carboxylated nanoparticles. Successful attachment of lipase to AuMPCs is evidenced by retarded migration of [Au, 14, 100%, EDC, Lipase] towards the positive pole.

The reaction conditions were optimized for the reproducible preparation of [Au, 14, 100%, EDC, Lipase]. In these experiments it has been demonstrated that lipase can be conjugated to the PEGylated MPCs ligand shell by an EDC coupling method. Catalytic activities of [Au, 14, 100%, EDC, Lipase] obtained in this way were not determined. However, this will be discussed in detail under the click chemistry method.

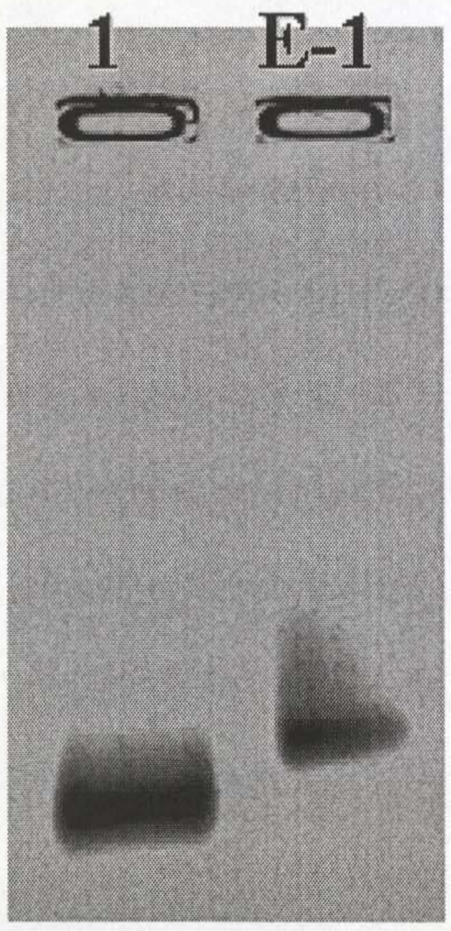

Figure 8. Gels of carboxylated Au MPCs (lane 1), and [Au, 14, 100%, EDC, Lipase] (lane E-1).

5.2.3.8 Lipase conjugation via click chemistry

[Au, 14, 100%, Click, Lipase]

Click chemistry according to Sharpless is "a modular approach that uses only the most practical and reliable chemical transformations.[33] Thus, those reactions that give products stereoselectively in high yields, produce inoffensive by-products, are insensitive to oxygen and water, utilise readily available starting materials, and have a thermodynamic driving force of at least 20 kcal mol^{-1}. Generally there are two widely studied click reactions that are reported to have influenced drug discovery, thus nucleophillic ring opening and 1,3-dipolar cycloadditions. The Huisgen 1,3-Dipolar cycloaddition reaction employing copper (I) as a catalyst has been well studied and is of interest in this investigation.

5.2.3.8.1 The creation of functional hybrids of enzymes and gold nanoparticles

The covalent linkage of enzymes to the ligand shell of gold nanoparticles to create a novel bionanomaterial is described. This is achieved by harnessing the copper-(I)-catalysed 1,2,3 triazole formation between azides and terminal acetylenes, known as "click" chemistry, which has recently emerged as a versatile, facile cross-linking reaction with wide-ranging applications.[34-37] The attraction of click chemistry is mainly due to its high degree of complete specificity and compatibility with both organic and aqueous reaction systems.[38-41] Thus has the potential to be an excellent method of conjugating biological materials to metal nanoparticles. The "click" chemistry linkage of enzymes to nanoparticles described here is achieved by preparing gold nanoparticles functionalized with an azide moiety and an enzyme modified with an acetylene moiety, and reacting these two functional groups together using copper(I) as a catalyst. The nanoparticles have been stabilized using a thiolated PEG ligand **1** in Figure 25, which is functionalized on the other end to contain "clickable" azide group.

These water-soluble nanoparticles have been characterized using transmission electron microscopy (TEM) and UV-vis spectroscopy. The acetylene-functionalized enzyme has been prepared (from Nijmegen, The Netherlands) using a variant of the bacterial lipase from the *Thermomyces lanuginosus* species. The binding of the enzyme to the particle via click chemistry has been demonstrated by agarose gel electrophoresis and by the lipase activity of the conjugates which was tested by a fluorometric lipase assay.

5.2.3.8.2 Preparation of azide modified gold nanoparticles (AzMPCs)

The preparation of the azide-modified nanoparticles is schematically illustrated in Figure 25. Citrate-stabilised gold hydrosols were treated with an aqueous solution of **1** to directly yield the azide-modified gold particles (AzMPCs). The AzMPCs exhibit a characteristic plasmon absorption band in the UV-vis spectrum at 523 nm and their size is that of the original citrate-stabilized particles, (RT-7, ~14 nm, chapter 3) as confirmed by TEM (Figure 26a). The particles are extremely stable and can be centrifuged, dried and re-suspended in aqueous solution several times without significant loss of material. Importantly for biological applications, they are also compatible with biological buffers and can tolerate salt concentrations up to 0.2 M before aggregation occurs.

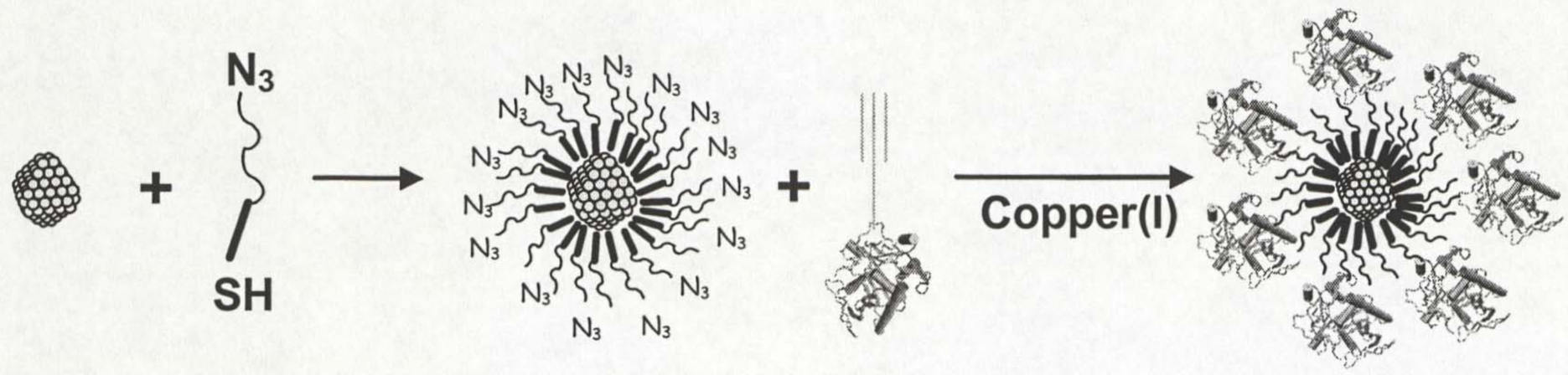

Figure 25. Reaction scheme depicting the stabilisation and functionalisation of gold nanoparticles with 1, and the linking of lipase to these nanoparticles using click chemistry. Box: the click chemistry linking reaction in detail.

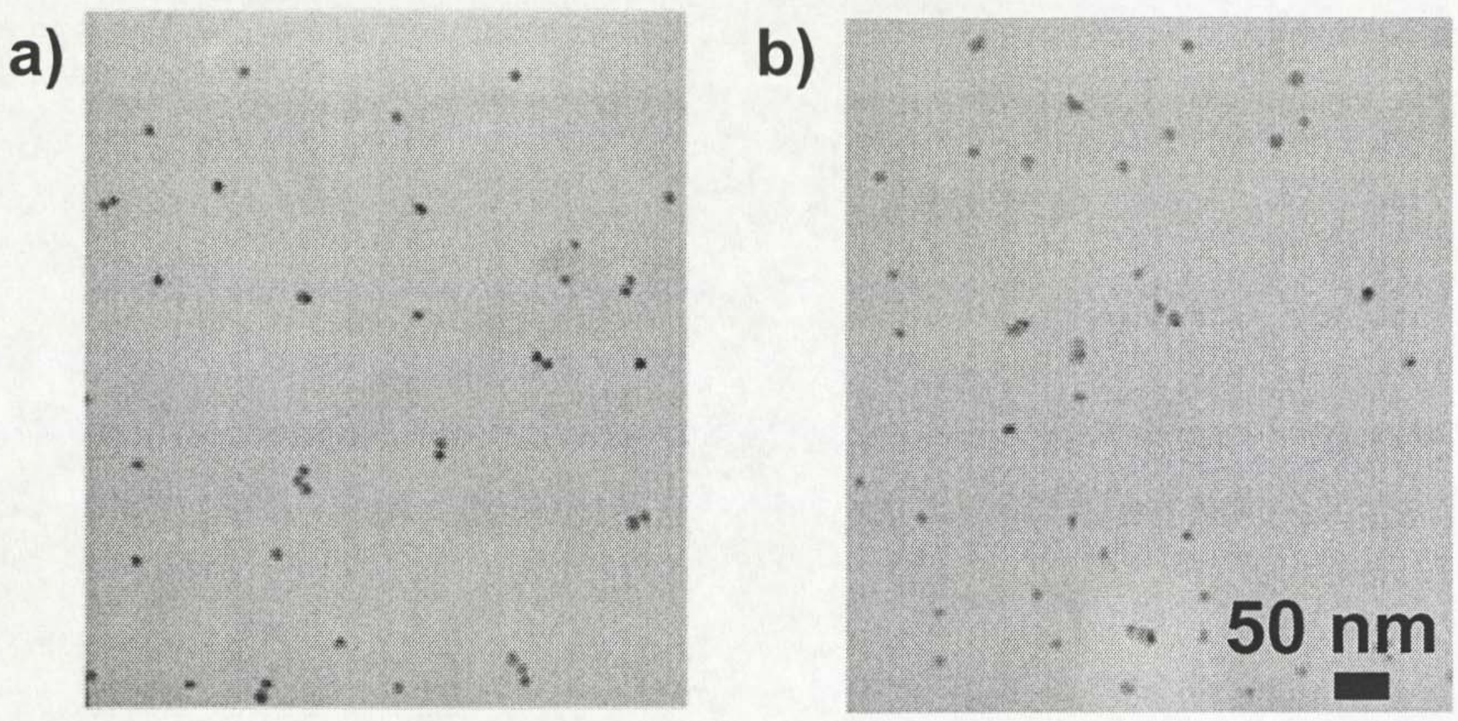

Figure 26. TEM images of a) azide modified MPCs and b) [Au, 14, 100%, Click, Lipase].

5.2.3.8.3 Preparation of lipase modified MPCs (Click reaction)

Azide modified MPCs have been "clicked" to an acetylene-modified lipase (Figure 25). It is a hydrolase that breaks down lipids via the cleaving of their ester bonds. Lipases are enzymes of commercial interest and are used widely within industry in, for example, detergents, baking, organic synthesis and the paper industry.[42, 43] The lipase utilized herein has been genetically altered to express just one solvent-accessible surface lysine residue (*i.e.* amino group, next to the active site). This surface amino group has been modified using standard carbodiimide coupling chemistry to yield a "clickable" enzyme with an accessible acetylene functional group on its surface.

To link this acetylene-lipase to the azide-modified AuMPCs, an excess of the lipase and copper (I) catalyst were incubated with the nanoparticle suspensions at room temperature for 3 days. A blank containing no copper (I) catalyst was also prepared, and was treated in an identical manner to the catalyst-containing sample.

Following extensive purification by centrifugation to remove the excess lipase, the particle suspensions were concentrated using centrifugation, loaded into a 1.5% (wt/v) agarose gel and electrophoretically separated at 100V for 60 min. In the gel shown in Figure 27, the band for the blank without copper catalyst (lane 2) moves an identical distance into the gel as a control band of un-reacted AzMPCs (lane 1). Proteins covalently linked to nanoparticles commonly show some non-specific association with the nanoparticle ligand shell.[44-51] This gel demonstrates that the purification method used removes all non-specifically bound protein from the nanoparticle surface. In another experiment it was shown that in a gel of samples prior to purification, the band for the blank moves further into the gel than the control band, indicating some non-specific protein binding to the nanoparticle. In both gels, the band for the sample with copper catalyst (lane 3) has partitioned even further into the gel, demonstrating a significant difference in molecular weight and/or electrostatic charge between the blank and the sample, which is attributed to the specific binding of lipase to the AzMPCs via the click chemistry 1,2,3-triazole linkage.

In conjunction with the electrophoretic evidence, the two samples have also been observed to behave differently when suspended in water. Whilst the blank is stable when suspended in de-ionized water, the [Au, 14, 100%, Click, Lipase] sample rapidly aggregates and changes color from ruby red to purple, with a measurable shift in the UV-vis λ_{max} from 528 to 540 nm, which can be reversed by adding some phosphate buffer, pH 7 to the sample. This behaviour may be attributed to the presence of bound lipase coating the AzMPC surface, as in de-ionized water, where the pH is ~ 5, the lipase is at its isoelectric point and is hence uncharged, which prevents the electrostatic repulsion between neighboring lipases which is present at pH 7, where the bound lipases are negatively charged (approx. eight negative charges per lipase molecule).

This electrostatic repulsion in buffer at pH 7 prevents the [Au, 14, 100%, Click, Lipase] from aggregating. This observation is supported by the TEM image of [Au. 14, 100%, Click, Lipase] in phosphate buffer presented in Figure 26b, which shows dispersed particles which are free from large aggregates.

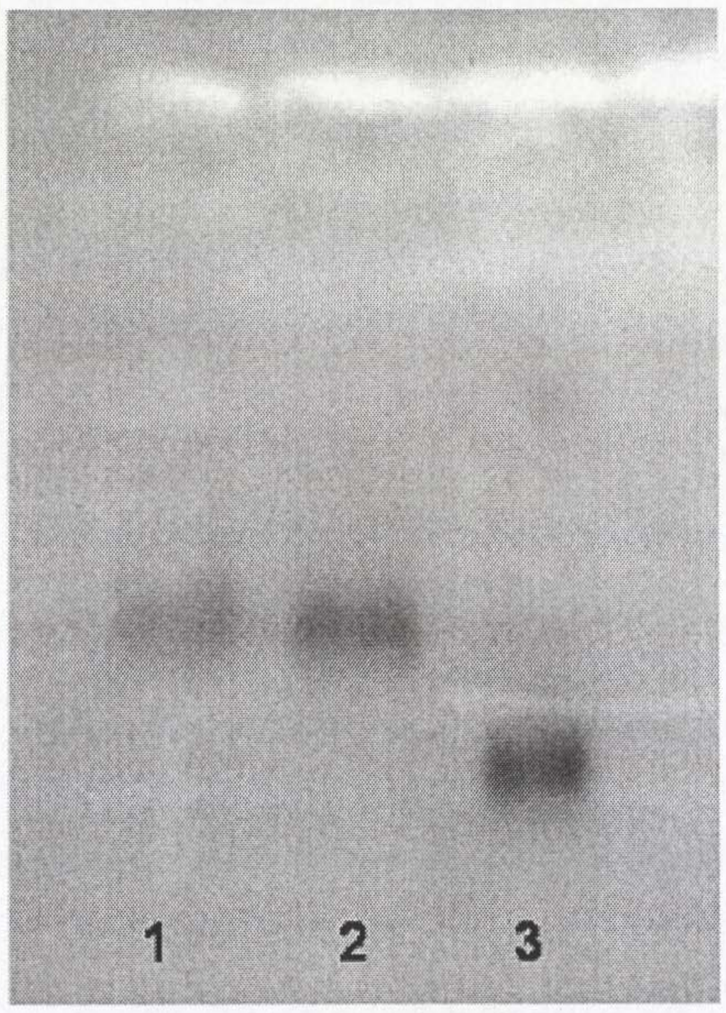

Figure 27. Gels of azide modified MPCs (lane 1), blank sample (no copper catalyst) (lane 2) and copper catalysed [Au. 14, 100%, Click, Lipase] (lane 3).

5.2.3.8.4 Lipase activity assay

Dr. Jennifer, Brennan primarily carried out this work and is presented as follows:

In developing chemistry to bind enzymes to nanomaterials, it is important to ensure that the enzyme retains its activity. Reports which describe enzymes conjugated to metal nanoparticles via non-covalent linking methods,[44,49] show that enzymatic activity is retained, although often lowered. There are remarkably few reports which utilize a specific covalent method of linking the enzyme to the nanoparticle ligand shell.[50, 51] High enzymatic activity is usually demonstrated by these conjugates. To investigate whether the bound lipases retain their activity, the lipase-labelled [Au. 14, 100%, Click, Lipase] and blank AzMPCs samples were tested using a fluorometric assay, which is schematically depicted in Figure 28a. Upon interaction with the lipase, the non-fluorescent substrate, 5-O-palmitoylindole, is cleaved at its ester bond, releasing the fluorescent 5-OH-indole product into solution. The emission of this product at 333 nm is monitored at intervals of 1 and 5 min after the addition of the sample, and the activity is expressed as activity units per ml (U ml^{-1}), with 1 unit equivalent to 1 micromole of 5-OH-indole product liberated per minute. The emission spectra for the [Au. 14, 100%, Click, Lipase] sample are presented in Figure 28b). The solid line is the spectrum after 1 min incubation and the dotted line after 5 min, showing the change in emission observed when the click sample is incubated with the substrate. This demonstrates that activity is retained when lipase is bound to the AzMPCs, with an enzyme activity of 1.82×10^{-3} U ml^{-1}. As expected, zero activity is observed for the blank sample, reaffirming the lack of non-specific protein binding observed in the electrophoresis gel. Lipase activity assays were also performed on the supernatants from the centrifugation/washing procedure used to purify the [Au. 14, 100%, Click, Lipase] samples, to ensure that all unbound lipase was removed from the MPCs suspensions. The results are presented in Figure 28c, showing the drop in supernatant lipase activity as the MPCs are repeated centrifuged and washed, eventually resulting in zero supernatant activity.

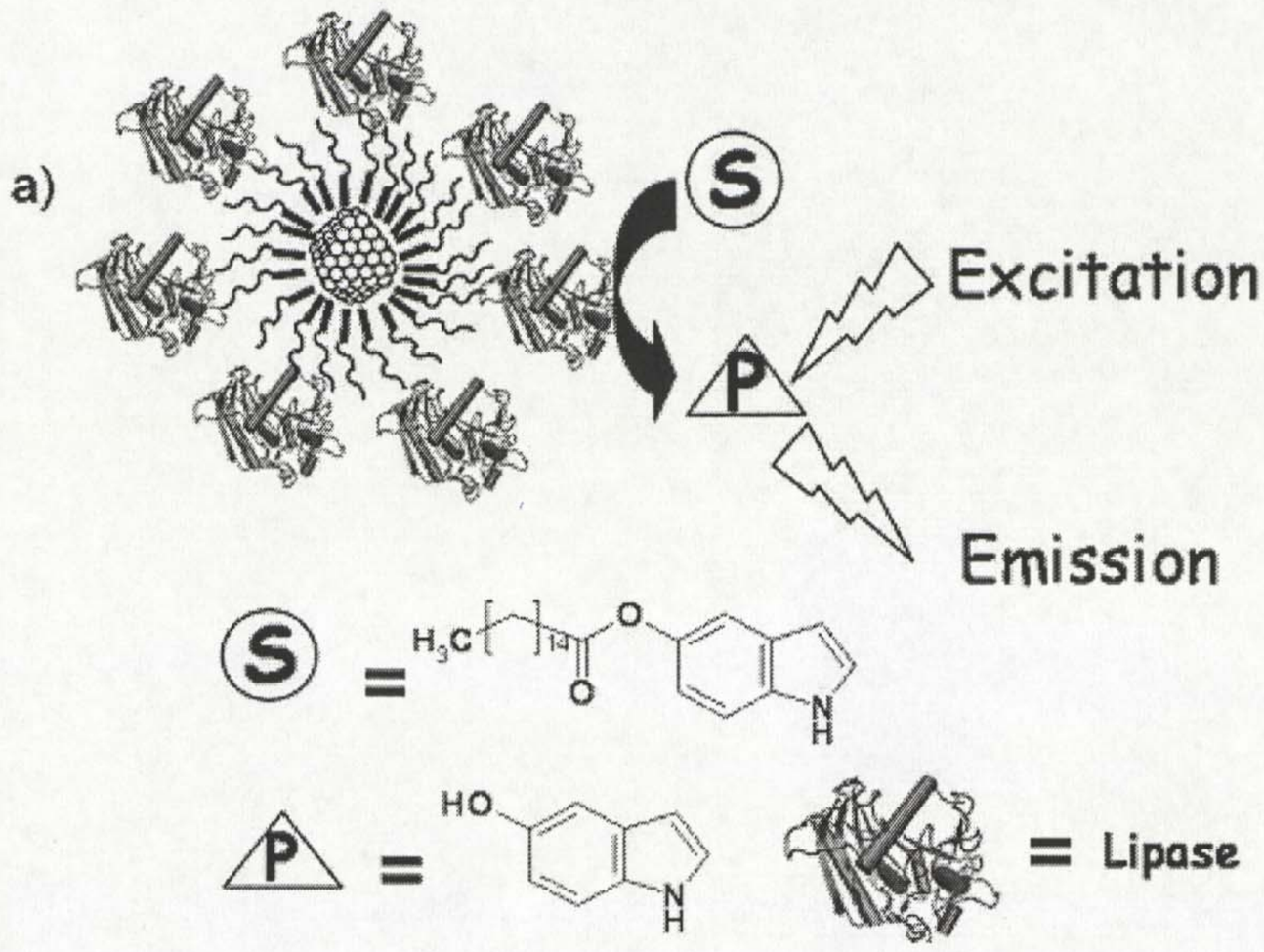

Sample	Activity ($\times 10^{-3}$ U L^{-1})
Wash 1	224.57
Wash2	67.06
Wash3	3.77
Wash 4	0.72
Wash 5	0.39
Wash 6	0.00
Wash 7	0.00
Wash 8	0.00
Blank-NPs	0.00
Lipase Labeled-NPs	1.82

Figure 28. a) Schematic representation of fluorometric lipase assay with the [Au. 14, 100%, Click, Lipase] hybrid acting on a fatty ester substrate b) Emission spectra recorded after 1 min (solid line) and 5 min (dotted line) of incubation with [Au. 14, 100%, Click, Lipase] c) Table describing the results of removing unbound lipase from nanoparticle samples using centrifugation, with nanoparticles washed until no activity is measured in the last three wash supernatants. Activity is displayed by the remaining nanoparticle suspension [Au. 14, 100%, Click, Lipase] (lipase labeled NPs), but not in the blank sample (Blank-NPs), where lipase is reacted with MPCs without the copper catalyst. 1 activity unit (U) is equivalent to 1 micromole of 5-OH-indole liberated per minute.

In summary, we have developed a functional hybrid nanomaterial consisting of lipase molecules covalently linked to AuMPCs ligand shell. For this purpose, we have introduced a simple route to water-soluble, azide-functionalized gold nanoparticles and have demonstrated the utility of click chemistry as a versatile approach to bioconjugation of nanoparticles. Importantly, the coupling chemistry used is very general and independent of the chemical nature of the nanoscopic subunits. This will allow the creation of similar composites containing a range of different biomolecular functionalities, which in the future may be used in applications such as biosensing, catalysis and controlled delivery.

5.3 Experimental

5.3.1 Materials

Unless stated otherwise, all reagents were purchased from Sigma-Aldrich (UK) and used without further purification. PEG-OH **3** and PEG-biotin **11** were either prepared following literature methods [52-54] or purchased from Prochimia (Poland). Milli-Q water (18.1MΩ) purified with ultrapure water system Milli-Q Plus 185 (Millipore purification pack) was used in all experiments. Tetrahydrofuran (THF) was distilled under nitrogen from sodium/benzophenone. Structures of some ligands used are presented in chapter 3 and few are listed below. Agarose gel electrophoresis of the nanoparticles was carried out using a Biorad Mini-PROTEAN 3-cell and Sub-Cell GT agarose gel electrophoresis system. Nanoparticles were loaded onto an agarose gel, which was run for 60 min at 100 V in tris-borate-EDTA (TBE) buffer. TEM and UV-vis experiments were carried out as described in Chapter 3.

i) N-[2-{2-{2-(1-mercaptoundec-11-yloxy)-ethoxy]-ethyl]Biotinamide (PEG-biotin)

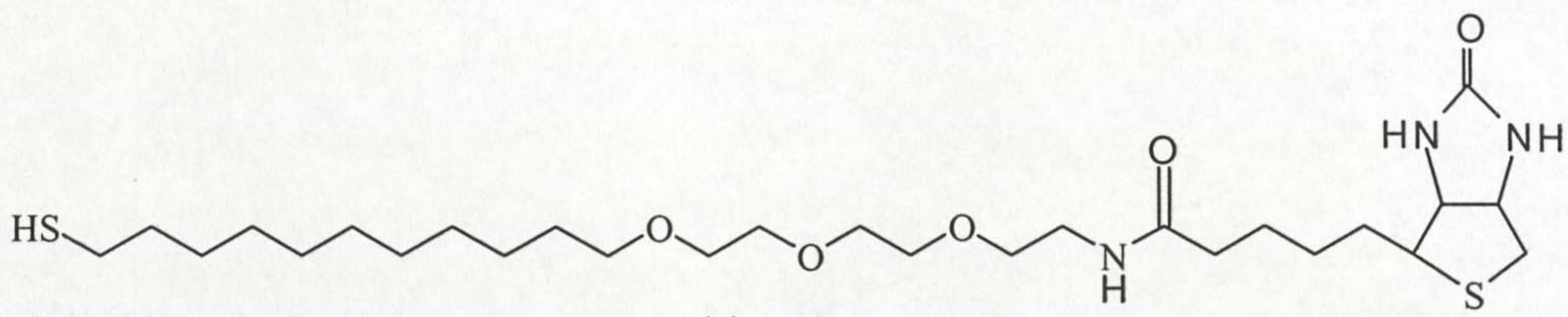

11

5.3.2 Synthetic procedures

5.3.2.1 General preparation of biotin modified MPCs (BAB method)

[Au, 14, 1%, B, -], [Au, 14, 10%, B, -], [Au, 6, 1%, B, -], [Au, 6, 10%, B, -]

Biotinylation was carried out following the synthetic approach described for the preparation of calix[4]arene modified MPCs (chapter 4), without THF.[55]

Preparation of **[Au, 14, 1%, B, -]**

A methanolic solution mixture of thioalkylated PEG-OH **3** (4.89 mg, 1.28 $x10^{-2}$ mmol) and thioalkylated PEG-biotin **11** (0.073 mg, 1.30 $x10^{-4}$ mmol) was added under stirring to filtered citrate-stabilised gold nanoparticles (20 ml, 2 nM) (prepared as described in chapter 3). The reaction mixture was stirred at room temperature overnight. Particles were centrifuged at least once (11 000 rpm, MIKRO 22 R centrifuge, Eppendorf) and re-dispersed in phosphate buffer (20 mM, pH 7.4). The resulting particles were purified by size-exclusion chromatography (Sephacryl S-100 HR support) with phosphate buffer as a mobile phase and finally particles were stored at 4 ^{0}C in 20 mM phosphate buffer pH (7.4) for later use.

Preparation of **[Au, 14, 10%, B, -]**

The experimental procedure described for the synthesis of [Au, 14, 1%, B, -] was followed using a methanolic mixture of thioalkylated PEG-OH **3** (4.45mg, 1.17 $x10^{-2}$ mmol) and PEG-biotin **11** (0.73mg, 1.3 x 10^{-3} mmol) added to filtered citrate stabilised gold nanoparticles (20 ml, 2nM) and worked up as described for [Au, 14, 1%, B, -] to obtain **[Au, 14, 10%, B, -]**.

Preparation of **[Au, 6, 1%, B, -]**

The experimental procedure described for the synthesis of [Au, 14, 1%, B, -] was followed using a methanolic mixture of thioalkylated PEG-OH **3** (4.89 mg, 1.28 $x10^{-2}$ mmol) and thioalkylated PEG-biotin **11** (0.073 mg, 1.30 $x10^{-4}$ mmol) added to

borohydride stabilised gold nanoparticles (40 ml, 75nM) (RT-5, chapter 3) and worked up as described for [Au, 14, 1%, B, -] to obtain **[Au, 6, 1%, B, -]**

Preparation of **[Au, 6, 10%, B, -]**

The experimental procedure described for the synthesis of [Au, 14, 1%, B, -] was followed using a methanolic mixture of thiolkylated PEG-OH **3** (4.45mg, 1.17 $x10^{-2}$ mmol) and PEG-biotin **11** (0.73mg, 1.3 x 10^{-3} mmol) added to borohydride stabilised gold nanoparticles (RT-5) (40 ml, 75nM) and worked up as described for [Au, 14, 1%, B, -] to obtain **[Au, 6, 10%, B, -]**

Note: Molar absorption coefficient of 4.2 x 10^8 M^{-1} cm^{-1} and 1.5 x 10^7 M^{-1} cm^{-1} were used for citrate stabilised gold nanoparticles (RT-7) and borohydride stabilised gold nanoparticles (RT-5) respectively and were adopted from [56]

5.3.2.2 General procedure for the preparation of avidin (streptavidin or neutravidin) modified MPCs (BAB method)

[Au, 14, 1%, BA, -], [Au, 14, 10%, BA, -], [Au, 6, 1%, BA, -], Au, 6, 10%, BA, -]

Preparation of **[Au, 14, 1%, BA, -] or [Au, 6, 1%, BA, -]**

Generally, to the purified 1% biotin modified AuMPCs *e.g.* [Au, 14, 1%, B, -] (1ml, 2.4 nM) was added an aqueous solution (8.6μL) of streptavidin (5mg/ml) and the mixture was left standing at ~ 4 °C overnight. Then particles were purified by repeated centrifugation (11000 rpm, 12 min, MIKRO 22 R centrifuge) re-dispersing in phosphate buffer (20 mM) (pH 7.4) until the avidin absorption peak (λ ~ 282 nm) in the supernatant was undetectable by UV-vis spectroscopy. Alternatively, particles were centrifuged at least once, and then purified by size-exclusion chromatography (S-100HR) using 20mM phosphate buffer (pH 7.4) mobile phase to obtain [Au, 14, 1%, BA, -] or [Au, 6, 1%, BA, -] which were stored in a 20 mM phosphate buffer.

Preparation of **[Au, 14, 10%, BA, -]**

The experimental procedure described for the synthesis of [Au, 14, 1%, BA, -] was followed using an aqueous solution (86 μL) of streptavidin (5mg/ml) added to biotinylated MPCs [Au, 14, 10%, B, -] (1m, 2.4 nM) and worked up as described for [Au, 14, 1%, BA, -] to obtain [Au, 14, 10%, BA, -] or [Au, 6, 10%, BA, -] which were stored in a phosphate buffer.

Note: It is important to consider Au core concentration during avidin saturation to prevent any possible aggregation. Basically the amount of avidin required to achieve optimum saturation is 300 or 3000 times the [Au, 14, 1%, B, -] or [Au, 14, 10%, B, -] respectively with relative to gold nanoparticles concentration. The biotin concentration with relative to Au core concentration for [Au, 14, 1%, B, -] and [Au, 14, 10%, B, -] is estimated 30 or 300 more respectively. For the aggregation studies described in section 5.2.1.3 the gold core concentration used is 3.5 nM for [Au, 14, 1%, B, -].

5.3.2.3 Preparation of IgG modified Au-MPCs

[Au, 14, 1%, BAB, IgG], [Au, 14, 10%, BAB, IgG] [Au, 6, 1%, BAB, IgG]

To the purified [Au, 14, 1 %, BA, -] (500μL, 4nM) in 20 mM phosphate buffer (pH 7.4) was added biotinylated anti-horse IgG (20μg/ml) Sigma-Aldrich, UK) in phosphate buffer (10mM, pH 7.4). The mixture was left standing at 4 ^{o}C overnight and then purified by either centrifugation (11 000 rpm, 12 min, until the IgG absorption peak in the supernatant is undetectable by UV-vis spectroscopy). Alternatively particles were purified by size-exclusion chromatography (S-100HR) to obtain [Au, 14, 1 %, BA, IgG].

The same procedure was followed for the preparation of [Au, 14, 10 %, BAB, IgG] using biotinylated anti-horse IgG (200μg/ml). The smaller core [Au, 6, 1 %, BA, IgG] and [Au, 6, 10 %, BA, IgG] were prepared as described for [Au, 14, 1 %, BA, IgG]. The [Au, 6, 1 %, BA, IgG] was prepared using biotinylated anti-horse IgG (20μg/ml) added to [Au, 6, 1 %, BA, -] (200μL, 132nM) and the [Au, 6, 10 %, BA, IgG] was

obtained by mixing [Au, 6, 10 %, BA, -] (400μL, 75nM) and biotinylated anti-horse IgG (40μg/ml). The smaller core was centrifuged at 25000g, ~ 30 min.

5.3.2.4 Preparation of sugar (antigen) modified Au-MPCs

[Au, 14, 1%, BAB, sugar] [Au, 6, 1%, BAB, Sugar]

To the purified [Au, 14, 1 %, BA,-] (500μL, 3.6nM) in 20 mM phosphate buffer (pH 7.4) was added Galα 1-3 Gal-biotin (50μg/ml) (Dextra Laboratories, Ltd, UK). The mixture was left standing at room temperature for 1hr and then particles were purified either by centrifugation (11000 rpm, 12 min) or by size-exclusion chromatography (S-100HR) to obtain [Au, 14, 1%, BAB, Sugar]. [Au, 14, 10%, BAB, Sugar] was obtained as described for [Au, 14, 1%, BAB, Sugar] using Galα 1-3 Gal-biotin (100μg/ml). [Au, 6, 1%, BAB, Sugar] was obtained from [Au, 6, 1 %, BA, -] (200μL, 132nM) and Galα 1-3 Gal-biotin (50μg/ml).

5.3.2.5 Preparation of fluorescein (dye) Au-MPCs

[Au, 14, 1%, BAB, Dye]

To the purified [Au, 14, 1 %, BA,-] (500μL, 3.6nM) in 20 mM phosphate buffer (pH 7.4) was added biotin-4-fluorescein (200μg/ml) (Sigma-Aldrich). The mixture was left standing overnight at ~ 4 ^{o}C. Particles were then purified by size-exclusion chromatography (Sephacryl-100HR).

5.3.2.6 Preparation of BSA modified Au-MPCs

[Au, 14, 1%, BAB, BSA], [Au, 14, 10%, BAB, BSA]

The experimental procedure described for the preparation of [Au, 14, 1%, BAB, IgG] was followed using albumin biotin labeled bovine (20μg/ml) (Sigma-Aldrich) added to [Au, 14, 1%, BA, -] (500μL, 3.6nM) to obtain [Au, 14, 1%, BAB, BSA]. [Au, 14, 10%, BAB, BSA] was obtained using biotin labeled bovine (40μg/ml) added to [Au, 14, 10%, BA, -] (500μL, 3.6nM).

5.3.2.7 Preparation of protein G or BSA primed silica bead

Two experiments were carried out (i) a warm molecular sieve bead (Aldrich, UK) was immersed into the solution of protein G (0.1mg/ml) (Aldrich, UK) in water (100μL) and allowed to sit at 4 °C overnight. It was then removed from the solution and washed extensively (2 times) with water and then allowed to dry at room temperature. (ii) BSA primed bead was prepared by immersion of warm molecular sieve bead into the aqueous BSA solution (2.5mg/ml) and allowed to stand at 4 °C for 24 hrs. Then it was washed extensively with water (2 times) and allowed to dry at room temperature.

5.3.2.8 Preparation of protein A primed silica bead

The experimental procedure described for the preparation of protein G primed silica bead was followed using a warm molecular sieve bead immersed into the solution of protein A (0.1mg/ml) in water (100μL).

5.3.2.9 Specific biomolecular recognition

Protein A or Protein G primed bead was each immersed into the [Au, 14, 1%, BAB, IgG] (200μL, 3.6 nM) and allowed to stand at room temperature overnight. After which it was washed extensively with water (2 times) and allowed to dry at room temperature. The same procedure was followed immersing BSA coated bead or uncoated molecular sieve bead.

5.3.2.10 Specific biomolecular recognition in solution

Two experiments were carried out (i) purified aqueous solutions of [Au, 14, 1%, BAB, IgG] (200µL, 3.6 nM) and [Au, 14, 1%, BAB, Sugar] (100µL, 1.5 nM) were incubated and allowed to react at room temperature overnight and then subjected to TEM analysis. (ii) Aqueous [Au, 14, 1%, BAB, IgG] (200µL, 3.6 nM) and [Au, 6, 1%, BAB, Sugar] (50µL, 2 nM) were incubated overnight at room temperature and the subjected to TEM analysis.

5.3.2.11 Preparation of avidin modified AMPCs (EDC)

[Au, 14, 100%, EDC, Avidin]

To the purified carboxylated Au-MPCs (RT-8, chapter 3) (1ml, 2.3 nM) was added 200 µL of avidin (10mg/ml) both in phosphate buffer (100 mM PB, pH 7). The mixture was shaken for 30 min at 150 x speed on a rotamax 120 (Heidolph). Then 350 µL of cold (1-ethyl-3-(3-dimethylaminopropyl) carbodiimide hydrochloride (EDC) (0.16M) (Pierce) in a phosphate buffer (100 mM, pH 7) was added and reaction mixture was further vortexed for an additional 2 hrs. Particles were then purified by repeated centrifugation (12 000 rpm, 12 min) re-suspending in PBS solution (100 mM PB, 0.28 M NaCl, pH 7.4) until avidin is undetectable in the supernatant from the UV-vis spectroscopy. Alternatively, after particles have been centrifuged at least once, they were purified by size exclusion chromatography Sephacryl (S-100HR), with buffer as the mobile phase.

5.3.2.12 Preparation of DNA-AuMPCs conjugates (EDC)

[Au, 14, 70%, EDC, DNA]

Preparation of maleimide activated Au-MPC

Purified amine functionalized MPCs (RT-10, 70% amine) (500 µL, 6nM) and sulfo-SMCC (1 ml, 5 mM) (Pierce) both in a phosphate buffer (0.1M PB, pH 7.21) solution, were incubated and protected from light. Mixture was shaken for few minutes and then

vortexed at 150 x speed (rotamax 120, Heidolph) for 2-3 hrs. Excess sulfo-SMCC was removed by repeated centrifugation, re-suspending the pellets in a buffer until the supernatant contains no sulfo-SMCC. As a final purification step particles were passed through a 5ml Zeba Desalt spin column (Pierce).

Preparation of thiolated single stranded DNA (ssDNA)

About 0.1M of DTT was placed into the 1 ml buffer (0.1M PB, pH 8.5, 0.2M NaCl) containing 5'- thiol modification ($OPO_3(CH_2)_6$-S-S-$(CH_2)_6OH$ single-stranded DNA of 22 bases (Sigma, Genosys Ltd), and allowed to stand at room temperature for 1hr. It was then purified by gel filtration chromatography (G-25) before use to make a final concentration of 30 nM in 500 μL buffer based on UV-vis absorption measurement DNA sequence: (5'HS-GCTGCCTCCCGTAGGAGTAAAA).

Preparation of DNA-AuMPCs [Au, 14, 70%, EDC, DNA]

To the maleimide activated AuMPCs (500μL, 3nM) in a conjugation buffer (0.1M PB, pH 7.43) was added 10 μL of 30 nM single-strand DNA prepared as described above. The mixture was shaken for a while and then vortexed at 150 x speed rotamax, Heidolph) overnight. Then excess DNA were removed by repeated centrifugation (11000 rpm, 12 min) and finally particles were passed through gel filtration chromatography (G-25) to obtain [Au, 14, 70%, EDC, DNA].

Preparation of particles with complementary DNA

Following a typical preparation [31], citrate stabilised particles were derivatised with thiolated single-stranded oligonucleotides by incubating gold hydrosols (500 μL, 5 nM) with disulfide protected oligonucleotides (thiol-ss DNA) (25 μL, 40 μM) in aqueous solution overnight. Solution was then diluted with 500 μL buffer solution (0.1 M PB, 0.2 M NaCl, pH 7.0) and further incubated for 3hrs. After 3 hrs, the volume of the particles (1 ml) was further evaporated slowly to 150 μL by vacuum centrifugation using Rota Vap apparatus (Labex Instruments AB, Helsingberg, model RVC2-18) for a period of 3-4 h at 40 ^{0}C. The concentrates were re-suspended in a NaCl (0.3M) and

sodium phosphate buffer (10 mM, pH 7) and the unbound oligonucleotides were removed by repeated centrifugation using a Sigma 1-13 Centrifuge (13 000 rpm x 2, for 25 min). The resulting complementary ssDNA-AuMPCs were stored at 4 ^{0}C in a phosphate buffer (10mM, 0.3 NaCl, pH 7) for later use.

Hybridization assay

Purified [Au, 14, 70%, EDC, DNA] (300 μL, 5 nM) and particles with complementary ssDNA (100 μL, 5 nM) both in a hybridization buffer (0.1M PB, 0.4 M NaCl, pH 7.43) were incubated and allowed to stand at room temperature overnight. Then a ruby red colour of the nanoparticles completely became blue and precipitated. Particles were heated up at 90 ^{0}C to recover the ruby red. Blue colour was re-gained on cooling the particles at room temperature.

5.3.2.13 Preparation of biotin modified Au MPCs

[Au, 14, 10%, EDC, Biotin] and [Au, 6, 10%, EDC, Biotin]

To the purified amine functionalized MPCs (500 μL, 6 nM) (RT-10, chapter 3 10% amine) in a phosphate buffer (100 mM, pH 7.4) was added 500 μL containing sulfo-NHS-LC-biotin ligand (11mg, 19 μmol) (Pierce) in a phosphate buffer. The mixture was vortexed at 150 x speed on rotamax 120 (Heidolph) for 2hr. Particles were then purified by size-exclusion chromatography (Sephacryl S-100HR) using phosphate buffer solution (100 mM, pH 7.4) as mobile phase. The same procedure was followed for the preparation of [Au, 6, 10%, EDC, Biotin] using sulfo-NHS-LC-biotin ligand (11mg, 19 μmol) and amine functionalized MPCs of smaller core (500 μL, 20 nM).

5.3.2.14 Preparation of biotin modified silver MPCs

[Ag, 5, 10%, EDC, Biotin]

The amine functionalized Ag MPCs (10 % amine) were prepared following the approach described for the synthesis of RT-21 particles chapter 3. The amine

functionalized particles were then used as precursors for the synthesis of Ag MPCs as follows. To the amine functionalized Ag MPCs (500μL, 3 nM) was added 500 μL of sulfo-NHS-LC-biotin ligand (15 mg, 26 μmol) both in phosphate buffer solution (100 mM, pH 7) and the mixture was were vigorously mixed (150 x speed, rotamax, Heidolph) for 2h. Then particles were purified by repeated centrifugation and alternatively purified by column chromatography (Sephadex G-25) using phosphate buffer (100 mM, pH 7).

5.3.2.15 Preparation of lipase-AuMPCs conjugates (EDC)

[Au, 14, 100%, EDC, Lipase]

Basically, carboxylated Au MPCs (RT-8, chapter 3) (500μL, 3.6nM) and lipase (300μL, 50μM) (30 000 daltons, HL1822a, Nijmegen) both in phosphate buffer (0.1M, pH 7.4) were mixed for few mins (~ 30 mins) and then EDC (250 mg, 1.3 mmol, 200 μL) in a cold buffer (0.1M PB, pH 7.4) was added and the mixture was vortexed overnight (150 x speed, rotamax 120, Heidolph). Excess lipase enzymes were removed by centrifugation (11 000 rpm, 12 min).

5.3.2.16 Preparation of lipase conjugation (Click- type method)

[Au, 14, 100%, Click, Lipase]

The citrate-stabilized gold nanoparticles were functionalized with **1** by mixing of a molar excess of **1** (Figure 25, section 5.2.3.8.2) (dissolved in water) with the gold nanoparticle suspension following a previous method. [55] Briefly, 500 μl of an aqueous solution (17 mg, 20 μmoles) of **1** was mixed with 10 μL of 0.1 M dithiothreitol, and was left to stand at room temperature for 25 min. This mixture was then added to filtered citrate-stabilized gold nanoparticles (20 ml, 2.8 nM) under stirring. After mixing for 18 hours at room temperature, the particles were purified by repeated centrifugation (3 times at ~ 11000 rpm) and re-dispersion in water. As a final purification step, the particles were passed through a 5 ml Zeba Desalt spin column (Pierce). Elemental analysis was carried out by ICP-AES (gold and sulphur) and combustion analysis (carbon, hydrogen and nitrogen). For a typical preparation of

AzMPCs a composition of gold = 95.8%, sulphur = 0.48%, carbon = 2.90%, hydrogen = 0.42% and nitrogen = 0.33 % was found.

5.3.2.17 Preparation of lipase modified nanoparicles

Lipase from *Thermomyces lanuginosus*, engineered to contain one solvent-accessible lysine NH_2 group, was prepared by Novozymes A/S using in-house protein engineering and expression techniques. It was labeled with an acetylene group using 4-pentynoic acid, and EDC (1-Ethyl-3-(3-dimethylaminopropyl)carbodiimide hydrochloride) as a coupling reagent. The reaction was carried out in 20 mM phosphate buffer, pH 7.0 (PB). 600 μL of lipase solution (0.0225 mM in water), 6.7 μL of 4-pentynoic acid solution (100 mM in 50% THF/PB), 13 μL of EDC solution (50 mM in PB), 300 μL THF and 130 μL of PB were mixed in a 10 ml plastic culture tube, yielding a final reaction volume of 1500 μL (20% v/v total THF content). The reaction mixture was shaken overnight at room temperature and the THF was evaporated off in a fumehood. The remaining mixture in 100% PB was dialyzed three times against 500 ml phosphate buffer for a total of 36 hrs using a molecular weight cut-of of 12 kDa.

Azide-functionalized gold nanoparticles were labelled with the acetylene-lipase using click chemistry. To 192 µl of a solution of azide-nanoparticles (AzMPCs, 13.0 nM in H_2O) was added 36 µl of acetylene-lipase (69 mM in phosphate buffer) and 2.5 µl of catalyst (10 mM $CuSO_4 \cdot 5H_2O$, 50mM ascorbic acid in H_2O), to a final volume of 1 ml in H_2O. This reaction mixture was stirred at room temperature for 3 days, after which the nanoparticles were purified by repeated centrifugation (8 times at ~ 10,000g) and re-dispersion in phosphate buffer. The supernatants were retained and tested for the presence of lipase using a lipase activity assay (described below). Agarose gel

electrophoresis of the nanoparticles was carried out using a Biorad Mini-PROTEAN 3-cell and Sub-Cell GT agarose gel electrophoresis system. Nanoparticles (in 10%

glycerol) were loaded onto a 1.5% agarose gel, which was run for 60 min at 100 V in tris-borate-EDTA (TBE) buffer.

5.3.2.18 Lipase activity assay

Lipase activity was determined using a fluorescence-based activity assay. A non-fluorescent substrate, 5-O-palmitoylindole was employed. In the presence of lipase, the palmitoyl chain of the substrate is cleaved at the ester bond, yielding a fluorescent 5-OH-indole product. Briefly, 30 μL of 5-O-palmitoylindole in 2-methoxyethanol was mixed with 70 μL of phosphate buffer, and 20 μL of lipase (or nanoparticle) sample was added, while a stop clock was started simultaneously. The emission intensity of the assay mixture at the start and end of 5 minutes incubation was monitored using a Perkin Elmer LS50B luminescence spectrometer (λex = 300 nm, λem = 333 nm). The rate of change of emission intensity w.r.t. time (min^{-1}) is converted to enzyme activity units (U ml^{-1}) using the molar fluorescence of 5-OH-indole (1.15 × 109 ml mol^{-1} in this assay). 1 activity unit (U) is equivalent to 1 micromole of 5-OH-indole product liberated per minute. The blank rate of the assay (auto-hydrolysis of the substrate) was determined by substituting 20 μL of phosphate buffer for the 20 μL of lipase sample in the assay mixture. This control experiment demonstrates that auto-hydrolysis of the substrate was negligible under these assay conditions. As nanoparticles absorb strongly at both the excitation and emission wavelength of 5-OH-indole, it is likely that the fluorescence quantum yield of the 5-OH-indole fluorophore will be lower when AzNPs are present in the lipase assay solution (due to the nanoparticles absorbing both the excitation and emission energy). To quantify this "quenching" effect, a Stern-Volmer-type quenching constant for the AzNPs and 5-OH-indole was determined. K_{sv} for this system is 3.3×10^8 M^{-1}. All quoted nanoparticle-lipase activity rates have been corrected using this K_{sv}.

5.4 References

[1] Salata, O. V., *Journal of Nanobiotechnology*, 2004, **2**, 3

[2] Kumar, C. S. S. R., *Biofunctionalisation of Nanomaterials (Nanotechnologies for the life sciences* 1), Wiley-VCH, Weinheim, 2005

[3] Katz, E and Willner, I., *Angew. Chem. Int. Ed.*, 2004, **43**, 6042

[4] Shenton, W., Davis, A. S and Mann, S., *Adv. Mater.*, 1999, **11**, 449

[5] Caruso, F., *Adv. Mater*. 2001, **13**, 11

[6] Caruso, F and Mohwald, H., *J. Am. Chem. Soc.*, 1999, **121**, 6039

[7] Taton, T. A., Mirkin, C. A and Letsinger, R. L., *Science,* 2000, **289**, 1757

[8] Niemeyer, C. M., *Angew. Chem. Int. Ed., 2001*, **113,** 4254

[9] Gestwicki, J. E., Strong, L. E and Kisseling, L. L., *Angew. Chem. Int. Ed.*, 2000, **112**, 4742

[10] Okano, K., Takahashi, S., Yasuda, K., Imai, K and Koga M., *Anal. Biochem*. 1992, **202,** 120

[11] Soukka, T., Harma, H., Paukunen, J and Lovgren, T., *Anal. Chem*., 2001, **73**, 2254

[12] Hermanson, G. T., *Bioconjugate Techniques*, Academic Press, London, 1996, 593

[13] Hong, H. G., Bohn, P. W and Sligar, S. G., *Anal. Chem*., 1993, **65,** 1635

[14] Hong, H. G., Jiang, M., Sligar, S. G and Bohn, P. W., *Langmuir*, 1994, **10**, 153

[15] Hainfield, J. F. and Powell, R. G., *The journal of Histochemistry & Cytochemistry*, 2000, **48**, 471

[16] Hayat, M. A, Colloidal Gold: *Principles, Methods and Applications*, Academic Press, New york, 1989

[17] Aubin-Tam, M and Hamad-Schifferli, K., *Langmuir,* 2005, **21**, 12080

[18] Dreshler, U., Erdogan, B and Rotello, V. M., *Chem. Eur. J.*, 2004, **10**, 5570

[19] Shenhar, R and Rotello, V. M., *Accounts of Chemical Research*, 2003, **36**, 549

[20] Manjula, B. N., Tsai, A., Upadhya, R., Perumalsamy, Smith, P. K, Malavalli, A., Vanderiff, K., Winslow, R. M., Intaglieta, M., Prabhakaran, M., Friedman, J. M and Archarya, A. S., *Bioconjugate Chem.,* 2003, **14**, 46

[21] Elghanian, R, Storhoff, J. J., Mucic, R. C., Letsinger, R. L and Mirkin, C. A., *Science*, 1997, **277**, 1078

[22] Rosi, N. L and Mirkin, C. A., *Chem. Rev*., 2005, **105,** 1547

[23] Mirkin, C. A., *Inorganic Chemistry*, 2000, **39**(11), 2258

[24] Goldman, E. R., Balighaian, E. D., Mattoussi, H., Kuno, M. K., Mauro, J. M., Tran, P. T and Anderson, G. P., *J. Am. Chem. Soc*., 2002, 1**24**, 6378

[25] Baeumie, M., Stamou, D., Segura, J. M., Hovius, R and Vogel, H., *Langmuir,* 2004, **314**, 529

[26] Wang, Z., Lee, J., Cossins, A. R and Brust, M., *Anal. Chem*., 2005, **77,** 5770

[27] Posekany, K. J., Pittman, K. H., Bradfield, J. F., Haisch, C. E and Verbanac, K. M., *Infection and Immunity*, 2002, **70**(11), 6215

[28] Pierce, F., Chakrabarti, A., Fry, D and Sorensen, C. M., *Langmuir*, 2004, **20**, 2498

[29] Pierce, F., Sorensen, C. M and Chakrabarti, A., *Langmuir*, 2005, **21**, 8992

[30] Hiddessen, A. L., Rodgers, S. D., Weitz, D. A and Hammer, D. A., *Langmuir*, 2000, **16**, 9744

[31] Kanaras, A. G., Wang, Z., Bates, A. D., Cosstick, R and Brust M., *Angew. Chem. Int. Ed.*, 2003, **2**, 42

[32] Reference 12, p 148

[33] Kolb, H. C and K. B. Sharpless, K. B., *DDT.*, 2003, **8**, 1128

[34] Kolb, H. C., Finn, M. G and Sharpless, K. B., *Angew. Chem. Int. Ed.,* 2001, **40**, 2004

[35] Rostovstev, V. V., Green, G. L., Fokin, V. F and Sharpless, K. B. *Angew. Chem. Int. Ed.* 2002, **41**, 2596

[36] Dirks, A. J., van Berkel, S. S., Hatzakis, N. S., Opsteen, J. A., van Delft, F. L., Cornelissen, J. J. L. M., Rowan, A. E., van Hest, J. C. M., Rutjes, F. P. J. T and. Nolte, R. J. M., *Chem. Comm.,* 2005, 4172

[37] Helms, B., Mynar, J. L., Hawker, C. J., Frechet, J. M. J., *J. Am. Chem. Soc.*, 2004, **126,** 15020

[38] Tornøe, C., Christensen, C and Meldal, M., *J. Org. Chem.,* 2002, **67**, 3057.

[39] Parrish, B., Breitenkamp, R.B and Emrick, T., *J. Am. Chem. Soc.,* 2005, **127**, 7404

[40] Kolb, H. C and Sharpless, K. B., *Drug Discovery Today*, 2003, **8**, 1128

[41] Mitsopoulous, G., Walsh, D. P and Chang, Y. T., *Curr. Op. Chem. Biol.*, 2004, **8**, 26

[42] Svendsen, A., *Biochim. Biophys. Acta,* 2000, **1543**, 223

[43] Valincius, G., Ignatjev, I., Niaura, G., Kazemekaite, M., Talaikyte, Z., Razumas, V and Svendsen, A., *Anal. Chem.*, 2005, **77,** 2632

[44] Ha, T. H., Jeong, J. Y and Chung, B. H., *Chem. Comm.*, 2005, 3959

[45] Aubin, M. E., Morales, D. G., Hamad-Schifferli, K. *Nano Lett.,* 2005, **5**, 519

[46] Stonehuerner, G., Zhao, J., O'Daly, J. P., Crumbliss, A. L and Henkens, R. W., *Biosens. Bioelectr.*, 1992, **7**, 421

[47] Keating, C. D., Kovaleski, K. M and Natan, M. J., *J. Phys. Chem. B.*, 1988, **102,** 9404

[48] Mandal, S., Phadthare, S and Sastry, M., *Curr. Appl. Phys.*, 2005, **5**, 118

[49] Fisher, N. O., McIntosh, C. M., Simard, J. M and Rotello, V. M., *Proc. Nat. Acad. Sci. U.S.A.*, 2005, **99**, 5018

[50] Abad, J. M., Mertens, S. F. L., Pita, M., Fernandez, V. M and Schiffrin, D. J. *J. Am. Chem. Soc.*, 2005, **127,** 5689

[51] Liobashevski, O., Chegel, V. I., Patolsky, F., Katz, E and Willner, I., *J. Am. Chem. Soc.*, 2004, **126**, 7133

[52] Tshikhudo, T. R., Wang, Z and Brust, M., *Materials Science & Technology*, 2004, **20**, 980

[53] Pale-Grosdemange, C., Simon, E. S., Prime, K. L and Whitesides, G. M., J. AM. *Chem. Commun.*, 1991, **113**, 12

[54] Kanaras, A. G., Kamounah, F. S., Schaumburg, K., Kiely, C. J and Brust, M., *Chem, Commun*., 2002, 2294

[55] Tshikhudo, T. R., D. Demuru, Z. Wang, M. Brust, A. Secchi, A. Arduini, A. Pochini, *Angew. Chem. Int. Ed*., **2005**, 44, 2913

[56] Demers, L. M., Mirkin, C. A., Mucic, D. C., Reynolds, R. A., Letsinger, R. L., Eighanian, R and Viswandham, G., *Anal. Chem*., 2000, **72**, 5535

CHAPTER 6

CONCLUSIONS AND FUTURE WORK

6 Conclusions and Future Perspectives

6.1 Conclusions

Thioalkylated polyethylene glycol (PEG) ligands containing specific functionalities such as amines, carboxylates, azide *etc* have been employed for the development of bio-molecularly functionalized monolayer protected clusters (MPCs) of gold and silver. They were designed to (i) impart water solubility and stability to the conventional alkanethioalted MPCs (ii) make MPCs bio-friendly by incorporating PEG segments containing the vacant functionality to permit facile conjugation with biomolecules and (iii) explore the versatility of the resulting materials in biological applications.

We have successfully employed these PEG ligands to prepare size-selective aqueous gold and silver MPCs. The smallest gold MPCs (~ 3 nm) were prepared by a single-phase reduction method, which encompasses reducing a gold salt by $NaBH_4$ in the presence of a thiolated PEG ligand in acidic alcoholic solution. Au-MPCs of the same size were also produced by the two-phase liquid/liquid route. Au-MPCs of around 6 nm were also prepared by two-phase route followed by transfer into water upon attachment of the PEG ligands. Slightly larger Au-MPCs (~7 nm) were prepared by reduction with borohydride, while citrate stabilised particles were used as precursors for the 14 nm Au-MPCs. We have also developed a simple route for the preparation of very large Au-MPCs (~ 55 nm) of varied morphologies by reduction with propanol. The amine stabilised MPCs by other routes were difficult to prepare, however, we developed a simple route in which the amine functionalized MPCs are stabilised by proportions of PEG-OH ligand. Above all, we have developed and prepared functionalized Au-MPCs, which could easily be manipulated without the loss of their materials. Importantly, for the purpose of meeting the requirements for biological applications, we tested the stability of all PEGylated Au-MPCs under

conditions likely to be encountered in a physiological environment, (such as high electrolyte concentrations varied pH ranges, *n*on-specific adsorption *etc*) and even conditions requiring the use of organic solvents. Our PEGylated Au-MPCs are very stable at high NaCl concentration (> 3 M) and at pH ranging from 1-14 irrespective of the length of the ligand used. We have employed size-exclusion chromatography to purify and to obtain narrow size distribution of PEGylated Au-MPCs.

Rational design for Ag-MPCs, incorporated pentapeptide CALNN ligand in addition to thioalkylated PEGS ligands to stabilize various types of Ag nanoparticles. Protocols have been developed for the preparation of CALNN stabilised Ag-MPCs (8 nm and 16 nm). These particles were derived from citrate stabilised particles or obtained by two-phase transfer method. Ligand exchange strategies were employed to prepare PEGylated Ag-MPCs of around 5 nm, while the two-phase negatively charged Ag-Br route was employed to obtain PEGylated Ag-MPC of comparable size (4.5 nm). We have carried out extensive stability studies which revealed that CALNN stabilised MPCs are stable in 1M NaCl and between pH 4 and 12 while PEGylated Ag-MPCs are stable in high NaCl concentrations (> 2 M) and between pH 1 and 14. The unprecedented stability conferred by both CALNN and in particular PEG ligands in combination with their compatibility in biological environment, opened platform in which Ag-MPCs can be used for biological applications. In addition they (particularly PEGylated Ag-MPCs) can be used in very harsh conditions without compromising their stability.

The versatility of our PEGylated MPCs has been demonstrated by developing a protocol for the incorporation of supramolecular chemistry to the MPCs ligand shell. It has been shown that water insoluble species, calix[4]arene moiety when introduced on MPCs ligand shell can be made water soluble and retain their specific molecular recognition properties in water. The specific molecular recognition properties of water soluble calix[4]arene modified MPCs towards cationic pyridinium moiety have been demonstrated.

In addition, calix[6]arene was used as wheel for the construction of pseudo/rotaxane assemblies in which gold nanoparticles act as alternative stoppers in organic solvent. It was found that, by constructing an octyl oriented pseudorotaxane complex (with calix[6]arene wheel oriented towards the molecular stopper) its immobilization on gold nanoparticles leads to the formation of gold based rotaxane in which the resulting gold nanoparticles are highly ordered.

Biomolecular functionalisation of gold and silver nanoparticles was achieved by covalent and non-covalent strategies. In a non-covalent approach, we have attached a number of biomolecules including IgG (antibody), sugar (antigen), dye and BSA via the biotin-avidin system (BAB). We have extensively carried out an aggregation assay studies which permitted us to attach any biotinylated functionalities of choice by the biotin-avidin system. A covalent strategy was carried out in two different approaches, thus, carbodiimide coupling and by click chemistry. By the carbodiimide approach, we developed protocols for the attachment of proteins (lipase, and avidin), biotin and oligonucleotide (DNA) to our PEGylated MPCs. A simple and reliable protocol for coupling the azide modified PEGylated MPCs and acetylene functionalized lipase an enzyme was developed by click chemistry.

Importantly, a proof of concept has been demonstrated that the attached biomolecules retain their biofunction. In the biotin-avidin approach (BAB), we have demonstrated specific biomolecular recognition properties of the antibody (IgG) modified Au-MPCs towards an antigen (Protein G), immobilized on a molecular sieve bead. The protein G coated silica bead becomes red when introduced into the ruby red IgG functionalized Au-MPCs solution. The specific biomolecular recognition properties demonstrated shows that the PEGylated antigenic particles developed are potential candidates for use in any colour based diagnostic applications. Moreover, we have showed the specific binding of these antibody modified Au-MPCs in solution, by mixing them with antigen (sugar) modified Au-MPCs. In solution, particles come together or aggregated when a low ratio of the smaller particles (sugar modified Au-MPCs) are mixed with the larger antigenic Au-MPCs a consequence of specific molecular recognition properties.

By the covalent approach, we have prepared and demonstrated that maleimide functionalized MPCs can be used as precursors for the construction of PEGylated Au-MPCs functionalized with DNA. We have successfully shown that, the DNA modified particles can be used as probes for the detection of target particles (particles functionalized with complementary strand DNA). A proof of concept was demonstrated by carrying out hydridisation and de-hybridisation experiments.

By click chemistry, it was shown that lipases do not loose their activities when attached on PEGylated Au-MPC ligand shell. It was demonstrated that lipase modified MPCs are capable of cleaving a non-fluorescent 5-O-palmitoylindole substrate at its ester bond releasing the fluorescent 5-OH-indole product into the solution with an emission at 333 nm. By monitoring the change in emission spectra of the product at 1 and 5 min intervals it was shown that an enzyme activity of 1.82×10^{-3} U ml^{-1} can be retained when the lipase is immobilised on MPCs ligand shell.

Finally, we have developed a generic approach to biomolecular functionalisation on gold and silver nanoparticles by PEGylation chemistry. The resulting PEGylated Au and Ag-MPCs kits can be used as alternative bio-labels, as delivery agents, bio-catalysts and for diagnostic purposes.

6.2 Future perspectives

Beyond the initial aims of project it is now important to find real applications of these special hydrophilic MPCs (diagnostics, bio-sensing *etc*). Dr. D.S.K. Ikah has recently shown that BSA-modified MPCs can be used for the removal of bilirubin. In his preliminary results, Dr. Ikah observed specific bilirubin binding by the BSA-modified MPCs prepared via the biotin-avidin approach. The efficiency of BSA-modified MPCs to significantly bind bilirubin and its transportation to the liver could be of great importance since free bilirubin is toxic and causes jaundice.

In addition, Dr. Ikah showed that cells can take-up these PEGylated MPCs into the cytoplasm and remain stable and monodispersed.

Designing probes for targeted nuclear entry is a highly desirable and challenging area of research that has to be investigated with immediate effect. In order to further exploit the applications of these materials in a wide biological and biomedical areas, the following targets have to be met;

- Monofunctionalisation (attachment of single molecule per particle) in particular for single-molecule detection studies
- Multifunctionalisation (attachment of multiple functionalities per particle- multiplexing)
- Improving the sensitivity of probes- to reach and exceed the current detection limit
- Preparing smaller probes (in particular for nuclear entry)
- Alloying probes (metals-magnetic-semiconductor nanocrystals) to fine tune the properties

All these application targets will allow the exploitation of these materials for specific drug delivery, detection of specific pathogens, MRI contrast enhancement etc to improve and exceed the scope of conventional technologies.

In order to exploit these particles (particularly by the BAB type), projects are currently underway and planned to address pressing needs facing the majority of Africans. This will not be limited to environmental, agricultural and health matters.